

# THE SPACE OF EMBEDDED MINIMAL SURFACES OF FIXED GENUS IN A 3-MANIFOLD $V$ ; FIXED GENUS

TOBIAS H. COLDING AND WILLIAM P. MINICOZZI II

ABSTRACT. This paper is the fifth and final in a series on embedded minimal surfaces. Following our earlier papers on disks, we prove here two main structure theorems for *non-simply connected* embedded minimal surfaces of any given fixed genus.

The first of these asserts that any such surface without small necks can be obtained by gluing together two oppositely-oriented double spiral staircases; see Figure 1.

The second gives a pair of pants decomposition of any such surface when there are small necks, cutting the surface along a collection of short curves; see Figure 2. After the cutting, we are left with graphical pieces that are defined over a disk with either one or two sub-disks removed (a topological disk with two sub-disks removed is called a pair of pants).

Both of these structures occur as different extremes in the two-parameter family of minimal surfaces known as the Riemann examples.

The results of [CM3]–[CM6] have already been used by many authors; see, e.g., the surveys [MeP], [P], [Ro] and the introduction in [CM6] for some of these applications. There is much current research on minimal surfaces with infinite topology. Some of the results of the present paper were announced previously and have already been widely used to study infinite topology minimal surfaces; see, e.g., [MeP], [MePRs1], [MePRs2], [MePRs3], and [P].

The two main structure theorems for non-simply connected surfaces:

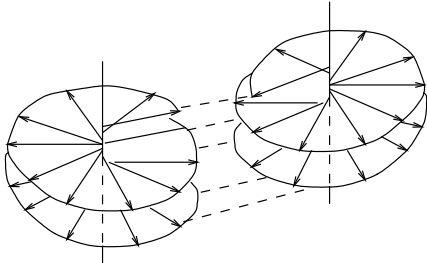
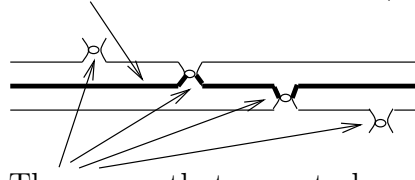


FIGURE 1. Absence of necks: The surface can be obtained by gluing together two oppositely-oriented double spiral staircases.

One of the “pair of pants” (in bold).



The curves that we cut along.

FIGURE 2. Presence of necks: The surface can be decomposed into a collection of pair of pants by cutting along short curves.

## CONTENTS

0.	Introduction	3
0.1.	Brief outline of the paper and overview of the proofs	10
1.	When the sequence has positive genus: Theorems and outlines of proofs	11

---

The authors were partially supported by NSF Grants DMS 0104453 and DMS 0104187.

1.1.	The sets $\mathcal{S}_{neck}$ and $\mathcal{S}_{ulsc}$ in the general case of fixed genus	11
1.2.	The statements of the theorems in the general case of fixed genus	12
1.3.	The local structure near points in $\mathcal{S}_{ulsc}$ and $\mathcal{S}_{neck}$	12
1.4.	The modifications in the proofs for positive genus	13
2.	Multi-valued graphs	15
<b>Part I.</b>	<b>Results for disks from [CM3]–[CM6]</b>	16
I.1.	The lamination theorem and one-sided curvature estimate	17
<b>Part II.</b>	<b>The singular set <math>\mathcal{S}</math> and limit lamination <math>\mathcal{L}'</math></b>	18
II.1.	The singular set $\mathcal{S}$	19
II.1.1.	Convergence away from $\mathcal{S}$	19
II.2.	The local structure of $\mathcal{L}'$ near a point of $\mathcal{S}_{ulsc}$	20
II.2.1.	Collapsed leaves of $\mathcal{L}'$	22
II.3.	The structure of the collapsed leaves of $\mathcal{L}'$	23
II.3.1.	Proving property (1) of Proposition II.3.1: Isolated removable singularities	24
II.3.2.	Each leaf is a limit of multi-valued graphs in the $\Sigma_j$ 's	28
II.3.3.	Property (2) of Proposition II.3.1: Each collapsed leaf is stable	29
II.3.4.	Property (3) of Proposition II.3.1: Opposite orientations at distinct points of $\Gamma_{Clos} \cap \mathcal{S}_{ulsc}$	35
<b>Part III.</b>	<b>When the surfaces are ULSC: The proof of Theorem 0.9</b>	37
III.0.5.	Property (1) in Proposition III.0.2: Collapsed leaves are planar	38
III.0.6.	Property (2) in Proposition III.0.2: Ruling out just one point of $\mathcal{S}_{ulsc}$ in a leaf	38
III.1.	Properness and the limit foliation	42
III.1.1.	Establishing properness: The proof of $(\star)$	43
III.2.	Completing the proof of Theorem 0.9	49
III.3.	Sequences with fixed genus	50
III.4.	An application: A one-sided property for ULSC surfaces	50
<b>Part IV.</b>	<b>When the surfaces are not ULSC: The proof of Theorem 0.14</b>	52
IV.1.	Proving (C1) in Theorem 0.14: A plane through each point of $\mathcal{S}_{neck}$	53
IV.1.1.	The proof of Proposition IV.1.1: A decomposition near each point of $\mathcal{S}_{neck}$	55
IV.1.2.	Step (1): Decomposing $\Sigma_j$ into ULSC pieces	63
IV.1.3.	Step (2): The ULSC pieces of $\Sigma_j$ contain graphs	64
IV.2.	The ULSC regions of the lamination: (C2) and (D) in Theorem 0.14	66
IV.2.1.	The leaf $\Gamma$ cannot cross the limit planes	67
IV.2.2.	The properties of a collapsed leaf $\Gamma$	68
IV.2.3.	$\Gamma_{Clos} \setminus \Gamma$ consists of exactly two points	69
IV.2.4.	The proof of Proposition IV.2.2	74
IV.2.5.	The proof of (C2) and (D) in Theorem 0.14	75
IV.3.	Putting it all together: The proof of Theorem 0.14	76
<b>Part V.</b>	<b>The no mixing theorem, Theorem 0.4</b>	76
<b>Part VI.</b>	<b>Completing the proofs of Theorem 0.6 and Theorem 0.12</b>	78
VI.1.	Blow up results for ULSC surfaces	79
VI.1.1.	Finding short separating curves	79
VI.2.	Complete leaves of $\mathcal{L}'$	81
VI.3.	Incomplete leaves of $\mathcal{L}'$	86

VI.3.1. If $\Gamma$ is not flat, then $\Gamma_{Clos} \cap \mathcal{S}$ consists of at most two points	87
VI.3.2. The proof of Lemma VI.3.1	88
VI.4. The proofs of Theorem 0.6 and Theorem 0.12	94
<b>Part VII. Appendices</b>	94
Appendix A. Compact connected exhaustions	94
Appendix B. Surfaces with stable covers	95
B.1. Going from stability of a covering space to stability of a surface itself	95
B.2. A surface and stable cover with cyclic holonomy group where the previous lemma applies	98
B.3. A Bernstein theorem for incomplete surfaces	99
Appendix C. An extension of [CM9]	101
C.1. Chord-arc bounds for ULSC surfaces	101
C.2. Chord-arc and area bounds for surfaces with bounded curvature	101
Appendix D. Estimates for stable surfaces	102
D.1. The regularity of the distance function to the interior boundary	102
D.2. The proof of the “stable graph” proposition	104
Appendix E. Blowing up intrinsically on the scale of non-trivial topology	108
Appendix F. Minimal surfaces with a quadratic curvature bound in a half-space	109
References	112

## 0. INTRODUCTION

This paper is the fifth and final in a series where we describe the space of all properly embedded minimal surfaces of fixed genus in a fixed (but arbitrary) closed 3-manifold. We will see that the key is to understand the structure of an embedded minimal planar domain in a ball in  $\mathbf{R}^3$ . Since the case of disks was considered in the first four papers, the focus here is on non-simply connected planar domains.

**We will first restrict to the case of planar domains, i.e., when the surfaces have genus zero. In particular, the main theorems will first be stated and proved for planar domains.** We will see that the general case of fixed genus requires only minor changes. The necessary changes to the main theorems and the modifications needed for their proofs will be given in Section 1.

Sequences of planar domains which are not simply connected are, after passing to a subsequence, naturally divided into two separate cases depending on whether or not the topology is concentrating at points. To distinguish between these cases, we will say that a sequence of surfaces  $\Sigma_i^2 \subset \mathbf{R}^3$  is *uniformly locally simply connected* (or ULSC) if for each compact subset  $K$  of  $\mathbf{R}^3$ , there exists a constant  $r_0 > 0$  (depending on  $K$ ) so that for every  $x \in K$ , all  $r \leq r_0^1$ , and every surface  $\Sigma_i$

$$\text{each connected component of } B_r(x) \cap \Sigma_i \text{ is a disk.} \quad (0.1)$$

For instance, a sequence of rescaled catenoids where the necks shrink to zero is not ULSC, whereas a sequence of rescaled helicoids is.

---

<sup>1</sup>If each component of the intersection of a minimal surface with a ball of radius  $r_0$  is a disk, then so are the intersections with all sub-balls by the convex hull property (see, e.g., lemma C.1 in [CM6]). Therefore, it would be enough that (0.1) holds for  $r = r_0$ .

Another way of locally distinguishing sequences where the topology does not concentrate from sequences where it does comes from analyzing the singular set. The singular set  $\mathcal{S}$  is defined to be the set of points where the curvature is blowing up. That is, a point  $y$  in  $\mathbf{R}^3$  is in  $\mathcal{S}$  for a sequence  $\Sigma_i$  if

$$\sup_{B_r(y) \cap \Sigma_i} |A|^2 \rightarrow \infty \text{ as } i \rightarrow \infty \text{ for all } r > 0. \quad (0.2)$$

We will show that for embedded minimal surfaces  $\mathcal{S}$  consists of two types of points. The first type is roughly modelled on rescaled helicoids and the second on rescaled catenoids:

- A point  $y$  in  $\mathbf{R}^3$  is in  $\mathcal{S}_{ulsc}$  if the curvature for the sequence  $\Sigma_i$  blows up at  $y$  and the sequence is ULSC in a neighborhood of  $y$ .
- A point  $y$  in  $\mathbf{R}^3$  is in  $\mathcal{S}_{neck}$  if the sequence is not ULSC in any neighborhood of  $y$ . In this case, a sequence of closed non-contractible curves  $\gamma_i \subset \Sigma_i$  converges to  $y$ .

The sets  $\mathcal{S}_{neck}$  and  $\mathcal{S}_{ulsc}$  are obviously disjoint and the curvature blows up at both, so  $\mathcal{S}_{neck} \cup \mathcal{S}_{ulsc} \subset \mathcal{S}$ . An easy argument will later show that, after passing to a subsequence, we can assume that

$$\mathcal{S} = \mathcal{S}_{neck} \cup \mathcal{S}_{ulsc}. \quad (0.3)$$

Note that  $\mathcal{S}_{neck} = \emptyset$  is equivalent to that the sequence is ULSC as is the case for sequences of rescaled helicoids. On the other hand,  $\mathcal{S}_{ulsc} = \emptyset$  for sequences of rescaled catenoids. These definitions of  $\mathcal{S}_{ulsc}$  and  $\mathcal{S}_{neck}$  are specific to the genus zero case that we are focusing on now; the slightly different definitions in the higher genus case can be found around equation (1.1).

We will show that every sequence  $\Sigma_i$  has a subsequence that is either ULSC or for which  $\mathcal{S}_{ulsc}$  is empty. This is the next “no mixing” theorem. We will see later that these two different cases give two very different structures.

**Theorem 0.4.** If  $\Sigma_i \subset B_{R_i} = B_{R_i}(0) \subset \mathbf{R}^3$  is a sequence of compact embedded minimal planar domains<sup>2</sup> with  $\partial\Sigma_i \subset \partial B_{R_i}$  where  $R_i \rightarrow \infty$ , then there is a subsequence with either  $\mathcal{S}_{ulsc} = \emptyset$  or  $\mathcal{S}_{neck} = \emptyset$ .

In view of Theorem 0.4 and the earlier results for disks, it is natural to first analyze sequences that are ULSC, so where  $\mathcal{S}_{neck} = \emptyset$ , and second analyze sequences where  $\mathcal{S}_{ulsc}$  is empty. We will do this next.

As already mentioned, our main theorems deal with sequences  $\Sigma_i \subset B_{R_i} = B_{R_i}(0) \subset \mathbf{R}^3$  of compact embedded minimal planar domains with  $\partial\Sigma_i \subset \partial B_{R_i}$  where  $R_i \rightarrow \infty$ . We will assume here that these planar domains are not disks (recall that the case of disks was dealt with in [CM3]–[CM6]). In particular, we will assume that for each  $i$ , there exists some  $y_i \in \mathbf{R}^3$  and  $s_i > 0$  so that

$$\text{some component of } B_{s_i}(y_i) \cap \Sigma_i \text{ is not a disk.} \quad (0.5)$$

Moreover, if the non-simply connected balls  $B_{s_i}(y_i)$  “run off to infinity” (i.e., if each connected component of  $B_{R'_i}(0) \cap \Sigma_i$  is a disk for some  $R'_i \rightarrow \infty$ ), then the results of [CM3]–[CM6] apply. Therefore, after passing to a subsequence, we can assume that the surfaces are uniformly not disks, namely, that there exists some  $R > 0$  so that (0.5) holds with  $s_i = R$  and  $y_i = 0$  for all  $i$ .

---

<sup>2</sup>The theorem holds also for sequences with fixed genus; see Section 1.

In general, we will allow our sequence of surfaces to have bounded genus. Recall that for a surface  $\Sigma$  with boundary  $\partial\Sigma$ , the *genus* of  $\Sigma$  is the genus of the closed surface  $\hat{\Sigma}$  obtained by adding a disk to each boundary circle. The genus of a union of disjoint surfaces is the sum of the genres. Therefore, a surface with boundary has nonnegative genus; the genus is zero if and only if it is a planar domain. For example, the disk and the annulus both have genus zero; on the other hand, a closed surface of genus  $g$  with any number of disks removed has genus  $g$ .

Common for both the ULSC case and the case where  $\mathcal{S}_{ulsc}$  is empty is that the limits are always laminations by flat parallel planes and the singular sets are always closed subsets contained in the union of the planes. This is the content of the next theorem:

**Theorem 0.6.** Let  $\Sigma_i \subset B_{R_i} = B_{R_i}(0) \subset \mathbf{R}^3$  be a sequence of compact embedded minimal planar domains<sup>3</sup> with  $\partial\Sigma_i \subset \partial B_{R_i}$  where  $R_i \rightarrow \infty$ . If

$$\sup_{B_1 \cap \Sigma_i} |A|^2 \rightarrow \infty, \quad (0.7)$$

then there exists a subsequence  $\Sigma_j$ , a lamination  $\mathcal{L} = \{x_3 = t\}_{t \in \mathcal{I}}$  of  $\mathbf{R}^3$  by parallel planes (where  $\mathcal{I} \subset \mathbf{R}$  is a closed set), and a closed nonempty set  $\mathcal{S}$  in the union of the leaves of  $\mathcal{L}$  such that after a rotation of  $\mathbf{R}^3$ :

- (A) For each  $1 > \alpha > 0$ ,  $\Sigma_j \setminus \mathcal{S}$  converges in the  $C^\alpha$ -topology to the lamination  $\mathcal{L} \setminus \mathcal{S}$ .
- (B)  $\sup_{B_r(x) \cap \Sigma_j} |A|^2 \rightarrow \infty$  as  $j \rightarrow \infty$  for all  $r > 0$  and  $x \in \mathcal{S}$ . (The curvatures blow up along  $\mathcal{S}$ .)

Before discussing the general ULSC case, it is useful to recall the case of disks. One consequence of [CM3]–[CM6] is that there are only two local models for ULSC sequences of embedded minimal surfaces. That is, locally in a ball in  $\mathbf{R}^3$ , one of following holds:

- The curvatures are bounded and the surfaces are locally graphs over a plane.
- The curvatures blow up and the surfaces are locally double spiral staircases.

Both of these cases are illustrated by taking a sequence of rescalings of the helicoid; the first case occurs away from the axis, while the second case occurs on the axis. Namely, recall that the helicoid is the minimal surface  $\Sigma$  in  $\mathbf{R}^3$  parametrized by

$$(s \cos t, s \sin t, t) \text{ where } s, t \in \mathbf{R}. \quad (0.8)$$

If we take a sequence  $\Sigma_i = a_i \Sigma$  of rescaled helicoids where  $a_i \rightarrow 0$ , then the curvature blows up along the vertical axis but is bounded away from this axis. Thus, we get that

- The intersection of the rescaled helicoids with a ball away from the vertical axis gives a collection of graphs over the plane  $\{x_3 = 0\}$ .
- The intersection of the rescaled helicoids with a ball centered on the vertical axis gives a double spiral staircase.

Loosely speaking, our next result shows that when the sequence is ULSC (but not simply connected), a subsequence converges to a foliation by parallel planes away from two lines  $\mathcal{S}_1$  and  $\mathcal{S}_2$ ; see Figure 3. The lines  $\mathcal{S}_1$  and  $\mathcal{S}_2$  are disjoint and orthogonal to the leaves of the foliation and the two lines are precisely the points where the curvature is blowing up. This is

---

<sup>3</sup>The theorem holds also for sequences with fixed genus; see Section 1.

similar to the case of disks, except that we get two singular curves for non-disks as opposed to just one singular curve for disks (the precise statement for disks is recalled in Part I).

**Theorem 0.9.** Let a sequence  $\Sigma_i$ , limit lamination  $\mathcal{L}$ , and singular set  $\mathcal{S}$  be as in Theorem 0.6.<sup>4</sup> Suppose that each  $\Sigma_i$  satisfies (0.5) with  $s_i = R > 1$  and  $y_i = 0$ . If every  $\Sigma_i$  is ULSC and

$$\sup_{B_1 \cap \Sigma_i} |A|^2 \rightarrow \infty, \quad (0.10)$$

then the limit lamination  $\mathcal{L}$  is the foliation  $\mathcal{F} = \{x_3 = t\}_t$  and the singular set  $\mathcal{S}$  is the union of two disjoint lines  $\mathcal{S}_1$  and  $\mathcal{S}_2$  such that:

- ( $C_{ulsc}$ ) Away from  $\mathcal{S}_1 \cup \mathcal{S}_2$ , each  $\Sigma_j$  consists of exactly two multi-valued graphs spiraling together. Near  $\mathcal{S}_1$  and  $\mathcal{S}_2$ , the pair of multi-valued graphs form double spiral staircases with opposite orientations at  $\mathcal{S}_1$  and  $\mathcal{S}_2$ . Thus, circling only  $\mathcal{S}_1$  or only  $\mathcal{S}_2$  results in going either up or down, while a path circling both  $\mathcal{S}_1$  and  $\mathcal{S}_2$  closes up (see Figure 6).
- ( $D_{ulsc}$ )  $\mathcal{S}_1$  and  $\mathcal{S}_2$  are orthogonal to the leaves of the foliation.

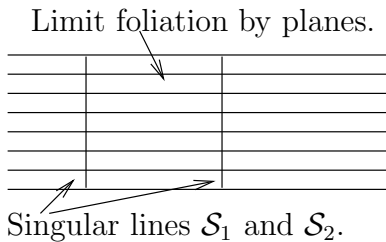


FIGURE 3. Theorem 0.9: Limits of sequences of non-simply connected, yet ULSC, surfaces with curvature blowing up. The singular set consists of two lines  $\mathcal{S}_1$  and  $\mathcal{S}_2$  and the limit is a foliation by flat parallel planes.

Notice that Theorem 0.9 shows that if the fixed genus ULSC surfaces  $\Sigma_j$  have curvature blowing up, then they essentially have genus zero. More precisely, given an arbitrarily large ball  $B_R \subset \mathbf{R}^3$ , then  $B_R \cap \Sigma_j$  has genus zero for  $j$  sufficiently large. To see this, combine the double spiral staircase structure near the two singular curves that holds for ULSC sequences (cf. Figure 6) with the smooth convergence elsewhere.

Despite the similarity of Theorem 0.9 to the case of disks, it is worth noting that the results for disks do not alone give this theorem. Namely, even though the ULSC sequence consists locally of disks, the compactness result for disks was in the global case where the radii go to infinity. One might wrongly think that Theorem 0.9 could be proven using the results for disks and a blow up argument. However, local examples constructed in [CM12]

<sup>4</sup>The theorem holds also for sequences with fixed genus with one minor change in the conclusion and one in the hypothesis. The change in the hypothesis is that we do not assume (0.5). The change in the conclusion is that there might be either one or two singular curves. The hypothesis (0.5) is used in the genus zero case to show that there cannot be just one singular curve. The reason that we will not assume (0.5) in the fixed genus case is that there can be either one or two singular curves in this case regardless; see Section 1.

shows the difficulty with such an argument.<sup>5</sup> We shall explain this further later together with what else is needed for the proof.

When the sequence is no longer ULSC, then there are other local models for the surfaces. The simplest example is a sequence of rescaled catenoids; the catenoid is the minimal surface in  $\mathbf{R}^3$  parametrized by

$$(\cosh s \cos t, \cosh s \sin t, s) \text{ where } s, t \in \mathbf{R}. \quad (0.11)$$

A sequence of rescaled catenoids converges with multiplicity two to the flat plane. The convergence is in the  $C^\infty$  topology except at 0 where  $|A|^2 \rightarrow \infty$ . This sequence of rescaled catenoids is not ULSC because the simple closed geodesic on the catenoid – i.e., the unit circle in the  $\{x_3 = 0\}$  plane – is non-contractible and the rescalings shrink it down to the origin.

One can get other types of curvature blow-up by considering the family of embedded minimal planar domains known as the Riemann examples.<sup>6</sup> Modulo translations and rotations, this is a two-parameter family of periodic minimal surfaces, where the parameters can be thought of as the size of the necks and the angle from one fundamental domain to the next. By choosing the two parameters appropriately, one can produce sequences of Riemann examples that illustrate both of the two structure theorems (cf. Figures 1 and 2):

- (1) If we take a sequence of Riemann examples where the neck size is fixed and the angles go to  $\frac{\pi}{2}$ , then the surfaces with angle near  $\frac{\pi}{2}$  can be obtained by gluing together two oppositely-oriented double spiral staircases. Each double spiral staircase looks like a helicoid. This sequence of Riemann examples converges to a foliation by parallel planes. The convergence is smooth away from the axes of the two helicoids (these two axes are the singular set  $\mathcal{S}$  where the curvature blows up). The sequence is ULSC since the size of the necks is fixed and thus illustrates the first structure theorem, Theorem 0.9.
- (2) If we take a sequence of examples where the neck sizes go to zero, then we get a sequence that is *not* ULSC. However, the surfaces can be cut along short curves into collections of graphical pairs of pants. The short curves converge to points and the graphical pieces converge to flat planes except at these points, illustrating the second structure theorem, Theorem 0.12 below.

With these examples in mind, we are now ready to state our second main structure theorem describing the case where  $\mathcal{S}_{ulsc}$  is empty.

---

<sup>5</sup>In [CM12], we constructed a sequence of embedded minimal disks  $\Sigma_i$  in the unit ball  $B_1$  with  $\partial\Sigma_i \subset \partial B_1$  where the curvatures blow up only at 0. This sequence converges to a lamination of  $B_1 \setminus \{0\}$  that cannot be extended smoothly to a lamination of  $B_1$ ; that is to say, 0 is not a removable singularity. This should be contrasted with Theorem 0.9 where every singular point is a removable singularity for the limit foliation by parallel planes.

<sup>6</sup>See <http://www.msri.org/publications/sgp/jim/geom/minimal/library/riemann/index.html> for a description, as well as computer graphics, of these surfaces.

**Theorem 0.12.** Let a sequence  $\Sigma_i$ , limit lamination  $\mathcal{L}$ , and singular set  $\mathcal{S}$  be as in Theorem 0.6.<sup>7</sup> If  $\mathcal{S}_{ulsc} = \emptyset$  and

$$\sup_{B_1 \cap \Sigma_i} |A|^2 \rightarrow \infty, \quad (0.13)$$

then  $\mathcal{S} = \mathcal{S}_{neck}$  by (0.3) and

( $C_{neck}$ ) Each point  $y$  in  $\mathcal{S}$  comes with a sequence of graphs in  $\Sigma_j$  that converge to the plane  $\{x_3 = x_3(y)\}$ . The convergence is in the  $C^\infty$  topology away from the point  $y$  and possibly also one other point in  $\{x_3 = x_3(y)\} \cap \mathcal{S}$ . If the convergence is away from one point, then these graphs are defined over annuli; if the convergence is away from two points, then the graphs are defined over disks with two subdisks removed.

Theorem 0.12, as well as Theorem 0.4, are proven by first analyzing sequences of minimal surfaces without any assumptions on the sets  $\mathcal{S}_{ulsc}$  and  $\mathcal{S}_{neck}$ . In this general case, we show that a subsequence converges to a lamination  $\mathcal{L}'$  divided into regions where Theorem 0.9 holds and regions where Theorem 0.12 holds. This convergence is in the smooth topology away from the singular set  $\mathcal{S}$  where the curvature blows up. Moreover, each point of  $\mathcal{S}$  comes with a plane and these planes are essentially contained in  $\mathcal{L}'$ ; see (P) below. The set of heights of the planes is a closed subset  $\mathcal{I} \subset \mathbf{R}$  but may not be all of  $\mathbf{R}$  as it was in Theorem 0.9 and may not even be connected. The behavior of the sequence is different at the two types of singular points in  $\mathcal{S}$  - the set  $\mathcal{S}_{neck}$  of “catenoid points” and the set  $\mathcal{S}_{ulsc}$  of ULSC singular points. We will see that  $\mathcal{S}_{ulsc}$  consists of a union of Lipschitz curves transverse to the lamination  $\mathcal{L}$ . This structure of  $\mathcal{S}_{ulsc}$  implies that the set of heights in  $\mathcal{I}$  which intersect  $\mathcal{S}_{ulsc}$  is a union of intervals; thus this part of the lamination is foliated. In contrast, we will not get any structure of the set of “catenoid points”  $\mathcal{S}_{neck}$ ; see (D) below. Given a point  $y$  in  $\mathcal{S}_{neck}$ , we will get a sequence of graphs in  $\Sigma_j$  converging to a plane through  $y$ ; see (C1) below. This convergence will be in the smooth topology away from either one or two singular points, one of which is  $y$ . Moreover, this limit plane through  $y$  will be a leaf of the lamination  $\mathcal{L}$ .

The precise statement of the compactness theorem for sequences that are neither necessarily ULSC nor with  $\mathcal{S}_{ulsc} = \emptyset$  is the following (see Figure 4):

**Theorem 0.14.** Let  $\Sigma_i \subset B_{R_i} = B_{R_i}(0) \subset \mathbf{R}^3$  be a sequence of compact embedded minimal planar domains<sup>8</sup> with  $\partial\Sigma_i \subset \partial B_{R_i}$  where  $R_i \rightarrow \infty$ . If

$$\sup_{B_1 \cap \Sigma_i} |A|^2 \rightarrow \infty, \quad (0.15)$$

then there is a subsequence  $\Sigma_j$ , a closed set  $\mathcal{S}$ , and a lamination  $\mathcal{L}'$  of  $\mathbf{R}^3 \setminus \mathcal{S}$  so that:

- (A) For each  $1 > \alpha > 0$ ,  $\Sigma_j \setminus \mathcal{S}$  converges in the  $C^\alpha$ -topology to the lamination  $\mathcal{L}'$ .
- (B)  $\sup_{B_r(x) \cap \Sigma_j} |A|^2 \rightarrow \infty$  as  $j \rightarrow \infty$  for all  $r > 0$  and  $x \in \mathcal{S}$ . (The curvatures blow up along  $\mathcal{S}$ .)
- (C1) ( $C_{neck}$ ) from Theorem 0.12 holds for each point  $y$  in  $\mathcal{S}_{neck}$ .
- (C2) ( $C_{ulsc}$ ) from Theorem 0.9 holds locally near  $\mathcal{S}_{ulsc}$ . More precisely, each point  $y$  in  $\mathcal{S}_{ulsc}$  comes with a sequence of multi-valued graphs in  $\Sigma_j$  that converge to the plane  $\{x_3 =$

<sup>7</sup>The theorem holds also for sequences with fixed genus with one small change in ( $C_{neck}$ ). Namely, the number of points in ( $C_{neck}$ ) is bounded by two plus the bound for the genus; see Section 1.

<sup>8</sup>The theorem holds also for sequences with fixed genus with one small change in ( $C_{neck}$ ). Namely, the number of points in ( $C_{neck}$ ) is bounded by two plus the bound for the genus; see Section 1.

$x_3(y)$ . The convergence is in the  $C^\infty$  topology away from the point  $y$  and possibly also one other point in  $\{x_3 = x_3(y)\} \cap \mathcal{S}_{ulsc}$ . These two possibilities correspond to the two types of multi-valued graphs defined in Section 2.

- (D) The set  $\mathcal{S}_{ulsc}$  is a union of Lipschitz curves transverse to the lamination. The leaves intersecting  $\mathcal{S}_{ulsc}$  are planes foliating an open subset of  $\mathbf{R}^3$  that does not intersect  $\mathcal{S}_{neck}$ . For the set  $\mathcal{S}_{neck}$ , we make no claim about the structure.
- (P) Together (C1) and (C2) give a sequence of graphs or multi-valued graphs converging to a plane through each point of  $\mathcal{S}$ . If  $P$  is one of these planes, then each leaf of  $\mathcal{L}'$  is either disjoint from  $P$  or is contained in  $P$ .

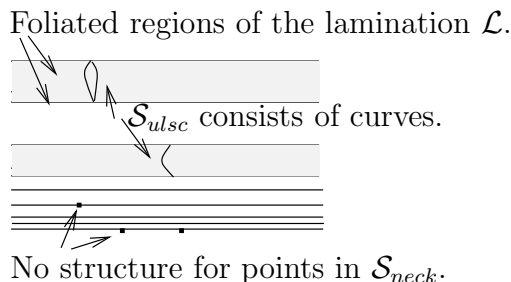


FIGURE 4. Theorem 0.14: Limits of sequences of non-ULSC surfaces with curvature blowing up. The limit is a lamination of  $\mathbf{R}^3 \setminus \mathcal{S}$ . The singular set  $\mathcal{S}$  consists of two types of points - the ones in  $\mathcal{S}_{neck}$  and the ones in  $\mathcal{S}_{ulsc}$ . Note that the set  $\mathcal{S}_{neck}$  is automatically closed, while the set  $\mathcal{S}_{ulsc}$  is not. The set  $\mathcal{S}_{ulsc}$  is a union of Lipschitz curves; the injectivity radius goes to zero at the endpoints of these curves, so these endpoints are in  $\mathcal{S}_{neck}$ . Finally, the part of the lamination containing  $\mathcal{S}_{ulsc}$  is foliated by planar leaves.

Note that Theorem 0.14 is a technical tool that will be used to prove the main compactness theorem in the non-ULSC case, Theorem 0.12. In particular, Theorem 0.14 itself will be superseded by the stronger compactness theorems in the ULSC and non-ULSC cases, Theorem 0.9 and Theorem 0.12. This is because eventually we will know by the no mixing theorem that either  $\mathcal{S}_{neck} = \emptyset$  or  $\mathcal{S}_{ulsc} = \emptyset$ , so that these cover all possible cases. Moreover, the assertions in Theorem 0.9 and Theorem 0.12 are stronger than those in Theorem 0.14.

After proving Theorem 0.14 in Part IV, we will be ready in Part V to prove the no mixing theorem, Theorem 0.4.

In Part VI, we will then complete the proof of Theorem 0.12. The main point left, which is not part of Theorem 0.14, is to prove that every leaf of the lamination  $\mathcal{L}$  in Theorem 0.12 is a plane. In contrast, Theorem 0.14 gives a plane through each point of  $\mathcal{S}_{neck}$ , but does not claim that the leaves of  $\mathcal{L}'$  are planar.

Finally, since the no mixing theorem implies that Theorem 0.9 and Theorem 0.12 cover all cases, Theorem 0.6 will be a corollary of these two theorems.

We refer to the introduction of [CM6] and the surveys [MeP], [P], and [Ro] for related results, including applications of the results of [CM3]–[CM6] as well as the results of this paper.

**0.1. Brief outline of the paper and overview of the proofs.** In Section 2, we will define the two notions of multi-valued graphs which will be needed to explain and prove the two main theorems.

Part I is devoted to recalling some of the earlier results for disks given in [CM3]–[CM6] and [CM9]. The first of these shows that embedded minimal disks are either graphs or are part of a double spiral staircase. The second result that we recall is the one-sided curvature estimate. Finally, we will recall the chord-arc bound for embedded minimal disks proven in [CM9].

In Part II, we will first define the singular set  $\mathcal{S}$  and prove the convergence to the lamination  $\mathcal{L}'$  away from  $\mathcal{S}$ . The rest of the part focuses on describing a neighborhood of each point in the ULSC singular set  $\mathcal{S}_{ulsc}$  and the leaves of  $\mathcal{L}'$  whose closure intersects  $\mathcal{S}_{ulsc}$ . A key point will be that the results of [CM3]–[CM6] for disks will give a sequence of multi-valued graphs in the  $\Sigma_j$ 's near each point  $x \in \mathcal{S}_{ulsc}$ . Moreover, these multi-valued graphs close up in the limit to give a leaf of  $\mathcal{L}'$  which extends smoothly across  $x$ . Such a leaf is said to be collapsed; in a neighborhood of  $x$ , the leaf can be thought of as a limit of double-valued graphs where the upper sheet collapses onto the lower. We will show that every collapsed leaf is stable, has at most two points of  $\mathcal{S}_{ulsc}$  in its closure, and these points are removable singularities. These results on collapsed leaves will be applied first in the USLC case in the next part and then later to get the structure of the ULSC regions of the limit in general, i.e., (C2) and (D) in Theorem 0.14.

In Part III, we prove Theorem 0.9 that gives the convergence of a ULSC sequence to a foliation by parallel planes away from two singular curves. Roughly speaking, there are two main steps to the proof:

- (1) Show that each collapsed leaf is in fact a plane punctured at two points of  $\mathcal{S}$  and, moreover, the sequence has the structure of a double spiral staircase near both of these points, with opposite orientations at the two points.
- (2) Show that leaves which are nearby a collapsed leaf of  $\mathcal{L}'$  are also planes punctured at two points of  $\mathcal{S}$ . (We call this “properness”.)

In Part IV we consider general sequences of minimal surfaces that are neither necessarily ULSC nor with  $\mathcal{S}_{ulsc} = \emptyset$  and we prove the general compactness theorem, Theorem 0.14. Recall that this theorem asserts that the limit lamination  $\mathcal{L}'$  can be divided into two disjoint sub-laminations. One of which is the support of a region where (a subsequence of) the surfaces are ULSC and all of the results about ULSC sequences from Part III hold, such as the structure of the singular set and the multi-valued graphs structure. In the other region, curvature blow up comes exclusively from neck pinching and, thus, in this region there are no helicoid like points. The key steps for proving the general structure theorem are the following:

- (1) Finding a stable plane through each point of  $\mathcal{S}_{neck}$ . This plane will be a limit of a sequence of stable graphical annuli that lie in the complement of the surfaces.
- (2) Finding graphs in  $\Sigma_j$  that converge to a plane through each point of  $\mathcal{S}_{neck}$ . To do this, we look in regions between consecutive necks and show that in any such region the surfaces are ULSC. The one-sided curvature estimate will then allow us to show that these regions are graphical.

- (3) Using (1) and (2) we then analyze the ULSC regions of a limit. That is, we show that if the closure of a leaf in  $\mathcal{L}'$  intersects  $\mathcal{S}_{ulsc}$ , then it has a neighborhood that is ULSC. This will allow us to use the argument for the proof of Theorem 0.9 to get the same structure for such a neighborhood as we did in case where the entire surfaces where ULSC.

In Part V, we will use the structure obtained in Theorem 0.14 to show the no mixing theorem; Theorem 0.4. The key here is to show that if  $\mathcal{S}_{ulsc}$  is non-empty, then  $\mathcal{S}_{ulsc}$  cannot stop.

In Part VI, we will complete the proofs of Theorem 0.6 and Theorem 0.12. The only thing that remains to be proven is that every leaf of the lamination  $\mathcal{L}'$  is contained in a plane. We have already proven that the leaves of  $\mathcal{L}'$  are planes when the sequence is ULSC; thus, by the no mixing theorem, the only remaining case is when  $\mathcal{S} = \mathcal{S}_{neck} \neq \emptyset$ . We will divide the proof that the leaves of  $\mathcal{L}'$  are contained in planes into two cases, depending on whether or not the leaf is complete. In both cases, we will use a flux argument to rule out a non-flat leaf of  $\mathcal{L}'$ .

## 1. WHEN THE SEQUENCE HAS POSITIVE GENUS: THEOREMS AND OUTLINES OF PROOFS

As we noted earlier, the main theorems were stated for sequences of planar domains, i.e., for genus zero. In this section, we will give the versions of these theorems for sequences with bounded genus and describe the necessary modifications for the proofs. The main change in the theorems is a change in the definitions of the singular sets  $\mathcal{S}_{neck}$  and  $\mathcal{S}_{ulsc}$ . The new definitions of  $\mathcal{S}_{neck}$  and  $\mathcal{S}_{ulsc}$ , as well as an example showing why a change is necessary, can be found in Subsection 1.1.

The general case of bounded genus can be divided into two subcases, depending on whether or not the genus concentrates at a point. An easy argument will show that the genus can concentrate at only finitely many points, so the most important subcase is when the sequence is *uniformly locally genus zero*. In the uniformly locally genus zero case, we do not need to change the definitions of  $\mathcal{S}_{neck}$  and  $\mathcal{S}_{ulsc}$  and the proofs go through with minor changes. The only change in the statement of the main theorems is in  $(C_{neck})$ : the number of punctures is now bounded by the genus plus two.

A reader interested only in the uniformly locally genus zero case can jump directly to Subsection 1.4.

**1.1. The sets  $\mathcal{S}_{neck}$  and  $\mathcal{S}_{ulsc}$  in the general case of fixed genus.** Before giving the new definitions of  $\mathcal{S}_{neck}$  and  $\mathcal{S}_{ulsc}$ , we will give an example illustrating why we have to change the definitions in the general case where the genus can concentrate. Namely, let the sequence  $\Sigma_j$  be a sequence of rescalings (“blow downs”) of the genus one helicoid constructed in [HoWeWo]. Since the genus one helicoid is asymptotic to the standard helicoid, the  $\Sigma_j$ ’s converge to a foliation by horizontal planes away from the vertical axis. However, the vertical axis contains both the origin where the injectivity radius goes to zero - since the genus concentrates there - and uniformly locally simply connected points. This was impossible in the case of genus zero because of the no mixing theorem.

This example of rescalings of the genus one helicoid illustrates that even if the injectivity radius goes to zero at a point, the point still might not belong in  $\mathcal{S}_{neck}$ . It is then reasonable to ask what it was about the injectivity radius going to zero that was useful in the genus zero

case. The answer is that this allowed one to use a barrier argument near a point  $y \in \mathcal{S}_{neck}$  to find stable graphs disjoint from the  $\Sigma_j$ 's that converge to a punctured plane through  $y$ . This motivates the following re-definition of  $\mathcal{S}_{ulsc}$  and  $\mathcal{S}_{neck}$ :

- A point  $y$  in  $\mathcal{S}$  is in  $\mathcal{S}_{ulsc}$  if there exist  $r_y > 0$  and a sequence  $r_{y,j} \rightarrow 0$  so that every component of  $B_{r_y}(y) \cap \Sigma_j$  has connected boundary and

$$B_{r_y}(y) \cap \Sigma_j \text{ and } B_{r_{y,j}}(y) \cap \Sigma_j \text{ have the same genus.} \quad (1.1)$$

- A point  $y$  in  $\mathcal{S}$  is in  $\mathcal{S}_{neck}$  if there exist  $r_y > 0$  and a sequence  $r_{y,j} \rightarrow 0$  so that some component of  $B_{r_{y,j}}(y) \cap \Sigma_j$  has dis-connected boundary and (1.1) holds.

Note that these definitions agree with the earlier ones when the sequence is uniformly locally genus zero, i.e., when the genus of  $B_{r_y}(y) \cap \Sigma_j$  is zero for every  $j$ . In particular, these definitions agree with the earlier ones when the sequence  $\Sigma_j$  has genus zero.

The sets  $\mathcal{S}_{neck}$  and  $\mathcal{S}_{ulsc}$  are obviously disjoint subsets of  $\mathcal{S}$ . It follows from proposition I.0.19 in [CM5] that, after passing to a subsequence, we can assume that

$$\mathcal{S} = \mathcal{S}_{neck} \cup \mathcal{S}_{ulsc}. \quad (1.2)$$

**1.2. The statements of the theorems in the general case of fixed genus.** Theorem 0.4 and Theorem 0.6 both apply verbatim to the general case of bounded genus with the new definitions of  $\mathcal{S}_{ulsc}$  and  $\mathcal{S}_{neck}$ .

On the other hand, Theorem 0.9 holds also for sequences with fixed genus with one minor change in the conclusion and one in the hypothesis. The change in the hypothesis is that we do not assume (0.5). The change in the conclusion is that there might be either one or two singular curves. The assumption (0.5), which says that the  $\Sigma_j$ 's are "uniformly not-disks", was used in the genus zero case to rule out the possibility of just one singular curve (as occurs both for sequences of disks and for rescalings of the genus one helicoid). However, we cannot rule out the possibility of just one singular curve in the fixed genus case regardless of whether we assume (0.5). For this reason, we will not assume (0.5) and we will allow for the possibility of just one singular curve.

Similarly, Theorem 0.12 and Theorem 0.14 require one small change in  $(C_{neck})$ . Recall that for each point  $y$  in  $\mathcal{S}_{neck}$ ,  $(C_{neck})$  gives a sequence of graphs in the  $\Sigma_j$ 's that converges to a plane through  $y$  away from a finite set of punctures. In the genus zero case, the number of punctures was at most two; in the higher genus case, the number of punctures is merely bounded by two plus the genus.

*The next two subsections will be devoted to sketching the modifications needed to prove the main theorems in the general case of bounded genus. However, we suggest that in the first reading the reader jump directly to Section 2 and then go through the rest of the paper in order to complete the proofs in the case of genus zero. Then, after completing the genus zero case in the first reading, it makes sense to return to the next two subsections for the case of bounded genus.*

**1.3. The local structure near points in  $\mathcal{S}_{ulsc}$  and  $\mathcal{S}_{neck}$ .** The starting point for understanding the sequence  $\Sigma_j$  is to describe the sequence in a neighborhood of each singular point, depending on whether the point is in  $\mathcal{S}_{ulsc}$  or  $\mathcal{S}_{neck}$ . Roughly speaking, we will get the same picture as in the case of planar domains. The precise statements are:

- ( $\alpha$ ) Given a point  $x$  in  $\mathcal{S}_{ulsc}$ , there is a ball  $B_r(x)$  and a sequence of multi-valued graphs in the  $\Sigma_j$ 's that “collapses” to a punctured graph in  $B_r(x)$  with a removable singularity at  $x$ .
- ( $\beta$ ) Given a point  $x$  in  $\mathcal{S}_{neck}$ , there is a ball  $B_r(x)$  and a sequence of graphs in the  $\Sigma_j$ 's that converges (with multiplicity) to a finitely punctured graph in  $B_r(x)$  with a removable singularity at  $x$ .

Sketch of proof of ( $\alpha$ ) and ( $\beta$ ): The structure ( $\alpha$ ) near a point in  $\mathcal{S}_{ulsc}$  follows from the results of [CM3]–[CM6] just as in the genus zero case; see Lemma II.2.3 in particular. This is because the arguments of [CM3]–[CM6] for disks generalize to surfaces with bounded genus and one end; in fact, many of these results were stated in that generality (see, e.g., theorem 1.22 in [CM4]).

Similarly, the structure ( $\beta$ ) near a point in  $\mathcal{S}_{neck}$  follows from a local version of the results of Section IV.1 for the genus zero case. There is only one minor difference:

- When we apply Proposition IV.1.1 to get the sequence of stable barriers, the outer radii of the extrinsic balls remains bounded. Hence, the limiting stable graph is defined over a disk and not the entire plane.

In particular, we cannot (yet) conclude that we get a plane through each singular point. This difference does not affect the arguments in Section IV.1 to get the sequence of local graphs mentioned above.

**1.4. The modifications in the proofs for positive genus.** In this subsection, we will explain how to extend the proofs of the main theorems to the general case of fixed genus. Many aspects of the proofs in the genus zero case were essentially local and will, therefore, extend easily now that we have the local structure near  $\mathcal{S}_{neck}$  and  $\mathcal{S}_{ulsc}$ . However, there are some global aspects to the proofs and these will require some work. The two main global facts are the existence of planes through each singular point and the flatness of nearby leaves (which we often call “properness”).

As in the genus zero case, a key point will be to prove that there is a limit plane through each point in the singular set  $\mathcal{S}$ . These planes were actually (the closure of) leaves of  $\mathcal{L}'$  when the sequence was ULSC, but this was not the case in general. However, these planes were always given as smooth limits of subsets of the  $\Sigma_j$ 's; cf. ( $C_{neck}$ ) in Theorem 0.12. This is the motivation for the following definition:

**Definition 1.3.** Let  $\Sigma_j$  be a sequence of surfaces with limit lamination  $\mathcal{L}'$  and singular set  $\mathcal{S}$ . We will say that a surface  $\Gamma$  is a *pseudo-leaf* of  $\mathcal{L}'$  if it is connected and there is a sequence of subsets  $\Sigma_j^I \subset \Sigma_j$  that converges smoothly to  $\Gamma$ . We will also require that  $\Gamma$  is maximal with respect to these properties, so that  $\Gamma$  is not a proper subset of a connected surface that is also a limit of subsets of the  $\Sigma_j$ 's.

Here “converges” means that for each open subset  $\Gamma_c \subset \Gamma$  with compact closure in  $\Gamma$ , then the  $\Sigma_j$ 's contain a sequence of graphs - or multi-valued graphs - over  $\Gamma_c$  and these converge smoothly to  $\Gamma_c$ . If we get multi-valued graphs, then we require that the number of sheets goes to infinity as  $j$  goes to infinity.

Note that every leaf of  $\mathcal{L}'$  is also a pseudo-leaf. We have already come across pseudo-leaves that may not be leaves. Namely, ( $C_{neck}$ ) in Theorem 0.12 implies that, for each point  $x$  in

$\mathcal{S}_{neck}$ , we get a flat pseudo-leaf whose closure is a plane through  $x$ . This pseudo-leaf is a plane punctured at  $x$  and possibly at one other point.

One useful property of a pseudo-leaf is that none of the leaves of  $\mathcal{L}'$  can intersect a pseudo-leaf transversely. It then follows from the local structure of nodal sets that the leaves of  $\mathcal{L}'$  cannot cross a pseudo-leaf.

We will need the following local property of pseudo-leaves which shows that they have isolated singularities:

**Lemma 1.4.** Suppose that  $x \in \mathcal{S}$  and  $B_r(x)$  is the ball given by  $(\alpha)$  or  $(\beta)$ , so that we get a punctured graph  $\Gamma_{x,r} \subset B_r(x)$  “through”  $x$  that is contained in a pseudo-leaf for  $\mathcal{L}'$ .

Inside the ball  $B_r(x)$ , every other pseudo-leaf of  $\mathcal{L}'$  sits on side of  $\Gamma_{x,r}$  and is complete away from an isolated set of points in  $\mathcal{S}$ .

*Proof.* (Sketch). Property (1) in Proposition II.3.1 proves the lemma when  $x$  is in  $\mathcal{S}_{ulsc}$  and the sequence has genus zero. The arguments there can be easily extended to the higher genus case. On the other hand, when  $x$  is in  $\mathcal{S}_{neck}$ , property (2) follows from a local version of Lemma VI.3.3.  $\square$

*From now on, we will assume that every pseudo-leaf is oriented. This slightly simplifies some of the arguments below involving stability. As we have seen several times, the unoriented case can be dealt with by going to a double cover. We will leave the easy modifications needed for this case to the reader.*

The key point for generalizing the main theorems from genus zero to fixed genus is to show that:

**Proposition 1.5.** For each point  $x \in \mathcal{S}$ , we get a flat pseudo-leaf whose closure is a plane through  $x$ . This pseudo-leaf is a plane punctured at a discrete set of points of  $\mathcal{S}$ .

We will need one more definition before proving Proposition 1.5. Recall that when we studied the leaves of  $\mathcal{L}'$ , we began with the collapsed leaves, i.e., the ones “through” a point in  $\mathcal{S}_{ulsc}$ . The collapsed leaves were shown to be stable and to have removable singularities at points in  $\mathcal{S}_{neck}$ . With this in mind, we will say that a pseudo-leaf  $\Gamma$  is *pinched* if it goes “through” a point in  $\mathcal{S}$ . There are two local models for the  $\Sigma_j$ ’s near a point  $x$  in  $\mathcal{S}$ , depending on whether  $x \in \mathcal{S}_{ulsc}$  or  $x \in \mathcal{S}_{neck}$ . First, if  $x \in \mathcal{S}_{ulsc}$ , then we know that there is a collapsed leaf of  $\mathcal{L}'$  through  $x$ ; see  $(\alpha)$ . Second, if  $x \in \mathcal{S}_{neck}$ , then it follows from the local version of  $(C_{neck})$  in Theorem 0.12 that there is a pinched pseudo-leaf through  $x$ ; see  $(\beta)$ .

*Proof.* (Sketch of proof of Proposition 1.5). Suppose that  $x \in \mathcal{S}$ . As mentioned above,  $x$  is in the closure of the pseudo-leaf  $\Gamma_x$  and there exists  $r_x > 0$  so that the component  $\Gamma_{x,r_x}$  of

$$B_{r_x}(x) \cap (\Gamma_x \cup \{x\}) \tag{1.6}$$

containing  $x$  is a smooth minimal graph, possibly with one point removed.

The lemma follows from the following steps:

- (1)  $\Gamma_x$  is stable: The local structure near points of  $\mathcal{S}_{neck}$  and  $\mathcal{S}_{ulsc}$  shows that  $\Gamma_{x,r_x}$  is either a limit of graphs with multiplicity or a limit of multi-valued graphs. Since every pseudo-leaf has isolated singularities by Lemma 1.4, it follows that the entire pseudo-leaf  $\Gamma_x$  is a limit with multiplicity (at least away from an isolated set of points). Therefore, we conclude that  $\Gamma_x$  is stable away from a finite set of points.

Note that in the case of multi-valued graphs, we need to appeal to Appendix B to get stability.

- (2)  $\Gamma_x$  is complete away from removable singularities: Note that  $\Gamma_x$  fails to be complete whenever we have a singular point  $y \in \mathcal{S}$  that is in the closure  $(\Gamma_x)_{Clos}$  of  $\Gamma_x$ . Suppose that  $y$  is such a point. We know that there is a pseudo-leaf with a removable singularity at  $y$ , namely  $\Gamma_y$ . The key point is that any component of  $\Gamma_x$  in  $B_{r_y}(y)$  with  $y$  in its closure is stable and complete away from  $y$  and, hence, has a removable singularity at  $y$  by a slight variation on Lemma B.26 in Appendix B.
- (3)  $\Gamma_x$  is flat: Combining these two facts and using a standard logarithmic cutoff function argument implies that the closure of  $\Gamma_x$  is a complete stable surface. Hence, the Bernstein theorem for stable surfaces implies that it is flat, completing the proof. □

We will next explain how to extend the main theorems to the general case of fixed genus. The main point is that once we have the planes through each singular point from Proposition 1.5, most of the arguments used for the main theorems are essentially local and, hence, carry over to the higher genus case. However, there is one key exception: the fact that all of the leaves of  $\mathcal{L}'$  are flat is unavoidably global; see Theorem 0.6. The fact that this is global is illustrated by the local examples constructed in [CM12]. This flatness of all of the leaves follows from three separate lemmas, all of which use global flux arguments to rule out a non-flat leaf.

The first global flux argument is the proof of “properness” in Lemma III.1.4, where we show that the set of flat leaves is an open subset of the ULSC part of the lamination (see  $(D_{ulsc})$ ). We indicate how to extend Lemma III.1.4 to the fixed genus case in Section III.3. In the proof of Lemma III.1.4, “genus zero” was used to conclude that some curves that were constructed in the  $\Sigma_j$ ’s must in fact divide in  $\Sigma_j$ . The key point is that the infinite multiplicity of the multi-valued graphs converging to a collapsed leaf means that there is an arbitrarily large number of disjoint curves to choose from. However, an elementary topological argument (see Lemma III.3.1) implies that only a bounded number of these can fail to divide in the  $\Sigma_j$ ’s.

Once we have extended  $(D_{ulsc})$  to the fixed genus case, the no-mixing theorem follows as well. We may therefore assume that  $\mathcal{S} = \mathcal{S}_{neck}$  from now on.

The other two global flux arguments are used to show that the leaves are flat in the non-ULSC case, i.e., when  $\mathcal{S} = \mathcal{S}_{neck}$ . This is divided into two cases, depending on whether or not the leaf is complete. The complete leaves were shown to be flat in Lemma VI.2.1 and the in-complete leaves were handled in Lemma VI.3.1. The flux arguments in these lemmas can also be extended to the fixed genus case using the same elementary topological argument as for Lemma III.1.4 (cf. Section III.3).

## 2. MULTI-VALUED GRAPHS

To explain the theorems stated in the introduction and their proofs, we will need two notions of multi-valued graphs - namely, the one used in [CM3]–[CM6] and a generalization.

In [CM3]–[CM6], we defined multi-valued graphs as multi-sheeted covers of the punctured plane. To be precise, let  $D_r$  be the disk in the plane centered at the origin and of radius  $r$  and let  $\mathcal{P}$  be the universal cover of the punctured plane  $\mathbf{C} \setminus \{0\}$  with global polar coordinates

$(\rho, \theta)$  so  $\rho > 0$  and  $\theta \in \mathbf{R}$ . Given  $0 \leq r \leq s$  and  $\theta_1 \leq \theta_2$ , define the “rectangle”  $S_{r,s}^{\theta_1, \theta_2} \subset \mathcal{P}$  by

$$S_{r,s}^{\theta_1, \theta_2} = \{(\rho, \theta) \mid r \leq \rho \leq s, \theta_1 \leq \theta \leq \theta_2\}. \quad (2.1)$$

An  $N$ -valued graph of a function  $u$  on the annulus  $D_s \setminus D_r$  is a single valued graph over (see Figure 5)

$$S_{r,s}^{-N\pi, N\pi} = \{(\rho, \theta) \mid r \leq \rho \leq s, |\theta| \leq N\pi\}. \quad (2.2)$$

( $\Sigma_{r,s}^{\theta_1, \theta_2}$  will denote the subgraph of  $\Sigma$  over the smaller rectangle  $S_{r,s}^{\theta_1, \theta_2}$ ). As in the earlier papers in the series, the multi-valued graphs that we will consider will never close up; in fact they will all be embedded. Note that embedded corresponds to that the separation never vanishes. Here the separation  $w$  is the difference in height between consecutive sheets and is therefore given by

$$w(\rho, \theta) = u(\rho, \theta + 2\pi) - u(\rho, \theta). \quad (2.3)$$

In the case where  $\Sigma$  is the helicoid [i.e.,  $\Sigma$  can be parametrized by  $(s \cos t, s \sin t, t)$  where  $s, t \in \mathbf{R}$ ], then

$$\Sigma \setminus x_3 - \text{axis} = \Sigma_1 \cup \Sigma_2, \quad (2.4)$$

where  $\Sigma_1, \Sigma_2$  are  $\infty$ -valued graphs.  $\Sigma_1$  is the graph of the function  $u_1(\rho, \theta) = \theta$  and  $\Sigma_2$  is the graph of the function  $u_2(\rho, \theta) = \theta + \pi$ . In either case the separation  $w = 2\pi$ .

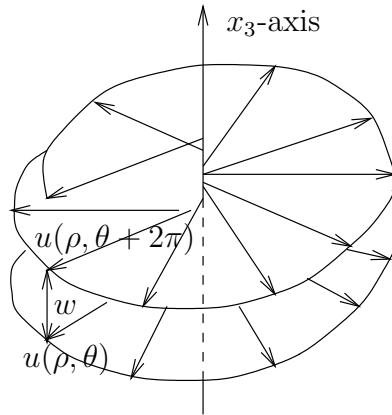


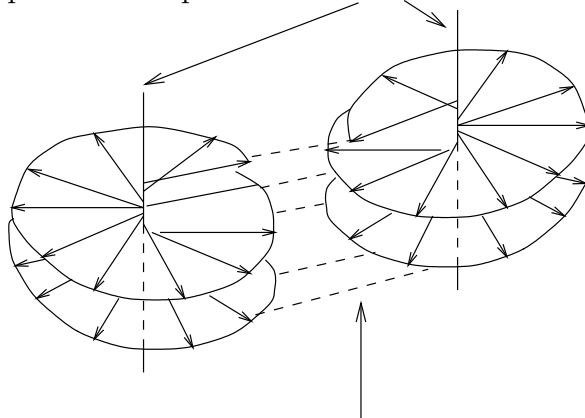
FIGURE 5. A multi-valued graph over the singly-punctured plane.

Locally, the above multi-valued graphs give the complete picture for a ULSC sequence. However, the global picture can consist of several different multi-valued graphs glued together. To allow for this, we are forced to consider multi-valued graphs defined over the universal cover of  $\mathbf{C} \setminus P$  where  $P$  is a discrete subset of the complex plane  $\mathbf{C}$  (see Figure 6). We will see that the bound on the genus implies that  $P$  consists of at most two points. The basic example of such a multi-valued graph comes from the family of minimal surfaces known as the Riemann examples.

### Part I. Results for disks from [CM3]–[CM6]

The results for non-simply connected minimal surfaces that are proven in this paper rely on the earlier results for disks given in [CM3]–[CM6]. For completeness and easy reference, we start by recalling those.

Locally graphical except over two points;  
those points correspond to the two axes.



The spiral staircases around each of the axes connect to each other between the axes.

FIGURE 6. A multi-valued graph over the doubly-punctured plane. The spiral staircases near each puncture are oppositely-oriented.

### I.1. THE LAMINATION THEOREM AND ONE-SIDED CURVATURE ESTIMATE

The first theorem that we recall shows that embedded minimal disks are either graphs or are part of double spiral staircases; moreover, a sequence of such disks with curvature blowing up converges to a foliation by parallel planes away from a singular curve  $\mathcal{S}$ . This theorem is modelled on rescalings of the helicoid and the precise statement is as follows (we state the version for extrinsic balls; it was extended to intrinsic balls in [CM9]):

**Theorem I.1.1.** (Theorem 0.1 in [CM6].) Let  $\Sigma_i \subset B_{R_i} = B_{R_i}(0) \subset \mathbf{R}^3$  be a sequence of embedded minimal disks with  $\partial\Sigma_i \subset \partial B_{R_i}$  where  $R_i \rightarrow \infty$ . If

$$\sup_{B_1 \cap \Sigma_i} |A|^2 \rightarrow \infty, \tag{I.1.2}$$

then there exists a subsequence,  $\Sigma_j$ , and a Lipschitz curve  $\mathcal{S} : \mathbf{R} \rightarrow \mathbf{R}^3$  such that after a rotation of  $\mathbf{R}^3$ :

1.  $x_3(\mathcal{S}(t)) = t$ . (That is,  $\mathcal{S}$  is a graph over the  $x_3$ -axis.)
2. Each  $\Sigma_j$  consists of exactly two multi-valued graphs away from  $\mathcal{S}$  (which spiral together).
3. For each  $1 > \alpha > 0$ ,  $\Sigma_j \setminus \mathcal{S}$  converges in the  $C^\alpha$ -topology to the foliation,  $\mathcal{F} = \{x_3 = t\}_t$ , of  $\mathbf{R}^3$ .
4.  $\sup_{B_r(\mathcal{S}(t)) \cap \Sigma_j} |A|^2 \rightarrow \infty$  for all  $r > 0$ ,  $t \in \mathbf{R}$ . (The curvatures blow up along  $\mathcal{S}$ .)

The second theorem that we need to recall asserts that every embedded minimal disk lying above a plane, and coming close to the plane near the origin, is a graph. Precisely this is the *intrinsic one-sided curvature estimate* which follows by combining [CM6] and [CM9]:

**Theorem I.1.3.** There exists  $\epsilon > 0$ , so that if

$$\Sigma \subset \{x_3 > 0\} \subset \mathbf{R}^3 \tag{I.1.4}$$

is an embedded minimal disk with  $\mathcal{B}_{2R}(x) \subset \Sigma \setminus \partial\Sigma$  and  $|x| < \epsilon R$ , then

$$\sup_{\mathcal{B}_R(x)} |A_\Sigma|^2 \leq R^{-2}. \quad (\text{I.1.5})$$

Theorem I.1.3 is in part used to prove the regularity of the singular set where the curvature is blowing up.

Note that the assumption in Theorem I.1.1 that the surfaces are disks is crucial and cannot even be replaced by assuming that the sequence is ULSC. To see this, observe that one can choose a one-parameter family of Riemann examples which is ULSC but where the singular set  $\mathcal{S}$  is given by a pair of vertical lines. Likewise, the assumption in Theorem I.1.3 that  $\Sigma$  is simply connected is crucial as can be seen from the example of a rescaled catenoid, see (0.11). Under rescalings the catenoid converges (with multiplicity two) to the flat plane. Thus a neighborhood of the neck can be scaled arbitrarily close to a plane but the curvature along the neck becomes unbounded as it gets closer to the plane. Likewise, by considering the universal cover of the catenoid, one sees that embedded, and not just immersed, is needed in Theorem I.1.3.

Finally, we recall the chord-arc bound for embedded minimal disks proven in theorem 0.5 of [CM9]:

**Theorem I.1.6.** [CM9]. There exists a constant  $C > 0$  so that if  $\Sigma \subset \mathbf{R}^3$  is an embedded minimal disk,  $\mathcal{B}_{2R} = \mathcal{B}_{2R}(0)$  is an intrinsic ball in  $\Sigma \setminus \partial\Sigma$  of radius  $2R$ , and  $\sup_{\mathcal{B}_{r_0}} |A|^2 > r_0^{-2}$  where  $R > r_0$ , then for  $x \in \mathcal{B}_R$  the intrinsic distance is bounded from above by the extrinsic distance as follows

$$C \operatorname{dist}_\Sigma(x, 0) < |x| + r_0. \quad (\text{I.1.7})$$

## Part II. The singular set $\mathcal{S}$ and limit lamination $\mathcal{L}'$

The three main results of this part are the convergence to the lamination  $\mathcal{L}'$  away from a singular set  $\mathcal{S}$ , the description of a neighborhood of each ULSC singular point, and the description of the leaves of  $\mathcal{L}'$  whose closure intersects  $\mathcal{S}_{ulsc}$ . We will explain these in a bit more detail next.

We start by defining the singular set  $\mathcal{S}$ ; roughly speaking,  $\mathcal{S}$  is the set of points where the curvature blows up (see Definition/Lemma II.1.1). The definition of  $\mathcal{S}$  will immediately imply that  $\mathcal{S}$  is a closed subset of  $\mathbf{R}^3$ . We next show that in the open subset  $\mathbf{R}^3 \setminus \mathcal{S}$ , a subsequence of the sequence of embedded minimal surfaces converges to a minimal lamination  $\mathcal{L}'$  of  $\mathbf{R}^3 \setminus \mathcal{S}$  (see Lemma II.1.2).

The results of [CM3]–[CM6] give a precise description of a neighborhood of each point in  $\mathcal{S}_{ulsc}$ . Namely, for  $j$  large,  $\Sigma_j$  must be a double-spiral staircase near each point in  $\mathcal{S}_{ulsc}$  and the set  $\mathcal{S}_{ulsc}$  must satisfy a local cone property which gives the regularity of the set. The description near a singular point and local cone property are given in Lemma II.2.3. We also recall in Lemma II.2.3 that, as  $j \rightarrow \infty$ , this sequence of double-spiral staircases near a singular point  $x$  closes up in the limit to give a leaf of  $\mathcal{L}'$  which extends smoothly across  $x$ . We will say that such a leaf is collapsed; in a neighborhood of  $x$ , the leaf can be thought of as a limit of double-valued graphs where the upper sheet collapses onto the lower.

Finally, we will show that every collapsed leaf is stable, has at most two points of  $\mathcal{S}_{ulsc}$  in its closure, and these points are removable singularities. The key for proving stability is to

use the separations of the limiting multi-valued graphs to construct a positive Jacobi field in the limit. The limit Jacobi field is not a priori well-defined, but is instead well-defined on a covering space of the collapsed leaf. However, we show in Appendix B that stability of a covering space implies stability of the surface itself as long as the covering space has sub-exponential area growth. We apply this to show that every collapsed leaf is stable. We will also use the fact that the surfaces  $\Sigma_j$  have bounded genus, to show that each collapsed leaf has at most two points of  $\mathcal{S}_{ulsc}$  in its closure.

These results on collapsed leaves will be applied first in the USLC case in the next part and then later to get the structure of the ULSC regions of the limit in general, i.e., (C2) and (D) in Theorem 0.14.

## II.1. THE SINGULAR SET $\mathcal{S}$

To define the singular set, recall from [CM6] that for any sequence of surfaces (minimal or not) in  $\mathbf{R}^3$ , after possibly going to a subsequence, then there is a well defined notion of points in  $\mathbf{R}^3$  where the second fundamental form of the sequence blows up. The set of such points will below be referred to as the singular set  $\mathcal{S}$  and is given by an elementary and straight-forward compactness argument.

**Definition/Lemma II.1.1.** (The singular set; Lemma I.1.4 in [CM6].) Let  $\Sigma_i \subset B_{R_i}$  with  $\partial\Sigma_i \subset \partial B_{R_i}$  and  $R_i \rightarrow \infty$  be a sequence of (smooth) compact surfaces. After passing to a subsequence,  $\Sigma_j$ , we may assume that for each  $x \in \mathbf{R}^3$  either of the two following properties holds:

- $\sup_{B_r(x) \cap \Sigma_j} |A|^2 \rightarrow \infty$  for all  $r > 0$ . (The set of such points  $x$  will be denoted by  $\mathcal{S}$ .)
- $\sup_j \sup_{B_r(x) \cap \Sigma_j} |A|^2 < \infty$  for some  $r > 0$ .

**II.1.1. Convergence away from  $\mathcal{S}$ .** The first result that we will need is that in the open subset  $\mathbf{R}^3 \setminus \mathcal{S}$ , a sequence of embedded minimal surfaces has a subsequence that converges to a minimal lamination  $\mathcal{L}'$  of  $\mathbf{R}^3 \setminus \mathcal{S}$ . This is an easy consequence of that the curvature is bounded on compact sets in the complement of  $\mathcal{S}$  and is proven in the next lemma.

**Lemma II.1.2.** Suppose that  $\Sigma_j$  and  $\mathcal{S}$  are as in Lemma II.1.1. If in addition the  $\Sigma_j$ 's are minimal and embedded, then there exists a subsequence (still denoted by  $\Sigma_j$ ) and a lamination  $\mathcal{L}'$  of  $\mathbf{R}^3 \setminus \mathcal{S}$  so that the following hold:

- $\Sigma_j \rightarrow \mathcal{L}'$  on compact subsets of  $\mathbf{R}^3 \setminus \mathcal{S}$ .
- The leaves of  $\mathcal{L}'$  are minimal.

*Proof.* For each compact subset  $K$  of  $\mathbf{R}^3 \setminus \mathcal{S}$ , then Lemma II.1.1 gives an open covering of  $K$  by finitely many balls where the curvatures of the  $\Sigma_j$ 's are bounded (independent of  $j$ ) in the concentric double balls. Both claims now follow from proposition B.1 in [CM6] and a diagonal argument.  $\square$

As in [CM6], convergence to  $\mathcal{L}'$  in the above lemma means that if we think of the embedded surfaces  $\Sigma_j$  themselves as laminations, then the coordinate charts for these laminations converge in the  $C^\alpha$  norm for any  $\alpha < 1$  and the leaves converge as sets. The convergence is actually  $C^\infty$  tangentially, meaning that if we write a leaf locally as a graph, then a sequence of local graphs in  $\Sigma_j$  converges smoothly to this leaf. This tangential regularity follows

from the  $C^\alpha$  convergence and elliptic estimates. However, easy examples show that the convergence in the transversal direction may only be in the Lipschitz topology; cf. [So].

Throughout the rest of this paper, we will assume that  $\Sigma_j \subset B_{R_j}$  with  $\partial\Sigma_j \subset \partial B_{R_j}$  and  $R_j \rightarrow \infty$  is a sequence of (smooth) compact embedded minimal surfaces that converges off of a singular set  $\mathcal{S}$  to a lamination  $\mathcal{L}'$  of  $\mathbf{R}^3 \setminus \mathcal{S}$  with minimal leaves. The lamination  $\mathcal{L}'$  is given by Lemma II.1.2. In order to obtain additional structure of  $\mathcal{S}$  and  $\mathcal{L}'$ , we will need to also make topological assumptions about the surfaces  $\Sigma_j$ . We will always assume that the  $\Sigma_j$ 's have bounded genus. In Part III, we will assume that the surfaces  $\Sigma_j$  are ULSC, i.e., that  $\mathcal{S}_{neck} = \emptyset$ ; in Part IV, we will consider the other case where  $\mathcal{S}_{neck} \neq \emptyset$ .

## II.2. THE LOCAL STRUCTURE OF $\mathcal{L}'$ NEAR A POINT OF $\mathcal{S}_{ulsc}$

We will eventually show that all of the leaves of the lamination  $\mathcal{L}'$  are flat (see Theorem 0.6), but we will need to first establish some initial structure of  $\mathcal{L}'$ . The first step will be accomplished in this section where we describe the local structure of  $\mathcal{L}'$  near a point in  $\mathcal{S}_{ulsc}$ .

The next lemma is going to show that each ULSC singular point lies in the closure of a leaf of  $\mathcal{L}'$  which extends smoothly across the singular point and, furthermore, ULSC singular points are leaf-wise isolated and they satisfy a local cone property. To state this cone property, let  $\mathbf{C}_\delta(z)$  be the (convex) double cone with vertex  $z$ , cone angle  $(\pi/2 - \arctan \delta)$ , and axis parallel to the  $x_3$ -axis. That is (see Figure 7),

$$\mathbf{C}_\delta(z) = \{x \in \mathbf{R}^3 \mid (x_3 - z_3)^2 \geq \delta^2 ((x_1 - z_1)^2 + (x_2 - z_2)^2)\}. \quad (\text{II.2.1})$$

The local cone property is now defined as follows. Given  $\delta > 0$  and  $r_0 > 0$ , we will say that a subset  $\mathcal{S}_{ulsc} \subset \mathbf{R}^3$  has the *local cone property* if  $\mathcal{S}_{ulsc}$  is nonempty and

$$\text{if } z \in \mathcal{S}_{ulsc}, \text{ then } B_{r_0}(z) \cap \mathcal{S}_{ulsc} \subset \mathbf{C}_\delta(z). \quad (\text{II.2.2})$$

As in [CM6], we will see in Section III.2 that this local cone property directly gives Lipschitz regularity of the subset  $\mathcal{S}_{ulsc}$ .

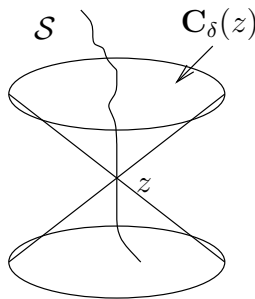


FIGURE 7. It follows from the one-sided curvature estimate that the ULSC singular set  $\mathcal{S}_{ulsc}$  has the local cone property and, as we will see, this gives Lipschitz regularity.

We can now state the lemma which gives the regularity of the leaves through  $\mathcal{S}_{ulsc}$  and the local cone property for  $\mathcal{S}_{ulsc}$ .

**Lemma II.2.3.** Given a point  $x \in \mathcal{S}_{ulsc}$ , there exists  $r_0 > 0$  so that  $B_{r_0}(x) \cap \mathcal{L}'$  has a component  $\Gamma_x$  whose closure  $\overline{\Gamma_x}$  is a smooth minimal graph containing  $x$  and with boundary in  $\partial B_{r_0}(x)$  (so  $x$  is a removable singularity for  $\Gamma_x$ ).

Furthermore,  $\overline{\Gamma_x} \cap \mathcal{S} = \{x\}$  and, after rotating  $\mathbf{R}^3$  so that  $\mathbf{n}_{\overline{\Gamma_x}}(x) = (0, 0, 1)$ , the set  $\mathcal{S}_{ulsc}$  satisfies the local cone property (II.2.2) for some  $\delta > 0$  and the above  $r_0$ . The rotation may vary with  $x$ , but the dependence is Lipschitz.

*Proof.* For simplicity, translate so that  $x = 0$ . Since  $0 \notin \mathcal{S}_{neck}$ , there exists some  $r_0 > 0$  so that the components of  $B_{r_0}(0) \cap \Sigma_j$  are disks for every  $j$ ; cf. (0.1).

The first two properties follow immediately from theorem 5.8 in [CM4] (this theorem combines the existence of multi-valued graphs near a blow up point and the sublinear growth of the separation). Namely, since  $0 \in \mathcal{S}$ , we first get a sequence of points  $y_j \in \Sigma_j$  with  $|A|^2(y_j) \rightarrow \infty$  and  $y_j \rightarrow 0$ . Since the component of  $B_{r_0}(0) \cap \Sigma_j$  containing  $y_j$  is a disk, theorem 5.8 in [CM4] then gives the following two properties:

- There is a rotation of  $\mathbf{R}^3$  and a subsequence so that  $\Sigma_j$  contains a 2-valued minimal graph  $\Sigma_{d,j} \subset \Sigma_j$  defined over an annulus  $D_{r_0/C} \setminus D_{r_j}$  where  $r_j \rightarrow 0$ .
- As  $j \rightarrow \infty$ , the 2-valued graphs close up in the limit to converge with multiplicity two to a graph  $\Gamma_x$  over  $D_{r_0/C} \setminus \{0\}$  with  $x \in \overline{\Gamma_x}$ .

Since any subsequence of a convergent sequence has the same limit, we conclude that  $\Gamma_x$  is contained in a leaf of  $\mathcal{L}'$ . Finally,  $x$  is a removable singularity for  $\Gamma_x$  by a standard removable singularity result for minimal graphs.

The cone property follows easily from corollary I.1.9 in [CM6] which gives a constant  $\delta_0 > 0$  so that if  $B_{2R} \cap \Sigma_j$  contains a 2-valued graph in  $\{x_3^2 \leq \delta_0^2(x_1^2 + x_2^2)\}$  over  $D_R \setminus D_{r_j}$  and with gradient  $\leq \delta_0$ , then each component of

$$B_{R/2} \cap \Sigma \setminus (\mathbf{C}_{\delta_0}(0) \cup B_{2r_j}) \quad (\text{II.2.4})$$

is a multi-valued graph with gradient  $\leq 1$ . After possibly shrinking the radius above given by theorem 5.8 in [CM4], we can assume that  $\Gamma_x$  is a graph with small gradient and hence corollary I.1.9 in [CM6] applies. It follows that

$$B_{r_0}(x) \cap \mathcal{S}_{ulsc} \subset \mathbf{C}_{\delta_0}(x). \quad (\text{II.2.5})$$

Finally, the embeddedness of the  $\Sigma_j$ 's implies that two limit minimal graphs through nearby singular points must be disjoint. It is now easy to see that the map which takes a singular point  $y$  to the tangent plane of the limit minimal graph through  $y$  is Lipschitz, giving the last claim.  $\square$

Lemma II.2.3 shows that each point  $x \in \mathcal{S}_{ulsc}$  is a removable singularity for a component  $\Gamma_x$  of  $B_{r_0}(x) \cap \mathcal{L}'$  for some  $r_0 > 0$ . Furthermore, the local cone property implies that the intersection of  $B_{r_0}(x) \cap \Sigma_j$  with the complement of (a tubular neighborhood of) a cone  $\mathbf{C}_{\delta'}(x)$  (for some  $\delta' > 0$ ) consists of two multi-valued graphs for  $j$  large (the fact that there are exactly two is established in proposition II.1.3 in [CM6]). However, it is worth noting that these two properties alone do not imply that  $x$  is a removable singularity for the lamination  $\mathcal{L}'$ , but rather there are two possibilities:

- (P) The multi-valued graphs in the complement of the cone  $\mathbf{C}_{\delta'}(x)$  close up in the limit.
- (N-P) These multi-valued graphs converge to a collection of graphs (such as  $\Gamma_x$ ) and *at least one* multi-valued graph that spirals infinitely on one side of  $\Gamma_x$ .

In the first case (P) (we will call this ‘‘properness’’ below), the sequence converges to a foliation in a neighborhood of  $x$ . The second case (N-P) (‘‘not proper’’) is illustrated in

[CM12] by a sequence of embedded minimal disks  $\Sigma_i$  in the unit ball  $B_1$  with  $\partial\Sigma_i \subset \partial B_1$  where the curvatures blow up only at 0 and

$$\Sigma_i \setminus \{x_3 = 0\} \tag{II.2.6}$$

converges to two embedded minimal disks

$$\Sigma^- \subset \{x_3 < 0\} \tag{II.2.7}$$

$$\Sigma^+ \subset \{x_3 > 0\}, \tag{II.2.8}$$

each of which spirals into  $\{x_3 = 0\}$  and thus is not proper. Thus, in the example from [CM12], 0 is the first, last, and only point in  $\mathcal{S}_{ulsc}$  and the limit lamination consists of three leaves:  $\Sigma^+$ ,  $\Sigma^-$ , and the punctured unit disk  $B_1 \cap \{x_3 = 0\} \setminus \{0\}$ . In this example of (N-P), the limit lamination cannot be extended smoothly to any neighborhood of 0.

To summarize, [CM12] shows that (N-P) can occur for a sequence of disks  $\Sigma_i \subset B_{R_i}$  with  $\partial\Sigma_i \subset \partial B_{R_i}$ ; however, [CM6] shows that (N-P) cannot occur for disks if the radii  $R_i$  go to infinity.

**II.2.1. Collapsed leaves of  $\mathcal{L}'$ .** One of the difficulties is that the leaves of the lamination  $\mathcal{L}'$  may not be complete; this occurs at points of  $\mathcal{S}$ . We will begin by analyzing a particular type of incomplete leaf that we will call *collapsed*.

To define this, note that Lemma II.2.3 shows that each point  $x \in \mathcal{S}_{ulsc}$  is a removable singularity for a component  $\Gamma_x$  of  $B_{r_0}(x) \cap \mathcal{L}'$ . We will say that the leaf  $\Gamma$  of  $\mathcal{L}'$  containing  $\Gamma_x$  is collapsed:

**Definition II.2.9.** A leaf  $\Gamma$  of  $\mathcal{L}'$  is *collapsed* if there exists some  $x \in \mathcal{S}_{ulsc}$  so that  $\Gamma$  contains the local leaf  $\Gamma_x$  given by Lemma II.2.3.

For a sequence of rescaled helicoids converging to a foliation by parallel planes away from an axis, every leaf is collapsed. We will eventually show that every leaf of  $\mathcal{L}'$  whose closure contains a point of  $\mathcal{S}_{ulsc}$  is collapsed. However, it is worth pointing out that this is not obvious. For example, in case (N-P) of the previous section, we get leaves of  $\mathcal{L}'$  that spiral infinitely into the collapsed leaf but are not themselves collapsed (we will eventually rule out this possibility using that the sequence of outer radii is going to infinity).

We will describe the structure of the collapsed leaves in the rest of this part. It is useful to first define the closure  $\Gamma_{Clos}$  of a leaf  $\Gamma$  of  $\mathcal{L}'$  to be the union of the closures of all bounded (intrinsic) geodesic balls in  $\Gamma$ ; that is, we fix a point  $x_\Gamma \in \Gamma$  and set

$$\Gamma_{Clos} = \bigcup_r \overline{\mathcal{B}_r(x_\Gamma)}, \tag{II.2.10}$$

where  $\overline{\mathcal{B}_r(x_\Gamma)}$  is the closure of  $\mathcal{B}_r(x_\Gamma)$  as a subset of  $\mathbf{R}^3$ .

Clearly, a leaf  $\Gamma$  is complete if and only if  $\Gamma_{Clos} = \Gamma$  and we always have that

$$\Gamma_{Clos} \setminus \Gamma \subset \mathcal{S}. \tag{II.2.11}$$

The incomplete leaves of  $\Gamma$  can be divided into several types, depending on how  $\Gamma_{Clos}$  intersects  $\mathcal{S}$ :

- Collapsed leaves, defined in Definition II.2.9, where  $\Gamma_{Clos} \cap \mathcal{S}_{ulsc}$  contains a removable singularity for  $\Gamma$ .

- Leaves  $\Gamma$  with  $\Gamma_{Clos} \cap \mathcal{S}_{ulsc} \neq \emptyset$ , but where  $\Gamma$  does not have a removable singularity. This would occur, for example, if  $\Gamma$  spirals infinitely into the collapsed leaf through  $\Gamma_{Clos} \cap \mathcal{S}_{ulsc}$  as in (N-P). (We will eventually show that this does not occur.)
- Leaves  $\Gamma$  where  $\Gamma_{Clos} \setminus \Gamma \subset \mathcal{S}_{neck}$ ; these won't be considered until Part IV.

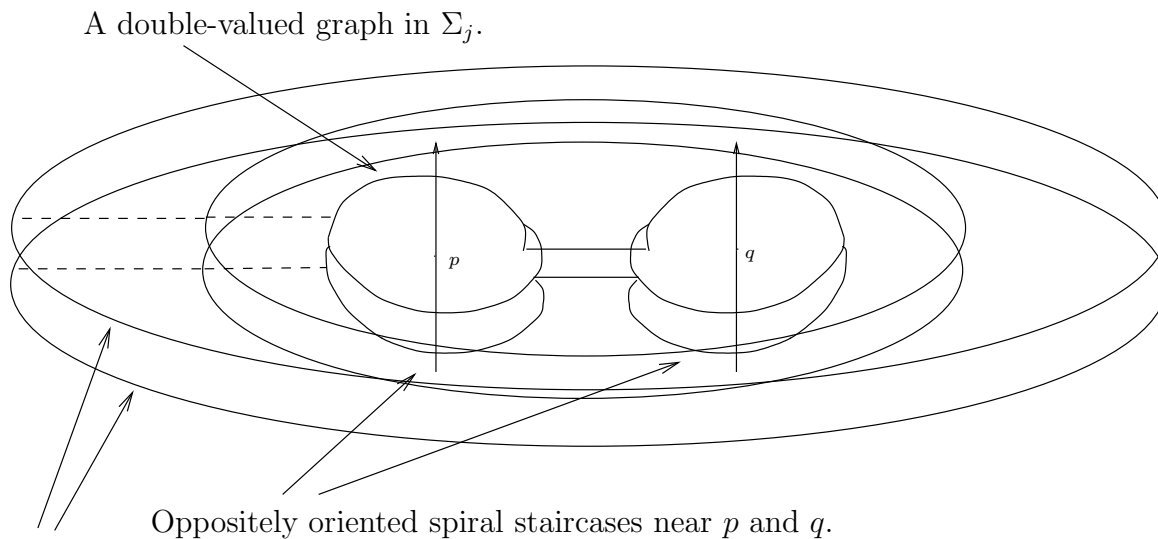
II.3. THE STRUCTURE OF THE COLLAPSED LEAVES OF  $\mathcal{L}'$

In the rest of this part, we will describe the structure of the collapsed leaves of  $\mathcal{L}'$  defined in Definition II.2.9. The most important properties of a collapsed leaf  $\Gamma$  are given in Proposition II.3.1 below that describes a neighborhood of the points of  $\mathcal{S}_{ulsc}$  in  $\Gamma$ . The proposition shows that such a  $\Gamma$  is stable and that the closure of  $\Gamma$  intersects  $\mathcal{S}_{ulsc}$  in at most two points. These results apply without additional assumptions on the sequence  $\Sigma_j$ ; we will see in the next part that  $\Gamma$  has more structure when we assume in addition that the sequence is ULSC.

The next proposition establishes the key properties of a collapsed leaf in the general case:

**Proposition II.3.1.** Each collapsed leaf  $\Gamma$  of  $\mathcal{L}'$  has the following properties:

- (1) Given any  $y \in \Gamma_{Clos} \cap \mathcal{S}_{ulsc}$ , there exists  $r_0 > 0$  so that the closure (in  $\mathbf{R}^3$ ) of each component of  $B_{r_0}(y) \cap \Gamma$  is a compact embedded disk with boundary in  $\partial B_{r_0}(y)$ .  
 Furthermore,  $B_{r_0}(y) \cap \Gamma$  must contain the component  $\Gamma_y$  given by Lemma II.2.3 and  $\Gamma_y$  is the only component of  $B_{r_0}(y) \cap \Gamma$  with  $y$  in its closure.
- (2) If  $\Gamma$  is oriented, then it is stable. (Otherwise, its oriented double cover is stable.)
- (3)  $\Gamma_{Clos}$  intersects  $\mathcal{S}_{ulsc}$  in at most two points. If  $\Gamma_{Clos} \cap \mathcal{S}_{ulsc}$  contains two points, then the multi-valued graphs in the  $\Sigma_j$ 's spiral in opposite directions around the two corresponding axes (see Figure 8).



Get 2 disjoint graphs after circling both  $p$  and  $q$ .

FIGURE 8. The multi-valued graph converging to  $\Gamma$  in Proposition II.3.1.

Properties (2) and (3) in Proposition II.3.1 are self-explanatory. However, to appreciate property (1), it may be useful to observe one implication of (1) and to also see an example

of what it rules out. First, (1) implies that  $\Gamma_{Clos} \cap \mathcal{S}_{ulsc}$  consists of a discrete set of points and each of these points is a removable singularity. Second, recall from (N-P) - “not proper” - that a priori there may be multi-valued graphs in  $B_{r_0}(y) \cap \mathcal{L}'$  that spiral infinitely into  $\Gamma_y$ ; (1) above says that these “infinite spirals” are not contained in any collapsed leaf.

Throughout this section  $\Gamma$  will be a collapsed leaf of  $\mathcal{L}'$ . By definition, a leaf  $\Gamma$  is a connected open surface, but may not be complete (and, in fact, collapsed leaves are incomplete by definition). We will let  $K \subset \Gamma$  denote a connected open subset with compact closure in  $\Gamma$ . Finally,  $T(K, \epsilon)$  is the  $\epsilon$ -tubular normal neighborhood of  $K$ , i.e.,

$$T(K, \epsilon) = \{x + s \mathbf{n}_\Gamma(x) \mid x \in K, |s| < \epsilon\}. \quad (\text{II.3.2})$$

**II.3.1. Proving property (1) of Proposition II.3.1: Isolated removable singularities.** To prove (1) of Proposition II.3.1, we will show the following claim:

Claim: If  $x \in \mathcal{S}_{ulsc}$  is a singular point in the closure  $\Gamma_{Clos}$  of a collapsed leaf  $\Gamma$ , then the component of  $B_{r_0}(x) \cap \overline{\Gamma}$  containing  $x$  is the one from Lemma II.2.3.

Property (1) then follows from the following two properties of the component  $\Gamma_x$  from Lemma II.2.3:

- $\Gamma_x \cup \{x\}$  is a smooth minimal surface.
- $\overline{\Gamma}_x \cap \mathcal{S} = x$ .

Thus, we will have at the same time shown that each ULSC singular point in the closure of  $\Gamma$  is a removable singularity and has a neighborhood in  $\Gamma$  where there are no other singular points, as desired.

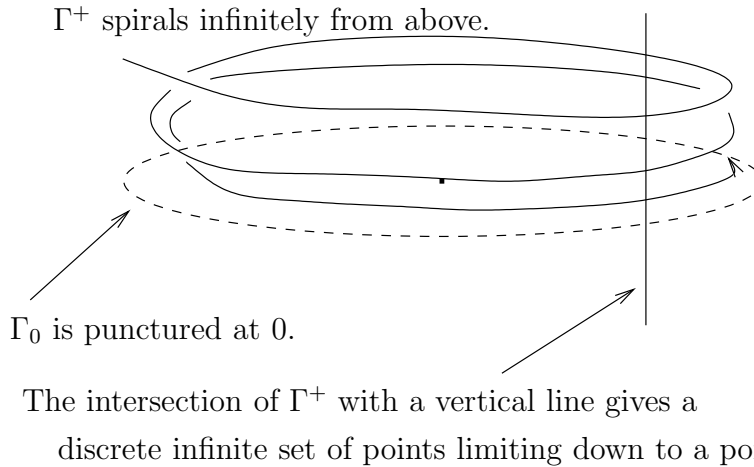


FIGURE 9. The “not proper” example (N-P): The sequence of disks  $\Sigma_j$  converges in  $B_1 \setminus \{0\}$  to a lamination with three leaves: the punctured disk  $\Gamma_0 = D_1 \setminus \{0\}$  (dotted),  $\Gamma^+$  spiralling into  $\Gamma_0$  infinitely from above, and  $\Gamma^-$  spiralling into  $\Gamma_0$  infinitely from below (not pictured). The collapsed leaf  $\Gamma_0$  is not discrete, but  $\Gamma^+$  and  $\Gamma^-$  are.

Lemma II.3.3 below establishes the above claim about the singular points in the closure of a collapsed leaf. The lemma is best illustrated using the “not proper” example in (N-P). In (N-P), a sequence of embedded minimal disks converges in  $B_1 \setminus \{0\}$  to a lamination with three leaves: the punctured disk  $\Gamma_0 = D_1 \setminus \{0\}$ ,  $\Gamma^+$  spiralling into  $\Gamma_0$  infinitely from above,

and  $\Gamma^-$  spiralling into  $\Gamma_0$  infinitely from below; see Figure 9. Notice that all three leaves contain 0 in their closure. The leaf  $\Gamma_0$  is collapsed at 0 (so 0 is a removable singularity for  $\Gamma_0$ ), but  $\Gamma^+$  and  $\Gamma^-$  cannot extend past the singularity 0. The conclusion of Lemma II.3.3 is that  $\Gamma^+$  and  $\Gamma^-$  cannot be contained in any collapsed leaf of  $\mathcal{L}'$ .

The above example from (N-P) also serves to illustrate the idea of the proof of Lemma II.3.3. Namely, a key distinction between the collapsed leaf  $\Gamma_0$  versus  $\Gamma^+$  and  $\Gamma^-$  is that  $\Gamma^+$  and  $\Gamma^-$  are discrete in the following sense:

Given any point  $y$  in  $\Gamma^+$  or  $\Gamma^-$ , there exists  $s > 0$  so that  $B_s(y) \cap \mathcal{L}'$  has only one connected component (i.e., the one containing  $y$ ).

On the other hand, since  $\Gamma^+$  and  $\Gamma^-$  spiral infinitely into  $\Gamma_0$ , the leaf  $\Gamma_0$  is not discrete in this sense. Likewise, the description of a neighborhood of a point in  $\mathcal{S}_{ulsc}$  shows that a collapsed leaf is never discrete.

**Lemma II.3.3.** Suppose that  $x \in \mathcal{S}_{ulsc}$  and  $\Gamma'$  is a component of  $B_{r_0}(x) \cap \mathcal{L}'$  with  $x$  in its closure  $\overline{\Gamma'}$ . If  $\Gamma'$  is contained in a collapsed leaf of  $\mathcal{L}'$ , then  $\Gamma'$  must be the component  $\Gamma_x$  given by Lemma II.2.3.

*Proof.* Since the component  $\Gamma'$  of  $B_{r_0}(x) \cap \mathcal{L}'$  contains the point  $x \in \mathcal{S}_{ulsc}$  in its closure, embeddedness and the cone property implies that  $\Gamma'$  has one of the following two properties:

- (L1)  $\Gamma'$  is the component  $\Gamma_x$  given by Lemma II.2.3 and hence extends smoothly across  $x$ .
- (L2)  $\Gamma'$  is not the component  $\Gamma_x$  given by Lemma II.2.3.

In Lemma II.3.4 below we will prove that the leaves satisfying (L2) are discrete in the following sense:

Given any point  $y$  in a leaf of  $\mathcal{L}'$  satisfying (L2), there exists  $s > 0$  so that  $B_s(y) \cap \mathcal{L}'$  has only one connected component (i.e., the one containing  $y$ ).

Completing the proof assuming discreteness: Suppose now that  $\Gamma$  is collapsed,  $y \in \Gamma$ , and the ball  $B_s(y)$  is disjoint from  $\mathcal{S}$ . Let  $\Gamma_{y,s}$  be the component of  $B_s(y) \cap \Gamma$  containing  $y$ . It follows from the Harnack inequality (since the curvature is locally bounded on  $\Gamma$ ) that  $\Gamma_{y,s}$  is the limit of distinct leaves of  $B_s(y) \cap \mathcal{L}'$ . In particular,  $\Gamma$  is not discrete and hence does not contain any leaves of  $B_{r_0}(x) \cap \mathcal{L}'$  that satisfy (L2). This completes the proof of the lemma modulo Lemma II.3.4 below.  $\square$

The next lemma shows that we always get discreteness for leaves of  $\mathcal{L}'$  that have a point of  $\mathcal{S}_{ulsc}$  in their closure but are not collapsed at this point (cf., the picture for  $\Gamma^+$  and  $\Gamma^-$  in Figure 9).

**Lemma II.3.4.** Given any point  $y$  in a leaf of  $\mathcal{L}'$  satisfying (L2), there exists  $s > 0$  so that  $B_s(y) \cap \mathcal{L}'$  has only one connected component (i.e., the one containing  $y$ ).

*Proof.* Suppose that a component  $\Gamma$  of  $B_{r_0}(x) \cap \mathcal{L}'$  contains the point  $x \in \mathcal{S}_{ulsc}$  in its closure but is not equal to  $\Gamma_x$ . It suffices to find one point in  $\Gamma$  where the leaf is locally discrete (since the leaf is connected, the Harnack inequality then implies that every point is discrete). We will next outline the argument to find this discrete point. The key will be to find a sequence of curves  $\gamma_j \subset \Sigma_j$  with uniformly bounded length, where one sequence of endpoints converges to a point in  $\Gamma$ , the  $\Sigma_j$ 's are uniformly discrete at the second endpoint of  $\gamma_j$ , and the  $\gamma_j$ 's stay away from the singular set  $\mathcal{S}$ . These properties are made precise in (G1)–(G4) below;

see Figure 10. Since the  $\gamma_j$ 's stay away from  $\mathcal{S}$  and have bounded length, a subsequence of the  $\gamma_j$ 's will converge to a curve  $\gamma$  in some leaf of  $\mathcal{L}'$ . However, one sequence of endpoints converges to a point in  $\Gamma$  and so the whole curve  $\gamma$  is in  $\Gamma$ . Finally, the second endpoint of  $\gamma$  will give the desired discrete point in  $\Gamma$ .

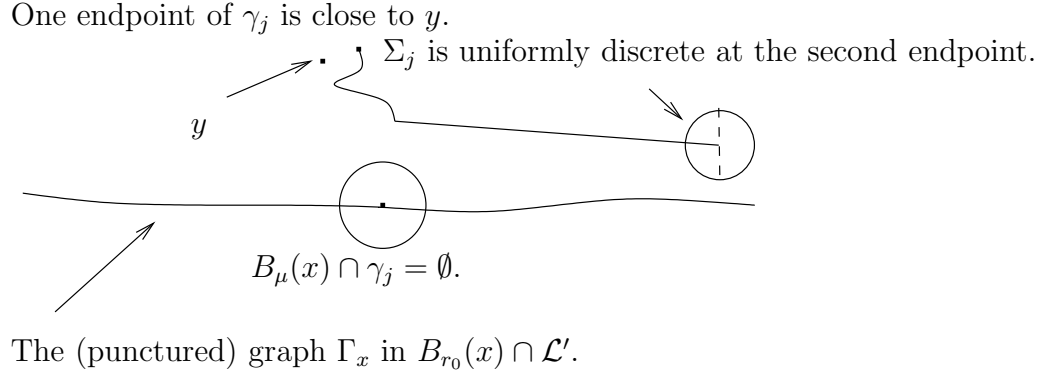


FIGURE 10. The curves  $\gamma_j$  in  $\Sigma_j$ .

Before making this precise, we need a few simple preliminaries. First, since  $\Gamma_x \cup \{x\}$  separates the ball  $B_{r_0}(x)$  and  $\Gamma \subset B_{r_0}(x) \setminus (\Gamma_x \cup \{x\})$  is connected, we may assume that  $\Gamma$  is contained in the component  $B_{r_0}^+(x)$  of  $B_{r_0}(x) \setminus (\Gamma_x \cup \{x\})$  that is above  $\Gamma_x$ . Since each point in  $\mathcal{S}_{ulsc}$  comes with a leaf through it with the same separating properties as  $\Gamma_x$ , the distance between  $x$  and  $B_{r_0}^+(x) \cap \mathcal{S}$  must be positive. Therefore, after shrinking  $r_0$ , we may as well assume that

$$B_{r_0}^+(x) \cap \mathcal{S} = \emptyset. \quad (\text{II.3.5})$$

As mentioned, the key point is to find a sequence of curves  $\gamma_j$  parameterized by arclength

$$\gamma_j : [0, \ell_j] \rightarrow B_{r_0}^+(x) \cap \Sigma_j \quad (\text{II.3.6})$$

with the following properties (see Figure 10):

- (G1) The endpoints  $\gamma_j(0)$  converge to a point  $y \in \Gamma$ .
- (G2) The lengths  $\ell_j$  are uniformly bounded, i.e.,  $\ell_j \leq \ell$  for every  $j$ .
- (G3) The minimal distance between  $\gamma_j$  and  $\mathcal{S}$  is at least  $\mu > 0$ .
- (G4) The  $\Sigma_j$ 's are “uniformly discrete” at the endpoint  $\gamma_j(\ell_j)$ ; precisely, there exists  $\delta > 0$  so that  $B_\delta(\gamma_j(\ell_j)) \cap \Sigma_j$  is a (connected) graph over its tangent plane at  $\gamma_j(\ell_j)$  with gradient bounded by one.

The discreteness follows immediately from (G1)–(G4). Namely, (G2) and (G3) imply that a subsequence of the curves  $\gamma_j$  converges to a curve  $\gamma$  contained in a leaf of  $\mathcal{L}'$ . Since the endpoints  $\gamma_j(0)$  converge to the point  $y$  in the leaf  $\Gamma$ , the entire curve  $\gamma$  must be contained in  $\Gamma$ . Finally, (G4) implies that  $\Gamma$  is discrete at the second endpoint of  $\gamma$  and, hence, discrete everywhere by the Harnack inequality.

Before establishing (G1)–(G4), we need to recall the following two additional facts:

- (1) Existence of nearby points of large curvature: Given any constants  $C_1$  and  $C_4$ , there exists  $\epsilon > 0$  so that for any  $s > 0$  and every  $j$  sufficiently large (depending also on  $s$ ) there is a point

$$q_j \in B_s(x) \cap \Sigma_j \setminus B_{\epsilon s}(x) \quad (\text{II.3.7})$$

so that  $q_j$  is above  $\Gamma_x \cup \{x\}$  and  $q_j$  satisfies

$$|A|^2(q_j) \geq C_4 C_1 |x - q_j|^{-2}. \quad (\text{II.3.8})$$

(2) Curvature bound away from  $x$ : Given any  $\mu > 0$ , there exists a constant  $C_2$  so that if  $y$  is any point in  $B_{r_0}^+(x) \cap \Sigma_j \setminus B_\mu(x)$ , then

$$|A|^2(y) \leq C_2. \quad (\text{II.3.9})$$

Property (1) was proven in corollary III.3.5 in [CM5]. Property (2) follows easily since the singular set  $\mathcal{S}$  does not intersect  $B_{r_0}^+(x)$  by (II.3.5) (the proof of (2) can be made precise using Lemma II.1.1 and a covering argument).

To complete the proof of discreteness, it suffices to establish (G1)–(G4). We will do this next. First, fix a point  $y \in \Gamma$  in a small ball  $B_h(x)$  about  $x$  ( $h$  will need to be sufficiently small relative to  $r_0$  but otherwise does not matter). Since  $y \in \Gamma$ , we can choose a sequence of points  $y_j \in \Sigma_j$  that converge to  $y$ . Now choose a constant  $s > 0$  with  $s$  much smaller than  $|y - x|$ .

Observe that property (1) gives points  $q_j \in B_s(x) \setminus B_{\epsilon s}(x)$  in  $\Sigma_j$  satisfying (II.3.8). A simple blow up argument (e.g., lemma 5.1 in [CM4]) then gives points  $p_j \in \Sigma_j$  near  $q_j$  and radii  $r_j$  so that

$$\sup_{B_{r_j}(p_j) \cap \Sigma_j} |A|^2 \leq 4 |A|^2(p_j) = 4 C_1 r_j^{-2}, \quad (\text{II.3.10})$$

and

$$B_{r_j}(p_j) \subset B_{\frac{2|x-q_j|}{\sqrt{C_4}}}(q_j). \quad (\text{II.3.11})$$

In particular, by taking  $C_4$  large in property (1), we can assume that the ratio

$$\frac{r_j}{|p_j - x|} \quad (\text{II.3.12})$$

is as small as we want and, hence, also that

$$B_{r_j}(p_j) \subset B_{2s}(x) \setminus B_{\epsilon s/2}(x). \quad (\text{II.3.13})$$

We called the pair  $(p_j, r_j)$  a *blow up pair* in [CM6]. The point about such a pair is that theorem 0.7 in [CM6] gives multi-valued graphs

$$\Sigma_j^g \subset \Sigma_j \quad (\text{II.3.14})$$

defined outside of a disk of radius  $r_j$  centered at  $p_j$  and whose initial separation is proportional to  $r_j$ . On the other hand, since  $p_j \notin B_{\epsilon s/2}(x)$ , property (2) implies that there is a uniform upper bound for  $|A|^2(p_j)$  – and, thus, a uniform lower bound for the initial scale  $r_j$ .

We will also need a positive lower bound for the minimum distance between  $\Sigma_j^g$  and  $x$ . The argument for this is very similar to an argument in section III.2 of [CM6]. We will sketch the argument next. The lower bound follows easily once we have a lower bound for the distance from  $B_{r_j}(p_j)$  to  $\Gamma_x$ . Since  $p_j \notin B_{\epsilon s/2}(x)$ , the one-sided curvature estimate gives a lower bound for the distance from  $p_j$  to  $\Gamma_x$  (otherwise  $p_j$  would lie in a narrow cone about  $\Gamma_x$  and the one-sided curvature estimate would contradict (II.3.10)). Using this and the fact that  $r_j$  is small relative to  $|p_j - x|$  (see (II.3.12)) then gives the desired lower bound for the distance from  $B_{r_j}(p_j)$  to  $\Gamma_x$ . We leave the details to the reader.

To summarize, we have established a positive lower bound for the distance from  $\Sigma_j^g$  to  $x$  and for the initial scale  $r_j$ . This lower bound on the initial scale also implies a lower bound

for the separation between the sheets of  $\Sigma_j^g$ .<sup>9</sup> Moreover, proposition II.1.3 in [CM6] says that  $\Sigma_j$  contains exactly two (oppositely oriented) multi-valued graphs in this region; the uniform curvature upper bound given by (2) then also implies a uniform lower bound for the distance between these two multi-valued graphs.

As a consequence of these uniform bounds, a (sub) sequence of the two (oppositely oriented) multi-valued graphs is guaranteed to converge (with multiplicity one) to two multi-valued graphs in  $B_{r_0}^+(x) \cap \mathcal{L}'$  and these limit multi-valued graphs will satisfy the same lower bounds. Fix a point  $z$  in one of the limit multi-valued graphs. We will now find the desired curves  $\gamma_j$  from  $y_j$  to  $z_j$  ((G1) and (G4) will then automatically be satisfied). We use two facts to find these curves. First, the chord-arc bound of Theorem I.1.6 allows us to connect  $y_j$  to the multi-valued graph  $\Sigma_j^g$  by a curve  $\gamma_j^+ \subset \Sigma_j$  with length at most  $C_3 h$  and, furthermore, we can assume that  $\gamma_j^+$  is above  $\Sigma_j^g$ .<sup>10</sup> Now that  $\gamma_j^+$  connects  $y_j$  to the multi-valued graph, we can use a curve  $\gamma_j^g$  in  $\Sigma_j^g$  to connect the endpoint of  $\gamma_j^+$  to points  $z_j \in \Sigma_j^g$  converging to  $z$ ; the  $\gamma_j^g$ 's automatically have uniformly bounded length and also stay uniformly away from  $x$ . This completes the proof of (G1)–(G4) and, consequently, also completes the proof of discreteness.  $\square$

**II.3.2. Each leaf is a limit of multi-valued graphs in the  $\Sigma_j$ 's.** Recall that, throughout this section,  $\Gamma$  is a leaf of  $\mathcal{L}'$  and  $K \subset \Gamma$  is a connected open subset that has compact closure in  $\Gamma$ .

We will first show in Lemma II.3.15 that the  $\Sigma_j$ 's are locally graphical over  $\Gamma$  in a tubular neighborhood of  $K$ . Corollary II.3.18 uses the local description of Lemma II.3.15 to construct multi-valued graphs  $\Sigma_j^g \subset \Sigma_j$  converging to  $K$ . Both Lemma II.3.15 and Corollary II.3.18 apply to any leaf  $\Gamma$  and do not require  $\Gamma$  to be collapsed.

The next lemma shows that  $\Sigma_j$  is locally graphical over  $\Gamma$  in a small tubular neighborhood of  $K$ .

**Lemma II.3.15.** Given any  $\delta > 0$ , there exist  $\epsilon > 0$  and  $J$  so that if  $j > J$  and  $x \in T(K, \epsilon) \cap \Sigma_j$ , then  $\mathcal{B}_\epsilon(x) \subset \Sigma_j$  is a graph over (a subset of)  $\Gamma$  with gradient bounded by  $\delta$ .

*Proof.* Since  $\Gamma$  is a leaf of  $\mathcal{L}'$ , it is disjoint from the singular set  $\mathcal{S}$ . Therefore, for each point  $y \in \Gamma$ , the convergence of the  $\Sigma_j$ 's to the lamination  $\mathcal{L}'$  away from  $\mathcal{S}$  gives a ball  $B_{\epsilon_y}(y)$  and a  $J_y$  so that if  $x \in B_{\epsilon_y}(y) \cap \Sigma_j$  for  $j > J_y$ , then  $\mathcal{B}_{\epsilon_y}(x) \subset \Sigma_j$  is a graph over (a subset of)  $\Gamma$  with gradient bounded by  $\delta$ .

However, the closure  $\bar{K}$  of  $K$  in  $\Gamma$  is compact, so it can be covered by a finite subcollection of the half-balls, i.e.,

$$\bar{K} \subset \cup_{i=1}^m B_{\frac{\epsilon_{y_i}}{2}}(y_i). \quad (\text{II.3.16})$$

It is then easy to see that this implies the lemma with

$$\epsilon = 1/2 \min_i \epsilon_{y_i}. \quad (\text{II.3.17})$$

$\square$

---

<sup>9</sup>The existence of some lower bound is easy and almost obvious; a fairly sharp lower bound is proven in lemma III.1.6 in [CM6].

<sup>10</sup>More precisely, the curve does not go below the union of  $\Sigma_j^g$  and the extrinsic ball  $B_{r_j}(p_j)$ .

The next corollary uses Lemma II.3.15 to get multi-valued graphs  $\Sigma_j^g \subset \Sigma_j$  over  $K$ ; see (A) below. Furthermore, (C) below shows that  $\Sigma_j^g$  contains a point  $p_j$  far from the boundary  $\partial\Sigma_j^g$  of the multi-valued graph. More precisely,  $\partial\Sigma_j^g$  divides naturally into two parts, depending on whether or not it projects to  $\partial K$ ; (C) shows that the point  $p_j$  is far from the part of  $\partial\Sigma_j^g$  that is not over  $\partial K$ . We will later use (C) to get multi-valued graphs with many sheets converging to a collapsed leaf.

**Corollary II.3.18.** Fix a point  $p_0 \in K$ . Given any (small) constant  $\delta > 0$  and a (large) constant  $N$ , there exist  $\epsilon > 0$  and  $J$  so that for each  $j > J$  we get the following:

- (A) There is a connected open subset  $\Sigma_j^g \subset T(K, \epsilon) \cap \Sigma_j$  so that, for each  $x \in \Sigma_j^g$ , the intrinsic ball  $\mathcal{B}_\epsilon(x)$  is a graph over (a subset of)  $\Gamma$  with gradient bounded by  $\delta$ .
- (B) The normal exponential map from  $K \times (-\epsilon, \epsilon)$  gives a diffeomorphism to  $T(K, 2\epsilon)$ . Let  $\Pi : T(K, \epsilon) \rightarrow K$  denote the projection to  $K$  and  $\Pi_j$  the restriction of  $\Pi$  to  $\Sigma_j^g$ .
- (C) There is a point  $p_j \in \Sigma_j^g$  with  $\Pi_j(p_j) = p_0$  satisfying

$$\text{dist}_{\Sigma_j^g}(p_j, \partial\Sigma_j^g \setminus \Pi_j^{-1}(\partial K)) > N. \quad (\text{II.3.19})$$

*Proof.* Lemma II.3.15 gives  $\epsilon > 0$  (depending only on  $\delta$ ) so that for every point  $x$  in  $T(K, \epsilon) \cap \Sigma_j$  the intrinsic ball  $\mathcal{B}_\epsilon(x)$  is a graph over (a subset of)  $\Gamma$  with gradient bounded by  $\delta$ .

Since  $K$  has compact closure in the (open) surface  $\Gamma$ , we can shrink  $\epsilon > 0$  so that the normal exponential map from  $K \times (-\epsilon, \epsilon)$  gives a diffeomorphism to  $T(K, 2\epsilon)$ .

Furthermore, since the  $\Sigma_j$ 's converge to  $\mathcal{L}'$  in a neighborhood of the point  $p_0 \in \Gamma$ , there is a sequence of points  $p_j \in \Sigma_j$  converging to  $p_0$  (in fact, there are many such sequences; just pick one). This determines the sequence of multi-valued graphs  $\Sigma_j^g \subset \Sigma_j$ .

It remains to prove that (C) holds for  $J$  sufficiently large. We will do this by contradiction, so suppose that no such  $J$  exists for some fixed  $N$ . In particular, we get infinitely many  $j$ 's where there exist curves  $\gamma_j \subset \Sigma_j$  with the following properties:

- $\gamma_j$  starts at  $p_j$  and ends at a point in  $\partial T(K, \epsilon)$  that is distance  $\epsilon$  from  $K$ .
- The length of  $\gamma_j$  is at most  $N$ .
- $\gamma_j$  is contained in  $T(K, \epsilon)$ .

After passing to a subsequence, the  $\gamma_j$ 's must converge to a curve  $\gamma \subset \overline{T(K, \epsilon)}$  that is contained in some leaf of  $\mathcal{L}'$  (we are using here that  $\gamma_j$  stays away from  $\mathcal{S}$ ). Since the  $p_j$ 's converge to  $p_0$ , the curve  $\gamma$  starts at  $p_0 \in K$  and, hence, we have

$$\gamma \subset \overline{K}. \quad (\text{II.3.20})$$

However, this is impossible since the second endpoints of  $\gamma_j$  are all distance  $\epsilon$  from  $K$  and, thus, could not have converged to a point in  $K$ . This contradiction completes the proof.  $\square$

**II.3.3. Property (2) of Proposition II.3.1: Each collapsed leaf is stable.** The main result of this subsection is that each oriented collapsed leaf of  $\mathcal{L}'$  is stable. The proof of stability has the following three main steps:

- Corollary II.3.18 gives multi-valued graphs  $\Sigma_j^g \subset \Sigma_j$  converging to  $K$  with large multiplicity. The  $\Sigma_j^g$ 's can be thought of as single-valued graphs over a (subset of a) covering space  $K_j$  over  $K$ .
- Corollary II.3.21 describes the covering spaces  $K_j$  by analyzing the ‘‘holonomy’’ action of  $\pi_1(K)$  on the fibers (the holonomy is defined below).

- Lemma II.3.22 then shows that a subsequence of the  $K_j$ 's satisfies (G1) and (G2) in Appendix B, so we can apply Corollary B.20 to see that  $K$  is stable.

Since this applies for any such  $K$ , and  $\Gamma$  can be exhausted by such  $K$ 's by Lemma A.1 in Appendix A, we conclude that  $\Gamma$  itself is stable.

The next corollary describes what the multi-valued graphs  $\Sigma_j^g$  look like as we follow them around a simple closed curve  $\gamma$  in  $K$ . Obviously, the pre-image  $\Pi_j^{-1}(\gamma)$  consists of a disjoint union of connected simple curves in the topological annulus  $\Pi^{-1}(\gamma)$ ; see Figure 11.

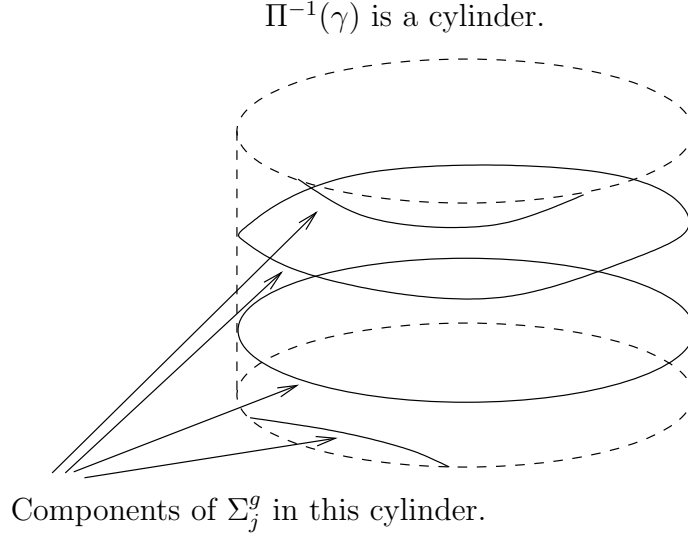


FIGURE 11. Each component of  $\Pi_j^{-1}(\gamma)$  is locally a graph over  $\gamma$ .

Some of the components of  $\Pi_j^{-1}(\gamma)$  are more important than others. To distinguish the components, we will say that one of these components is “short” if it has two endpoints contained in the same boundary circle of  $\Pi^{-1}(\gamma)$ ; otherwise, we will say the component is “long” (so a long component either has no boundary, or it has endpoints in distinct boundary circles of  $\Pi^{-1}(\gamma)$ ). The corollary describes these long components:

**Corollary II.3.21.** Suppose that  $\Pi_j : \Sigma_j^g \rightarrow K$  is as in Corollary II.3.18.

If  $\gamma \subset K$  is a simple closed curve, then either (1A) or (1B) holds:

- (1A) Each long component of  $\Pi_j^{-1}(\gamma)$  is closed and is a graph over  $\gamma$ ; see Figure 12.
- (1B) The long components of  $\Pi_j^{-1}(\gamma)$  are disjoint simple curves spiralling together from one boundary circle of  $\Pi^{-1}(\gamma)$  to the other; see Figure 13.

If, in addition,  $K$  contains a simple closed curve  $\sigma$  that circles  $p \in \Gamma_{Clos} \cap \mathcal{S}_{ulsc}$  but is contractible in  $\Gamma \cup \{p\}$ , then

- (2)  $\Pi_j^{-1}(\sigma)$  has a single long component<sup>11</sup>; this long component spirals from one boundary circle of the topological annulus  $\Pi^{-1}(\sigma)$  to the other.

<sup>11</sup>Note that even though  $\Pi_j^{-1}(\sigma)$  is all of where  $\Pi^{-1}(\sigma)$  intersects the multi-valued graph,  $\Pi_j^{-1}(\sigma)$  is not all of  $\Pi^{-1}(\sigma) \cap \Sigma_j$ . At the least, there must be another oppositely oriented component of  $\Pi^{-1}(\sigma) \cap \Sigma_j$  that spirals together; cf. the example of rescaled helicoids.

Schematic picture of Corollary II.3.21 (the two boundary circles of  $\Pi^{-1}(\gamma)$  are dotted):

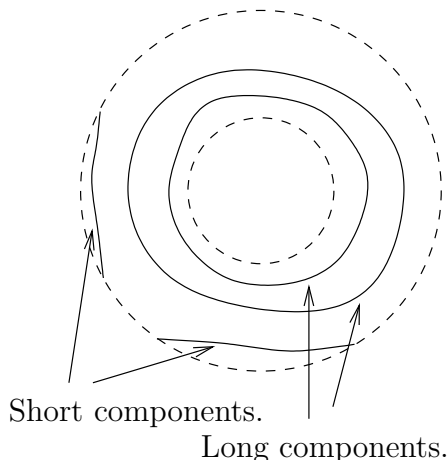


FIGURE 12. Case (1A): The long components of  $\Pi_j^{-1}(\gamma)$  are graphs.

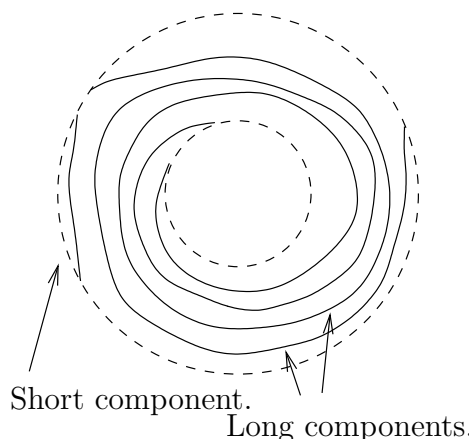


FIGURE 13. Case (1B): The long components of  $\Pi_j^{-1}(\gamma)$  are multi-valued graphs spiralling together from one boundary circle of  $\Pi^{-1}(\gamma)$  to the other.

*Proof.* Since we are working in the compact embedded surface  $\Sigma_j$  and not in the limit, each component of  $\Pi_j^{-1}(\gamma)$  is a simple curve with compact closure. In particular, these curves cannot spiral infinitely. Moreover, since  $\Pi_j^{-1}(\gamma)$  is contained in the multi-valued graph, each component of  $\Pi_j^{-1}(\gamma)$  is also locally a graph over  $\gamma$ .

If any long component is closed (and hence a graph over  $\gamma$ ), then it separates the two boundary components of the topological annulus  $\Pi^{-1}(\gamma)$  and, by embeddedness, every long component must be a closed graph over  $\gamma$ ; this is case (1A). Suppose, on the other hand, that one (and, hence, every) long component connects the two boundary components of  $\Pi^{-1}(\gamma)$ . In this case, the embeddedness of  $\Pi_j^{-1}(\gamma)$  forces all of these curves to spiral together; this is case (1B).

Suppose now that a simple closed curve  $\sigma \subset K$  circles  $p \in \Gamma_{Clos} \cap \mathcal{S}_{ulsc}$  but is contractible in  $\Gamma \cup \{p\}$  and, in particular, does not circle any other points in  $\Gamma_{Clos} \cap \mathcal{S}_{ulsc}$ . It follows from Lemma II.2.3 (and its proof) that the long components of  $\Pi_j^{-1}(\sigma)$  do not close up and, hence, we are in case (1B). It remains to see that there is just one long component. This follows immediately from proposition II.1.3 in [CM6] which shows that  $\Pi^{-1}(\sigma) \cap \Sigma_j$  consists of exactly two oppositely oriented double spiral staircases.<sup>12</sup> Since  $\Sigma_j^g$  is a multi-valued graph over the connected set  $K$ , and hence can achieve only one of these orientations, it can contain only one of these.  $\square$

We will say that  $K$  is *sufficiently large* when it contains a simple closed curve  $\sigma$  that circles exactly one point  $p \in \Gamma_{Clos} \cap \mathcal{S}_{ulsc}$  but is contractible in  $\Gamma \cap \{p\}$ , i.e., when (2) applies in Corollary II.3.21. We will assume in the rest of this section that  $K$  is sufficiently large.

<sup>12</sup>Technically, this description applies only when  $\sigma$  is in a neighborhood of  $p$ . This is sufficient for us since our  $\sigma$  is homotopic to a curve in a neighborhood of  $p$  and  $\Sigma_j^g$  is locally graphical over  $K$ .

**Lemma II.3.22.** If the  $\Sigma_j$ 's are planar domains,  $K$  is sufficiently large, and  $\gamma \subset K$  is a simple closed curve, then there can be only one long curve in (1B) of Corollary II.3.21 for  $j$  sufficiently large.

More generally, when the  $\Sigma_j$ 's have bounded genus, then we get a bound for the number of distinct curves in (1B).

*Proof.* We will give the proof for genus zero, i.e., when the  $\Sigma_j$ 's are planar domains; the easy modifications needed for the general case are left to the reader.

Let  $\sigma \subset K$  be a simple closed curve circling  $p \in \Gamma_{Clos} \cap \mathcal{S}_{ulsc}$  and so  $\sigma$  is contained in a small neighborhood of  $p$  (this exists since  $K$  was assumed to be sufficiently large). Let  $\gamma \subset K$  be a second simple closed curve. After possibly perturbing  $\sigma$  slightly, we can assume that it is disjoint from  $\gamma$ . Fix points  $x \in \sigma$  and  $y \in \gamma$  and let  $\eta \subset K$  be a simple curve from  $x$  to  $y$ . Again, after perturbing things, we can assume that  $\eta$  intersects  $\sigma$  and  $\gamma$  only at its endpoints  $x$  and  $y$ ; see Figure 14.

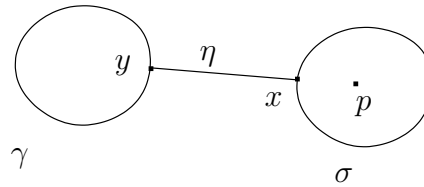


FIGURE 14. The proof of Lemma II.3.22: The curves  $\sigma$ ,  $\eta$ , and  $\gamma$  in  $K$ .

Suppose now that  $\Sigma_j^g \subset \Sigma_j$  contains two distinct long curves,  $\gamma_1$  and  $\gamma_2$ , in  $\Pi_j^{-1}(\gamma)$  that spiral together; see Figure 15. We will show that this leads to a contradiction by constructing two simple closed curves,  $\mu_1$  and  $\mu_2$ , in  $\Sigma_j$  that have linking number one in  $\Sigma_j$ . This is impossible for a planar domain (it implies that the genus is at least one).

We will first construct the curve  $\mu_2 \subset \Sigma_j$  out of four parts; see Figure 16. The first part of  $\mu_2$  is a 1-valued graph over  $\gamma$  that is contained in  $\gamma_2$  and has both of its endpoints over  $y$ . These two endpoints are distinct since they are at different heights over  $y$ . The next two parts of  $\mu_2$  are graphs over  $\eta$  that connect these two endpoints to two distinct points over  $x \in \sigma$ . Finally, we close the curve up by connecting the two points over  $x$  by a multi-valued graph over  $\sigma$ . Here, we have used that  $\Pi_j^{-1}(\sigma)$  has exactly one long component to show that these endpoints can be connected and to see that the curve connecting them is at least 2-valued. Furthermore, we have also implicitly used that  $j$  is large to ensure that we can find the graphs over  $\eta$  and to ensure that the endpoints of these over  $x$  lie in a long component of  $\Pi_j^{-1}(\sigma)$ . (We will use that  $j$  is large in the same way later in the paper, usually without mentioning that we are doing so.)

The curve  $\mu_1 \subset \Sigma_j$  is constructed similarly, with two notable differences; see Figure 17. First, the 1-valued graph over  $\gamma$  is chosen to be in  $\gamma_1$  this time, as opposed to  $\gamma_2$  before. Consequently, the one-valued graphs over  $\gamma$  in  $\mu_1$  and  $\mu_2$  are disjoint and, furthermore, the graphs over  $\eta$  are at four distinct heights. Second, instead of closing  $\mu_1$  up with a multi-valued graph over  $\sigma$ , do it over a slight outward perturbation of  $\sigma$  (see Figure 17). This makes the two “closing up” curves for  $\mu_1$  and  $\mu_2$  disjoint. However, since there is just one long component over  $\sigma$  (and also over its slight outward perturbation), we see that the “closing up” curve for  $\mu_1$  must cross one of the graphs over  $\eta$  in  $\mu_2$ . Moreover, this intersection is

The proof of Lemma II.3.22:

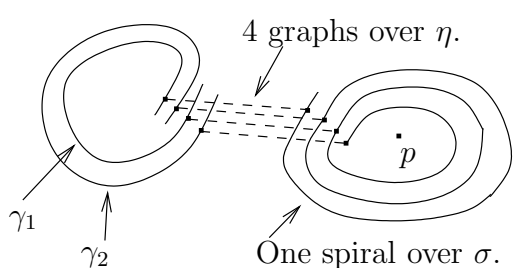


FIGURE 15. Two curves  $\gamma_1$  and  $\gamma_2$  in  $\Sigma_j$  spiral together over  $\gamma$ , but only one curve spirals over  $\sigma$ .

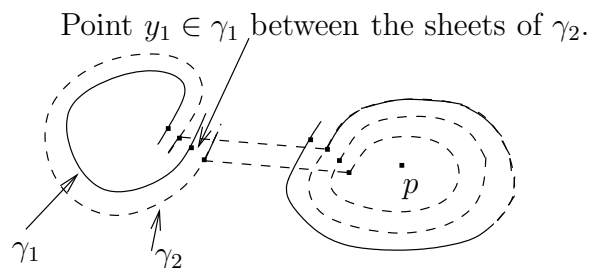


FIGURE 16. The (dashed) simple closed curve  $\mu_2$  in  $\Sigma_j$  has four parts:  
 A 1-valued graph over  $\gamma$  in  $\gamma_2$ .  
 A multi-valued graph over  $\sigma$ .  
 Two graphs over  $\eta$ .

transverse and the curves are otherwise disjoint. This implies that  $\mu_1$  and  $\mu_2$  have linking number one in  $\Sigma_j$ , which gives the desired contradiction.  $\square$

The contradiction for the proof of Lemma II.3.22:

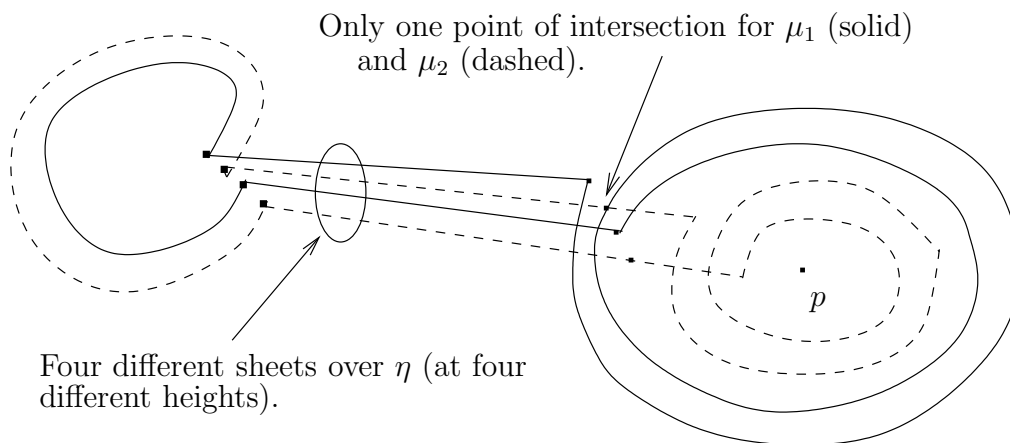


FIGURE 17. Repeating the construction with  $\gamma_1$  in place of  $\gamma_2$  gives a second simple closed curve  $\mu_1$ . Perturbing the 1-valued graph over  $\sigma$  slightly outside of  $\sigma$ ,  $\mu_1$  and  $\mu_2$  intersect in exactly one point and do so transversely. Hence,  $\mu_1$  and  $\mu_2$  have linking number one, which is impossible in the planar domain  $\Sigma_j$ .

Each  $\Sigma_j^g$  is a multi-valued graph over  $K$ , but can be thought of as a single-valued graph over a domain  $K_j$  in some covering space of  $K$ . However, this covering space may depend on  $j$ . Therefore, in order to apply the results of Appendix B, we need to pass to a subsequence so that:

- The  $K_j$ 's all lie in the same covering space  $\hat{K}$  (independent of  $j$ ).
- The  $K_j$ 's exhaust  $\hat{K}$ .

- The holonomy group of the covering space  $\hat{K}$  is  $\mathbf{Z}$  (the definition of the holonomy group is recalled below).

In order to achieve these three points, we need a few elementary facts about covering spaces. First, recall that a covering space  $\hat{\Pi} : \hat{K} \rightarrow K$  with base point  $x \in K$  is uniquely determined by the *holonomy homomorphism*  $\text{Hol}$  from  $\pi_1(K)$  to the automorphisms of the fiber  $\hat{\Pi}^{-1}(x)$ . To define this homomorphism, suppose that

$$\gamma : [0, 1] \rightarrow K \tag{II.3.23}$$

is a curve with  $\gamma(0) = \gamma(1) = x$  and  $\hat{x}$  is a point in  $\hat{\Pi}^{-1}(x)$ . The lifting property for covering spaces gives a unique lift<sup>13</sup>

$$\gamma_{\hat{x}} : [0, 1] \rightarrow \hat{K} \tag{II.3.24}$$

of  $\gamma$  with  $\gamma_{\hat{x}}(0) = \hat{x}$ . We define  $\text{Hol}(\gamma)(\hat{x})$  to be the endpoint  $\gamma_{\hat{x}}(1)$ . Finally, define the holonomy group to be the image  $\text{Hol}(\pi_1(K))$ .

We are now ready to prove that each oriented collapsed leaf is stable:

*Proof.* (of (2) in Proposition II.3.1). We will show that any connected open subset  $K \subset \Gamma$  that has compact closure in  $\Gamma$  and is sufficiently large must be stable. Since  $\Gamma$  can be exhausted by such  $K$ 's by Lemma A.1 in Appendix A, we will conclude that  $\Gamma$  itself is stable.

Fix a point  $x \in K$ . By repeatedly applying Corollary II.3.18 with  $\delta = 1/j$  and passing to a subsequence, we get a sequence of connected multi-valued graphs  $\Sigma_j^g$  over  $K$ , covering spaces  $\Pi_j : \hat{K}_j \rightarrow K$ , domains  $K_j \subset \hat{K}_j$ , and functions  $u_j : K_j \rightarrow \mathbf{R}$  with

$$|u_j| + |\nabla u_j| \leq 1/j, \tag{II.3.25}$$

so that there is a bijection from  $K_j$  to  $\Sigma_j^g$  given by

$$x \rightarrow \Pi_j(x) + u_j(x) \mathbf{n}_{\Gamma}(\Pi_j(x)). \tag{II.3.26}$$

Furthermore, (II.3.19) gives a point  $x_j \in \Sigma_j^g$  with  $\Pi_j(x_j) = x$  satisfying

$$\text{dist}_{\Sigma_j^g}(x_j, \partial \Sigma_j^g \setminus \Pi_j^{-1}(\partial K)) > j. \tag{II.3.27}$$

We must do two things in order to apply Corollary B.20 in Appendix B. Namely, we must pass to a subsequence so that the  $K_j$ 's all sit in the same covering space  $\hat{K}$  and we must show that the holonomy group of  $\hat{K}$  is  $\mathbf{Z}$ . Once we have done these, (II.3.27) will imply that the  $K_j$ 's exhaust  $\hat{K}$ .

We will deal with the second one first, i.e., we will show that the holonomy group is always  $\mathbf{Z}$ . This follows immediately from Corollary II.3.21. Namely, (2) in Corollary II.3.21 implies that the fiber over  $x$  in each  $K_j$  can be identified with  $\mathbf{Z}$  and the holonomy from circling the point  $p \in \mathcal{S}_{ulsc}$  is just  $n \rightarrow (n + 1)$  or  $n \rightarrow (n - 1)$ , depending on whether the multi-valued graph spirals up or down. Suppose now that  $\gamma$  is a simple closed curve through  $x$  representing a homotopy class  $[\gamma]$  in  $\pi_1(K)$ . Furthermore, (1A) and (1B) in Corollary II.3.21 imply that either:

- If (1A) holds, then  $\text{Hol}([\gamma])$  is the identity map, i.e.,  $n \rightarrow n$ .

---

<sup>13</sup>Recall that  $\gamma_{\hat{x}}$  is said to be a *lift* of  $\gamma$  if  $\gamma = \hat{\Pi} \circ \gamma_{\hat{x}}$ . The lifting property for covering spaces says that we get a unique lift of  $\gamma$  for each choice of point  $\hat{x}$  with  $\hat{\Pi}(\hat{x}) = x$ .

- If (1B) holds, then  $\text{Hol}([\gamma])$  maps to  $n \rightarrow (n \pm k)$ , where  $k$  is the number of disjoint curves spiralling together in (1B).

In particular, the image of the holonomy is always in  $\mathbf{Z}$  in either case.

Finally, we will use Lemma II.3.22 to prove that only a finite set of distinct covering spaces arise as one of the  $\hat{K}_j$ 's and, consequently, one of the  $\hat{K}_j$ 's occurs infinitely many times. We have already established that each holonomy group is  $\mathbf{Z}$ , but the covering space is determined by the holonomy homomorphism (and not just the group). Each holonomy homomorphism

$$\text{Hol}_j : \pi_1(K) \rightarrow \mathbf{Z} \tag{II.3.28}$$

is determined by the image of a fixed (finite) set of generators  $\gamma_1, \dots, \gamma_m$  of  $\pi_1(K)$ , so we need only to show a uniform bound for  $\text{Hol}_j(\gamma_n)$  for every  $j$  and  $n$ . However, (1B) in Corollary II.3.21 implies that  $\text{Hol}_j(\gamma_n)$  is just the number of disjoint (long) curves spiralling together in  $\Pi_j^{-1}(\gamma_n)$  and Lemma II.3.22 bounds this uniformly, completing the proof.  $\square$

**Remark II.3.29.** We have assumed throughout this subsection that the leaf  $\Gamma$  is oriented. When this is not the case, the same argument applies to show that the oriented double cover is stable.

**II.3.4. Property (3) of Proposition II.3.1: Opposite orientations at distinct points of  $\Gamma_{Clos} \cap \mathcal{S}_{ulsc}$ .**

*Proof.* (of (3) in Proposition II.3.1). We must show that if  $p$  and  $q$  are distinct points in  $\Gamma_{Clos} \cap \mathcal{S}_{ulsc}$ , then the multi-valued graphs in  $\Sigma_j$  near  $p$  spiral in the opposite direction as the ones near  $q$ . Since there are only two possible directions, this implies that  $\Gamma_{Clos} \cap \mathcal{S}_{ulsc}$  contains at most two points (if there were three such points, then two would have to be oriented the same way which we will show is impossible).

We will argue by contradiction, so suppose that the multi-valued graphs near  $p$  and  $q$  have the same orientation. In this case, we can choose a closed “figure eight” curve  $\gamma_j$  in  $\Sigma_j$  with the following properties (see Figure 18):

- $\gamma_j$  is a graph over a fixed (immersed) figure eight curve  $\gamma$  in  $\Gamma$  which circles  $p$  and  $q$  in opposite directions. Let  $r \in \gamma$  be the double point where  $\gamma$  is not embedded.
- The two points in  $\gamma_j$  above the double point  $r$  are in distinct sheets of  $\Sigma_j$ ; hence  $\gamma_j$  is embedded.

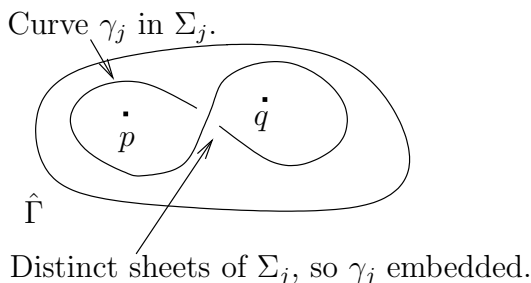


FIGURE 18. The figure eight curves  $\gamma^j$  in  $\Sigma_j$ .

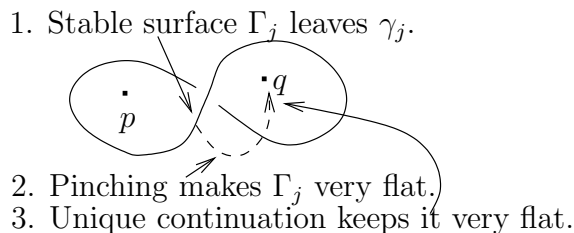


FIGURE 19. The stable surface  $\Gamma_j$  would be forced to cross an axis.

The second condition has a very useful consequence. Namely, the unit normal to  $\Sigma_j$  is always either upward or downward pointing along  $\gamma_j$  since  $\Sigma_j$  is graphical along  $\gamma_j$ ; therefore, elementary topology implies that:

- The two points in  $\gamma_j$  above  $r$  are separated by an oppositely-oriented sheet of  $\Sigma_j$ .

We will now use these properties of the  $\gamma_j$ 's to find stable minimal surfaces  $\Gamma_j$  disjoint from the  $\Sigma_j$ 's which contain a graph near either  $p$  or  $q$ , contradicting that these points are in  $\mathcal{S}_{ulsc}$ . Since  $\Sigma_j$  has genus zero, the curve  $\gamma_j$  separates in  $\Sigma_j$ ; let  $\Sigma_j^+$  be one of the two components of  $\Sigma_j \setminus \gamma_j$ . Since  $B_{R_j} \setminus \Sigma_j$  is mean convex in the sense of Meeks-Yau, the existence theory of [MeYa2] gives a stable embedded minimal planar domain

$$\Gamma_j^+ \subset B_{R_j} \setminus \Sigma_j \text{ with } \partial\Gamma_j^+ = \partial\Sigma_j^+. \quad (\text{II.3.30})$$

Let  $\Gamma_j$  be the component of  $\Gamma_j^+$  with  $\gamma_j \subset \partial\Gamma_j$ . Using estimates for stable surfaces ([Sc1], cf. [CM2]) and the fact that  $\gamma_j$  is a figure eight, it is now not hard to see that  $\Gamma_j$  must contain a graph near either  $p$  or  $q$  (see Figure 19). This can be seen as follows:

1. After leaving the upper portion of  $\gamma_j$  over  $r$ , the stable surface  $\Gamma_j$  is separated from the lower portion of  $\gamma_j$  by an oppositely oriented sheet of  $\Sigma_j$  and, hence,  $\Gamma_j$  has an a priori curvature bound there by [Sc1], cf. [CM2].

To see that  $\Gamma_j$  does indeed leave the upper portion of  $\gamma_j$  over  $r$ , intersect  $\Gamma_j$  with a large transverse<sup>14</sup> ball  $B_R(z)$  to get a collection of closed curves and one segment  $\sigma_j$  where  $\sigma_j$  connects the upper and lower portions of  $\gamma_j$  (see Figure 20). Since these are separated near  $r$  by an oppositely-oriented sheet of  $\Sigma_j$ , the segment  $\sigma_j$  moves away from  $\gamma_j$  as desired.

2. Away from the singular points  $p$  and  $q$ , the surface  $\Gamma_j$  is locally pinched between sheets of  $\Sigma_j$ . Combining this pinching with the curvature bound from 1. implies that  $\Gamma_j \rightarrow \Gamma$  away from  $p$ ,  $q$ , and  $\gamma_j$ . (Here “away” is with respect to distance along paths in  $B_{R_j} \setminus \Sigma_j$ .)
3. Combining the a priori bound of 1. with the flatness given by 2., unique continuation forces  $\Gamma_j \rightarrow \Gamma_{Clos}$  even as it approaches  $p$  or  $q$  (this unique continuation argument is spelled out in lemma II.1.38 in [CM5]). However, the one-sided curvature estimate, i.e., Theorem I.1.3, would then apply to the  $\Sigma_j$ 's near  $p$  or  $q$ , contradicting that  $|A| \rightarrow \infty$  near  $p$  and  $q$ .

This contradiction shows that the multi-valued graphs near  $p$  and  $q$  are oppositely-oriented, completing the proof of (3).  $\square$

This completes the proof of Proposition II.3.1.

**Remark II.3.31.** The genus bound on the  $\Sigma_j$ 's can be used to directly see that  $\Gamma_{Clos} \cap \mathcal{S}_{ulsc}$  cannot contain three points. To see this, suppose that  $p, q$ , and  $r$  are three distinct points in  $\Gamma_{Clos} \cap \mathcal{S}_{ulsc}$  and  $\gamma_{pq}$  is a geodesic in  $\Gamma$  from  $p$  to  $q$ . For  $j$  large, Theorem I.1.6 allows us to find simple closed curves  $\gamma_{pq}^j \subset \Sigma_j$  with the following properties:

- $\gamma_{pq}^j$  is contained in the  $\epsilon$ -tubular neighborhood of  $\gamma_{pq}$ .
- $\gamma_{pq}^j \setminus (B_\epsilon(p) \cup B_\epsilon(q))$  consists of two graphs over  $\gamma_{pq}$  which are in distinct sheets of  $\Sigma_j$ .

<sup>14</sup>The application of transversality uses the regularity of  $\tilde{\Gamma}_j$  up to the interior of  $\tilde{\gamma}$ . Local boundary regularity was established for two-dimensional minimal surfaces in [Hi].

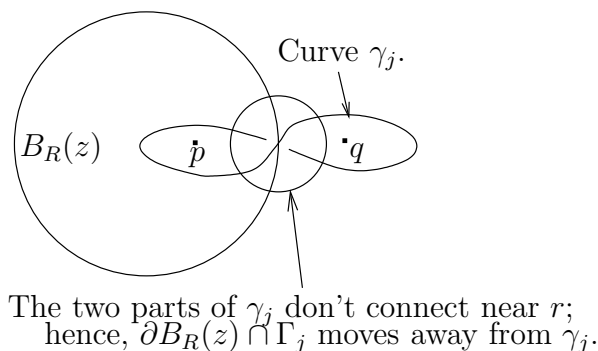


FIGURE 20. The stable surface moves away from its boundary near  $r$ .

Since  $\Sigma_j$  has genus zero, the curve  $\gamma_{pq}^j$  must separate  $\Sigma_j$  into two distinct components. However, it is easy to see that this is impossible by using the local connecting property near the third point  $r$ . Namely, we can take two points near  $p$  on opposite sides of  $\gamma_{pq}^j$  and connect each of them to  $B_\epsilon(r)$  by curves in  $\Sigma_j$  which do not intersect  $\gamma_{pq}^j$ . These two curves can then be connected to each other in  $B_\epsilon(r) \cap \Sigma_j$ , giving the desired contradiction.

### Part III. When the surfaces are ULSC: The proof of Theorem 0.9

In this part, we will prove Theorem 0.9, i.e., the main structure theorem for ULSC sequences where  $\mathcal{S}_{neck} = \emptyset$ . The key will be to analyze the ULSC singular set  $\mathcal{S}_{ulsc}$  and, in particular, the collapsed leaves of  $\mathcal{L}'$ . Although the emphasis will be on the ULSC case, many of the arguments will actually apply to a neighborhood of a collapsed leaf whose closure does not intersect  $\mathcal{S}_{neck}$ . This will be used later when we analyze the general case.

In the previous section, we showed that a collapsed leaf  $\Gamma$  of  $\mathcal{L}'$  is a stable, incomplete minimal surface with isolated removable singularities at points in  $\mathcal{S}_{ulsc}$ . In general,  $\Gamma$  may have worse singularities at points of  $\Gamma_{clos} \cap \mathcal{S}_{neck}$ , but we will assume that  $\Gamma_{clos} \cap \mathcal{S}_{neck} = \emptyset$  in this part.

In addition to what we have shown in the previous section, we need to establish two facts to complete the proof of Theorem 0.9. First, we must show that every collapsed leaf is a plane (it then follows easily from embeddedness that all of these planes are parallel). Since we have shown in Proposition II.3.1 that the collapsed leaves are stable with isolated removable singularities at each point of  $\mathcal{S}_{ulsc}$ , this follows easily from the Bernstein theorem for complete stable surfaces in  $\mathbf{R}^3$ . The second additional fact that must be established is the “properness” of the limit in the sense of [CM7]. Roughly speaking, the local cone property already implies that the closed set  $\mathcal{S}$  is contained in two Lipschitz curves each of which is transverse to the limit planes. The properness consists of showing that  $\mathcal{S}$  actually fills out these curves completely, i.e., there cannot be a first or last point in  $\mathcal{S}$ . See  $(\star)$  in Section III.1 for the precise statement. As in [CM7], we will prove properness by showing that the vertical flux of a potential non-proper limit would have to be positive, which is impossible by Stokes’ theorem.

All of this will show the following:

- The ULSC sequence of surfaces converges to the foliation by parallel planes

$$\mathcal{F} = \{x_3 = t\}_t \tag{III.0.1}$$

- away from the singular set  $\mathcal{S}$ .
- $(C_{ulsc})$  from Theorem 0.9 holds.
  - $(D'_{ulsc})$ :  $\mathcal{S}$  consists of two disjoint Lipschitz graphs  $\mathcal{S}_1 : \mathbf{R} \rightarrow \mathbf{R}^3$  and  $\mathcal{S}_2 : \mathbf{R} \rightarrow \mathbf{R}^3$  over the  $x_3$ -axis.

From this, it follows immediately from the main theorem of [Me1] that  $\mathcal{S}_1$  and  $\mathcal{S}_2$  are in fact straight lines *orthogonal* to the leaves of the foliation, giving  $(D_{ulsc})$  from Theorem 0.9 and completing the proof of Theorem 0.9.

Recall that collapsed leaves are the leaves of  $\mathcal{L}'$  that “go through” a point of  $\mathcal{S}_{ulsc}$ , i.e., that contain the local leaf  $\Gamma_x$  given by Lemma II.2.3 for some  $x \in \mathcal{S}_{ulsc}$ ; see Definition II.2.9. The next proposition establishes the key properties of a collapsed leaf in the ULSC case:

**Proposition III.0.2.** Suppose that  $\Gamma$  is a collapsed leaf of  $\mathcal{L}'$ . If  $\Gamma_{Clos} \cap \mathcal{S}_{neck} = \emptyset$ , then

- (1)  $\Gamma_{Clos}$  is a plane.

If, in addition,  $\mathcal{S}_{neck} = \emptyset$  (i.e., the sequence is ULSC), then

- (2)  $\Gamma_{Clos}$  intersects  $\mathcal{S}_{ulsc}$  in exactly two points and the multi-valued graphs in the  $\Sigma_j$ 's spiral in opposite directions around the two corresponding axes (see Figure 8).

This proposition will be proven over the rest of this section.

**III.0.5. Property (1) in Proposition III.0.2: Collapsed leaves are planar.** To prove that  $\Gamma$  is flat, we first use property (3) in Proposition II.3.1 to see that  $\Gamma_{Clos}$  is the union of  $\Gamma$  together with at most two points in  $\mathcal{S}_{ulsc}$  since we are assuming that  $\Gamma_{Clos} \cap \mathcal{S}_{neck} = \emptyset$ . In particular, since each point in  $\Gamma_{Clos} \cap \mathcal{S}_{ulsc}$  is a removable singularity by (1) in Proposition II.3.1, we conclude that  $\Gamma_{Clos}$  is a smooth complete surface without boundary.

Assuming first that  $\Gamma$  is oriented, (2) in Proposition II.3.1 implies that  $\Gamma$  is stable. We can then use a standard logarithmic cutoff argument at each point in  $\Gamma_{Clos} \setminus \Gamma$  to conclude that  $\Gamma_{Clos}$  is itself stable. The Bernstein theorem for stable complete minimal surfaces, [FiSc], [DoPe], then implies that  $\Gamma_{Clos}$  is a plane, as desired. When  $\Gamma$  is not oriented, the preceding discussion applies to show that its oriented double cover is flat – and hence so is  $\Gamma$ . The obvious details are left to the reader.

**III.0.6. Property (2) in Proposition III.0.2: Ruling out just one point of  $\mathcal{S}_{ulsc}$  in a leaf.** In contrast to property (1), we will need to use that the sequence is ULSC in order to prove (2). We will later see that this assumption can be removed. However, the argument we will give to prove (2) in general will use the ULSC case that we are proving now (this is why we are not proving the general case directly).

We have shown in property (3) of Proposition II.3.1 that the closure of a collapsed leaf contains at most two ULSC singular points and that the  $\Sigma_j$ 's spiral in opposite directions around two such points. Hence, to prove (2) in Proposition III.0.2, we must show that  $\Gamma_{Clos}$  cannot intersect  $\mathcal{S}$  in just one point.

Before proving (2), we need to recall a useful property of stable minimal surfaces. Namely, the following lemma shows that a stable surface that starts out on one side of a plane where the interior boundary is in a small ball is graphical away from its boundary (see Figure 21):

**Lemma III.0.3.** There exists a small constant  $0 < \delta < 1$  so that if  $r_0 < \delta R_0$  and  $\Gamma \subset B_{R_0}$  is a connected embedded stable minimal planar domain with non-empty inner boundary

$\gamma = \partial\Gamma \setminus \partial B_{R_0}$  contained in the small ball  $B_{\delta r_0}$ , outer boundary  $\partial\Gamma \setminus B_{\delta r_0}$  non-empty, and

$$B_{r_0} \cap \Gamma \cap \{x_3 = 0\} = \emptyset, \tag{III.0.4}$$

then  $\Gamma$  contains a graph over the annulus  $D_{\delta R_0} \setminus D_{r_0} \subset \{x_3 = 0\}$ . Moreover, this graph can be connected to the inner boundary  $\gamma$  by a curve in  $B_{2r_0} \cap \Gamma$ .

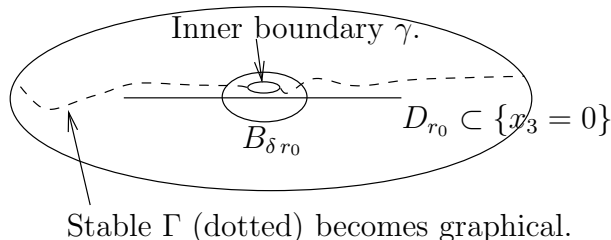


FIGURE 21. Lemma III.0.3: The stable surface  $\Gamma$  starts off close to - but above - a disk and is forced to become graphical.

*Proof.* The proof has two steps. Namely, we first show that  $\Gamma$  contains an initial graph over a small annulus on the scale of  $\delta r_0$ . The next step uses the initial graph to apply the “stable graph proposition” - Proposition D.2 in Appendix D - to get the desired graph over the large annulus  $D_{\delta R_0} \setminus D_{r_0}$ .

Producing the initial graph: Observe first that the a priori curvature estimates for stable surfaces of [Sc1], [CM2] and the gradient estimate imply that each point in  $\Gamma$  close to  $D_{r_0}$  - but outside of  $B_{2\delta r_0}$  - is graphical (see, e.g., lemma I.0.9 in [CM3] for a precise statement and proof). Moreover, a standard catenoid barrier argument (lemma 3.3 in [CM8]) guarantees the existence of such “low points” that can be connected to the inner boundary  $\gamma$  by a curve in  $B_{2C_1\delta r_0} \cap \Gamma$ . Starting from one such low point, we can then build up a graph  $\Gamma^g$  over the annulus  $D_{2C_1\delta r_0} \setminus D_{C_1\delta r_0}$  by applying the Harnack inequality a fixed number of times, thereby staying low as we go around (we get a graph and not a multi-valued graph since the surface  $\Gamma$  is embedded and does not spiral infinitely).<sup>15</sup>

Applying Proposition D.2 to get the graph from  $r_0$  to  $\delta R_0$ : Let  $\hat{\gamma}$  be the graph in  $\Gamma^g$  defined over the inner boundary  $\partial D_{C_1\delta r_0}$ . The simple closed curve  $\hat{\gamma}$  separates the planar domain  $\Gamma$  into two components; let  $\Gamma_{Clos}$  be the “outer” one, so that  $\gamma$  is not in  $\partial\Gamma_{Clos}$ . Since the tubular neighborhood  $An_{C_1\delta r_0}(\hat{\gamma})$  of radius  $C_1\delta r_0$  of  $\hat{\gamma}$  in  $\Gamma_{Clos}$  is contained in the graph  $\Gamma^g$ , we get uniform bounds for the area and total curvature of  $An_{C_1\delta r_0}(\hat{\gamma})$ . We can now apply Proposition D.2 to  $\hat{\gamma}$  to get a graph in  $\Gamma$  defined over the annulus  $D_{R_0/\omega} \setminus D_{\omega C_1\delta r_0}$ . The lemma follows by taking  $\delta > 0$  sufficiently small.  $\square$

We note next that the local cone property has two important consequences for the singular set  $\mathcal{S}_{ulsc}$ , and in particular, for how the singular set changes as we move from one collapsed leaf to the next:

- (S1)  $\mathcal{S}_{ulsc}$  cannot run off to infinity.
- (S2) Distinct points of  $\mathcal{S}_{ulsc}$  in a collapsed leaf cannot combine in another collapsed leaf.

<sup>15</sup>The constant  $C_1$  depends on the constants from the Harnack inequality and lemma 3.3 in [CM8] but is independent of  $\delta$ .

*Proof.* (of property (2) in Proposition III.0.2). To prove that  $\Gamma_{Clos} \cap \mathcal{S}_{ulsc}$  contains exactly two points, suppose for a moment that there was only one singular point (there is always at least one by definition). In particular, after a translation and rotation of  $\mathbf{R}^3$ , we may suppose that

$$\Gamma_{Clos} \cap \mathcal{S}_{ulsc} = \{0\}. \quad (\text{III.0.5})$$

and the collapsed leaf through 0 is the punctured horizontal plane  $\{x_3 = 0\} \setminus \{0\}$ . We will show that (III.0.5) implies that every leaf of  $\mathcal{L}'$  is a plane with one point removed, these planes foliate  $\mathbf{R}^3$ , and as a consequence the intersection of any fixed ball with the surfaces  $\Sigma_j$  is simply connected for  $j$  sufficiently large. However, this is impossible since we have assumed an upper bound for the injectivity radii of the  $\Sigma_j$ 's in Theorem 0.9, so we conclude that (III.0.5) cannot hold.

Properness: We will show next that every open neighborhood of  $\{x_3 = 0\}$  contains points of  $\mathcal{S}_{ulsc}$  both above and below  $\{x_3 = 0\}$ ; the proof will use only that  $\Gamma_{Clos} \cap \mathcal{S}_{neck} = \emptyset$ . We called this properness in [CM6] and the argument is essentially the same, with one caveat: [CM6] argues for embedded minimal disks, whereas presently we only know that the  $\Sigma_j$ 's are ULSC near 0. The disk hypothesis was used for two things in [CM6]:

- (D1) The  $\Sigma_j$ 's are multi-valued graphs in the cone  $\{|x_3| < \mu|x|\}$  for some  $\mu > 0$ .
- (D2) The portions of these two multi-valued graphs in a fixed ball combine to be part of a single embedded minimal disk in this small ball (this disk property was used in [CM6] to apply Stokes' theorem).

The second fact (D2) holds in this case since  $0 \in \mathcal{S}_{ulsc}$ . The first fact (D1) will follow immediately from the one-sided curvature estimate once we establish the following scale invariant ULSC property:

- (D) There exists  $\tau > 0$  so that, for  $z \in \{x_3 = 0\}$  and  $j$  large, each component of  $B_{\tau|z|}(z) \cap \Sigma_j$  that connects to the multi-valued graph in  $\Sigma_j$  is a disk.

We will next prove (D) by contradiction, using a variation of the ‘‘between the sheets’’ estimate of [CM3]. To do this, assume that  $\tau > 0$  is small and  $z \in \{x_3 = 0\}$  is the first time that (D) fails (i.e.,  $|z|$  is minimal); obviously, we must have  $|z| > r_0$  since the  $0 \in \mathcal{S}_{ulsc}$ . Fix a sequence of simple closed non-contractible curves  $\gamma_j \subset B_{\tau|z|}(z) \cap \Sigma_j$ . We will see that this leads to a contradiction:

- (1) See Figure 22. The existence results of Meeks-Yau, [MeYa2], gives stable embedded connected minimal surfaces  $\Gamma_j \subset B_{R_j} \setminus \Sigma_j$  with  $\partial\Gamma_j \setminus \partial B_{R_j} = \gamma_j$  and  $\partial\Gamma_j \cap \partial B_{R_j} \neq \emptyset$ .<sup>16</sup> Since these stable surfaces start out on one side of, but close to, the multi-valued graphs in  $\Sigma_j$  converging to  $\{x_3 = 0\} \setminus \{0\}$ , Lemma III.0.3 implies that the  $\Gamma_j$ 's quickly become graphical.
- (2) See Figure 23. The portion  $\Sigma_j^+$  of  $\Sigma_j$  between  $\partial B_{|z|/2} \cap \{x_3 = 0\}$  and the graph in  $\Gamma_j$  must be simply connected in extrinsic balls of radius  $\tau|z|/2$  since it is trapped ‘‘between the sheets’’ of the multi-valued graph in  $\Sigma_j$  and the graph in  $\Gamma_j$  (and these two can be connected). Namely, if  $\Sigma_j^+$  contained a non-contractible curve in an extrinsic ball of radius  $\tau|z|/2$  centered there, then we could apply [MeYa2] to get a second stable surface  $\tilde{\Gamma}_j$  disjoint from both  $\Sigma_j$  and  $\Gamma_j$ . The surface  $\tilde{\Gamma}_j$  would be forced to become graphical (again by Lemma III.0.3) but would then have to cross

<sup>16</sup>This is a standard application of [MeYa2]; see, e.g., lemma 3.1 in [CM8] for details.

the curve in  $\Sigma_j \cup \Gamma_j$  which connects the two graphical regions. (Compare the proof of theorem I.0.8 in [CM3].)

- (3) Since each ball of radius  $\tau|z|/2$  centered on  $\Sigma_j^+$  is simply connected by (2), the set  $\Sigma_j^+$  is locally graphical by the one-sided curvature estimate and, since it contains a multi-valued graph but cannot pass through  $\Gamma_j$ , it spirals infinitely. This is impossible since each  $\Sigma_j$  is compact, giving the contradiction needed to establish (D).

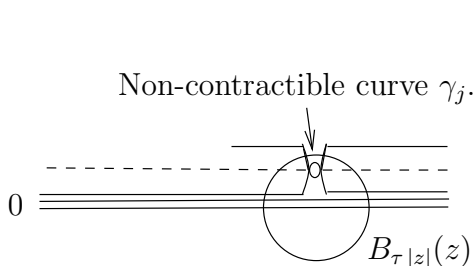


FIGURE 22. The stable surface  $\Gamma_j$  is dotted.

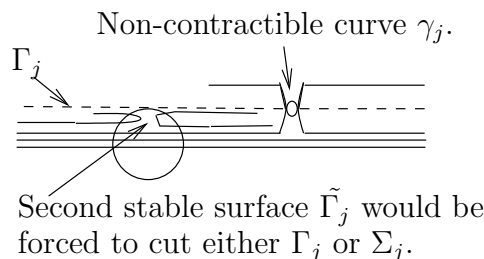


FIGURE 23.  $\Sigma_j$  is simply connected between the multi-valued graph in  $\Sigma_j$  and the graph in  $\Gamma_j$ .

Now that we have established (D), we can argue precisely as in [CM6] using [CM7] (see lemma I.1.10 there) to prove that every open neighborhood of this plane contains points of  $\mathcal{S}_{ulsc}$  both above and below this plane.

It follows easily from this properness - as in [CM6] - that an entire slab  $\{-\epsilon < x_3 < \epsilon\}$  must be foliated by (the closures of) planar leaves of  $\mathcal{L}'$ . In order to extend this foliated structure to all of  $\mathbf{R}^3$ , we will need to use the ULSC assumption next.

Using the ULSC hypothesis to repeat the argument: Since the set  $\mathcal{S}_{ulsc}$  is automatically closed and transverse to these planes (by the one-sided curvature estimate), we see that a neighborhood of this plane is foliated by parallel planes and, in this neighborhood,  $\mathcal{S}_{ulsc}$  is a single Lipschitz curve. However, since the constant  $\tau > 0$  was uniform and did not depend on the particular singular point, we can now repeat the above argument to extend the set of foliated planes to the whole of  $\mathbf{R}^3$ . Once we have the foliation by parallel planes, the ULSC condition and one-sided curvature estimate imply that  $\mathcal{S}_{ulsc}$  is a discrete collection of transverse Lipschitz curves. The transversality implies that each curve hits every leaf and hence there is only one curve. In sum, the sequence is converging to a foliation of  $\mathbf{R}^3$  by parallel planes away from a single Lipschitz curve  $\mathcal{S}_{ulsc}$  transverse to the planes. (This was exactly the result of [CM3]–[CM6] for sequences of disks.) This has two consequences:

- Near  $\mathcal{S}_{ulsc}$ , the sequence looks like a double spiral staircase.
- Away from  $\mathcal{S}_{ulsc}$ , the sequence is locally converging (with bounded curvature) to a foliation by parallel planes.

The second fact allows us to extend the double spiral staircase structure away from the singular curve  $\mathcal{S}_{ulsc}$ , so that we get a sequence  $R'_j \rightarrow \infty$  where the component of  $B_{R'_j} \cap \Sigma_j$  intersecting  $B_{R'_j/C}$  is a double spiral staircase. In particular, this component is also a disk. Since we have assumed that no such sequence of expanding disks in  $\Sigma_j$  exists, we rule out (III.0.5) as promised.  $\square$

## III.1. PROPERNESS AND THE LIMIT FOLIATION

We have now shown that each collapsed leaf is a plane that is transverse to  $\mathcal{S}_{ulsc}$  (with a definite lower bound on the angle of intersection). As in [CM6], we must show that nearby leaves are also planes; we call this *properness* of the limit foliation. Since each singular point in  $\mathcal{S}_{ulsc}$  has a plane through it, this properness will follow from showing that there cannot be a first or last such singular point. In fact, it is not hard to see that these properties are equivalent. Namely, a planar leaf nearby a collapsed leaf must also contain singular points since otherwise the one-sided curvature estimate would give a curvature bound at the singular point in the collapsed leaf. In [CM6], a similar properness for disks (where each plane had only one puncture as opposed to the current situation of two) was proven using [CM7].

Before giving the precise statement of properness, observe that we can rotate  $\mathbf{R}^3$  so that the closure of each collapsed leaf of  $\mathcal{L}'$  is a horizontal plane, i.e., is given by  $\{x_3 = t\}$  for some  $t \in \mathbf{R}$ . This is because the closure of each collapsed leaf is some plane by Proposition III.0.2 and these planes must all be parallel since the surfaces  $\Sigma_j$  are embedded. With this normalization, the precise statement of properness is:

( $\star$ ) If  $t \in x_3(\mathcal{S}_{ulsc})$  and  $\epsilon > 0$ , then  $\mathcal{S} \cap \{t < x_3 < t + \epsilon\} \neq \emptyset$  and  $\mathcal{S} \cap \{t - \epsilon < x_3 < t\} \neq \emptyset$ .

We should point out that when the sequence is ULSC, ( $\star$ ) automatically implies that  $\{x_3 = s\} \cap \mathcal{S}_{ulsc}$  contains at least two points (cf. (S1) and (S2)). Namely, once  $\{x_3 = s\} \cap \mathcal{S}_{ulsc}$  contains one point  $p'$ , then Proposition III.0.2 implies that there is a second point  $q' \in \{x_3 = s\} \cap \mathcal{S}_{ulsc}$  so that

$$\{x_3 = s\} \setminus \{p', q'\} \tag{III.1.1}$$

is a collapsed leaf of  $\mathcal{L}'$ .

As in [CM6] and [CM7], the key to proving ( $\star$ ) is a careful analysis of the vertical flux of the multi-valued graphs. Recall that if  $\Sigma$  is a minimal surface and  $\sigma \subset \Sigma$  is a simple closed curve, then the vertical flux across  $\sigma$  is

$$\int_{\sigma} \frac{\partial x_3}{\partial n}, \tag{III.1.2}$$

where  $\frac{\partial x_3}{\partial n}$  is the derivative of  $x_3$  in the direction normal to  $\sigma$  but tangent to  $\Sigma$ . By Stokes' theorem, the integral (III.1.2) depends only on the homology class of  $\sigma$  since the coordinate function  $x_3$  is harmonic on a minimal surface.

We will prove ( $\star$ ) by contradiction as we now outline: If ( $\star$ ) does not hold for  $t = 0$ , then we can assume, after possibly reflecting across  $\{x_3 = 0\}$ , that

$$\mathcal{S} \cap \{0 < x_3 < \epsilon\} = \emptyset. \tag{III.1.3}$$

We will use this to show that there is a unique leaf  $\Sigma$  of  $\mathcal{L}'$  which spirals into the plane  $\{x_3 = 0\}$  from above and this leaf is a multiplicity one limit of the  $\Sigma_j$ 's. Moreover, near the singular points in  $\{x_3 = 0\}$ ,  $\Sigma$  will be a double spiral staircase which spirals infinitely into the plane; see Figure 24. The ends of  $\Sigma$  coming from circling both double spiral staircases will be graphs lying above the plane  $\{x_3 = 0\}$ ; we will see that this implies that each such end has non-negative vertical flux. This structure of the ends also allows us to cutoff  $\Sigma$  below a carefully chosen horizontal plane  $\{x_3 = \epsilon\}$ ; it will be almost automatic that the boundary curve produced has positive vertical flux. Using the fact that the plane  $\{x_3 = 0\}$  contains two points of  $\mathcal{S}_{ulsc}$ , we will find a sequence of separating curves in  $\Sigma$  whose vertical flux goes

to zero. This gives a sequence of compact domains in  $\Sigma$  bounded at the top by a curve in the plane  $\{x_3 = \epsilon\}$  with positive flux, bounded at the bottom by curves with flux going to 0, and with boundary curves on the sides with non-negative flux. Combining all of this will give the desired contradiction since, by Stokes' theorem, the total flux of any compact domain must sum to zero.

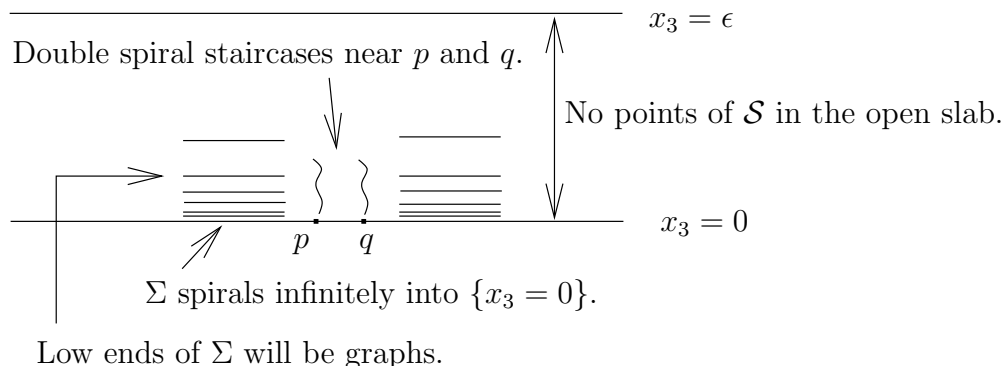


FIGURE 24. The limit  $\Sigma$  when properness fails.

There are in general two ways to show that the vertical flux in (III.1.2) is small; one can either show that the curve  $\sigma$  is short (since  $|\nabla x_3| \leq 1$ ) or show that  $|\nabla x_3|$  is small and the length of  $\sigma$  is bounded. Since the length of any closed non-contractible curve near  $\{x_3 = 0\}$  is bounded away from zero, we must take the second approach here to bound the flux of the bottom boundary curves (we will use the first approach in the next part near points in  $\mathcal{S}_{neck}$ ). In our application, the harmonic function  $x_3$  will be positive on the surface  $\Sigma$  and the estimate on  $|\nabla x_3|$  will follow from the gradient estimate.

**III.1.1. Establishing properness: The proof of  $(\star)$ .** The next lemma shows that  $(\star)$  holds as long as we have properties (1) and (2) in Proposition III.0.2. In particular, since these properties always hold when the sequence is ULSC, we get  $(\star)$  in the ULSC case.

**Lemma III.1.4.** If (1) and (2) in Proposition III.0.2 hold, then  $(\star)$  holds. That is, if the horizontal plane  $\{x_3 = t\}$  is the closure of a collapsed leaf satisfying (2) in Proposition III.0.2, and  $\epsilon > 0$ , then

$$\mathcal{S} \cap \{t < x_3 < t + \epsilon\} \neq \emptyset \text{ and } \mathcal{S} \cap \{t - \epsilon < x_3 < t\} \neq \emptyset. \tag{III.1.5}$$

*Proof.* For simplicity, we will assume that the  $\Sigma_j$ 's have genus zero. The general case follows with easy modifications.

We will argue by contradiction, so suppose that  $\mathcal{S}_{ulsc} \cap \{x_3 = 0\} = \{p, q\}$ ,  $\epsilon > 0$ , and

$$\mathcal{S} \cap \{0 < x_3 < \epsilon\} = \emptyset. \tag{III.1.6}$$

Fix a radius  $R > 0$  so that the disk  $D_R \subset \{x_3 = 0\}$  contains both  $p$  and  $q$ .

We will first record four consequences of (III.1.6) that will be proven below and then use these properties to rule out the possibility of such a non-proper limit (see Figure 25):

- (P1) There is exactly one leaf  $\Sigma$  of  $\mathcal{L}'$  in  $\{x_3 > 0\}$  whose closure intersects the plane  $\{x_3 = 0\}$ . This leaf  $\Sigma$  is a multiplicity one limit of the  $\Sigma_j$ 's. Furthermore, after possibly reducing  $\epsilon > 0$ , the leaf  $\Sigma$  is proper in compact subsets of  $\{0 < x_3 < \epsilon\}$ .

- (P2) Each “low” end of  $\Sigma$  is an asymptotic graph with non-negative vertical flux. Here “low” will be made precise below but roughly means starting off close to  $\{x_3 = 0\}$  over the disk  $D_R$  containing  $p$  and  $q$ .
- (P3) Intersecting  $\Sigma$  with a carefully chosen horizontal plane where  $x_3$  is constant will give a vertically separating curve  $\gamma_+ \subset \Sigma$  with positive vertical flux. Here *vertically separating* means that if a curve in  $\overline{\Sigma}$  is over  $D_R$  and intersects both of

$$\{x_3 = 0\} \text{ and } \{x_3 = \epsilon\}, \quad (\text{III.1.7})$$

then the curve also intersects  $\gamma_+$ .

- (P4) There is a sequence of vertically separating curves  $\gamma_i \subset B_1 \cap \Sigma$  with  $x_3(\gamma_i) \rightarrow 0$  and vertical flux going to zero.

(P3): Intersecting with a plane between two ends gives a curve  $\gamma_+$  that is vertically separating and has positive flux.

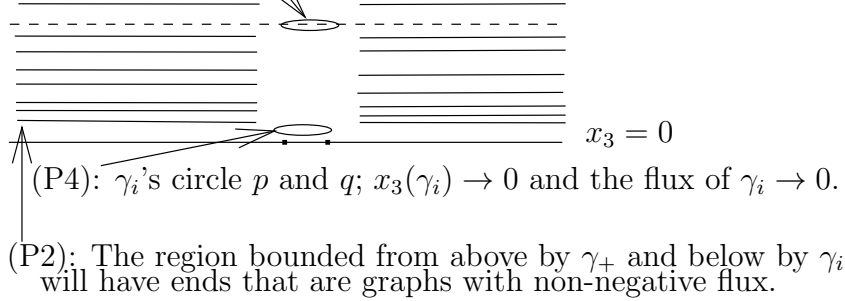


FIGURE 25. Properties (P2)–(P4) of  $\Sigma$  when properness fails.

The proof of (P1). Since  $p$  and  $q$  are locally the last points in  $\mathcal{S}_{ulsc}$ , we are in case (L2) in the proof of Lemma II.3.3 near  $p$  and  $q$  (cf. the “not proper” example (N-P)). Consequently, Lemma II.3.4 implies that near  $p$  and  $q$ , but above  $\{x_3 = 0\}$ , the  $\Sigma_j$ 's converge with multiplicity one to double spiral staircases which spiral infinitely into  $\{x_3 = 0\}$ .<sup>17</sup> In particular, only one leaf  $\Sigma$  of  $\mathcal{L}$  (namely, the one containing these double spiral staircases) can spiral into  $D_R \subset \{x_3 = 0\}$  from above. It remains to show that if  $\Sigma' \subset \{x_3 > 0\}$  is a leaf of  $\mathcal{L}$  that contains a point  $q' \in \{x_3 = 0\}$  in its closure  $\overline{\Sigma'}$ , then  $\Sigma' = \Sigma$ . This has already been established when  $q'$  is near  $p$  or  $q$  since there is only leaf there (cf. the chord arc property of Theorem I.1.6). However, this easily gives the general case. Namely, first fix a compact disk

$$\overline{D_S} = \{x_1^2 + x_2^2 \leq S^2\} \cap \{x_3 = 0\}. \quad (\text{III.1.8})$$

containing  $p$ ,  $q$ , and  $q'$ . Since, by assumption (see (1) in Proposition III.0.2), we have that  $\overline{D_S} \cap \mathcal{S}_{neck} = \emptyset$ , an easy compactness argument and the convex hull property give some  $r_1 > 0$  so that

$$\text{each component of } B_{r_1}(y) \cap \Sigma_j \text{ is a disk for every } y \in \overline{D_S}. \quad (\text{III.1.9})$$

Hence, by the one-sided curvature estimate, the  $\Sigma_j$ 's are locally graphical in a cylindrical slab about  $\{x_3 = 0\}$  and over  $D_S$ , as long as we stay away from  $p$  and  $q$ . If we now choose

<sup>17</sup>This is proven within the proof of Lemma II.3.4.

a point  $\bar{q}$  in  $\Sigma'$  with  $|\bar{q} - q'|$  sufficiently small (depending on both  $|p - q'|$  and  $r_1$ ), then we can repeatedly apply the Harnack inequality to connect  $\bar{q}$  by a curve in  $\Sigma'$  back to a small neighborhood of  $p$ . Therefore, since  $\Sigma$  is the only leaf in  $\{x_3 > 0\}$  that intersects a sufficiently small neighborhood of  $p$ , we conclude that  $\Sigma' = \Sigma$ .

Finally, we show that there exists some  $\epsilon_0 > 0$  so that  $\Sigma$  is proper in compact subsets of

$$\{0 < x_3 < \epsilon_0\}. \tag{III.1.10}$$

This properness will follow by combining the two following facts:

- (Fact 1) There exists some  $\epsilon_1 > 0$  so that  $\mathcal{L}'$  does not contain any horizontal planes in the slab  $\{0 < x_3 < \epsilon_1\}$ .
- (Fact 2) There exists  $\epsilon_2 > 0$  so that if  $y \in \{0 < x_3 < \epsilon_2\}$  is an ‘‘accumulation point’’ of  $\Sigma$ , then the leaf of  $\mathcal{L}'$  containing  $y$  is a horizontal plane. A point  $y$  is said to be ‘‘accumulation point’’ of  $\Sigma$  if there exists a sequence of points  $y_j \in \Sigma$  so that

$$\lim_{j \rightarrow \infty} \text{dist}_{\mathbf{R}^3}(y, y_j) = 0, \tag{III.1.11}$$

$$\lim_{j \rightarrow \infty} \text{dist}_{\Sigma}(y_1, y_j) = \infty. \tag{III.1.12}$$

Obviously, the two facts together easily imply the properness of  $\Sigma$  in the slab between 0 and the minimum of  $\epsilon_1$  and  $\epsilon_2$ .

To prove (Fact 1), note that  $\inf_{\Sigma} x_3 = 0$  and  $\sup_{\Sigma} x_3 > 0$  (since  $\Sigma$  is not flat). Consequently, since the leaves of  $\mathcal{L}'$  are disjoint and the leaf  $\Sigma$  is connected,  $\mathcal{L}'$  cannot contain any horizontal planes in the open slab  $\{0 < x_3 < \sup_{\Sigma} x_3\}$ . This gives (Fact 1).

(Fact 2) follows easily from the proof of lemma 1.3 in [MeRo] (in fact, one can even take  $\epsilon_2 = \epsilon$  but we will not need this). We will give the proof next for completeness. Suppose therefore that  $\Sigma$  accumulates at a point  $y \in \{0 < x_3 < \epsilon_2\}$  in a leaf  $\hat{\Sigma} \in \mathcal{L}'$  ( $y$  is in a leaf since the union of the leaves of  $\mathcal{L}'$  is a closed subset of  $\mathbf{R}^3 \setminus \mathcal{S}$  and  $\mathcal{S}$  does not intersect the open slab  $\{0 < x_3 < \epsilon\}$ ). Since  $\Sigma$  is discrete by Lemma II.3.4, we must have  $\hat{\Sigma} \neq \Sigma$  and, hence, also

$$\overline{\hat{\Sigma}} \cap \{x_3 = 0\} = \emptyset. \tag{III.1.13}$$

First, we can use the Harnack inequality to extend the local sequence of graphs converging to  $\hat{\Sigma}$  to graphs over a sequence of expanding subdomains of  $\hat{\Sigma}$ , eventually obtaining a positive Jacobi field on the universal cover of  $\hat{\Sigma}$  (cf. lemma 2.1 in [CM4]). In particular, the existence of such a positive Jacobi field implies stability of the universal cover of  $\hat{\Sigma}$  (see, e.g., proposition 1.26 in [CM1]). Combining the local curvature estimate for stable surfaces, [Sc1], with the gradient estimate and (III.1.13) gives  $\epsilon_2 > 0$  (depending only on  $\epsilon$ ) so that

$$\{x_3 \leq \epsilon_2\} \cap \hat{\Sigma} \text{ is } \underline{\text{locally}} \text{ graphical over } \{x_3 = 0\}. \tag{III.1.14}$$

(See, e.g., lemma I.0.9 in [CM3] for a detailed proof of (III.1.14).) However, the theory of covering spaces (see lemma 1.4 in [MeRo]) now implies that each component of  $\{x_3 \leq \epsilon_2\} \cap \hat{\Sigma}$  is globally a graph of a function  $u$  with  $0 < u \leq \epsilon_2$  over a domain  $\Omega \subset \{x_3 = 0\}$  with boundary values  $u|_{\partial\Omega} = \epsilon_2$ . However, the proof of the strong halfspace theorem of Hoffman-Meeks, [HoMe], implies that such a  $u$  must be identically equal to its boundary values and, by unique continuation, we see that  $\hat{\Sigma}$  is a horizontal plane as claimed. This completes the proof of (Fact 2) and, hence, also of (P1).

The proof of (P2). The proof of the asymptotic graph structure in (P2) will be similar to the proof of property (D1) in subsection III.0.6. First, we fix a large constant  $\Omega > 1$  and some disk  $D_R \subset \{x_3 = 0\}$  containing both  $p$  and  $q$ . Since  $\{x_3 = 0\} \setminus \{p, q\}$  is a leaf of  $\mathcal{L}'$  (and, in particular, disjoint from  $\mathcal{S}$ ), an easy covering argument gives constants  $\mu_A > 0$  and  $C_A$  so that

$$\sup_{\{0 < x_3 < \mu_A\} \cap \{x_1^2 + x_2^2 \leq 4\Omega^2 R^2\} \setminus (B_\epsilon(p) \cup B_\epsilon(q))} |A|^2 \leq C_A. \quad (\text{III.1.15})$$

The gradient estimate and (III.1.15) then give a constant  $\mu > 0$  (and less than  $\mu_A$ ) so that:

See Figure 26. Each point  $y \in \{0 < x_3 < \mu\} \cap \Sigma$  over  $\partial D_R$  is contained in a graph  $\Sigma_y \subset \Sigma$  over the annulus  $D_{\Omega R} \setminus D_R$  with  $\Sigma_y \subset \{0 < x_3 < \epsilon\}$ . Furthermore, the graph  $\Sigma_y$  extends over (a large part of)  $D_R$  as a graph, connecting to the two double spiral staircase structures near  $p$  and  $q$ .

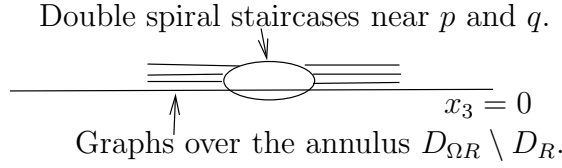


FIGURE 26. The graphs  $\Gamma_y$  in  $\Sigma$ .

This allows us to make the notion of a “low” end precise. Namely, a low end is the component of  $\Sigma \setminus \Sigma_y$  – with  $\Sigma_y$  as above – whose closure does not contain the boundary graph over  $\partial D_R$ .

It remains to show that each of the graphs  $\Sigma_y$  extends as a graph indefinitely, i.e., past  $\partial D_{\Omega R}$ . This is where we argue as the proof of (D) in subsection III.0.6, proving the following scale invariant ULSC property:

- (D’) There exists  $\tau > 0$  so that, for  $z \in \{x_3 = 0\} \setminus D_R$  and  $j$  large, each component of  $B_{\tau|z|}(z) \cap \Sigma_j$  that connects to the multi-valued graph in  $\Sigma_j$  is a disk.

Once we have shown (D’), then the one-sided curvature estimate and gradient estimate will allow us to extend  $\Sigma_y$  as a graph indefinitely. We will leave this easy extension argument to the reader.

We will next prove (D’) by contradiction; suppose therefore that some  $\Sigma_y$  connects outside  $D_R$  to a component of  $B_{\tau|z|}(z) \cap \Sigma_j$  which is not a disk. (Here and below we are identifying  $\Sigma_y$  with the portion of the  $\Sigma_j$ ’s converging to it. This identification should not lead to confusion since we have already shown that the convergence is multiplicity one.) We observe that this “non-disk component” leads to a contradiction, roughly following the proof of (D) in subsection III.0.6 as follows:

- Figure 27. A curve  $\gamma_j$  which is non-contractible in  $B_{\tau|z|}(z) \cap \Sigma_j$  is also non-contractible in  $\Sigma_j$  by the convex hull property. We can therefore apply [MeYa2] to find a stable surface  $\Gamma_j \subset B_{R_j} \setminus \Sigma_j$  with interior boundary  $\gamma_j$  as in (1) in subsection III.0.6. As before, using the plane  $\{x_3 = 0\}$  allows us to conclude by Lemma III.0.3 that these stable surfaces quickly become graphs as we move away from the interior boundary  $\gamma_j$ .
- Figure 28. Fix a graph  $\Sigma_{y'}$  above  $\Sigma_y$  and let  $\sigma_{y'}$  be the component of  $\partial \Sigma_{y'}$  over  $\partial D_R$ . As in (2) in subsection III.0.6, we could then apply [MeYa2] to put in a second stable

surface  $\tilde{\Gamma}_j \subset B_{R_j} \setminus (\Gamma_j \cup \Sigma_j)$  with interior boundary equal to  $\sigma_{y'}$ . Furthermore, this surface also quickly becomes graphical by Lemma III.0.3. Finally, the graph in  $\tilde{\Gamma}_j$  must start off between the two graphs  $\Sigma_y$  and  $\Gamma_j$  because (1) its interior boundary  $\sigma_{y'}$  was chosen to be above  $\Sigma_y$  and (2) every point near  $D_R$  in  $\Sigma$  which connects back to the multi-valued graph in  $\Sigma$  must be below  $\Gamma_j$ .

This easily gives the desired contradiction: The construction of  $\Gamma_j$  guarantees that there is a curve in  $\Sigma_j \cup \Gamma_j$  connecting  $\Sigma_y$  to the graph in  $\Gamma_j$  and moreover is a graph over the  $x_1$ -axis except for in a small neighborhood of  $z$ . The graph in  $\tilde{\Gamma}_j$  is consequently forced to intersect this curve, giving the desired contradiction.

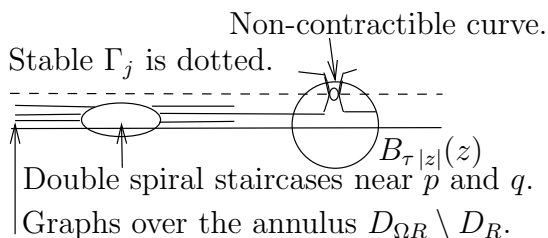


FIGURE 27. The proof of (D’): Constructing  $\Gamma_j$ .

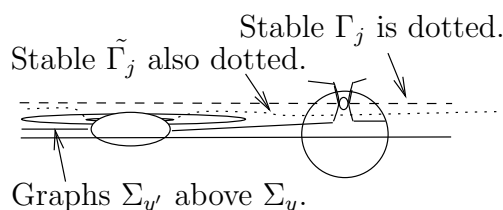


FIGURE 28. The proof of (D’):  $\tilde{\Gamma}_j$  must intersect  $\Gamma_j \cup \Sigma_j$ .

The final part of (P2), i.e., the non-negativity of the vertical flux of the low ends, follows immediately since the ends are asymptotic to planes (vertical flux zero) or upper-halves of catenoids (vertical flux positive). This is because the only other possibility would be an end asymptotic to the lower half of a catenoid which is impossible since one of these would eventually go below the plane  $\{x_3 = 0\}$ . (Recall that any embedded minimal end with finite total curvature is asymptotic to either a plane or half of a catenoid by proposition 1 in [Sc2].)

The proof of (P3). To prove (P3), recall first that there is a positive distance between consecutive ends by the maximum principle at infinity of [LaRo]. This positive distance allows us to intersect  $\Sigma$  with a horizontal plane which intersects  $\Sigma$  transversely between the heights of two consecutive ends, giving a finite collection  $\gamma_+$  of disjoint simple closed curves separating these ends; see Figure 29. This finiteness follows from the compactness of the level set which in turn used the properness of  $\Sigma$ . Since we will be considering the part of  $\Sigma$  below this plane, the outward normal derivative of  $x_3$  is non-negative at every point along  $\gamma_+$ . However, this plane was chosen to be transverse to the surface, so this derivative must in fact be pointwise positive along  $\gamma_+$ . That is, the flux integrand is pointwise positive along  $\gamma_+$  so the vertical flux across  $\gamma_+$  is clearly positive.

Finally, we will sketch briefly why the fact that  $\Sigma$  has genus zero implies that we can choose a single component of  $\gamma^+$  that is vertically separating. We must show that only one component of  $\Sigma \setminus \gamma^+$  connects  $\gamma^+$  to the “the ceiling”  $\{x_3 = \epsilon\}$ . The point is that if there were two such components of  $\Sigma \setminus \gamma^+$ , then we could solve a sequence of Plateau problems to get a stable surface  $\Gamma^+$  between them with the following properties:

- $\partial\Gamma^+ \subset \gamma^+$  is a finite collection of disjoint simple closed curves in a plane.
- $\Gamma^+$  does not go below the plane containing  $\gamma^+$ .
- $\Gamma^+$  is above one of the components of  $\Sigma \setminus \gamma^+$  and below the other.

It is not hard to see that this is impossible. The connectedness of  $\gamma^+$  is not actually necessary for the proof, so we will leave the details for the reader.

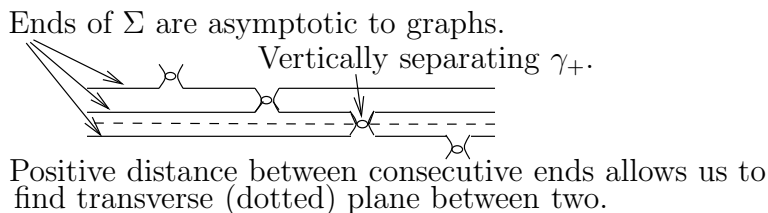


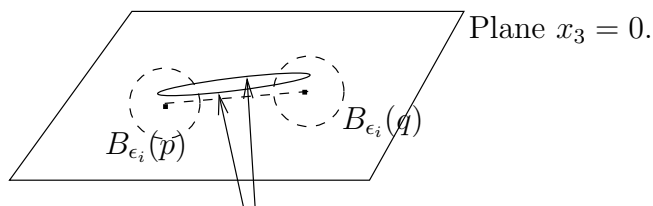
FIGURE 29. The vertically separating curve  $\gamma_+$ .

The proof of (P4). The last claim (P4) essentially follows from the description of  $\Sigma$  near the plane  $\{x_3 = 0\}$  and the gradient estimate. To see this, let

$$\gamma_{pq} \subset \{x_3 = 0\} \quad (\text{III.1.16})$$

be the line segment from  $p$  to  $q$ . Using the description of  $\Sigma$  near  $\{x_3 = 0\}$  and the chord arc bound of Theorem I.1.6, we can find simple closed curves  $\gamma_i \subset \Sigma$  with the following properties (see Figure 30):

- $\gamma_i$  is contained in the  $\epsilon_i$ -tubular neighborhood of  $\gamma_{pq}$  where  $\epsilon_i \rightarrow 0$ .
- $\gamma_i \setminus (B_{\epsilon_i}(p) \cup B_{\epsilon_i}(q))$  consists of two graphs over  $\gamma_{pq}$  which are in oppositely-oriented sheets of  $\Sigma$ .
- The length of  $(B_{\epsilon_i}(p) \cup B_{\epsilon_i}(q)) \cap \gamma_i$  is at most  $C \epsilon_i$  for a fixed constant  $C$ .



Away from  $p$  and  $q$ , the closed curve  $\gamma_i$  has two components; these lie in oppositely oriented graphs in  $\Sigma$ .

FIGURE 30. The separating curves  $\gamma_i$ .

It is easy to see that the  $\gamma_i$ 's are vertically separating since the sheets containing

$$\gamma_i \setminus (B_{\epsilon_i}(p) \cup B_{\epsilon_i}(q)) \quad (\text{III.1.17})$$

are oppositely-oriented (meaning that the unit normals point in nearly opposite directions). Namely, if we fix a spiralling curve in either of the two multi-valued graphs near either singular curve, then the third component to the unit normal to  $\Sigma$  does not change sign along this curve. Consequently, such a spiralling curve intersects exactly one of the  $\gamma_i$ 's and does so exactly once. It follows that the  $\gamma_i$ 's are vertically separating as claimed.

We can now use the gradient estimate to bound  $|\nabla x_3|$  along  $\gamma_i$  away from  $p$  and  $q$  to see that the vertical flux on

$$\gamma_i \setminus (B_\delta(p) \cup B_\delta(q)) \quad (\text{III.1.18})$$

goes to zero for any fixed  $\delta > 0$ . To get this bound, note first that the height function  $x_3$  is positive and harmonic on the multi-valued graphs in  $\Sigma$  that spiral infinitely into  $\{x_3 = 0\}$  and these graphs have bounded curvature away from  $p$  and  $q$ . Therefore, the gradient estimate (for positive harmonic functions) implies that

$$\sup_{\gamma_i \setminus (B_\delta(p) \cup B_\delta(q))} |\nabla x_3| \rightarrow 0 \text{ uniformly as } i \rightarrow \infty. \quad (\text{III.1.19})$$

Combining this gradient bound with the bound on the length of

$$(B_\delta(p) \cup B_\delta(q)) \cap \gamma_i \quad (\text{III.1.20})$$

gives the last claim. This completes the proof of the properties (P1)–(P4) of  $\Sigma$ .

Using (P1)–(P4) to deduce a contradiction. We now see that these properties are contradictory. Namely, by Stokes' theorem, the total flux across  $\gamma_i$ ,  $\gamma_+$ , and the “ends” of  $\Sigma$  between  $\gamma_i$  and  $\gamma_+$  must sum to zero. However, the flux across  $\gamma_+$  is positive and every other flux is either non-negative or approaches zero. This contradiction shows that (III.1.6) could not have held, proving the lemma.  $\square$

### III.2. COMPLETING THE PROOF OF THEOREM 0.9

We will now use the properties of the singular set  $\mathcal{S}_{ulsc}$  and lamination  $\mathcal{L}'$  to show that  $\mathcal{L}'$  is a foliation by parallel planes with two Lipschitz curves removed, thereby completing the proof of Theorem 0.9. The two main steps are:

- Using properness (Lemma III.1.4) to see that the (collapsed) planar leaves of  $\mathcal{L}'$  intersect every height.
- Using the local cone property to get regularity of  $\mathcal{S}_{ulsc}$ .

*Proof.* (of Theorem 0.9.) Lemma II.1.2 gives a subsequence  $\Sigma_j$ , singular set  $\mathcal{S}$ , and lamination  $\mathcal{L}'$  of  $\mathbf{R}^3 \setminus \mathcal{S}$  with minimal leaves. The set  $\mathcal{S} = \mathcal{S}_{ulsc}$  is nonempty by assumption.

For each point  $x$  in  $\mathcal{S}_{ulsc}$ , properties (1) and (2) of Proposition III.0.2 give a (collapsed) leaf of  $\mathcal{L}'$  which is a plane with two points removed ( $x$  is one of the two points). It follows easily from the convergence to these planes and the embeddedness of  $\Sigma_j$  that all of the limit planes are parallel so, after a rotation of  $\mathbf{R}^3$ , we can assume that these planes are horizontal, i.e., given as level sets  $\{x_3 = t\}$ . Furthermore, since  $\mathcal{S}_{ulsc} \subset \mathbf{R}^3$  is a nonempty closed set, the local cone property implies that  $x_3(\mathcal{S}_{ulsc}) \subset \mathbf{R}$  is also closed (and nonempty).

We will show first that the collapsed leaves (or, rather, their closures) foliate  $\mathbf{R}^3$ , more precisely, that

$$x_3(\mathcal{S}_{ulsc}) = \mathbf{R}. \quad (\text{III.2.1})$$

To prove (III.2.1), we assume that  $\{x_3 = t_0\} \cap \mathcal{S}_{ulsc} = \emptyset$  for some  $t_0 \in \mathbf{R}$  and will see that this leads to a contradiction. Namely, since  $x_3(\mathcal{S}_{ulsc})$  is closed, there exists  $t_s \in x_3(\mathcal{S}_{ulsc})$  which is a closest point in  $x_3(\mathcal{S}_{ulsc})$  to  $t_0$ . The desired contradiction now easily follows from Lemma III.1.4 since either  $\{t_s < x_3 < t_0\} \cap \mathcal{S}_{ulsc}$  or  $\{t_0 < x_3 < t_s\} \cap \mathcal{S}_{ulsc}$  is empty. We conclude therefore that  $x_3(\mathcal{S}_{ulsc}) = \mathbf{R}$ .

Finally, the Lipschitz regularity of the curves now follows as in lemma I.1.2 of [CM6]; the same argument applies with obvious minor modifications to deal with the fact that each horizontal plane now contains two singular points as opposed to just one in [CM6].  $\square$

### III.3. SEQUENCES WITH FIXED GENUS

Most of the arguments in the preceding sections have assumed that the surfaces  $\Sigma_j$  have genus zero as opposed to just some fixed finite genus. The arguments for the genus zero case are slightly simpler, however, the modifications needed for the general case are straightforward. The key point is that the infinite multiplicity of the multi-valued graphs converging to a collapsed leaf means that there is an arbitrarily large number of disjoint curves to choose from that “circle both axes” and thus have the desired properties for the preceding arguments. In the general case of finite (but nonzero) genus, we can therefore follow the preceding argument using the following lemma:

**Lemma III.3.1.** If  $\Sigma$  is oriented with genus  $g$  and  $\sigma_1, \dots, \sigma_{g+1} \subset \Sigma$  are disjoint simple closed curves, then  $\Sigma \setminus \cup_i \sigma_i$  is disconnected.

*Proof.* The first integral homology group of  $\Sigma$  is  $2g$ -dimensional and the intersection form is a bilinear form of full rank (cf. lemma I.0.9 of [CM5]). Therefore the maximal subspaces on which the intersection form vanishes have dimension  $g$ . Consequently, there is a nontrivial linear (integral) relation between the  $\sigma_i$ 's and the lemma follows easily.  $\square$

### III.4. AN APPLICATION: A ONE-SIDED PROPERTY FOR ULSC SURFACES

The compactness theorem for ULSC sequences, Theorem 0.9, can be used to prove estimates for embedded minimal surfaces that have a lower bound on their injectivity radius. We will prove several such estimates in this paper, including Lemma III.4.1 in this section. This lemma proves a one-sided property for non-simply connected surfaces on the smallest scale of non-trivial topology, showing that an intrinsic ball in such a surface cannot lie on one side a plane and have its center close to the plane on this scale. This result requires that we work on this scale since, after all, large balls in the catenoid can be rescaled to lie above a plane and yet come arbitrarily close to the plane.

The proof of the lemma divides naturally into two extreme cases, depending on whether the (inverse of the) curvature is comparable to the injectivity radius or is much larger. In the first case, the surface looks more like a catenoid while in the second it looks like a pair of oppositely oriented helicoids joined together. In the first case, the lemma essentially follows from the logarithmic growth of the ends of the catenoid; the second case follows from that these double-helicoids converge to a foliation of all of  $\mathbf{R}^3$  by the compactness theorem for ULSC sequences, Theorem 0.9.

**Lemma III.4.1.** Let  $\Sigma$  be an embedded minimal planar domain with  $0 \in \Sigma$  and so that  $\mathcal{B}_{4r_1}(0) \subset \Sigma$  is not a disk. Given any  $H > 0$ , there exists  $C_1 > H$  so that if  $\mathcal{B}_{C_1 r_1}(0) \cap \partial\Sigma = \emptyset$  and  $\mathcal{B}_{r_1}(x)$  is a disk for each  $x \in \mathcal{B}_{C_1 r_1}(0)$ , then

$$\sup_{\mathcal{B}_{C_1 r_1}(0)} x_3 > H r_1. \quad (\text{III.4.2})$$

*Proof.* After rescaling, we can assume that  $r_1 = 1$ . We will argue by contradiction, so suppose that  $\Sigma_j$  is a sequence of embedded minimal planar domains containing 0 with

$$\mathcal{B}_j(0) \subset (\Sigma_j \setminus \partial\Sigma_j) \cap \{x_3 \leq H\}, \quad (\text{III.4.3})$$

$$\mathcal{B}_4(0) \text{ is not a disk}, \quad (\text{III.4.4})$$

$$\mathcal{B}_1(x) \text{ is a disk for each } x \in \mathcal{B}_j(0). \quad (\text{III.4.5})$$

Observe first that Lemma C.1 in Appendix C gives a sequence  $R_j \rightarrow \infty$  so that the component  $\Sigma_{0,R_j}$  of  $B_{R_j} \cap \Sigma_j$  containing 0 is compact and has boundary in  $\partial B_{R_j}$ .<sup>18</sup> Replacing the sequence  $\Sigma_j$  by  $\Sigma_{0,R_j}$  gives a ULSC sequence – still denoted  $\Sigma_j$  – of embedded minimal planar domains in extrinsic balls whose radius goes to infinity. We will now divide the proof into two cases depending on whether or not the curvatures of the sequence blows up.

Case 1: Suppose first that  $|A|^2 \rightarrow \infty$  in some fixed ball of  $\mathbf{R}^3$  (for some subsequence). We can then apply the compactness theorem for ULSC sequences, Theorem 0.9, to get a subsequence of the  $\Sigma_j$ 's that converges to a foliation by parallel planes away from two lines orthogonal to the leaves of the foliation. Since the foliation is of all of  $\mathbf{R}^3$ , this contradicts the upper bound for  $x_3$  in (III.4.3).

Case 2: Suppose now that  $|A|^2$  is uniformly bounded on compact subsets of  $\mathbf{R}^3$  for every  $\Sigma_j$ . In this case, a subsequence of the  $\Sigma_j$ 's converges smoothly to a minimal lamination  $\mathcal{L}$  of  $\mathbf{R}^3$  by proposition B.1 in [CM6]. We will first see that (III.4.3)–(III.4.5) imply that there is a non-flat leaf  $\Gamma$  of  $\mathcal{L}$  satisfying

$$\Gamma \subset \{x_3 \leq H\}, \tag{III.4.6}$$

$$\mathcal{B}_1(x) \text{ is a disk for each } x \in \Gamma. \tag{III.4.7}$$

To see this, first note that (III.4.4) implies that each  $\mathcal{B}_4(0) \subset \Sigma_j$  cannot be written as a graph over any plane and hence contains a point  $y_j$  with  $|A|^2(y_j) > \delta_0$  for some  $\delta_0 > 0$ . A subsequence of these points converges to a point  $y$  in some leaf – call it  $\Gamma$  – of  $\mathcal{L}$  with  $|A|^2(y) \geq \delta_0$ . Thus  $\Gamma$  is not flat. Equation (III.4.6) follows immediately from (III.4.3).

Observe next that the leaf  $\Gamma$ :

- is a multiplicity one limit of the  $\Sigma_j$ 's.
- is locally isolated in  $\mathcal{L}$  in the sense that each point  $y \in \Gamma$  has a neighborhood  $B_r(y)$  so that  $B_r(y) \cap \mathcal{L}$  consists only of the component of  $B_r(y) \cap \Gamma$  containing  $y$ .

If either of these was not the case, then the universal cover of  $\Gamma$  would be stable and, hence, flat; cf. the proof of Corollary B.20 for more details. As a consequence, if  $K$  is any compact subset of  $\Gamma$ , then for  $j$  sufficiently large (depending on  $K$ )  $\Sigma_j$  contains a normal graph  $K_j$  over  $K$ ; as  $j \rightarrow \infty$ , the  $K_j$ 's converge smoothly to  $K$ . Using this convergence and the convex hull property, it is easy to see that (III.4.5) implies (III.4.7). Moreover, this convergence and the fact that the  $\Sigma_j$ 's are planar domains implies that  $\Gamma$  is also a planar domain. To see this, suppose instead that  $\Gamma$  contains a pair of non-separating curves  $\gamma$  and  $\tilde{\gamma}$  that have linking number one (i.e., so they are transverse and intersect at exactly one point). Then for  $j$  large, we would get a similar pair of curves in  $\Sigma_j$ ; since this is impossible for planar domains, we conclude that  $\Gamma$  is also a planar domain.

We have shown that  $\Gamma$  is a planar domain satisfying (III.4.6) and (III.4.7). We can assume that  $H = \sup_{\Gamma} x_3$ . Recall that [MeRo] gives

$$\sup_{\Gamma \cap \{H-1 < x_3 < H\}} |A|^2 = \infty. \tag{III.4.8}$$

Namely, by the first paragraph of the proof of lemma 1.5 in [MeRo], if instead we had

$$\sup_{\Gamma \cap \{H-1 < x_3 < H\}} |A|^2 < \infty, \tag{III.4.9}$$

---

<sup>18</sup>This will be needed later to apply the compactness results for ULSC sequences.

then  $\Gamma = \{x_3 = H\}$ . However,  $\Gamma$  is not flat, so we conclude that (III.4.8) must hold.

We will now use (III.4.8) to define a new sequence of planar domains where we can argue to a contradiction as in Case 1. Namely, (III.4.8) gives a sequence of points  $p_n \in \Gamma \cap \{H-1 < x_3 < H\}$  with

$$|A|^2(p_n) \rightarrow \infty. \quad (\text{III.4.10})$$

By (III.4.7), we can apply Lemma C.1 to conclude that the component  $\Gamma_{p_n, n}$  of  $B_n(p_n) \cap \Gamma$  containing  $p_n$  is compact and has boundary in  $\partial B_n(p_n)$ . Translate  $\Gamma_{p_n, n}$  by moving  $p_n$  to the origin to get a ULSC sequence

$$\Gamma_n = \Gamma_{p_n, n} - p_n \quad (\text{III.4.11})$$

of compact embedded minimal planar domains with  $\Gamma_n \subset B_n$ ,  $\partial\Gamma_n \subset \partial B_n$ , and  $|A|^2(0) \rightarrow \infty$ . As in Case 1, a subsequence converges to a foliation of all of  $\mathbf{R}^3$  by parallel planes away from two lines orthogonal to the leaves of the foliation. However, by (III.4.6), the translated surfaces  $\Gamma_n$  are in the half-space  $\{x_3 < 1\}$ . This contradiction completes the proof of the lemma in Case 2, completing the proof of the lemma.  $\square$

**Remark III.4.12.** Using this one-sided property, we can go back and prove a stronger version of Lemma C.1. This stronger result gives that ULSC surfaces are proper – as opposed to just knowing that each component in a ball is proper.

#### Part IV. When the surfaces are not ULSC: The proof of Theorem 0.14

We will now turn to the case where the sequence is not ULSC and there is consequently no longer a lower bound for the injectivity radius of the  $\Sigma_j$ 's in compact subsets of  $\mathbf{R}^3$ . As we did in the ULSC case, we will initially argue for the genus zero case and then explain the easy modifications needed for the general case of fixed finite genus.

We have already defined the singular set  $\mathcal{S}$  in Definition/Lemma II.1.1 to be the set of points where the curvature blows up. Furthermore, Lemma II.1.2 gives a subsequence  $\Sigma_j$  that converges to a minimal lamination  $\mathcal{L}'$  of  $\mathbf{R}^3 \setminus \mathcal{S}$ . This gives (A) and (B) in Theorem 0.14.

In the ULSC case, every singular point was essentially the same; namely, in a neighborhood of each singular point, the surfaces were double-spiral staircases. However, we now have the possibility that the injectivity radius of the  $\Sigma_j$ 's is going to zero at the singular point. This occurs, for example, by taking a sequence of rescalings of a catenoid or one of the Riemann examples. Recall that the Riemann examples are singly-periodic embedded minimal planar domains which are topologically - and conformally - equivalent to an infinite cylinder with a one-dimensional lattice of punctures.

For the sequence of rescaled catenoids, the singular set  $\mathcal{S}$  consists of just the origin and we get  $C^\infty$  convergence to a single plane with multiplicity two away from the origin. Rescaling one of the Riemann examples gives a line of singular points and convergence to a foliation by parallel planes away from this line. By choosing different sequences of rescaled Riemann examples, we can get different singular sets – but we always get a foliation by parallel planes.

The local behavior of the surfaces near a singular point is quite different, depending on whether or not the injectivity radius is going to zero there. To account for this, we define the subset  $\mathcal{S}_{neck} \subset \mathcal{S}$  to be the set of points where the injectivity radius goes to zero. Proposition I.0.19 of [CM5] implies that, after passing to a further subsequence, each point  $y \in \mathcal{S} \setminus \mathcal{S}_{neck}$

has a radius  $r_y > 0$  so that each component of  $B_{r_y}(y) \cap \Sigma_j$  is a disk for every  $j$ . In other words, this proposition implies that  $\mathcal{S}$  is given as the disjoint union

$$\mathcal{S} = \mathcal{S}_{neck} \cup \mathcal{S}_{ulsc}. \quad (\text{IV.0.1})$$

Recall that  $\mathcal{S}_{ulsc}$  was defined in the introduction to be the set of points where the curvature blows up but where the sequence is locally ULSC.

**An overview of this part:** In Section IV.1, we prove the main structure result for the non-ULSC part of the limit lamination  $\mathcal{L}'$ , i.e., (C1) in Theorem 0.14. Namely, we show that for each point  $y$  in  $\mathcal{S}_{neck}$ , we get a sequence of graphs in the  $\Sigma_j$ 's that converges to a plane through  $y$ . These graphs will be defined over a sequence of expanding domains and the convergence will be smooth away from  $y$  and possibly one other point in the limit plane. In the process of proving this, we will also establish (P) in Theorem 0.14.

In Section IV.2, we prove the main structure results for the ULSC part of the lamination, i.e., (C2) and (D) in Theorem 0.14. Namely, we show that this part of the lamination is actually a foliation by an open set of parallel planes in  $\mathbf{R}^3$  and the ULSC singular set  $\mathcal{S}_{ulsc}$  is a collection of Lipschitz curves transverse to these planes.

In Section IV.3, we combine all of this and complete the proof of Theorem 0.14.

**Remark IV.0.2.** Theorem 0.14 gives a flat leaf of  $\mathcal{L}'$  through every singular point in  $\mathcal{S}$  but does not show that all of the leaves of  $\mathcal{L}'$  are flat. This will be proven in Part VI.

#### IV.1. PROVING (C1) IN THEOREM 0.14: A PLANE THROUGH EACH POINT OF $\mathcal{S}_{neck}$

For each point  $y$  in  $\mathcal{S}_{neck}$ , we will prove in this section that there is a sequence of graphs in  $\Sigma_j$  converging to a plane through  $y$ . The graphs converge smoothly to the plane away from  $y$  and possibly one other point (the other point is also in  $\mathcal{S}_{neck}$ ).

The key tool in this section is Proposition IV.1.1 that allows us to decompose an embedded minimal planar domain  $\Sigma \subset B_{r_0}$  with  $\partial\Sigma \subset \partial B_{r_0}$  by ‘‘cutting it’’ inside a small ball  $B_{r_1}$  whenever some component of  $B_{r_1} \cap \Sigma$  is not a disk. Moreover, the proposition uses a barrier construction to find a stable graph disjoint from  $\Sigma$  so that the pieces of  $\Sigma$  are on opposite sides of this graph; see Figure 31. The basic example to keep in mind is the catenoid: Cutting the catenoid along the unit circle in the  $\{x_3 = 0\}$  plane gives two pieces; these pieces are on opposite sides of the stable graph  $\{x_3 = 0\} \cap \{x_1^2 + x_2^2 > 1\}$ .

**Proposition IV.1.1.** There exists a constant  $C > 1$  so that the following holds:

Let  $\Sigma \subset B_{r_0}$  be an embedded minimal planar domain with  $\partial\Sigma \subset \partial B_{r_0}$  and  $0 \in \Sigma$ . If  $B_{r_1} \subset \Sigma$  is not a topological disk for some  $r_1 < r_0/C^2$ , then there exists a stable embedded minimal surface  $\Gamma \subset B_{r_0} \setminus \Sigma$  with  $\partial\Gamma \subset \partial B_{r_0} \cup \mathcal{B}_{r_1}$  and satisfying the following properties:

- (A) A component  $\Gamma_0$  of  $B_{r_0/C} \cap \Gamma \setminus B_{Cr_1}$  is a graph with gradient bounded by one and so that  $\partial\Gamma_0$  intersects both  $\partial B_{r_0/C}$  and  $\partial B_{Cr_1}$ .
- (B) There are distinct components  $H^+$  and  $H^-$  of  $B_{r_0/C} \setminus (\Gamma_0 \cup B_{Cr_1})$ , a separating curve  $\tilde{\sigma} \subset B_{Cr_1} \cap \Sigma$ , and distinct components  $\Sigma^+$  and  $\Sigma^-$  of  $B_{r_0/C} \cap \Sigma \setminus \tilde{\sigma}$  so that  $\Sigma^\pm \subset H^\pm \cup B_{Cr_1}$  and  $\tilde{\sigma} = \partial\Sigma^+ \cap \partial\Sigma^-$ .

As mentioned above, Proposition IV.1.1 will be the key tool for getting the limit plane through each point of  $\mathcal{S}_{neck}$  that was promised in (C1) in Theorem 0.14. To see why, we will first use Proposition IV.1.1 to get a sequence of stable graphs that are disjoint from  $\Sigma_j$

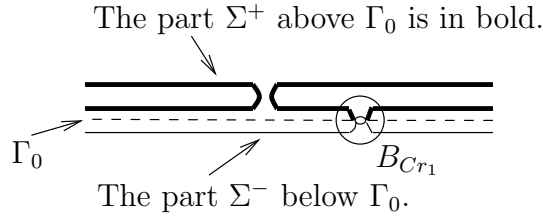


FIGURE 31. Proposition IV.1.1: A stable graph  $\Gamma_0$  separates  $\Sigma$  into parts above and below the graph.

and converge, away from  $y$ , to a plane through  $y$ . Since the outer radii  $R_j$  go to infinity, applying Proposition IV.1.1 to the sequence  $\Sigma_j$  will give a sequence of stable graphs that are disjoint from  $\Sigma_j$  and defined over larger and larger annuli centered at  $y$ . As  $j \rightarrow \infty$ , the inner radii of these annuli go to zero and the outer radii go to infinity. Consequently, the stable graphs will converge (subsequentially) to a minimal graph over a plane punctured at  $y$  and this graph will have  $y$  in its closure. By a standard removable singularity theorem, this limit graph extends smoothly across  $y$  to an entire minimal graph and, hence, is flat by the Bernstein theorem. The easy details will be left to the reader.

Now that we have this stable limit plane through  $y \in \mathcal{S}_{neck}$ , the proof of (C1) in Theorem 0.14 will consist of two main steps. We will sketch these two steps next:

- (1) **Decomposing  $\Sigma_j$  into ULSC pieces:** Let  $\Sigma_j^+$  denote the portion of  $\Sigma_j$  above the stable graph. There are now two possibilities:
  - $\Sigma_j^+$  is scale-invariant ULSC away from  $y$ . More precisely, there exists a constant  $C'$  and a sequence  $r_j \rightarrow 0$  so that if  $x \notin B_{C'r_j}(y)$ , then each component of  $B_{|x|/C'}(x) \cap \tilde{\Sigma}_j^+$  is a disk.<sup>19</sup>
  - Otherwise, we can apply Proposition IV.1.1 to cut along a second non-contractible curve; see Figure 32.

In the second case, we replace  $\Sigma_j^+$  by the portion  $\Sigma_j^{+-}$  of  $\Sigma_j^+$  that is below the second stable graph. After repeating this a finite number of times, we will eventually get down to a scale-invariant ULSC subset of  $\Sigma_j$  with two interior boundary components (one component for the cut near  $y$  and one component for the last cut that we make).

- (2) **The ULSC pieces contain graphs:** In either case, Lemma 3.3 in [CM8] will then give low points in  $\Sigma_j$  on either side of these stable graphs (see Figure 38). Here “low points” roughly means points close to the stable graph but away from its boundary. The one-sided curvature estimate<sup>20</sup> from [CM6] and the gradient estimate will imply that the low points in the resulting ULSC subsets of  $\Sigma_j$  are graphical. Piecing this together will easily give the desired global graphs.

In the first case in (2) above, the graphs in the  $\Sigma_j$ 's will be defined over annuli; in the second case, the graphs will be over pairs of pants, i.e., over disks with two subdisks removed. We will refer to the second case as a “pair of pants” decomposition; see Figure 32.

The steps (1)–(3) above are modelled on similar arguments for topological annuli in [CM8]. Some new complications will arise here because of the more complicated topological types of the surfaces, especially in the second case in step (2).

<sup>19</sup>This intersection is empty when  $|x|$  is larger than  $C' R_j$ .

<sup>20</sup>The one-sided curvature estimate is recalled in this paper in Theorem I.1.3.

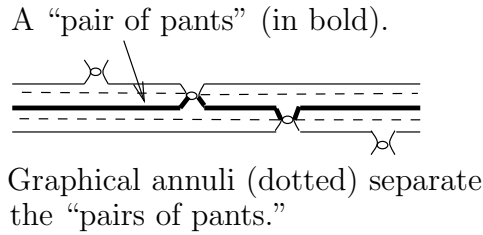


FIGURE 32. A pair of pants decomposition near a point where the injectivity radius goes to zero.

**IV.1.1. The proof of Proposition IV.1.1: A decomposition near each point of  $\mathcal{S}_{neck}$ .**

The next lemma will first give stable surfaces disjoint from  $\Sigma$  and with “interior boundary” contained in a small ball. In order to prove Proposition IV.1.1, we will later show that these stable surfaces contain the desired graphs. More precisely, the next lemma assumes that a component of a minimal planar domain  $\Sigma$  in a small ball is not a disk so that it must contain a simple closed curve  $\tilde{\gamma}$  separating two components  $\sigma_1$  and  $\sigma_2$  of  $\partial\Sigma$ . The lemma then uses the separating curve  $\tilde{\gamma}$  as “interior boundary” for a Plateau problem to get a stable minimal surface “between”  $\sigma_1$  and  $\sigma_2$ ; see (C) in Lemma IV.1.2 below.

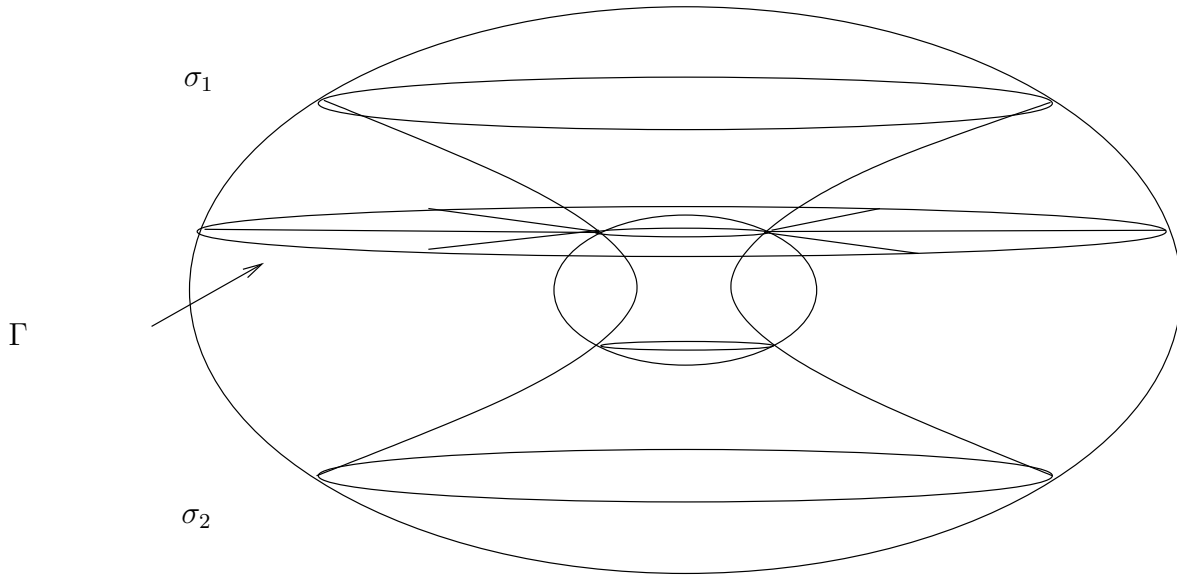


FIGURE 33. Lemma IV.1.2: If the planar domain  $\Sigma$  contains a closed non-contractible curve in the small ball  $B_{r_1}$ , then  $\Sigma$  has distinct boundary components  $\sigma_1$  and  $\sigma_2$ . Moreover, there is a stable surface  $\Gamma$  that is disjoint from  $\Sigma$  and separates  $\sigma_1$  and  $\sigma_2$  in a component  $\Omega$  of  $B_{r_0} \setminus \Sigma$ . The boundary of  $\Gamma$  has two parts, an outer boundary in  $\partial B_{r_0}$  and an inner boundary curve  $\tilde{\gamma} \subset \partial B_{r_1} \cap \Sigma$ .

**Lemma IV.1.2.** Let  $\Sigma \subset B_{r_0}$  be an embedded minimal planar domain with  $\partial\Sigma \subset \partial B_{r_0}$ . If  $r_1 < r_0$  and a component  $\Sigma_{r_1}$  of  $B_{r_1} \cap \Sigma$  is not a topological disk, then the following four properties hold (see Figure 33):

- (A)  $\Sigma \setminus \Sigma_{r_1}$  has at least two connected components; each of these components has at least one component of  $\partial\Sigma$  in its closure.
- (B) If  $\sigma_1$  and  $\sigma_2$  are components of  $\partial\Sigma$  that are separated by  $\Sigma_{r_1}$  (i.e.,  $\sigma_1$  and  $\sigma_2$  are in the closure of distinct components of  $\Sigma \setminus \Sigma_{r_1}$ ), then we can choose a simple closed curve

$$\tilde{\gamma} \subset \partial\Sigma_{r_1} \subset \partial B_{r_1} \tag{IV.1.3}$$

that separates  $\sigma_1$  and  $\sigma_2$  in  $\Sigma$ .

- (C) There is a component  $\Omega$  of  $B_{r_0} \setminus \Sigma$  and an embedded stable minimal surface  $\Gamma \subset \Omega$  with interior boundary  $\partial\Gamma \setminus \partial B_{r_0}$  equal to  $\tilde{\gamma}$ , and so that  $\Gamma$  separates  $\sigma_1$  and  $\sigma_2$  in  $\Omega$ .<sup>21</sup>
- (D)  $\Gamma$  is area-minimizing amongst surfaces in  $\Omega$  with boundary equal to  $\partial\Gamma$ .

*Proof.* The first two claims, i.e., (A) and (B), follow from that  $\Sigma$  is a planar domain and, by the maximum principle, any homologically nontrivial curve in  $\Sigma_{r_1}$  is also homologically nontrivial in  $\Sigma$ .

We will next solve the Plateau problem to get the desired stable surface in the complement of  $\Sigma$ . To do this, we need to choose the boundary of the stable surface and decide which of the two components of  $B_{r_0} \setminus \Sigma$  that we will solve in.

To get the boundary, simply let  $\Sigma_0$  be the component of  $\Sigma \setminus \tilde{\gamma}$  that contains  $\sigma_1$  in its boundary; we will minimize area among surfaces with boundary equal to

$$\partial\Sigma_0. \tag{IV.1.4}$$

Note that  $\partial\Sigma_0$  has “interior boundary” equal to  $\tilde{\gamma}$  and  $\sigma_2$  is not in  $\partial\Sigma_0$ .

We will use a simple linking argument to choose the domain  $\Omega$  to solve in. First, fix a smooth curve  $\eta \subset \Sigma$  from  $\sigma_1$  to  $\sigma_2$  that intersects  $\tilde{\gamma}$  exactly once and does so transversely (such a curve exists since  $\tilde{\gamma}$  separates  $\sigma_1$  and  $\sigma_2$  in  $\Sigma$ ). Since  $\Sigma$  is compact and embedded, we can “push  $\eta$  off of  $\Sigma$ ” - on either side of  $\Sigma$  - to get curves  $\eta^+$  and  $\eta^-$  that are disjoint from  $\Sigma$  and in distinct components of  $B_{r_0} \setminus \Sigma$ . It follows that the (mod 2) linking numbers of  $\eta^+$  and  $\eta^-$ , respectively, with  $\tilde{\gamma}$  differ by one.<sup>22</sup> In particular, one of these - say  $\eta^-$  - has linking number 1 (mod 2) with  $\tilde{\gamma}$ . Let  $\Omega$  be the component of  $B_{r_0} \setminus \Sigma$  that contains the *other* curve  $\eta^+$ .

It follows that we have the following three properties:

- The domain  $\Omega$  is mean convex in the sense of [MeYa2].
- $\partial\Sigma_0$  is contained in  $\partial\Omega$  and bounds the planar domain  $\Sigma_0$  in  $\partial\Omega$ .
- $\tilde{\gamma} = \partial\Sigma_0 \setminus \partial B_{r_0}$  has linking number 1 (mod 2) with the curve  $\eta^-$  *that is not in  $\Omega$* .

Using the first two properties, a result of Hardt-Simon, [HSi], gives an embedded minimal surface  $\tilde{\Gamma} \subset \Omega$  with  $\partial\tilde{\Gamma} = \partial\Sigma_0$  and so that  $\tilde{\Gamma}$  minimizes area amongst surfaces in  $\Gamma$  with the same boundary.<sup>23</sup> In particular,  $\tilde{\Gamma}$  must be stable.

<sup>21</sup>One must be careful interpreting this “separation” since  $\partial\Gamma$  may intersect  $\sigma_1$  or  $\sigma_2$ . In this case, we mean that  $\Gamma$  separates points in the interior of  $\Sigma$  that are arbitrarily close to  $\sigma_1$  and  $\sigma_2$ .

<sup>22</sup>Recall that if  $\eta \subset B_r$  is a curve with endpoints in  $\partial B_r$  and  $\gamma \subset B_r$  is a closed curve, then their linking number is defined to be the number of times (mod 2) that  $\eta$  intersects a surface  $\Gamma \subset B_r$  with  $\partial\Gamma = \gamma$ . As usual, we assume that  $\Gamma$  and  $\eta$  intersect transversely when counting intersections. The point is that this number does not depend on the particular choice of bounding surface  $\Gamma$ .

<sup>23</sup>We could of course have applied a result of Meeks-Yau to get a stable planar domain. However, this planar domain would have minimized area only amongst planar domains. We will later use this minimizing

The surface  $\tilde{\Gamma}$  may have several components. We will use the third property above to show that the component  $\Gamma$  containing  $\tilde{\gamma}$  in its boundary separates  $\sigma_1$  and  $\sigma_2$  in  $\Omega$  and, hence, satisfies (C). First of all,  $\tilde{\gamma}$  alone cannot be the entire boundary of  $\partial\Gamma$ ; indeed, any surface  $\Gamma_{\tilde{\gamma}} \subset B_{r_0}$  with  $\partial\Gamma_{\tilde{\gamma}} = \tilde{\Gamma}$  would be forced to intersect the curve  $\eta^-$  that is not in  $\Omega$ . Therefore, we must have that

$$\partial B_{r_0} \cap \partial\Gamma \neq \emptyset. \quad (\text{IV.1.5})$$

A similar use of the linking condition implies that  $\Gamma$  separates  $\sigma_1$  and  $\sigma_2$  in  $\Omega$ , giving (C).  $\square$

The minimizing property given in (D) will be used to give an upper bound for the area of  $\Gamma$  by constructing comparison surfaces with the same boundary. To carry this out, we will need two elementary lemmas. The first is a simple topological lemma showing that any collection of disjoint simple closed curves in a planar domain is homologous to a collection of distinct boundary curves. Moreover, together the initial curves and the boundary curves bound a subdomain of the planar domain. The second lemma uses this to construct comparison surfaces and hence, using (D), deduce an area bound for the surface  $\Gamma$  above.

**Lemma IV.1.6.** Let  $P$  be a (possibly disconnected) compact planar domain with boundary  $\partial P$ . Given any collection  $\sigma_1, \dots, \sigma_n$  of disjoint simple closed curves in  $P$ , then there is a subdomain  $P_0 \subset P$  with

$$\partial P_0 = (\cup_{i=1}^n \sigma_i) \cup (\cup_{i=1}^m \eta_i), \quad (\text{IV.1.7})$$

where  $\eta_1, \dots, \eta_m$  are distinct components of  $\partial P$ .

**Remark IV.1.8.** Before giving the proof of Lemma IV.1.6, it may be helpful to make two remarks. First, it is possible that  $m = 0$  in IV.1.7, i.e., that  $\partial P_0 = \cup_{i=1}^n \sigma_i$ . Second, notice that all of the above curves - both the  $\sigma_i$ 's and  $\eta_i$ 's - are thought of as unoriented curves.

*Proof.* (of Lemma IV.1.6.) Since we can consider each connected component of  $P$  separately, we may as well assume that  $P \subset \mathbf{R}^2$  is connected. The set  $P_0$  will be given as the level set  $f^{-1}(1)$  of a map

$$f : P \setminus (\cup_{i=1}^n \sigma_i) \rightarrow \{-1, +1\}. \quad (\text{IV.1.9})$$

To define  $f$ , first fix a point  $p_0 \in P \setminus (\cup_{i=1}^n \sigma_i)$ . For each point  $p \in P \setminus (\cup_{i=1}^n \sigma_i)$ , choose a curve  $\gamma_p \subset P$  from  $p_0$  to  $p$  that is transverse to the  $\sigma_i$ 's and let  $n(p)$  be the number of times that  $\gamma_p$  crosses  $(\cup_{i=1}^n \sigma_i)$ ; see Figure 34. It follows from elementary topology that  $n(p) \pmod{2}$  does not depend on the choice of the curve  $\gamma_p$  and, hence, we can define the function  $f$  by

$$f(p) = (-1)^{n(p)}. \quad (\text{IV.1.10})$$

Define  $P_0$  by

$$P_0 = \{p \mid f(p) = +1\}. \quad (\text{IV.1.11})$$

It follows easily that  $f$  changes sign as we cross each  $\sigma_i$  and, therefore, each  $\sigma_i \subset \partial P_0$  as desired.  $\square$

---

property to bound the area of  $\Gamma$  by constructing comparison surfaces. It will be convenient not to have to restrict the topological type of the comparison surfaces.

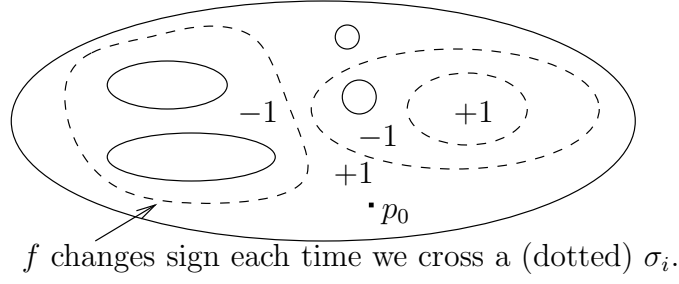


FIGURE 34. The proof of Lemma IV.1.6: The curves  $\sigma_i$  are dashed while  $\partial P$  is dotted. After fixing a basepoint  $p_0$ , we define a function  $f(p)$  to be  $+1$  or  $-1$ , depending on whether you have to cross an even or odd number of the  $\sigma_i$ 's to get from  $p_0$  to  $p$ . The domain  $P_0$  is then defined to be the level set where  $f$  is  $+1$ . In the example pictured,  $P_0$  has two components.

**Lemma IV.1.12.** Given a constant  $C_1$ , there exists  $C_2 > C_1$  so that if  $\Sigma \subset B_{r_0}$ ,  $\tilde{\gamma}$ , and  $\Gamma \subset \Omega \subset B_{r_0} \setminus \Sigma$  are as in Lemma IV.1.2 and for some  $r$  between  $r_0$  and  $r_1$  we have

$$r^{-1} \text{Length}(\partial B_r \cap \Sigma) \leq C_1, \quad (\text{IV.1.13})$$

then we get an area bound for  $B_r \cap \Gamma$

$$r^{-2} \text{Area}(B_r \cap \Gamma) \leq C_2. \quad (\text{IV.1.14})$$

*Proof.* Note first that (IV.1.13) and Stokes' theorem (using that  $\text{div}(\nabla|x|^2) = 4$  on a minimal surface) gives

$$r^{-2} \text{Area}(B_r \cap \Sigma) \leq 1/2 r^{-1} \text{Length}(\partial B_r \cap \Sigma) \leq C_1/2. \quad (\text{IV.1.15})$$

The minimizing property (D) in Lemma IV.1.2 implies that  $B_r \cap \Gamma$  is itself area minimizing among surfaces in its homology class in  $\Omega$ . It will suffice therefore to construct a comparison surface in  $\overline{\Omega}$  with bounded area. This follows from the following steps:

- (1) The outer boundary of  $B_r \cap \Gamma$  – i.e.,  $(\partial B_r) \cap \Gamma$  – sits inside the (possibly disconnected) planar domain  $\Omega \cap \partial B_r$ . Consequently, Lemma IV.1.6 gives a subset  $P_0$  of the planar domain  $\Omega \cap \partial B_r$  with

$$(\partial B_r \cap \Gamma) \subset \partial P_0 \text{ and } \partial P_0 \setminus (\partial B_r \cap \Gamma) \subset (\partial B_r) \cap \Sigma. \quad (\text{IV.1.16})$$

Note that  $P_0$  has bounded area since it is contained in  $\partial B_r$ .

- (2) Let  $\Sigma_0$  denote the component of  $B_r \cap \Sigma$  containing  $\tilde{\gamma}$  and let  $\Sigma_0^+$  be one of the components of  $\Sigma_0 \setminus \tilde{\gamma}$ . Note that  $\Sigma_0^+$  has bounded area by (IV.1.15).
- (3) By the previous two steps, the boundary of  $P_0 \cup \Sigma_0^+$  contains all of  $\partial(B_r \cap \Gamma)$  (both  $\tilde{\gamma}$  and the outer boundary). Ideally, we would have that  $\partial(P_0 \cup \Sigma_0^+) = \partial(B_r \cap \Gamma)$  so that  $P_0 \cup \Sigma_0^+$  would be a valid comparison surface. However, this does not have to be the case since  $\partial(P_0 \cup \Sigma_0^+)$  may have some additional components. We can therefore assume that

$$\partial(P_0 \cup \Sigma_0^+) \setminus \partial(B_r \cap \Gamma) \neq \emptyset. \quad (\text{IV.1.17})$$

- (4) Observe that  $\partial(P_0 \cup \Sigma_0^+) \setminus \partial(B_r \cap \Gamma)$  is itself the boundary of a surface in  $\overline{\Omega}$ , namely of the surface  $P_0 \cup \Sigma_0^+ \cup (B_r \cap \Gamma)$ . We can therefore solve the Plateau problem for a

surface  $\tilde{\Gamma}$  in  $B_r \cap \Omega$  with

$$\partial\tilde{\Gamma} = \partial(P_0 \cup \Sigma_0^+) \setminus \partial(B_r \cap \Gamma) \subset (\partial B_r) \cap \Sigma. \quad (\text{IV.1.18})$$

The length bound on  $(\partial B_r) \cap \Sigma$  and the isoperimetric inequality for minimal surfaces then give an area bound for  $\tilde{\Gamma}$ .

(5) Finally, it follows that

$$\partial(P_0 \cup \Sigma_0^+ \cup \tilde{\Gamma}) = \partial(B_r \cap \Gamma), \quad (\text{IV.1.19})$$

so that  $P_0 \cup \Sigma_0^+ \cup \tilde{\Gamma}$  is the desired comparison surface.<sup>24</sup> This gives (IV.1.14) since each of the three pieces of the comparison surface has the desired area bound.  $\square$

The next lemma gives an area estimate for the components of the stable surface constructed in Lemma IV.1.2 on the largest scale  $r_1$  where  $\Sigma$  is ULSC. Recall that  $\Sigma$  contains a non-contractible curve  $\tilde{\gamma}$  in  $\partial B_{r_1}$ , so  $\Sigma$  is not ULSC on scales larger than  $r_1$ . On the other hand, the assumption (IV.1.21) below gives that  $\Sigma$  is ULSC on this scale.

**Lemma IV.1.20.** Given a constant  $C_1$ , there exists  $C_2 > C_1$  so that if  $\Sigma \subset B_{r_0}$ ,  $\tilde{\gamma}$ , and  $\Gamma \subset \Omega \subset B_{r_0} \setminus \Sigma$  are as in Lemma IV.1.2 with  $r_1 < r_0/C_2$  and, in addition,

$$\mathcal{B}_{r_1/4}(x) \subset \Sigma \text{ is a disk for every } x \in \mathcal{B}_{C_2 r_1}, \quad (\text{IV.1.21})$$

then each component  $\Gamma'$  of  $B_{C_1 r_1} \cap \Gamma \setminus B_{8r_1}$  which can be connected to  $\tilde{\gamma}$  by a curve in  $B_{17r_1} \cap \Gamma$  satisfies

$$\text{Area}(\Gamma') \leq C_2 r_1^2. \quad (\text{IV.1.22})$$

*Proof.* Observe first that the chord-arc bound for ULSC surfaces, Lemma C.1 in Appendix C, shows that the ULSC hypothesis (IV.1.21) also holds for  $x$  in the component of  $\Sigma$  containing 0 in an extrinsic ball  $B_{C'_2 r_1}$  where  $C'_2$  goes to infinity as  $C_2$  does. In particular, after replacing  $\Sigma$  by this component, we may as well assume that

$$\mathcal{B}_{r_1/4}(x) \text{ is a disk for every } x \in \Sigma. \quad (\text{IV.1.23})$$

The proof of (IV.1.22) will be by contradiction, using a compactness argument. Suppose therefore that  $\Sigma_j, \Gamma_j$  is a sequence of counter-examples where (IV.1.22) fails with  $C_2 = j \rightarrow \infty$ . After translating and rescaling, we may assume that  $r_1 = 4$ .

We will consider two cases depending on whether  $|A|^2 \rightarrow \infty$  on a compact set for the sequence  $\Sigma_j$ .

Case 1: Suppose first that  $|A|^2 \rightarrow \infty$  in some fixed ball of  $\mathbf{R}^3$  (for some subsequence of the  $\Sigma_j$ 's). We can then apply the compactness theorem for non-simply connected ULSC sequences, Theorem 0.9, to get a subsequence of the  $\Sigma_j$ 's that converges to a foliation by parallel planes away from two lines orthogonal to the leaves of the foliation.

Observe that both of these orthogonal ‘‘singular’’ lines intersect the leaf through 0 inside the ball  $B_4$  since  $\Sigma_j$  is assumed to be non-simply connected inside that ball. It follows easily from the description of the convergence near the lines (as oppositely oriented double spiral staircases) that any such component  $\Gamma'_j$  is sandwiched between the almost planar leaves of the foliation (for  $j$  sufficiently large). This sandwiching, together with interior curvature

<sup>24</sup>This surface is not embedded and it may not even have the same topological type, but it is nonetheless a valid comparison surface.

estimates for stable surfaces, implies that  $\Gamma'_j$  is itself a graph and hence has bounded area as desired.

Case 2: Suppose now that  $|A|^2$  is uniformly bounded on compact subsets of  $\mathbf{R}^3$  for every  $\Sigma_j$ . In this case, we will get uniform area bounds for the surfaces  $\Sigma_j$  in the ball  $B_{4C_1}$ . Once we have these area bounds for the  $\Sigma_j$ 's, then the comparison argument in Lemma IV.1.12 will give a uniform bound for area of the  $\Gamma_j$ 's in the same ball. However, we assumed that there was no such area bound for  $\Gamma_j$ 's. This contradiction will complete the proof of the lemma.

Therefore, to complete the proof of the lemma, it suffices to bound the area of  $\Sigma_j$  in  $B_{4C_1}$ . This area bound follows immediately from combining the following two facts:

- By Lemma C.3 in Appendix C, the uniform curvature bound implies uniform area bounds for each component of  $\Sigma_j$  in extrinsic balls (the bound depends on the ball but not on  $j$ ). More precisely, if  $\Sigma_{j,R}$  is a component of  $B_R \cap \Sigma_j$ , then Lemma C.3 implies that

$$\text{Area}(\Sigma_{j,R}) \leq C_c R^2, \quad (\text{IV.1.24})$$

where the constant  $C_c$  depends only on the supremum of  $|A|^2$  on  $B_{C_0 R} \cap \Sigma_j$ . The constant  $C_0$  here is universal and does not depend on the upper bound for the curvature.

- Even though each intrinsic ball of radius one in  $\Sigma_j$  is a disk, there is a component of  $B_4 \cap \Sigma_j$  that is not a disk. Therefore, it follows easily from a barrier argument and the one-sided lemma for non-simply connected surfaces, Lemma III.4.1, that there exists  $R > 4C_1$  so that only one component of  $B_R \cap \Sigma_j$  intersects  $B_{4C_1}$  for  $j$  large.<sup>25</sup>

□

The last result that we will need to recall before proving Proposition IV.1.1 is the following elementary property of connected planar domains:

**Lemma IV.1.25.** Let  $\Sigma$  be a connected planar domain and  $\sigma_1, \dots, \sigma_n$  the components of  $\partial\Sigma$ . Given  $k < n$  and a collection  $\{\sigma_{i_1}, \dots, \sigma_{i_k}\}$ , there is a simple closed curve  $\tilde{\sigma} \subset \Sigma$  which separates  $\cup_{j \leq k} \sigma_{i_j}$  from  $\partial\Sigma \setminus \cup_{j \leq k} \sigma_{i_j}$ .

*Proof.* (of Proposition IV.1.1). We will first use a rescaling argument to locate the smallest scale of non-trivial topology, choose a non-contractible curve  $\gamma$  on this scale, and then solve the Plateau problem with  $\gamma$  as interior boundary. We will then obtain an area bound for the components of  $\Gamma$  on this scale. This area bound will allow us to apply the “stable graph proposition”, Proposition D.2, to get the graph  $\Gamma_0 \subset \Gamma$  and thus prove (A). Finally, in the last step of the proof, we will find the separating curve  $\tilde{\sigma}$  and prove (B).

Blowing up on the smallest scale of non-trivial topology. Fix a large constant  $C_1 > 1$  to be chosen. Applying the blow up lemma, Lemma E.1 in Appendix E, at 0 gives an intrinsic ball

$$\mathcal{B}_{C_1 s_1}(y_1) \subset \mathcal{B}_{5C_1 r_1}, \quad (\text{IV.1.26})$$

---

<sup>25</sup>This follows exactly as does the analogous result for disks given in corollary 0.4 in [CM6]. Namely, if there were two such components, then we could put a stable surface between them. Interior estimates for stable surfaces then imply that each of the original components lies on one side of a plane that comes close to the center of the ball. However, this would contradict the one-sided lemma for non-simply connected surfaces, Lemma III.4.1, so we conclude that there could not have been two such components.

so that  $\mathcal{B}_{4s_1}(y_1)$  is not a disk but  $\mathcal{B}_{s_1}(y)$  is a disk for each  $y \in \mathcal{B}_{C_1s_1}(y_1)$ . We can now use this topologically non-trivial region  $\Sigma$  to solve a Plateau problem. Namely, applying Lemma IV.1.2 to the component of  $B_{4s_1}(y_1) \cap \Sigma$  containing  $\mathcal{B}_{4s_1}(y_1)$  gives a simple closed non-contractible<sup>26</sup> curve  $\gamma \subset B_{4s_1}(y_1) \cap \Sigma$ , a mean convex domain  $\Omega \subset B_{r_0} \setminus \Sigma$ , and a stable embedded minimal surface

$$\Gamma \subset \Omega, \tag{IV.1.27}$$

with interior boundary  $\partial\Gamma \setminus \partial B_{r_0}$  equal to  $\gamma$ . Moreover, there are distinct components  $\sigma_1$  and  $\sigma_2$  of  $\partial\Sigma \subset \partial B_{r_0}$  that are separated in  $\Sigma$  by  $\gamma$  and separated in  $\Omega$  by  $\Gamma$ . Finally,  $\Gamma$  is area-minimizing amongst surfaces in  $\Omega$  with boundary equal to  $\partial\Gamma$ .

An area estimate on the smallest scale of non-trivial topology. Suppose that  $\Gamma'$  is a component of  $B_{24s_1}(y_1) \cap \Gamma \setminus B_{8s_1}(y_1)$  which can be connected to  $\gamma$  by a curve in  $B_{17s_1}(y_1) \cap \Gamma$ . If the constant  $C_1$  from the previous step is sufficiently large (independent of  $\Sigma$  and  $\Gamma$ ), then Lemma IV.1.20 gives a constant  $C_2$  so that

$$\text{Area}(\Gamma') \leq C_2 s_1^2. \tag{IV.1.28}$$

Finding the graph in  $\Gamma$ . Using the area bound (IV.1.28), we can apply Proposition D.2 to get that each component of  $B_{r_0/C} \cap \Gamma \setminus B_{Cr_1}$  is a graph. A linking argument as in Lemma IV.1.2 then implies that one of these components  $\Gamma_0$  has the property that  $\Gamma_0 \cup B_{Cr_1}$  separates  $B_{r_0/C}$  into components  $H^+$  above and  $H^-$  below  $\Gamma_0$  where  $\sigma_1 \subset H^+$  and  $\sigma_2 \subset H^-$ .<sup>27</sup>

Finding the separating curve. To complete the proof, we need only find the separating curve  $\tilde{\sigma} \subset \Sigma$  and prove (B). In doing this, we will increase the constant  $C$  several times below.

The key to this step is to prove that there is a constant  $C_3 > 1$  so that

$$\text{only one component of } B_{C_3r_1} \cap \Sigma \text{ intersects both } H^+ \text{ and } H^-. \tag{IV.1.29}$$

Before proving (IV.1.29), it may be helpful to make a few remarks. First, it is not hard to see that (IV.1.29) is necessary to establish (B). Namely, if there were two distinct components of  $B_{C_3r_1} \cap \Sigma$  that each connected  $H^+$  and  $H^-$ , then it would be impossible to find a single connected curve in  $B_{C_3r_1} \cap \Sigma$  that separates  $H^+$  and  $H^-$ . Second, it is easy to see that there must be at least one component of  $B_{C_3r_1} \cap \Sigma$  that intersects both  $H^+$  and  $H^-$ . This is because  $\Sigma$  has boundary components  $\sigma_1 \subset H^+$  and  $\sigma_2 \subset H^-$  and the only way to connect these without crossing the annular graph  $\Gamma_0$  is to go through the ‘‘hole’’ in the middle. Finally, the basic idea behind (IV.1.29) is that if there were two components passing through the ‘‘hole’’ in  $\Gamma_0$ , then a barrier argument would also give a stable surface between the two components that also passes through the hole. However, such a stable surface would have to be very flat if  $C_3$  is large, so it cannot pass through this hole. This is essentially the argument that we will give below, but it will take a little work to make it precise.

Once we establish (IV.1.29), the rest of the proof of the proposition will follow easily. Namely, if let  $\hat{\Sigma}$  be the component of  $B_{Cr_1} \cap \Sigma$  intersecting both  $H^+$  and  $H^-$ , then Lemma IV.1.25 gives a simple closed curve  $\tilde{\sigma} \subset \hat{\Sigma}$  separating  $H^+ \cap \partial\hat{\Sigma}$  from  $H^- \cap \partial\hat{\Sigma}$ . In particular, the components  $\Sigma^\pm$  of  $\Sigma \setminus \tilde{\sigma}$  satisfy  $\Sigma^\pm \subset H^\pm \cup B_{Cr_1}$ .

<sup>26</sup>Since  $\Sigma$  has non-positive curvature and  $\gamma$  is non-contractible in the intrinsic ball  $\mathcal{B}_{4s_1}(y_1)$ , it is also non-contractible in  $\Sigma$ .

<sup>27</sup>Technically, this is not quite right since  $\partial\Sigma$  is contained in the boundary of the larger ball  $B_{r_0}$ . Rather, the linking argument gives two components – call them  $\tilde{\sigma}_1$  and  $\tilde{\sigma}_2$  – of  $\partial B_{r_0/C} \cap \Sigma$  that are separated by  $\Gamma_0$ .

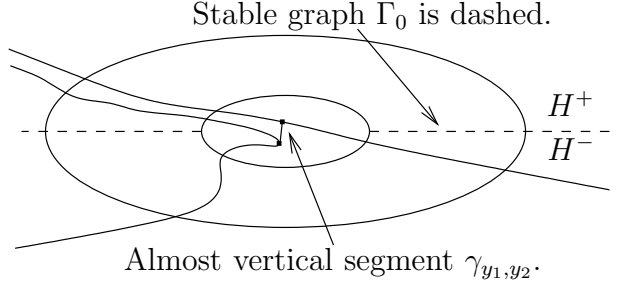


FIGURE 35. The key step in finding the separating curve: Ruling out that two components of  $B_{C_3 r_1} \cap \Sigma$  both intersect both  $H^+$  and  $H^-$ .

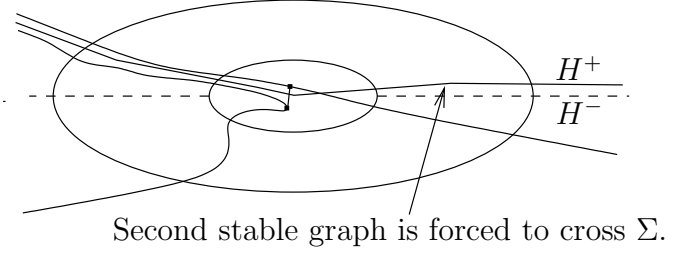


FIGURE 36. The contradiction: We cannot have a second stable graph that is between the two components of  $\Sigma$  and on one side of  $\Gamma_0$ .

Finally, to complete the proof of the proposition, it remains only to prove (IV.1.29). We will do this by contradiction, so suppose that  $\hat{\Sigma}_1$  and  $\hat{\Sigma}_2$  are distinct components of  $B_{C_3 r_1} \cap \Sigma$  each of which intersects both  $H^+$  and  $H^-$ . Since the only “hole” in the graph  $\Gamma_0$  is in  $B_{C r_1}$ , there must be components  $\tilde{\Sigma}_i \subset \hat{\Sigma}_i$  of  $B_{C r_1} \cap \Sigma$  intersecting both  $H^+$  and  $H^-$ ; see Figure 35. Label these components so  $\gamma \cap \hat{\Sigma}_2 = \emptyset$ . To get the contradiction, we will solve a Plateau problem to get a second stable graph that is between the  $\tilde{\Sigma}_i$ ’s and also disjoint from the graph  $\Gamma_0$ ; such a graph would be forced to sit on one side of  $\Gamma_0$  and hence would not allow both of the  $\tilde{\Sigma}_i$ ’s to intersect both  $H^+$  and  $H^-$ ; see Figure 36.

To set this up, note first that we can assume that  $\Gamma_0$  is a graph with arbitrarily small gradient – say at most  $\delta > 0$  – after possibly increasing  $C$ . This follows from estimates for minimal graphs; see proposition 1.12 in [CM13]. After a rotation of  $\mathbf{R}^3$ , we can assume that  $\Gamma_0$  is a graph over the horizontal plane  $\{x_3 = 0\}$ .

Fix a point  $y_1$  in  $B_{C r_1} \cap \tilde{\Sigma}_1$  and choose a point  $y_2$  in  $B_{2C r_1} \cap \tilde{\Sigma}_2$  so that the segment  $\gamma_{y_1, y_2}$  from  $y_1$  to  $y_2$  is “almost vertical”; see Figure 35. More precisely, applying lemma A.8 of [CM3] (as in (I.0.20) of [CM3]) gives  $y_2 \in B_{2C r_1} \cap \tilde{\Sigma}_2$  with

$$|\Pi(y_2 - y_1)| \leq |y_2 - y_1| \cos \theta_0, \quad (\text{IV.1.30})$$

where  $\Pi$  is orthogonal projection to the horizontal plane and the constant  $\theta_0$  is defined in the appendix of [CM3]. It now follows that there is a component  $\tilde{\Omega}$  of  $B_{C_3 r_1} \setminus (\Gamma \cup \Sigma)$  so (some subsegment of)  $\gamma_{y_1, y_2}$  is linked with  $\partial \tilde{\Sigma}_2$  in  $\tilde{\Omega}$ . Note that  $\tilde{\Omega}$  is mean convex in the sense of [MeYa2]. A result of [MeYa1]–[MeYa2] gives a stable embedded minimal surface

$$\hat{\Gamma}^0 \subset \tilde{\Omega} \quad (\text{IV.1.31})$$

with  $\partial \hat{\Gamma}^0 = \partial \tilde{\Sigma}_2$ . Since  $\partial \tilde{\Sigma}_2$  and  $\gamma_{y_1, y_2}$  are linked in  $\tilde{\Omega}$ , a component  $\hat{\Gamma}$  of  $B_{C_4 C r_1} \cap \hat{\Gamma}^0$  intersects  $\gamma_{y_1, y_2}$  at least once. However, combining curvature estimates [Sc1], [CM2] for stable surfaces with the fact that  $\hat{\Gamma}^0$  is disjoint from the graph  $\Gamma_0$  with small gradient (but comes close to this graph) implies that  $\hat{\Gamma}^0$  is also a graph with small gradient over the horizontal plane. Choosing the constants appropriately so the gradient of these graphs is sufficiently small, we see that  $\hat{\Gamma}^0$  can only intersect the “almost vertical” segment  $\gamma_{y_1, y_2}$  exactly once (see (IV.1.30)). In particular,  $\hat{\Gamma}^0$  separates  $\tilde{\Sigma}_1$  and  $\tilde{\Sigma}_2$ , forcing one of these to lie on the same

side of  $\Gamma_0$  as does  $\hat{\Gamma}^0$ . This gives the desired contradiction; see Figure 36. Consequently, we conclude that  $B_{C_3 r_1}(x_1) \cap \Sigma$  contains only one component  $\hat{\Sigma}$  which intersects both  $H_1^+$  and  $H_1^-$ , i.e., (IV.1.29) holds.  $\square$

**IV.1.2. Step (1): Decomposing  $\Sigma_j$  into ULSC pieces.** Suppose now that  $0 \in \mathcal{S}_{neck}$ , so that Proposition IV.1.1 gives

- (1) A sequence of stable graphs  $\Gamma_j$  that are disjoint from  $\Sigma_j$  and that converge to a punctured plane through 0; after rotating  $\mathbf{R}^3$ , we can assume that the stable graphs converge to  $\{x_3 = 0\} \setminus \{0\}$ .
- (2) A sequence of closed curves  $\tilde{\sigma}_j \subset B_{r_j} \cap \Sigma_j$  with  $r_j \rightarrow 0$  and so that  $\tilde{\sigma}_j$  divides  $\Sigma_j$  into a component  $\Sigma_j^+$  above  $\{x_3 = 0\}$  and a component  $\Sigma_j^-$  below.<sup>28</sup>

We will show next that each  $\Sigma_j^+$  contains a large scale-invariant ULSC piece  $\Sigma_j^{ulsc}$ . Before stating this precisely, it may be helpful to recall two simple examples:

- If we consider a sequence of shrinking catenoids, then 0 is the only point in  $\mathcal{S}_{neck}$  and each half of the catenoids is easily seen to be scale-invariant ULSC (in fact, given any point  $x \neq 0$  in one of the catenoids, the ball  $B_{|x|}(x)$  has two simply connected components).
- Consider now a sequence of rescalings of one of the Riemann examples. In this case,  $\mathcal{S}_{neck}$  is a line through the origin and  $\Sigma_j^+$  is *not* scale-invariant ULSC. However, if we cut  $\Sigma_j^+$  along a second short curve (the “neck” immediately above the first curve), then the resulting “pair of pants” is scale-invariant ULSC with respect to the distance to the closer of the two necks.

The precise statement of the decomposition into ULSC pieces is given in the next lemma. For simplicity, we will suppose that  $0 \in \mathcal{S}_{neck}$ ,  $\Sigma_j^+ \subset \Sigma_j$  are as above, and the constant  $C$  is given by Proposition IV.1.1.

**Lemma IV.1.32.** Let  $\tilde{\Sigma}_j^+$  denote the connected component of  $B_{R/(2C)} \cap \Sigma_j^+$  with  $\tilde{\sigma}_j$  in its boundary and fix a constant  $\alpha > 1$ . For each  $j$  sufficiently large, one of the following two cases holds:

- (1)  $\tilde{\Sigma}_j^+$  is scale-invariant ULSC: Given any  $x \notin B_{\alpha C r_j}$ , then each component of  $B_{|x|/(C\alpha)}(x) \cap \tilde{\Sigma}_j^+$  is a disk.
- (2)  $\tilde{\Sigma}_j^+$  contains a non-contractible curve  $\tilde{\sigma}_j^+$  in a ball  $B_{s_j}(y_j)$  with

$$|y_j| > \alpha C r_j \text{ and } s_j < |y_j|/(C\alpha), \quad (\text{IV.1.33})$$

so that the component  $\Sigma_j^{ulsc}$  of  $\tilde{\Sigma}_j^+ \setminus \tilde{\sigma}_j^+$  with  $\tilde{\sigma}_j$  in its boundary is scale-invariant ULSC: Given any  $x \notin (B_{\alpha C r_j} \cup B_{\alpha C s_j}(y_j))$ , then each component of

$$B_{\frac{\min\{|x|, |x-y_j|\}}{C\alpha}}(x) \cap \Sigma_j^{ulsc} \quad (\text{IV.1.34})$$

is a disk.

*Proof.* The key for establishing this lemma is that the decomposition into a  $\Sigma_j^+$  and a  $\Sigma_j^-$  can be repeated anywhere that the topology is concentrating. Namely, suppose that (1) does

<sup>28</sup>More precisely, there are shrinking extrinsic balls  $B_{r_j}$  so that  $\Sigma_j^+ \setminus B_{r_j}$  is above  $\Gamma_j$  and similarly for  $\Sigma_j^-$ .

not hold and, hence, there exists some  $z_1$  in  $B_{R_j/(2C)} \setminus B_{\alpha C r_j}$  so that some component of

$$B_{|z_1|/(\alpha C)}(z_1) \cap \tilde{\Sigma}_j^+ \quad (\text{IV.1.35})$$

is not a disk. We can repeat the argument of Proposition IV.1.1 to get a second stable graph  $\Gamma'_j$ , separating curve  $\tilde{\sigma}'_j$ , and components  $\Sigma_j^{++}$  and  $\Sigma_j^{+-}$  of  $\Sigma_j^+ \setminus \tilde{\sigma}'_j$  that are above and below, respectively, the graph  $\Gamma'_j$ ; see Figure 37.<sup>29</sup> Observe that the “middle component”  $\Sigma_j^{+-}$  is between the two stable graphs and has only two components in its interior boundary. If  $\Sigma_j^{+-}$  satisfies (2), then we are done. Otherwise, there is a third non-contractible simple closed curve. We can repeat the argument to cut  $\Sigma_j^{+-}$  to get an even lower component  $\Sigma_j^{+--}$ . The key point is that this new surface  $\Sigma_j^{+--}$  also has only two components in its interior boundary. Since  $\Sigma_j$  is compact, this process must eventually terminate to give a lowest component  $\Sigma_j^{+---}$  that satisfies (2).  $\square$

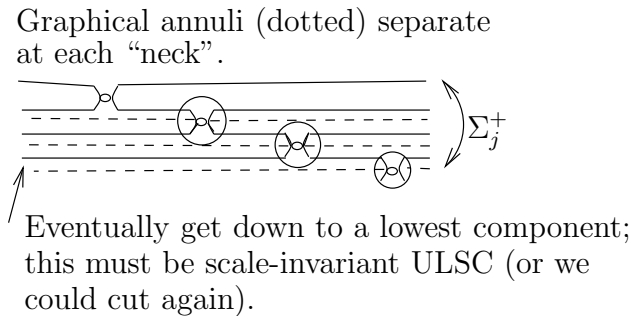


FIGURE 37. Cutting repeatedly to get the pair of pants decomposition.

**Remark IV.1.36.** The reader may find the constant  $\alpha$  in Lemma IV.1.32 somewhat mysterious. The point is that taking  $\alpha$  large forces the two interior boundary components in case (2) to be relatively far apart. This will be used to guarantee that the ULSC piece is sufficiently large, i.e., goes all the way out to the outer boundary in  $\partial B_{R_j/(2C)}$ .

**IV.1.3. Step (2): The ULSC pieces of  $\Sigma_j$  contain graphs.** We will next find the graphs in  $\Sigma_j$  converging to the plane  $\{x_3 = 0\}$  away from 0 and possibly one other point. The argument for this is slightly simpler in case (1) where  $\tilde{\Sigma}_j^+$  is itself scale-invariant ULSC and we do not need to cut along a second curve, but this simpler case already illustrates the key ideas. The argument follows a similar one in [CM11].

Suppose now that case (1) in Lemma IV.1.32 holds for (a subsequence of) the  $\Sigma_j$ 's. The existence of the graphs in the  $\tilde{\Sigma}_j^+$ 's converging to  $\{x_3 = 0\} \setminus \{0\}$  follows immediately from combining three facts:

- As  $j \rightarrow \infty$ , the minimum distance between  $\partial B_1 \cap \tilde{\Sigma}_j^+$  and  $\{x_3 = 0\}$  goes to zero. This was actually proven in lemma 3.3 of [CM8] that gave the existence of low points

<sup>29</sup>Proposition IV.1.1 directly gives the second stable graph disjoint from  $\Sigma_j$ . However, the proposition does not explicitly give that the two stable surfaces can be chosen to be disjoint. This is easy to achieve since the components of  $B_{R_j} \setminus (\Sigma_j \cup \Gamma_j)$  are also mean convex in the sense of Meeks-Yau.

in a connected minimal surface contained on one side of a plane and with interior boundary close to this plane.<sup>30</sup> We will recall this lemma from [CM8] next:

**Lemma IV.1.37.** Lemma 3.3 in [CM8]; see Figure 38. If  $0 < \epsilon < 4r_0/5$  and  $\Sigma \subset B_{r_0}$  is a connected immersed minimal surface with  $B_\epsilon \cap \Sigma \neq \emptyset$ ,  $\Sigma \setminus B_\epsilon \neq \emptyset$ , and

$$\partial\Sigma \subset B_\epsilon \cup (\partial B_{r_0} \cap \{x_3 > -3r_0/5\}), \tag{IV.1.38}$$

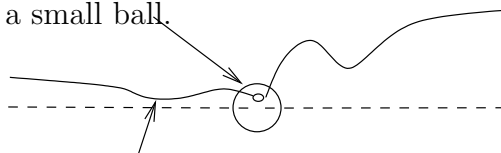
then

$$\min_{\Sigma \cap \{x_1^2 + x_2^2 \geq (4r_0/5)^2\}} x_3 \leq 4\epsilon \cosh^{-1}(3r_0/\epsilon) < 4\epsilon \log(6r_0/\epsilon). \tag{IV.1.39}$$

- The one-sided curvature estimate and the scale-invariant ULSC property give a scale-invariant curvature estimate for the  $\tilde{\Sigma}_j^+$ 's in a narrow cone about the plane  $\{x_3 = 0\}$ . Here we have used that the  $\tilde{\Sigma}_j^+$ 's stay on one side of the graphs  $\Gamma_j$  converging to  $\{x_3 = 0\} \setminus \{0\}$ . Similarly, this curvature estimate and the barrier limit plane imply that the  $\tilde{\Sigma}_j^+$ 's are locally graphical in a slightly narrower cone about  $\{x_3 = 0\}$ .
- The first step gives a sequence of points in the  $\tilde{\Sigma}_j^+$ 's converging to a point in  $\partial B_1 \cap \{x_3 = 0\}$ . The second step allows us to apply the Harnack inequality to build this out into expanding, locally graphical, subsets of the  $\tilde{\Sigma}_j^+$ 's that are converging to the plane.

These locally graphical regions piece together to give graphs over expanding annuli; the other possibility would be to form a multi-valued graph, but this is impossible since such a multi-valued graph would be forced to spiral infinitely (since it cannot cross itself and also cannot cross the stable graph  $\Gamma_j$ ).

A minimal surface  $\Sigma$  above a plane and with  $\partial\Sigma$  intersecting a small ball.



$\Sigma$  must contain points near the plane but far out.

FIGURE 38. The existence of low points near a plane.

Finally, we will briefly describe the modifications needed for case (2) in Lemma IV.1.32 when the  $\Sigma_j^{ulsc}$ 's have two interior boundary components. The complication arises in the second step. Namely, we can no longer locally extend the graph over  $\{x_3 = 0\} \setminus \{0\}$ ; this is because  $\tilde{\Sigma}_j^+$  is not scale-invariant ULSC in the second ball  $B_{s_j}(y_j)$ . To deal with this, we will consider several different cases.

The two simplest possibilities are when the points  $y_j$  go to either zero or infinity. When  $y_j \rightarrow 0$ , then we can replace the radii  $r_j$  by another sequence  $r'_j > \max\{r_j, |y_j|\}$  where

<sup>30</sup>The argument for this was by contradiction. Namely, if there were no low points, then we would get a contradiction from the strong maximum principle by first sliding a catenoid up under the surface and then sliding the catenoid horizontally away, eventually separating two boundary components of the surface. Here the strong maximum principle is used to keep the sliding catenoids and the surface disjoint. See, for instance, corollary 1.18 in [CM1] for a precise statement of the strong maximum principle.

$r'_j \rightarrow 0$ ; with the new choice of  $r'_j$ , the new  $\tilde{\Sigma}_j^+$ 's are ULSC and we can proceed as in case (1). On the other hand, when  $|y_j| \rightarrow \infty$ , we can replace the outer radii  $R_j$  by  $|y_j|$  and the new sequence of  $\tilde{\Sigma}_j^+$ 's will again be scale-invariant ULSC.

Suppose therefore that the points  $y_j$  converge to a finite point  $y \neq 0$ . We will consider two separate subcases here (we can reduce to these after taking subsequences):

- Suppose first that  $s_j$  goes to 0. In this case, the one-sided curvature estimate gives estimates for the  $\Sigma_j^{ulsc}$ 's as long as we stay away from the points 0 and  $y$ . We can then argue as in (1) to get the desired graphs – these graphs converge to  $\{x_3 = 0\} \setminus \{0, y\}$ .
- Suppose now that  $\liminf s_j = s_\infty > 0$ . In this case, the sequence is ULSC away from 0 but not scale-invariant ULSC (i.e., the injectivity radius stays away from zero, but it does not necessarily grow as we go away from 0). To make this precise, we will need an additional property of the balls  $B_{s_j}(y_j)$  that was not recorded in Lemma IV.1.32 but follows easily from its proof.<sup>31</sup> Namely, we can assume that  $s_j$  is the “smallest scale of non-trivial topology.” More precisely, we can assume that the component of  $B_{s_j}(y_j) \cap \Sigma_j$  containing the second interior boundary curve has injectivity radius at least  $\beta s_j$  for some fixed constant  $\beta > 0$ . In particular, since  $\liminf s_j > 0$ , the one-sided curvature estimate gives uniform estimates on these components of  $B_{s_j}(y_j) \cap \Sigma_j$ . We can now argue as in (1) to get the desired graphs; this time the graphs converge to  $\{x_3 = 0\} \setminus \{0\}$ .

This completes the proof of (C1) in Theorem 0.14.

#### IV.2. THE ULSC REGIONS OF THE LAMINATION: (C2) AND (D) IN THEOREM 0.14

In this section, we will prove that the ULSC regions of the lamination have the same structure as in the globally ULSC case of Theorem 0.9. Namely, we will prove that:

- The leaves intersecting the ULSC part of the singular set  $\mathcal{S}_{ulsc}$  are parallel planes. Each plane intersects  $\mathcal{S}_{ulsc}$  at two points.
- $\mathcal{S}_{ulsc}$  is a union of Lipschitz curves transverse to the leaves. The leaves intersecting  $\mathcal{S}_{ulsc}$  foliate an open subset of  $\mathbf{R}^3$  that does not intersect  $\mathcal{S}_{neck}$ .

The key for the proof of these two properties will be to show that each collapsed leaf has a neighborhood that is ULSC; this will be done in Proposition IV.2.2. Recall that a leaf  $\Gamma$  of  $\mathcal{L}'$  is said to be collapsed if its closure  $\Gamma_{Clos}$  contains a point in  $\mathcal{S}_{ulsc}$  and this point is a removable singularity for  $\Gamma$ ; see Definition II.2.9. We have already established a great deal of structure for collapsed leaves in Proposition II.3.1 and much of this will be used below.

Here, and elsewhere in this section, the closure  $\Gamma_{Clos}$  of a leaf  $\Gamma$  is defined to be the union of the closures of all bounded geodesic balls in  $\Gamma$ ; that is, we fix a point  $x_\Gamma \in \Gamma$  and set

$$\Gamma_{Clos} = \bigcup_r \overline{\mathcal{B}_r(x_\Gamma)}, \quad (\text{IV.2.1})$$

where  $\overline{\mathcal{B}_r(x_\Gamma)}$  is the closure of  $\mathcal{B}_r(x_\Gamma)$  as a subset of  $\mathbf{R}^3$ . Eventually we will show that  $\Gamma_{Clos}$  is a flat plane and hence, in particular,  $\Gamma_{Clos} = \bar{\Gamma}$ . However, a priori  $\Gamma$  may not be proper, and thus the two notions could a priori differ.

<sup>31</sup>See “Blowing up on the smallest scale of non-trivial topology.” in the proof of Proposition IV.1.1.

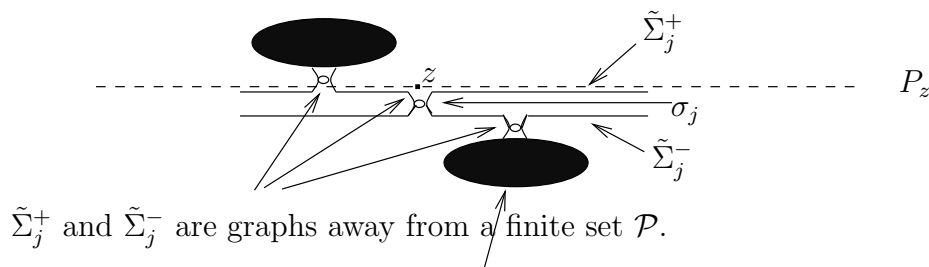
The main result of this section is Proposition IV.2.2 below showing that  $\Gamma_{Clos}$  does not intersect  $\mathcal{S}_{neck}$ . Since  $\mathcal{S}_{neck}$  is a closed subset of  $\mathbf{R}^3$ , it follows that every compact subset of  $\Gamma_{Clos}$  has a neighborhood in  $\mathbf{R}^3$  that does not intersect  $\mathcal{S}_{neck}$ .

**Proposition IV.2.2.** If  $\Gamma$  is a collapsed leaf of  $\mathcal{L}'$ , then  $\Gamma_{Clos} \cap \mathcal{S}_{neck} = \emptyset$ .

The rough idea of the proof is to first show that  $\Gamma_{Clos} \setminus \Gamma$  consists of exactly two points (this is analogous to each leaf having at most two singular points in the ULSC case); see Corollary IV.2.6 below. Consequently, the union of  $\Gamma$  and the given point in  $\Gamma_{Clos} \cap \mathcal{S}_{ulsc}$  will give a stable surface that is “complete away from a point” and, hence flat by Lemma B.26. Finally, once we know that  $\Gamma$  is flat, it will be easy to check that  $\Gamma_{Clos} \cap \mathcal{S}_{neck} = \emptyset$ .

Before we can get into the proof just outlined, we will need to recall a little of the structure that has already been proven. We will do this in the next two subsections. The next subsection establishes a key property of the stable limit planes that we get through each point of  $\mathcal{S}_{neck}$ . The second subsection below reviews the properties of a general collapsed leaf of  $\mathcal{L}'$ .

**IV.2.1. The leaf  $\Gamma$  cannot cross the limit planes.** The structure result  $(C_{neck})$  from Theorem 0.12 gives graphs  $\tilde{\Sigma}_j^+$  and  $\tilde{\Sigma}_j^-$  in  $\Sigma_j$  that converge to a plane  $P_z$  through each point  $z \in \mathcal{S}_{neck}$ ; see Figure 39. The graphs  $\tilde{\Sigma}_j^+$  converge smoothly away from  $z$  and possibly one other point (call it  $z^+$ ); this second point must also be in  $\mathcal{S}_{neck}$ . Similarly, the  $\tilde{\Sigma}_j^-$  converge away from  $z$  and possibly a point  $z^- \in \mathcal{S}_{neck}$ . Furthermore,  $\tilde{\Sigma}_j^+$  and  $\tilde{\Sigma}_j^-$  are separated in  $\Sigma_j$  by the curve  $\sigma_j$ .<sup>32</sup> One expects that the limit plane  $P_z$  should be the closure of a leaf of  $\mathcal{L}'$ , but this is not a priori clear; for instance,  $\mathcal{S}$  might even be dense in  $P_z$ .



The multi-valued graphs are contained in the dark regions.

FIGURE 39. The structure near  $z$ : The two graphs  $\tilde{\Sigma}_j^+$  and  $\tilde{\Sigma}_j^-$  are separated by curves  $\sigma_j$  shrinking to  $z$ . The multi-valued graph  $\Sigma_j^g$  comes near  $z$ .

Using this structure, the next lemma proves that the leaves of  $\mathcal{L}'$  do not cross any of these limit planes. This is almost obvious since the stable surfaces converging to the limit plane are disjoint from the  $\Sigma_j$ 's that are converging to the leaves of  $\mathcal{L}'$ . The only possible difficulty comes from that the convergence is only away from the singular set  $\mathcal{S}$ , but this will be easy to handle. The lemma applies to an arbitrary leaf  $\Gamma$  of  $\mathcal{L}'$ , i.e., we do not need  $\Gamma$  to be collapsed.

<sup>32</sup>Property  $(C_{neck})$  from Theorem 0.12 holds at  $z$  by (C1) in Theorem 0.14; this was proven in Section IV.1. The last “separation” claim is not explicit in  $(C_{neck})$  but follows immediately from Proposition IV.1.1; using the notation from that proposition, we have that  $\tilde{\Sigma}_j^+ \subset \Sigma_j^+$  and  $\tilde{\Sigma}_j^- \subset \Sigma_j^-$ .

**Lemma IV.2.3.** Suppose that  $\Gamma$  is an arbitrary leaf of  $\mathcal{L}'$ , collapsed or not. If  $z$  is any point in  $\mathcal{S}_{neck}$  and  $P_z$  is the corresponding limit plane through  $z$ , then  $\Gamma$  does not cross  $P_z$ .

*Proof.* Fix an open connected set  $K \subset \Gamma$  with compact closure in  $\Gamma$  and recall that the  $\Sigma_j$ 's contain:

- Graphs  $\tilde{\Sigma}_j^+$  and  $\tilde{\Sigma}_j^-$  that both converge to  $P_z$  away from a finite set  $\mathcal{P}$  of points; see Figure 39. Moreover,  $\tilde{\Sigma}_j^+$  and  $\tilde{\Sigma}_j^-$  are separated in  $\Sigma_j$  by curves  $\sigma_j$  shrinking to  $z$ .
- Connected subsets  $\Sigma_j^g \subset \Sigma_j$  given by Lemma II.3.15 that are locally graphical over  $K$  and that converge with multiplicity to  $K$ . These locally graphical subsets might globally be graphs or multi-valued graphs over  $K$ .

We will show first that the  $\Sigma_j^g$ 's cannot intersect both  $\tilde{\Sigma}_j^+$  and  $\tilde{\Sigma}_j^-$ . First, using that  $z$  is not in  $\Gamma$  and  $K \subset \Gamma$  has compact closure, we can fix a ball  $B_s(z)$  so that

$$B_s(z) \cap \Sigma_j^g = \emptyset \quad (\text{IV.2.4})$$

for all  $j$  sufficiently large. On the other hand, the curves  $\sigma_j$  separating  $\tilde{\Sigma}_j^+$  and  $\tilde{\Sigma}_j^-$  are shrinking to  $z$ . Therefore, the curves  $\sigma_j$  don't intersect  $\Sigma_j^g$  when  $j$  is large and, hence, the connected set  $\Sigma_j^g$  cannot intersect both  $\tilde{\Sigma}_j^+$  and  $\tilde{\Sigma}_j^-$ . Without loss of generality, we can assume that

$$\Sigma_j^g \cap \tilde{\Sigma}_j^+ = \emptyset. \quad (\text{IV.2.5})$$

We will next use (IV.2.5) to show that the two smooth open surfaces  $P_z$  and  $K$  do not have any points of transverse intersection. Namely, if  $P_z$  and  $K$  have points of transverse intersection, then, since the singular set  $\mathcal{P}$  for the convergence to  $P_z$  is finite,  $P_z \setminus \mathcal{P}$  and  $K$  would also have points of transverse intersection. However, this contradicts (IV.2.5) since  $\tilde{\Sigma}_j^+ \rightarrow P_z$  smoothly away from  $\mathcal{P}$  and  $\Sigma_j^g \rightarrow K$ .

Finally, recall that if a connected minimal surface intersects both sides of a plane, then the surface and plane must have a point of transverse intersection; this follows from the local structure of the nodal set of a harmonic function, see, e.g., lemma 4.28 in [CM1]. Therefore, since  $K$  is connected and does not intersect  $P_z$  transversely at any point, we see that  $K$  must be on one side of  $P_z$ . Since this holds for every such  $K$  and these exhaust  $\Gamma$  by Lemma A.1 in Appendix A, we see that  $\Gamma$  also lies on one side of  $P_z$ .  $\square$

*Throughout the rest of this section,  $\Gamma$  will be a collapsed leaf of  $\mathcal{L}'$ .*

**IV.2.2. The properties of a collapsed leaf  $\Gamma$ .** Before getting into the proof, it may be useful to recall the properties of the leaf  $\Gamma$ . Eventually, we will use these properties to show that  $\Gamma_{Clos}$  is a plane.

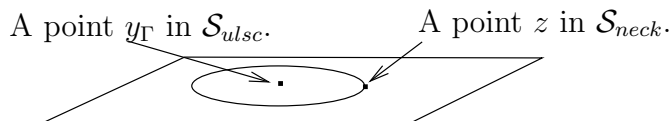
- $\Gamma$  is by definition an injective immersion of a connected surface without boundary, but not necessarily complete. Furthermore, the immersion is not necessarily proper.
- Since  $\Gamma$  is a leaf of  $\mathcal{L}'$ , it follows that  $\Gamma$  does not intersect  $\mathcal{S}$  – and hence, since  $\mathcal{S}$  is closed (as a subset of  $\mathbf{R}^3$ ), each point in  $\Gamma$  has a neighborhood where the curvatures of the  $\Sigma_j$ 's are uniformly bounded.
- The following local structure of  $\Gamma$  near a point of  $\Gamma_{Clos} \cap \mathcal{S}_{ulsc}$  was established in (1) in Proposition II.3.1:

(Loc) Given any  $y \in \Gamma_{Clos} \cap \mathcal{S}_{ulsc}$ , there exists  $r_0 > 0$  so that the closure (in  $\mathbf{R}^3$ ) of each component of  $B_{r_0}(y) \cap \Gamma$  is a compact embedded disk with boundary in  $\partial B_{r_0}(y)$ .

Furthermore,  $B_{r_0}(y) \cap \Gamma$  must contain the component  $\Gamma_y$  given by Lemma II.2.3 and  $\Gamma_y$  is the only component of  $B_{r_0}(y) \cap \Gamma$  with  $y$  in its closure.

- $\Gamma$  (or its oriented double cover) must be stable by (2) in Proposition II.3.1.
- $\Gamma_{Clos}$  intersects  $\mathcal{S}_{ulsc}$  in at most two points by (3) in Proposition II.3.1.

These properties will be essential for proving Proposition IV.2.2. The main difficulty will be that  $\Gamma$  is not complete. This occurs where  $\Gamma_{Clos}$  intersects  $\mathcal{S}$ ; see Figure 40 for such an example. By (Loc), the points in  $\Gamma_{Clos} \cap \mathcal{S}_{ulsc}$  are isolated removable singularities of  $\Gamma$  and thus are easily dealt with. Consequently, the first step will be to control the number of points of  $\Gamma_{Clos} \cap \mathcal{S}_{neck}$  when  $\Gamma$  is collapsed. This will be done in the next subsection.



Each point in  $\partial\Gamma$  is in  $\mathcal{S}$ .

FIGURE 40. A priori  $\Gamma$  could be a punctured disk in a plane.

IV.2.3.  $\Gamma_{Clos} \setminus \Gamma$  **consists of exactly two points.** The next corollary is the first step needed for the proof of Proposition IV.2.2 that gives  $\Gamma_{Clos} \cap \mathcal{S}_{neck} = \emptyset$ . This corollary shows that if  $\Gamma_{Clos} \cap \mathcal{S}_{neck} \neq \emptyset$ , then  $\Gamma_{Clos} \setminus \Gamma$  consists of exactly two points.

**Corollary IV.2.6.** Let  $\Gamma$  be a collapsed leaf of  $\mathcal{L}'$ . If  $\Gamma_{Clos} \cap \mathcal{S}_{neck} \neq \emptyset$ , then  $\Gamma_{Clos} \setminus \Gamma$  consists of exactly two points with one each in  $\mathcal{S}_{ulsc}$  and  $\mathcal{S}_{neck}$ .

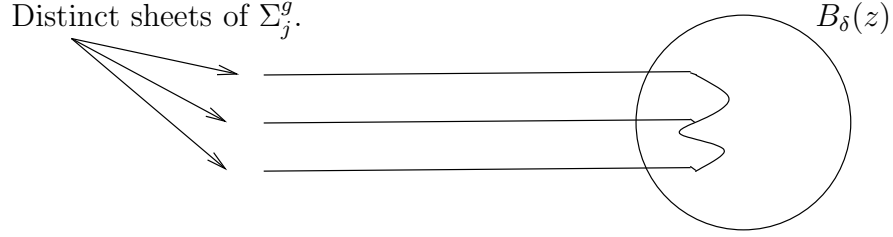
This will be an easy corollary of Lemma IV.2.7 below that shows that the sheets of the multi-valued graphs over  $\Gamma$  connect in a small neighborhood of any singular point. Previously, we used the one-sided curvature estimate to establish a similar connecting property near a point of  $\mathcal{S}_{ulsc}$ .

Before making this connecting property precise, we need to set up some notation. Recall that if  $K$  is a “sufficiently large” open connected subdomain of  $\Gamma$  with compact closure in  $\Gamma$ , then Corollary II.3.18 gives a sequence of multi-valued graphs  $\Sigma_j^g \subset \Sigma_j$  that converges to  $K$  with infinite multiplicity. Since  $\Gamma$  can be exhausted by a nested sequence  $K_j$  of such  $K$ ’s by Lemma A.1, we can assume that the following holds (after passing to a subsequence):

- (Graph)  $\Sigma_j$  contains a  $j$ -valued graph  $\Sigma_j^g$  over  $K_j$  of a function whose values are bounded by  $1/j$  and whose gradient is bounded by  $1/j$ . Here  $K_j \subset \Gamma$  is a nested sequence of connected open sets with compact closure in  $\Gamma$  with  $\Gamma = \cup_j K_j$ .

We actually know a good deal more about these multi-valued graphs, but this additional structure will not be needed until the proof of Corollary IV.2.6.

**Lemma IV.2.7.** The sheets of the multi-valued graph  $\Sigma_j^g$  connect near  $z \in \Gamma_{Clos} \cap \mathcal{S}_{neck}$ ; see Figure 41. Precisely, given any  $r > 0$ , there exist  $\delta > 0$  and  $J$  so that if  $x \in B_\delta(z) \cap \Gamma$ ,



The sheets all intersect the same component of  $B_\delta(z) \cap \Sigma$  for  $j$  sufficiently large.

FIGURE 41. Lemma IV.2.7: The sheets of the multi-valued graph  $\Sigma_j^g$  must connect near  $z \in \Gamma_{\text{Clos}} \cap \mathcal{S}_{\text{neck}}$ .

$j > J$ , and

$$z_j^+ \text{ and } z_j^- \text{ are points in the multi-valued graph } \Sigma_j^g \text{ over } x, \quad (\text{IV.2.8})$$

then  $z_j^+$  and  $z_j^-$  are in the same connected component of  $B_r(z) \cap \Sigma_j$ .

*Proof.* We will argue by contradiction, so suppose there exists some  $r > 0$  so that for every  $\delta > 0$  there exists  $x \in B_\delta(z) \cap \Gamma$  and infinitely  $j$ 's so that  $B_r(z) \cap \Sigma_j$  has (at least) two distinct components that both contain points in  $\Sigma_j^g$  over  $x$ . After passing to a subsequence, we can assume that there is a sequence of points  $z_j^+$  and  $z_j^-$  in  $\Sigma_j^g$  with

$$z_j^+ \text{ and } z_j^- \text{ converging to } z, \quad (\text{IV.2.9})$$

so that  $z_j^+$  and  $z_j^-$  are in distinct components of  $B_r(z) \cap \Sigma_j$ .

We will use the  $\Sigma_j$ 's as barriers for a Plateau problem to construct stable surfaces  $\tilde{\Gamma}_j$  between these distinct components. Before constructing the stable surfaces  $\tilde{\Gamma}_j$ , recall the following useful consequence of the interior curvature estimates for stable surfaces of [Sc1], [CM2] (see, e.g., lemma 2.2 in [CM1]):

(Stab) There exists a positive constant  $\alpha < 1$  so that if  $\Gamma_s$  is a stable embedded minimal surface with  $\partial\Gamma_s \subset \partial B_R$ , then each component of  $B_{\alpha R} \cap \Gamma_s$  is a graph over some plane with gradient bounded by one.

Set

$$r' = \alpha r. \quad (\text{IV.2.10})$$

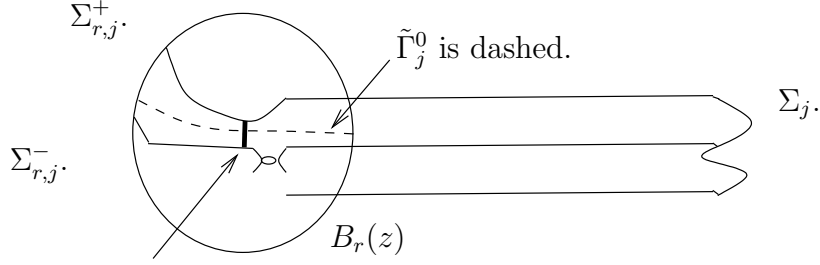
**The properties of the stable graphs  $\tilde{\Gamma}_j$ :** We will below find (stable) graphs  $\tilde{\Gamma}_j$  between these distinct components so that the following three properties hold:

$$\tilde{\Gamma}_j \subset B_{r'}(z) \setminus \Sigma_j \text{ with } \partial\tilde{\Gamma}_j \subset \partial B_{r'}(z). \quad (\text{IV.2.11})$$

$$B_{\epsilon_j}(z) \cap \tilde{\Gamma}_j \neq \emptyset \text{ where } \epsilon_j \rightarrow 0. \quad (\text{IV.2.12})$$

$$\text{The multi-valued graph } \Sigma_j^g \text{ in } \Sigma_j \text{ intersects both sides of } \tilde{\Gamma}_j. \quad (\text{IV.2.13})$$

Recall that a properly embedded (connected) surface in  $\mathbf{R}^3$  will automatically have two sides. Properties (IV.2.12) and (IV.2.13) will follow from a standard linking argument.



Bold  $\ell_j$  connects the two components  $\Sigma_{r,j}^+$  and  $\Sigma_{r,j}^-$  of  $B_r(z) \cap \Sigma_j$

FIGURE 42. We argue by contradiction to show that the sheets connect near  $z$ . Assuming that they don't, we first construct stable surfaces  $\tilde{\Gamma}_j$ .

**Constructing the stable graphs  $\tilde{\Gamma}_j$ :** We will construct  $\tilde{\Gamma}_j$  in two steps, first finding stable surfaces  $\tilde{\Gamma}_j^0$  in the larger ball  $B_r(z)$  and then letting  $\tilde{\Gamma}_j$  be an appropriate component of  $B_{r'}(z) \cap \tilde{\Gamma}_j^0$  where  $r'$  is given by (IV.2.10).

To construct  $\tilde{\Gamma}_j^0$ , first choose two distinct components  $\Sigma_{r,j}^+$  and  $\Sigma_{r,j}^-$  of  $B_r(z) \cap \Sigma_j$  that both contain points in  $\Sigma_j^g$  over  $z_j$ ; these exist by assumption. Let  $\ell_j$  be a line segment connecting the two points over  $x_j$  in  $\Sigma_{r,j}^+$  and  $\Sigma_{r,j}^-$ ; see Figure 42. Fix a component  $\ell_j^0$  of  $\ell_j \setminus (\Sigma_{r,j}^+ \cup \Sigma_{r,j}^-)$  that also connects  $\Sigma_{r,j}^+$  and  $\Sigma_{r,j}^-$  but intersects  $\Sigma_{r,j}^+$  and  $\Sigma_{r,j}^-$  only at its endpoints  $\partial\ell_j^0$ . The surface  $\Sigma_{r,j}^+$  sits in the boundary of two components of  $B_r(z) \setminus \Sigma_j$  – one component on each side of  $\Sigma_{r,j}^+$ .<sup>33</sup> Let  $\Omega_j$  be the component that  $\ell_j^0$  points into as it leaves  $\Sigma_{r,j}^+$ ; i.e., let  $\Omega_j$  be the component of  $B_r(z) \setminus \Sigma_j$  with

$$\Sigma_{r,j}^+ \subset \partial\Omega_j \text{ and } \Omega_j \cap (\ell_j^0 \setminus \partial\ell_j^0) \neq \emptyset. \quad (\text{IV.2.14})$$

The point of choosing  $\Omega_j$  in this way is that the curve  $\ell_j^0$  has linking number one with  $\partial\Sigma_{r,j}^+$  in  $\Omega_j$ . The domain  $\Omega_j$  is mean convex and, hence, [MeYa1]–[MeYa2] gives a stable embedded minimal surface  $\tilde{\Gamma}_j^0 \subset \Omega_j$  with  $\partial\tilde{\Gamma}_j^0 = \partial\Sigma_{r,j}^+$ .

Since  $\partial\tilde{\Gamma}_j^0$  has linking number one with  $\ell_j^0$  in  $\Omega_j$ , the endpoints of  $\ell_j^0$  are separated in  $B_r(z)$  by  $\tilde{\Gamma}_j^0$ . However, the endpoints of  $\ell_j^0$  connect to the endpoints of  $\ell_j$  by curves in  $\Sigma_{r,j}^+$  and  $\Sigma_{r,j}^-$ ; these curves do not cross  $\tilde{\Gamma}_j^0$  and, consequently, the endpoints of  $\ell_j$  are also separated in  $B_r(z)$  by  $\tilde{\Gamma}_j^0$ . We can therefore choose a component  $\tilde{\Gamma}_j$  of  $B_{r'}(z) \cap \tilde{\Gamma}_j^0$  that separates the endpoints of  $\ell_j$ ; so

$$\tilde{\Gamma}_j \cap \ell_j \neq \emptyset. \quad (\text{IV.2.15})$$

Since  $z_j^+$  and  $z_j^-$  go to  $z$ , it follows that each  $\ell_j$  is contained in a ball  $B_{\epsilon_j}(z)$  where  $\epsilon_j \rightarrow 0$ . In particular, (IV.2.15) gives (IV.2.12). Since the endpoints of  $\ell_j$  are both in the multi-valued graph, we also get (IV.2.13).

**Using the stable graphs  $\tilde{\Gamma}_j$  to show that  $\Gamma \subset P_z$ :** Now that we have constructed the  $\tilde{\Gamma}_j$ 's, we are ready to return to the proof of the lemma. The first step will be to show that

<sup>33</sup>In the simplest case where  $\Sigma_{r,j}^+$  and  $\Sigma_{r,j}^-$  are the only components of  $B_r(z) \cap \Sigma_j$ , we would choose  $\Omega_j$  to be the component of  $B_r(z) \setminus \Sigma_j$  between them, i.e., the component containing the interior of  $\ell_j^0$ . In general, there are other components of  $B_r(z) \cap \Sigma_j$  intersecting  $\ell_j^0$  so we cannot do this. This slightly complicates the choice of  $\Omega_j$ .

a subsequence of the  $\tilde{\Gamma}_j$ 's converges to a subset of  $P_z$ . First, by (Stab), the surface  $\tilde{\Gamma}_j$  is a graph with gradient bounded by one. After passing to a subsequence, we can therefore assume that  $\tilde{\Gamma}_j$  converges to a minimal graph  $\tilde{\Gamma}$ . Since  $\epsilon_j \rightarrow 0$ ,  $\tilde{\Gamma}$  contains  $z$ . On the other hand,  $\tilde{\Sigma}_j^+ \subset \Sigma_j$  does not intersect the graph  $\tilde{\Gamma}_j$ ; since  $\tilde{\Sigma}_j^+$  converges to  $P_z$  away from a finite set, we conclude that  $\tilde{\Gamma}$  must be on one side of  $P_z$ . Since  $\tilde{\Gamma}$  is on one side of  $P_z$  and intersects it at  $z$ , the strong maximum principle implies that  $\tilde{\Gamma}$  is contained in  $P_z$ , as desired.

We will next show that

$$\Gamma \subset P_z. \quad (\text{IV.2.16})$$

First, by (IV.2.13), there is at least one sheet of the multi-valued graph  $\Sigma_j^g$  on each side of the graph  $\tilde{\Gamma}_j$  for every  $j$ . Since both of these sheets converge to  $\Gamma$  by (Graph), we can fix a point  $\tilde{y}$  in  $B_{r'} \cap \Gamma$  that is both a limit of points  $\tilde{y}_j^+$  above  $\tilde{\Gamma}_j$  and a limit of points  $\tilde{y}_j^-$  below  $\tilde{\Gamma}_j$ . For each  $j$ , the line segment connecting  $\tilde{y}_j^+$  to  $\tilde{y}_j^-$  must intersect  $\tilde{\Gamma}_j$  at a point  $\tilde{y}_j$ . The sequence of points  $\tilde{y}_j \in \tilde{\Gamma}_j$  must also converge to the common limit  $\tilde{y}$  of  $\tilde{y}_j^+$  and  $\tilde{y}_j^-$ . In particular, we conclude that  $\tilde{y} \in P_z \cap \Gamma$ , so that  $\Gamma \subset P_z$  by the strong maximum principle.

**The contradiction: We cannot have  $\Gamma \subset P_z$ :** To complete the proof of the lemma, we explain next how (IV.2.16) leads to a contradiction. Since we will need the same argument later, it will be useful to isolate it out as a claim:

**Claim:** (IV.2.16) cannot hold, i.e., we cannot have  $\Gamma \subset P_z$ .

**Proof of Claim:** We will argue by contradiction, so suppose that  $\Gamma \subset P_z$ . Since  $\Gamma_{Clos}$  is the closure of  $\Gamma$ , it follows that  $\Gamma_{Clos} \subset P_z$  as well. Since  $\Gamma$  is collapsed,  $\Gamma_{Clos}$  contains a point

$$y_\Gamma \in \mathcal{S}_{ulsc} \cap \Gamma_{Clos} \subset P_z. \quad (\text{IV.2.17})$$

Both of the graphs  $\tilde{\Sigma}_j^+$  and  $\tilde{\Sigma}_j^-$  are converging to  $P_z$  away from punctures in  $\mathcal{S}_{neck}$ , so we get sequences of points  $y_j^+ \in \tilde{\Sigma}_j^+$  and  $y_j^- \in \tilde{\Sigma}_j^-$  with

$$y_j^+ \rightarrow y_\Gamma \text{ and } y_j^- \rightarrow y_\Gamma. \quad (\text{IV.2.18})$$

We will next use the one-sided curvature estimate to prove that  $y_j^+$  and  $y_j^-$  can be connected in  $\Sigma_j$  in any small neighborhood of  $y_\Gamma$  as  $j \rightarrow \infty$ . To see this, note first that  $y_\Gamma$  is in  $\mathcal{S}_{ulsc}$  and hence each component of  $B_r(y_\Gamma) \cap \Sigma_j$  is a disk for some  $r > 0$ ; after possibly choosing  $r$  smaller, we can assume that  $|y_\Gamma - z| > r$ . If there were at least two of these disks in  $B_r(y_\Gamma) \cap \Sigma_j$  intersecting the concentric sub-ball  $B_{C''r}(y_\Gamma)$  where  $C'' > 0$  is a sufficiently small constant, then the one-sided curvature estimate would give a uniform curvature bound for each component of  $\Sigma_j$  in this sub-ball.<sup>34</sup> Since no such curvature bound holds near a point of  $\mathcal{S}$  by definition, we conclude that the points  $y_j^+$  and  $y_j^-$  must be in the same connected component of  $B_r(y_\Gamma) \cap \Sigma_j$  for all  $j$  sufficiently large.

This local connectedness near  $y_\Gamma$  will easily lead to a contradiction. This is because  $y_j^+$  and  $y_j^-$  were proven to be separated in  $\Sigma_j$  by the curve  $\sigma_j$  and the  $\sigma_j$ 's are shrinking to the point  $z \neq y_\Gamma$ . This contradiction completes the proof of the Claim and hence of the lemma.  $\square$

---

<sup>34</sup>We actually use a corollary of the one-sided curvature estimate recorded in corollary 0.4 in [CM6]. This corollary states that if there are two disjoint surfaces in a ball in  $\mathbf{R}^3$ , both intersect a sufficiently small ball around the center, and one is a disk, then we get an interior curvature estimate for the disk-type component.

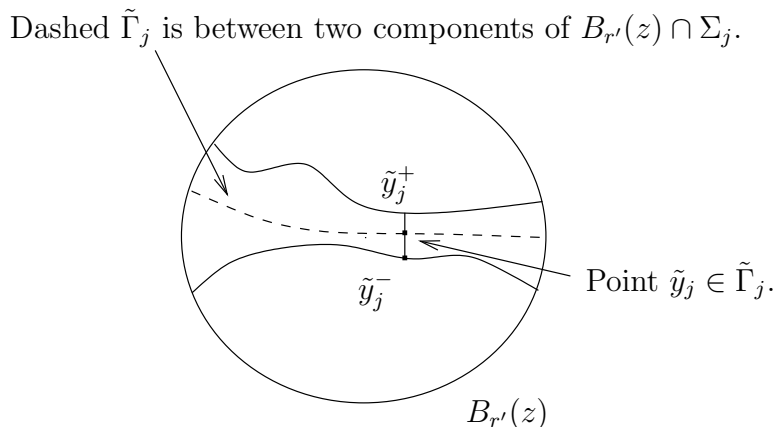


FIGURE 43. The points  $\tilde{y}_j^+$  and  $\tilde{y}_j^-$  converge to a point  $\tilde{y} \in \Gamma$  from opposite sides of the graph  $\tilde{\Gamma}_j$ . Thus, the points  $\tilde{y}_j \in \tilde{\Gamma}_j$  between them also converge to  $\tilde{y} \in \Gamma$ , giving Lemma IV.2.7.

*Proof.* (of Corollary IV.2.6.) By assumption,  $\Gamma_{Clos} \cap \mathcal{S}$  contains at least one point in each of  $\Gamma_{Clos} \cap \mathcal{S}_{ulsc}$  and  $\Gamma_{Clos} \cap \mathcal{S}_{neck}$ . We will argue by contradiction to prove that  $\Gamma_{Clos} \cap \mathcal{S}$  cannot contain a third point. For simplicity, we will assume that the  $\Sigma_j$ 's are planar domains; the general finite genus case follows with easy modifications.

The proof follows the argument given in Remark II.3.31 and the basic idea is simple:

Suppose that  $p$ ,  $q$ , and  $r$  are distinct points in  $\Gamma_{Clos} \cap \mathcal{S}$ . The local connecting property near each point of  $\mathcal{S}$  allows us to construct closed non-contractible curves in the  $\Sigma_j$ 's that converge with multiplicity two to a curve in  $\Gamma$  connecting  $p$  and  $q$ . These curves must separate in the planar domain  $\Sigma_j$ . However, if we connect points on opposite sides of these curves to the third point  $r$ , the local connecting property near  $r$  gives a contradiction.

The only difficulty in carrying out this argument will be that the surface  $\Gamma$  is not complete.

**Step 1: Choosing the singular points and curves in  $\Gamma$ .** We will first choose the points  $p$ ,  $q$ , and  $r$  in  $\Gamma_{Clos} \cap \mathcal{S}$ . Let  $p$  be the given point in  $\Gamma_{Clos} \cap \mathcal{S}_{ulsc}$  and then let  $q$  be a closest point in  $\Gamma_{Clos} \cap \mathcal{S}$  to  $p$  (a priori there may be many possible choices). Since we are arguing by contradiction, there is a third distinct point  $r \in \Gamma_{Clos} \cap \mathcal{S}$ .

By our choice of  $q$ , there must be a minimizing geodesic  $\gamma_{pq} : [0, L] \rightarrow \Gamma_{Clos}$  parameterized by arclength and with the following properties:

- $\gamma_{pq}(0) = p$  and  $\gamma_{pq}(L) = q$ .
- The interior of  $\gamma_{pq}$  is contained in  $\Gamma$ .

Since the closed geodesic  $\gamma_{pq}$  is compact, we must have

$$\text{dist}_{\mathbb{R}^3}(\gamma_{pq}, r) > 0. \tag{IV.2.19}$$

Since  $p \in \mathcal{S}_{ulsc}$  and  $\Gamma$  is collapsed, property (1) in Proposition II.3.1 gives a ball  $B_\delta(p)$  and a component  $\Gamma_p$  of  $B_\delta(p) \cap \Gamma$  so that  $\Gamma_p \cup \{p\}$  is a smooth minimal graph. Since  $\gamma_{pq}$  is minimizing, it is not hard to see that  $\partial\Gamma_p$  intersects  $\gamma_{pq}$  in a single point  $p'$ .

Fix a constant  $\epsilon > 0$  that is much smaller than the distance from  $r$  to  $\gamma_{pq}$ . By the definition of  $\Gamma_{Clos}$ , there must be a point  $r'$  in  $\Gamma$  that is distance  $\epsilon$  from  $r$ . Since  $\Gamma$  is connected, we

can choose a compact curve  $\tilde{\gamma}_{p'r'}$  that is contained in  $\Gamma$  and connects  $p'$  to  $r'$ . The curve  $\tilde{\gamma}_{p'r'}$  may intersect  $\gamma_{pq}$  many times, so we replace it with the component of  $\tilde{\gamma}_{p'r'} \setminus \gamma_{pq}$  with  $r'$  in its boundary. This gives a curve in  $\Gamma$  from  $\gamma_{pq}$  to  $r'$  and whose interior does not intersect  $\gamma_{pq}$ . After adding a subsegment of  $\gamma_{pq}$  and perturbing the resulting curve slightly off of  $\gamma_{pq}$ , we get a compact curve  $\gamma_{p'r'} \subset \Gamma$  from  $p'$  to  $r'$  and whose interior does not intersect  $\gamma_{pq}$ ; see Figure 44.

The point about the curve  $\gamma_{p'r'}$  is that it will give a way to connect points near  $p'$  to  $r'$  in  $\Gamma \setminus \gamma_{pq}$ ; see Figure 44. This will be especially useful since the curve  $\partial\Gamma_p$  allows us to connect points near  $p'$  that are on the opposite sides of  $\gamma_{pq}$ .

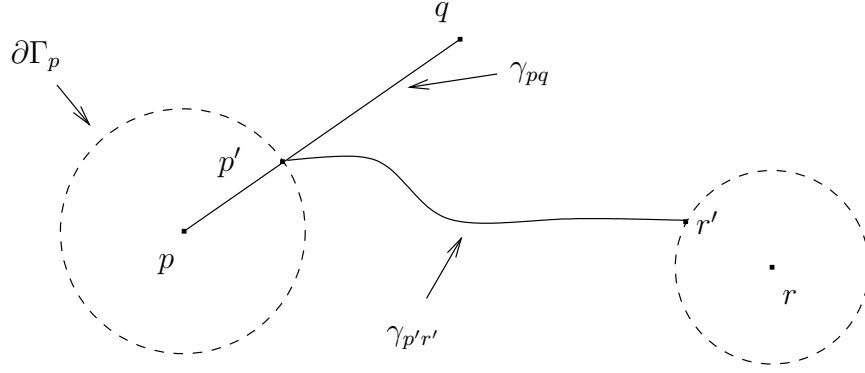


FIGURE 44. The curves  $\gamma_{pq}$  and  $\gamma_{p'r'}$ .

**Step 2: Choosing the curves in the  $\Sigma_j$ 's.** We can now argue as in Remark II.3.31. The key point is that Theorem I.1.6 and Lemma IV.2.7 imply that the  $\Sigma_j$ 's are locally connected in a small neighborhood of any of the singular points in  $\Gamma_{Clos} \cap \mathcal{S}$ . These connecting properties allow us to find simple closed curves  $\gamma_{pq}^j \subset \Sigma_j$  with the following properties:

- $\gamma_{pq}^j$  is contained in the  $\epsilon$ -tubular neighborhood of  $\gamma_{pq}$ .
- $\gamma_{pq}^j \setminus (B_\epsilon(p) \cup B_\epsilon(q))$  consists of two graphs over  $\gamma_{pq}$  which are in distinct sheets of  $\Sigma_j$ .

**Step 3: The contradiction.** Since  $\Sigma_j$  has genus zero, the curve  $\gamma_{pq}^j$  must separate  $\Sigma_j$  into two distinct components. However, it is easy to see that this is impossible by using the local connecting property near the third point  $r$ . Namely, we can take two points near  $p$  on opposite sides of  $\gamma_{pq}^j$  and connect each of them to  $r'$  by curves in  $\Sigma_j$  which do not intersect  $\gamma_{pq}^j$ . One of these connecting curves will be a graph over  $\gamma_{p'r'}$  while the other is a graph over  $\partial\Gamma_p \cup \gamma_{p'r'}$ . These two connecting curves can then be connected to each other in  $B_{C\epsilon}(r) \cap \Sigma_j$ , giving the desired contradiction.  $\square$

**IV.2.4. The proof of Proposition IV.2.2.** We can now use Corollary IV.2.6 and the properties of a collapsed leaf to prove Proposition IV.2.2. Recall that this proposition claims that  $\Gamma_{Clos} \cap \mathcal{S}_{neck} = \emptyset$  whenever  $\Gamma$  is a collapsed leaf of  $\mathcal{L}'$ .

*Proof.* (of Proposition IV.2.2.) We will argue by contradiction, so suppose that  $\Gamma$  is a collapsed leaf of  $\mathcal{L}'$  and  $\Gamma_{Clos} \cap \mathcal{S}_{neck} \neq \emptyset$ . By Corollary IV.2.6, we know that  $\Gamma_{Clos} \setminus \Gamma$  consists of one point  $y$  in  $\mathcal{S}_{ulsc}$  and one point  $z$  in  $\mathcal{S}_{neck}$ . Furthermore, property (1) in

Proposition II.3.1 implies that the point  $y$  is a removable singularity for  $\Gamma$  so that  $\Gamma \cup \{y\}$  is smooth and complete away from the point  $z$ .

We will show next that  $\Gamma$  is flat. The starting point for this is that  $\Gamma$  (or its oriented double cover) is stable by property (2) in Proposition II.3.1. A standard “logarithmic cutoff function” argument then implies that  $\Gamma \cup \{y\}$  (or its oriented double cover) is also stable; we leave the simple argument to the reader. If  $\Gamma \cup \{y\}$  had been complete, then the Bernstein theorem for stable surfaces would have implied that it was flat. However, even in this case where  $\Gamma \cup \{y\}$  is complete away from the single point  $z$ , Lemma B.26 in Appendix B implies that  $\Gamma$  is flat.

We have now established that  $\Gamma$  is a plane with two points removed and one of these points (namely  $z$ ) is in  $\mathcal{S}_{neck}$ . Since  $\Gamma$  cannot cross the limit plane  $P_z$  through  $z$  by Lemma IV.2.3, it follows that

$$\Gamma \subset P_z. \tag{IV.2.20}$$

However, we already saw in the Claim at the end of the proof of Lemma IV.2.7 that (IV.2.20) is impossible. This contradiction completes the proof of the proposition.  $\square$

**IV.2.5. The proof of (C2) and (D) in Theorem 0.14.** We can now argue as in the ULSC case of Part III to prove (C2) and (D) in Theorem 0.14. As we saw in Part III, the argument requires that we establish the following four properties of an arbitrary collapsed leaf  $\Gamma$  of  $\mathcal{L}'$ :

- (0)  $\Gamma_{Clos} \cap \mathcal{S}_{neck} = \emptyset$ .
- (1)  $\Gamma_{Clos}$  is a plane and  $\Gamma_{Clos} \setminus \Gamma$  contains at most two points.
- (2)  $\Gamma_{Clos} \setminus \Gamma$  contains exactly two points.
- ( $\star$ ) If  $t \in x_3(\mathcal{S}_{ulsc})$  and  $\epsilon > 0$ , then

$$\mathcal{S}_{ulsc} \cap \{t < x_3 < t + \epsilon\} \neq \emptyset \text{ and } \mathcal{S}_{ulsc} \cap \{t - \epsilon < x_3 < t\} \neq \emptyset. \tag{IV.2.21}$$

Once we show that (0), (1), (2), and ( $\star$ ) hold, then (C2) and (D) in Theorem 0.14 follow exactly as in Part III; we will not repeat the argument here.

It suffices therefore to check that (0), (1), (2), and ( $\star$ ) hold in this setting. The first two are quite easy: (0) is exactly the conclusion of Proposition IV.2.2 and (1) follows from (0) together with (1) in Proposition III.0.2.

We will prove (2) by contradiction, so suppose that  $\Gamma_{Clos} \cap \mathcal{S}_{ulsc} = \{0\}$ . It follows immediately that the  $\Sigma_j$ 's contain multi-valued graphs over (subsets of) the punctured plane  $\Gamma = \{x_3 = 0\} \setminus \{0\}$  that converge to  $\Gamma$  with infinite multiplicity. Moreover, (D) in the proof of property (2) in Proposition III.0.2 gives the following scale invariant ULSC property:

- (D) There exists  $\tau > 0$  so that, for  $z \in \{x_3 = 0\}$  and  $j$  large, each component of  $B_{\tau|z|}(z) \cap \Sigma_j$  that connects to the multi-valued graph in  $\Sigma_j$  is a disk.

Note that the proof of (D) did not use that the sequence was ULSC. It follows from (D) and the one-sided curvature estimate that the multi-valued graphs in  $\Sigma_j$  converging to  $\Gamma$  spiral through an entire cone about  $\Gamma$ . Note that the  $\Sigma_j$ 's are assumed to be uniformly non-simply connected. Therefore, Proposition IV.1.1 gives stable graphs  $\Gamma_j$  that are disjoint from  $\Sigma_j$ . The  $\Gamma_j$ 's are graphs with bounded gradient that start out in a fixed ball and are defined over annuli with a fixed inner radius and with outer radii going to infinity. Standard results for exterior graphs then imply that the  $\Gamma_j$ 's grow sublinearly. Consequently, the  $\Gamma_j$ 's are eventually contained in the narrow cone that the multi-valued graphs in the  $\Sigma_j$ 's spiral

through. However, this is impossible since the two are disjoint. This contradiction completes the sketch of the proof of (2); we leave the details to the reader.

**Remark IV.2.22.** The argument that we gave here is actually simpler than in the ULSC case; cf. (2) in Proposition III.0.2. However, we could not yet use this argument for the ULSC case since Proposition IV.1.1 relies on the ULSC case.

Finally,  $(\star)$  follows from (1) and (2) together with Lemma III.1.4 that proved  $(\star)$  in the ULSC case. However, Lemma III.1.4 did not actually require the sequence to be ULSC, but rather requires only that (1) and (2) above hold. This completes the sketch of (C2) and (D) in Theorem 0.14.

#### IV.3. PUTTING IT ALL TOGETHER: THE PROOF OF THEOREM 0.14

We have now completed the proof of all six of the claims in Theorem 0.14 over the course of this part (the six claims are (A), (B), (C1), (C2), (D), and (P) in Theorem 0.14). For the reader's convenience, we will review next where each was proven:

*Proof.* (of Theorem 0.14). The singular set  $\mathcal{S}$  is defined in Definition/Lemma II.1.1, where we also prove property (B). Lemma II.1.2 gives a subsequence  $\Sigma_j$  that converges to a minimal lamination  $\mathcal{L}'$  of  $\mathbf{R}^3 \setminus \mathcal{S}$ , thus giving (A). Property (C1) that describes the points in  $\mathcal{S}_{neck}$  is established in Section IV.1. The properties (C2) and (D) that describe the points in  $\mathcal{S}_{ulsc}$  are established in Section IV.2. Finally, property (P) that shows that the leaves of  $\mathcal{L}'$  don't cross the limit planes given by (C1) is proven in Lemma IV.2.3.  $\square$

#### Part V. The no mixing theorem, Theorem 0.4

This part is devoted to the proof of the no mixing theorem, i.e., Theorem 0.4. Recall that this theorem asserts that the singular set  $\mathcal{S}$  consists of either exclusively helicoid points or exclusively catenoid points, i.e., either  $\mathcal{S}_{neck} = \emptyset$  or  $\mathcal{S}_{ulsc} = \emptyset$ . We have already shown in (D) of Theorem 0.14 that the leaves intersecting  $\mathcal{S}_{ulsc}$  foliate an open subset of  $\mathbf{R}^3$  that does not intersect  $\mathcal{S}_{neck}$ . Using in part that  $\mathcal{S}$  is closed, we will show that the closure of this foliated region will also intersect  $\mathcal{S}$ ; therefore, the boundary of the foliated region must intersect  $\mathcal{S}_{neck} = \mathcal{S} \setminus \mathcal{S}_{ulsc}$ . We will prove the no mixing theorem by showing that also the closure of this foliated region does not intersect  $\mathcal{S}_{neck}$  and, hence, the foliated region is either empty or all of  $\mathbf{R}^3$ . The argument for this will be very similar to the one that we used earlier to show that the leaves intersecting  $\mathcal{S}_{ulsc}$  do not intersect  $\mathcal{S}_{neck}$ .

*Proof.* (of Theorem 0.4). Suppose that  $\mathcal{S}_{ulsc} \neq \emptyset$ ; we will show that  $\mathcal{S}_{neck} = \emptyset$ . By (D) of Theorem 0.14, the set  $\mathcal{S}_{ulsc}$  is a union of Lipschitz curves transverse to the leaves of the lamination and the leaves intersecting  $\mathcal{S}_{ulsc}$  foliate an open subset of  $\mathbf{R}^3$  that does not intersect  $\mathcal{S}_{neck}$ ; we will call this foliated region the "ULSC region". Moreover, each connected component of the ULSC region contains exactly two curves in  $\mathcal{S}_{ulsc}$  and each of these two curves intersects each leaf exactly once. We will prove the theorem by showing that these ULSC leaves foliate all of  $\mathbf{R}^3$ . It is easy to see that this is equivalent to showing that a curve in  $\mathcal{S}_{ulsc}$  cannot just stop.

Note first that each curve in  $\mathcal{S}_{ulsc}$  is in fact a line segment *orthogonal* to the leaves of the lamination. This follows from the main theorem of [Me1] since we have already proven here that the ULSC regions are foliated.

Foliated ULSC region of the lamination  $\mathcal{L}$ .

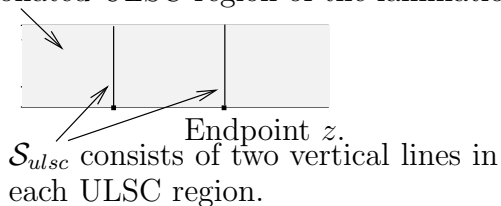


FIGURE 45. A limit lamination where the ULSC region has non-empty boundary; we will rule this out.

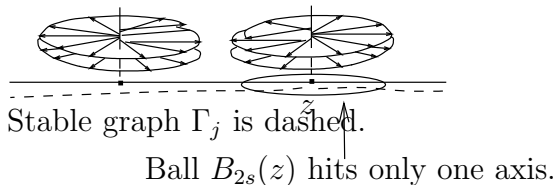


FIGURE 46. Properties of a sequence  $\Sigma_j$  that converges to a lamination where the ULSC region has non-empty boundary.

Suppose now that one of the line segments in  $\mathcal{S}_{ulsc}$  does stop, i.e., has an endpoint  $z$ . Since the set  $\mathcal{S}$  is closed and  $\mathcal{S}_{ulsc}$  is open in  $\mathcal{S}$ , the endpoint must be in  $\mathcal{S}_{neck}$ . To complete the proof, we will use the properties of the sequence  $\Sigma_j$  to show that having  $z$  in  $\mathcal{S}_{neck}$  leads to a contradiction. This contradiction follows from the following four steps:

- (1) Since  $z \in \mathcal{S}_{neck}$ , Proposition IV.1.1 gives a sequence of stable graphs  $\Gamma_j \subset B_{R_j} \setminus \Sigma_j$  converging to a horizontal plane through  $z$ ; this convergence is smooth away from the point  $z$ . Proposition IV.1.1 also gives separating curves  $\gamma_j \subset \Sigma_j$  with  $\gamma_j \rightarrow z$  where  $\gamma_j$  divides  $\Sigma_j$  into a component  $\Sigma_j^+$  above  $\Gamma_j$  and a component  $\Sigma_j^-$  below.<sup>35</sup> After possibly reflecting about the horizontal plane through  $z$ , we can assume that the segment in  $\mathcal{S}_{ulsc}$  lies above the plane.
- (2) Since  $z$  is in the closure of  $\mathcal{S}_{ulsc}$ , (C2) of Theorem 0.14 gives double spiral staircases in  $\Sigma_j^+$  above the horizontal plane through  $z$ . More precisely, fix a ball  $B_{2s}(z)$  that intersects only one of the two vertical line segments in  $\mathcal{S}_{ulsc}$  approaching the plane through  $z$  from above. After possibly shrinking  $s$ , we can also assume that  $B_{2s}(z) \cap \{x_3 > x_3(z)\}$  is contained in one connected component of the ULSC foliated region. Then, by (C2) of Theorem 0.14, in each compact subset of  $B_{2s}(z) \cap \{x_3 > x_3(z)\}$ ,  $\Sigma_j^+$  will consist of a double spiral staircase for all  $j$  sufficiently large. This will be used in (4) to pull the double spiral staircases into an appropriate region near the plane.
- (3) We will show next that  $\Sigma_j^+$  must be ULSC away from  $z$ . Namely, we will show that:
  - There exists some  $\epsilon > 0$  so that if  $y \in (B_{2s}(z) \setminus B_s(z)) \cap \{x_3 = x_3(z)\}$ , then each component of  $B_{\epsilon s}(y) \cap \Sigma_j$  is a disk for  $j$  sufficiently large.

We will prove this by contradiction, so suppose that there is a sequence of non-contractible curves  $\tilde{\gamma}_j$  in  $B_{\epsilon s}(y) \cap \Sigma_j^+$ ; the constant  $\epsilon$  will be given by Proposition IV.1.1. Applying Proposition IV.1.1 to the  $\tilde{\gamma}_j$ 's will lead to the desired contradiction. Namely, Proposition IV.1.1 gives a second stable graph  $\tilde{\Gamma}_j$  that is disjoint from both  $\Sigma_j$  and  $\Gamma_j$ . Since  $\tilde{\Gamma}_j$  starts off from  $\tilde{\gamma}_j$ , we see that  $\tilde{\Gamma}_j$  is above  $\Gamma_j$ . However, it follows from (1) that the axis of the double spiral staircase in  $\Sigma_j^+$  can be connected to  $\Gamma_j$  by a short curve  $\sigma_j$  in  $\Sigma_j$ ; here short means that the length of  $\sigma_j$  goes to zero as  $j \rightarrow \infty$ .

<sup>35</sup>When we say that “ $\Sigma_j^+$  is above  $\Gamma_j$ ”, we have to be a little bit careful since each  $\Gamma_j$  is defined only over an annulus. The precise statement is given in Proposition IV.1.1: There are shrinking balls  $B_{r_j}(z)$  with  $r_j \rightarrow 0$  so that  $\Gamma_j \cup B_{r_j}(z)$  divides  $B_{R_j/C}$  into components  $H_j^+$  above  $\Gamma_j$  and  $H_j^-$  below  $\Gamma_j$ ; we then have that  $\Sigma_j^+$  is contained in  $H_j^+ \cup B_{r_j}(z)$ .

In particular, the short curve  $\sigma_j$  does not pass through the “hole” in the annulus  $\tilde{\Gamma}_j$ . Therefore, the graph  $\tilde{\Gamma}_j$  must intersect  $\Sigma_j \cup \Gamma_j$  which is a contradiction.

(4) Finally, (3) will allow us to apply the one-sided curvature estimate<sup>36</sup> to show that the  $\Sigma_j^+$ 's continue to spiral as graphs below the plane  $\{x_3 = x_3(z)\}$ , contradicting (1). To do this, suppose that  $y$  is any given point in  $(B_{2s}(z) \setminus B_s(z)) \cap \{x_3 = x_3(z)\}$ . Observe that (1) gives the sequence of stable  $\Gamma_j$ 's disjoint from  $\Sigma_j^+$  converging in  $B_s(y)$  to the horizontal disk  $B_s(y) \cap \{x_3 = x_3(z)\}$ . It follows from this and (3) that we can apply the one-sided curvature estimate to get that each component of  $B_{\epsilon' s}(y) \cap \Sigma_j$  is a graph for  $j$  large; here  $\epsilon' > 0$  depends on  $\epsilon$  and the constant from the one-sided curvature estimate. Since these components are graphical for every such point  $y$  and start out as part of a multi-valued graph, there are now two possibilities:

- The multi-valued graph can be continued down to  $x_3 = x_3(z) - \epsilon' s$ .
- The multi-valued graphs spiral infinitely into some horizontal plane above  $x_3 = x_3(z) - \epsilon' s$ .

The latter is impossible since each  $\Sigma_j$  is a compact surface. This completes the proof of the fourth step and, hence, gives the promised contradiction to (1). □

## Part VI. Completing the proofs of Theorem 0.6 and Theorem 0.12

The only thing that remains to be proven is that every leaf of the lamination  $\mathcal{L}'^{37}$  is contained in a plane. This is the remaining claim in Theorem 0.6 (the planar lamination convergence theorem). We have already proven that the leaves of  $\mathcal{L}'$  are planes when the sequence is ULSC; thus, by the no mixing theorem, the only remaining case is when  $\mathcal{S} = \mathcal{S}_{neck} \neq \emptyset$ .

Recall that each point in  $\mathcal{S}_{neck}$  comes with a plane through it that is a limit of stable graphs in the complement of the sequence  $\Sigma_j$ . Since  $\mathcal{S}_{neck} \neq \emptyset$  by assumption, there is at least one such plane and, hence, every leaf of  $\mathcal{L}'$  is contained in a half-space (by Lemma IV.2.3). We will divide the proof that the leaves of  $\mathcal{L}'$  are contained in planes into two cases, depending on whether or not the leaf is complete. Recall that a leaf  $\Gamma$  is complete when  $\Gamma_{Clos} = \Gamma$ , where the closure  $\Gamma_{Clos}$  is defined by fixing a point  $x_\Gamma \in \Gamma$  and setting

$$\Gamma_{Clos} = \bigcup_r \overline{\mathcal{B}_r(x_\Gamma)}; \tag{VI.0.1}$$

see (II.2.10). We will prove that complete leaves of  $\mathcal{L}'$  are planes in Lemma VI.2.1; the in-complete leaves will be shown to be planes in Lemma VI.3.1.

It may be useful to give an example of the kind of thing that we need to rule out and a rough idea of why it cannot happen. Suppose therefore that a leaf  $\Gamma$  of  $\mathcal{L}'$  contains infinitely many necks, one on top of the next, and that these necks “shrink” to a point  $p \in \mathcal{S}_{neck}$ . It follows that we have a limit plane through  $p$  and that  $\Gamma$  is contained on one side of this plane. We will use a flux argument to rule out such an example. Roughly speaking, we will find a “top” curve with positive flux and then find a sequence of “bottom” curves shrinking to  $p$  whose flux goes to zero. We will then show that all of the ends of  $\Gamma$  between these curves

<sup>36</sup>The one-sided curvature estimate from [CM6] is recalled in Theorem I.1.3.

<sup>37</sup>Recall that  $\mathcal{L}'$  is a lamination of  $\mathbf{R}^3 \setminus \mathcal{S}$  given in Lemma II.1.2.

are asymptotic to planes or upward sloping catenoids - and hence make a non-negative contribution to the total flux. This will give the desired contradiction since Stokes' theorem implies that the total flux is zero.

## VI.1. BLOW UP RESULTS FOR ULSC SURFACES

We will later need to analyze the structure of the sequence  $\Sigma_j$  in Theorem 0.6 (the planar lamination convergence theorem) near points where the topology is concentrating. In doing so, it will often be useful to work on the smallest scale of non-trivial topology (this is similar to blowing up on the scale of the curvature in the ULSC case; cf. the notion of blow up pairs in [CM6]). This can be achieved using a simple rescaling argument given in Lemma E.1 in Appendix E.

The advantage of working on the smallest scale of non-trivial topology is that we can use the compactness theorem for ULSC sequences – Theorem 0.9 – to prove a great deal of structure for the surfaces on this scale. We will use two such structure results below:

- Lemma III.4.1 proves a one-sided property for non-simply connected surfaces on the smallest scale of non-trivial topology. This shows that an intrinsic ball in such a surface cannot lie on one side a plane and have its center close to the plane on this scale; in the extreme case as the radius of the intrinsic ball goes to infinity, the surface would be forced to grow out of any half-space.
- Lemma VI.1.1 finds short curves on the smallest scale of non-trivial topology separating the ends. These short curves will be used in the flux argument for the main results in this part.

**VI.1.1. Finding short separating curves.** The next lemma finds short separating curves and stable graphs near points with small injectivity radius. These curves will separate the surface into two parts: a part  $\Sigma^+$  above the graph and a part  $\Sigma^-$  below the graph; cf. Figure 31. Earlier, in Proposition IV.1.1, we found separating curves contained in small extrinsic balls; in fact (1) and (2) below are proven in Proposition IV.1.1. The new point here is the bound on the length of the curves in (3) below. To prove this length bound, we will work on the smallest scale of non-trivial topology.

**Lemma VI.1.1.** Let  $\Sigma \subset B_{r_0}$  be an embedded minimal planar domain with  $\partial\Sigma \subset \partial B_{r_0}$ . Suppose also that  $\mathcal{B}_{r_1} \subset \Sigma$  is not a disk and  $\Gamma \subset B_{r_0} \setminus \Sigma$  is the stable surface given by Lemma IV.1.2.<sup>38</sup>

The following three properties hold (the first two are just Proposition IV.1.1):

- (1) Given  $\tau > 0$ , there exists  $C \geq 1$  so a component  $\Gamma_0$  of  $B_{r_0/C} \cap \Gamma \setminus B_{Cr_1}$  is a graph of a function  $v$  with  $|\nabla v| \leq \tau$  and  $\partial\Gamma_0$  intersects both  $\partial B_{r_0/C}$  and  $\partial B_{Cr_1}$ .
- (2) There are distinct components  $H^+$  and  $H^-$  of  $B_{r_0/C} \setminus (\Gamma_0 \cup B_{Cr_1})$ , a separating curve  $\tilde{\sigma} \subset B_{Cr_1} \cap \Sigma$ , and components  $\Sigma^\pm$  of  $B_{r_0/C} \cap \Sigma \setminus \tilde{\sigma}$  so that  $\Sigma^\pm \subset H^\pm \cup B_{Cr_1}$  and  $\tilde{\sigma} \subset \partial\Sigma^\pm$ .
- (3) There exists  $C_1$  so that if  $r_0 \geq C_1 r_1$  and  $\mathcal{B}_{r_1/4}(x)$  is a disk for each  $x \in \mathcal{B}_{C_1 r_1}$ , then  $\tilde{\sigma}$  is homologous to a collection of curves whose total length is at most  $C_1 r_1$ .

---

<sup>38</sup> $\Gamma$  is given by solving a Plateau problem using a non-contractible curve in  $\mathcal{B}_{r_1} \subset \Sigma$  as “interior” boundary.

**Remark VI.1.2.** We will call this the “short curve lemma” and call the separating curve  $\tilde{\sigma}$  the “short curve.” Of course,  $\tilde{\sigma}$  itself may not be short; rather it is homologous to a collection of curves whose total length is at most  $C_1 r_1$ .

*Proof.* Claims (1) and (2) are proven in Proposition IV.1.1. We will prove the last claim by contradiction, so suppose that (3) fails with  $C_1 = j$  for a sequence  $\Sigma'_j$ . After rescaling, we can assume that  $r_1 = 4$ .

Observe first that Lemma C.1 in Appendix C gives a sequence  $R_j \rightarrow \infty$  so that the component  $\Sigma_j$  of  $B_{R_j} \cap \Sigma'_j$  containing 0 is contained in the intrinsic ball  $\mathcal{B}_{4j}$  and, hence, each intrinsic ball of radius one in  $\Sigma_j$  is a disk. The  $\Sigma_j$ 's therefore give a ULSC sequence of embedded minimal planar domains in extrinsic balls whose radii go to infinity. As in the proof of Lemma III.4.1, we will now divide into two cases depending on whether or not the curvatures of the sequence blows up.

Case 1: Suppose first that there exists some  $R$  so that

$$\limsup_{j \rightarrow \infty} \sup_{B_R \cap \Sigma_j} |A|^2 = \infty. \quad (\text{VI.1.3})$$

We can then apply the compactness theorem for ULSC sequences, Theorem 0.9, to get a subsequence of the  $\Sigma_j$ 's that converges to a foliation by parallel planes away from two lines orthogonal to the leaves of the foliation. It follows easily from the description of the convergence near the lines (as double spiral staircases) that we get a uniform length bound for the separating curve. This length bound is proven in “The proof of (P4)” within the proof of Lemma III.1.4 and will not be repeated here.

Case 2: Suppose now that  $|A|^2$  is uniformly bounded on each compact subset of  $\mathbf{R}^3$  for the sequence  $\Sigma_j$ . The length bound in this case follows by combining three facts:

- By Lemma C.3 in Appendix C, the uniform curvature bounds implies uniform area bounds for each component of  $\Sigma_j$  in extrinsic balls (the bound depends on the ball but not on  $j$ ). More precisely, if  $\Sigma_{j,R}$  denotes the component of  $B_R \cap \Sigma_j$  containing 0, then Lemma C.3 implies that

$$\text{Area}(\Sigma_{j,R}) \leq C_c R^2, \quad (\text{VI.1.4})$$

where the constant  $C_c$  depends only on

$$\sup_{B_{C_0 R} \cap \Sigma_j} |A|^2. \quad (\text{VI.1.5})$$

The constant  $C_0$  here is universal and does not depend on the upper bounds for the curvature.

- The area bound (VI.1.4) and the co-area formula give uniform length bounds for the boundary  $\partial\Sigma_{j,R}$  for most values of  $R$ . Precisely, at least one-half of the  $R$ 's between  $R_0/2$  and  $R_0$  must satisfy

$$\text{Length}(\partial\Sigma_{j,R}) \leq 2 C_c R_0 \leq 4 C_c R. \quad (\text{VI.1.6})$$

- In the proof of Proposition IV.1.1, the components of  $\partial\Sigma_{j,R}$  were divided into two groups, depending on whether they connected to  $\Sigma_j^+$  or  $\Sigma_j^-$ ; the separating curve  $\tilde{\sigma}_j$  was then chosen to separate these two groups.<sup>39</sup> However, if we do not ask for a

---

<sup>39</sup>This is described in more detail in the proof of Proposition IV.1.1.

single connected separating curve, then we can instead use either of the two groups to separate. Finally, (VI.1.6) gives a uniform bound for the total length.

Therefore, in either case, we get uniform length bounds, hence proving the lemma.  $\square$

## VI.2. COMPLETE LEAVES OF $\mathcal{L}'$

We will show next that any complete leaf  $\Gamma$  of the lamination  $\mathcal{L}'$  is a plane ( $\mathcal{L}'$  is the lamination of  $\mathbf{R}^3 \setminus \mathcal{S}$  given in Lemma II.1.2). Such a leaf  $\Gamma$  is a complete embedded minimal surface in  $\mathbf{R}^3$ , but is not *a priori* known to be proper.

**Lemma VI.2.1.** Suppose that  $\Gamma$  is a complete leaf of the lamination  $\mathcal{L}'$ , i.e, suppose that  $\Gamma_{\text{clos}} = \Gamma$ . Then  $\Gamma$  must be a plane.

*Proof.* We will assume that  $\Gamma$  is not a plane and show that this leads to a contradiction.

The ULSC case was already completed in Theorem 0.9, so we can assume that

$$\mathcal{S} = \mathcal{S}_{\text{neck}} \neq \emptyset \tag{VI.2.2}$$

by the no mixing theorem (Theorem 0.4). Recall that, by Proposition IV.1.1, each point in  $\mathcal{S}_{\text{neck}}$  comes with a plane through it that is a limit of stable graphs in the complement of the sequence  $\Sigma_j$ .<sup>40</sup> Furthermore, by Lemma IV.2.3, the leaves of  $\mathcal{L}'$  do not cross any of these planes. Since there is at least one such plane,  $\Gamma$  is contained in a half-space. After a translation and a rotation, we may assume that  $\Gamma \subset \{x_3 \geq 0\}$  and

$$\inf_{\Gamma} x_3 = 0. \tag{VI.2.3}$$

Claim: If  $\Gamma$  satisfies (VI.2.3) and is not a plane, then there is a sequence of points  $p_n \in \Gamma$  satisfying:

$$i(p_n) \rightarrow 0, \tag{VI.2.4}$$

$$x_3(p_n) \rightarrow 0. \tag{VI.2.5}$$

Here  $i(p_n)$  is the injectivity radius of  $\Gamma$  at  $p_n$ . Since  $\Gamma$  is a complete smooth surface, (VI.2.4) immediately implies that

$$\text{dist}_{\Gamma}(p_1, p_n) \rightarrow \infty. \tag{VI.2.6}$$

Proof of Claim: Since  $\Gamma$  satisfies (VI.2.3) but is not a plane, [MeRo] (see the first paragraph of the proof of lemma 1.5 there) implies that for any  $\epsilon > 0$  we have

$$\sup_{\Gamma \cap \{0 < x_3 < \epsilon\}} |A|^2 = \infty. \tag{VI.2.7}$$

Therefore, we get a sequence of points  $p_n$  in  $\Gamma$  satisfying (VI.2.5) and with

$$|A|^2(p_n) \rightarrow \infty. \tag{VI.2.8}$$

Equation (VI.2.4) then follows immediately from this and the one-sided curvature estimate.

QED of Claim

---

<sup>40</sup>More precisely, repeatedly applying Proposition IV.1.1 gave a sequence of stable graphs defined over larger and larger annuli and this sequence converges to a limit graph over a punctured plane. The limit graph is bounded at the puncture and extends smoothly across the puncture to an entire graph; consequently, the limit graph is a plane by the Bernstein theorem.

Return to the proof of the lemma: We will use the Claim above to deduce a flux contradiction (similar to the proof of  $(\star)$  in the ULSC case given in Subsection III.1.1) as follows:

- (a) The leaf  $\Gamma$  must be a multiplicity one limit of the  $\Sigma_j$ 's. To see this, observe that if this was not the case, then the universal cover of  $\Gamma$  would be stable and, hence, flat; cf. the proof of Corollary B.20 for more details.
- (b) Blowing up at  $p_1$  to get a separating curve. Fix a large constant  $C_1 > 1$  (it will be chosen depending on both Lemma VI.1.1 - the ‘‘short curve lemma’’ - and Lemma III.4.1 - the ‘‘one-sided lemma’’ for non-simply connected surfaces). Applying the blow up lemma, Lemma E.1, at  $p_1$  gives an intrinsic ball

$$\mathcal{B}_{C_1 s_1}(y_1) \subset \mathcal{B}_{5 C_1 i(p_1)}(p_1), \quad (\text{VI.2.9})$$

so that  $\mathcal{B}_{4 s_1}(y_1)$  is not a disk but  $\mathcal{B}_{s_1}(y)$  is a disk for each  $y \in \mathcal{B}_{C_1 s_1}(y_1)$ .

Taking  $C_1$  sufficiently large, it follows that  $\mathcal{B}_{C_1 s_1}(y_1)$  satisfies the hypotheses of both Lemma VI.1.1 and Lemma III.4.1 (where the constant  $H$  in Lemma III.4.1 is set equal to a large constant  $C_2 > 1$ ). Hence, the short curve lemma, Lemma VI.1.1, gives an initial short separating curve

$$\gamma_1 \subset B_{4 s_1}(y_1) \cap \Gamma \quad (\text{VI.2.10})$$

and a stable graph

$$\Gamma_0 \subset \mathbf{R}^3 \setminus \Gamma. \quad (\text{VI.2.11})$$

Since the surface  $\Gamma$  is not known to be proper in all of  $\mathbf{R}^3$ , the graph  $\Gamma_0$  would at first appear to be defined only over a bounded annulus. However, the multiplicity one convergence of (a) implies that the short curve  $\gamma_1 \subset \Gamma$  is actually a smooth limit of curves  $\gamma_{1,j}$  contained in the proper surfaces  $\Sigma_j$ . We can therefore apply the barrier construction to these curves in  $\Sigma_j$  and take the limit of the resulting stable graphs to get the desired  $\Gamma_0$  as a graph defined outside the ball  $B_{C s_1}(y_1)$ . It follows that the graph  $\Gamma_0$  is asymptotic to either a plane or an upward sloping half-catenoid (the other possibility would be a downward sloping half-catenoid which is clearly impossible since  $\Gamma$  is above  $\{x_3 = 0\}$ ).

Moreover, since  $\Gamma \subset \{x_3 \geq 0\}$ , the one-sided lemma for non-simply connected surfaces, Lemma III.4.1, guarantees that

$$C_2 s_1 < x_3(y_1), \quad (\text{VI.2.12})$$

where  $C_2 > 1$  is a large fixed constant (we can make  $C_2$  as large as we want by increasing  $C_1$ ). By the same argument, the extrinsic ball  $B_{C_2 s_1}(y_1)$  does not intersect any of the horizontal planes associated to the singular set  $\mathcal{S}$ .

Finally, since  $x_3(p_n)$  and  $i(p_n)$  both go to zero, we can pass to a subsequence of the  $p_n$ 's so that

$$\sup_{\Gamma} x_3 > \sup_{B_{C s_1}(y_1)} x_3, \quad (\text{VI.2.13})$$

and then for  $n \geq 1$

$$\inf_{B_{C s_n}(y_n)} x_3 > \sup_{B_{C s_{n+1}}(y_{n+1})} x_3. \quad (\text{VI.2.14})$$

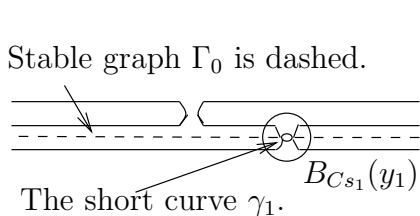


FIGURE 47. (b): Lemma VI.1.1 gives a short curve  $\gamma_1 \subset \Gamma$  and a stable graph  $\Gamma_0$ .

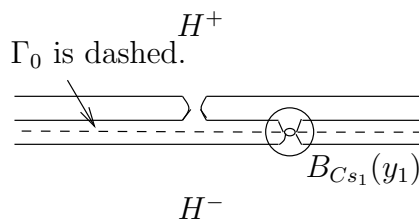


FIGURE 48. (c’):  $\mathbf{R}^3 \setminus (\Gamma_0 \cup B_{C_{s_1}}(y_1))$  has components  $H^+$  above and  $H^-$  below  $\Gamma_0 \cup B_{C_{s_1}}(y_1)$ .  $\Gamma$  is the only leaf of  $\mathcal{L}'$  intersecting both  $H^+$  and  $H^-$ .

(c)  $\Gamma$  is the only leaf of  $\mathcal{L}'$  that intersects  $\overline{B_{C_{s_1}}(y_1)}$ . A barrier argument and the one-sided lemma for non-simply connected surfaces, Lemma III.4.1 give  $\tilde{C} > C$  so that if  $C_1 \geq \tilde{C}$ , then only one proper component of  $B_{\tilde{C}_{s_1}}(y_1) \cap \mathcal{L}'$  intersects  $\overline{B_{C_{s_1}}(y_1)}$ .<sup>41</sup> Here  $\tilde{C}$  depends only on  $C$ .

To complete the argument for (c), we need to verify that each component of any leaf of  $\mathcal{L}'$  in  $B_{\tilde{C}_{s_1}}(y_1)$  is proper. Fortunately, this will follow directly from Lemma C.3 that gives the compactness of each component of an embedded minimal surface in a ball  $B_R$  if there is some curvature bound in the fixed larger ball  $B_{C_d R}$ .<sup>42</sup> Namely, (VI.2.12) implies that  $B_{2C_d \tilde{C}_{s_1}}(y_1)$  is disjoint from  $\mathcal{S}$  so long as  $C_2$  is sufficiently large. We can then conclude that every leaf of  $\mathcal{L}'$  has bounded curvature in  $B_{C_d \tilde{C}_{s_1}}(y_1)$  and hence has compact components in  $B_{\tilde{C}_{s_1}}(y_1)$  by Lemma C.3.

(c’)  $\Gamma$  is the only leaf of  $\mathcal{L}'$  that intersects both sides of  $B_{C_{s_1}}(y_1) \cup \Gamma_0$ . Since the graph  $\Gamma_0$  is a limit of surfaces that are disjoint from the  $\Sigma_j$ ’s, it follows that none of the leaves of  $\mathcal{L}'$  can cross  $\Gamma_0$ . However,  $\Gamma_0$  is a graph over an annulus, so the leaves of  $\mathcal{L}'$  may “go through the hole” to get from one side of  $\Gamma_0$  to the other; this is exactly what  $\Gamma$  does. However, by (c),  $\Gamma$  is the only leaf that intersects  $B_{C_{s_1}}(y_1)$ , so we conclude that  $\Gamma$  is the only leaf of  $\mathcal{L}'$  that intersects both sides of  $B_{C_{s_1}}(y_1) \cup \Gamma_0$ .

(d) Repeating (b) at each  $p_n$ . Using (VI.2.4), we can argue as in (b) at each point  $p_n$  to get shrinking curves

$$\gamma_n \subset B_{4s_n}(y_n) \text{ where } \mathcal{B}_{C_1 s_n}(y_n) \subset \mathcal{B}_{5C_1 i(p_n)}(p_n), \tag{VI.2.15}$$

as well as stable graphs that are defined outside  $B_{C_{s_n}}(y_n)$  and are disjoint from  $\Gamma$ . Since  $i(p_n) \rightarrow 0$ , Lemma VI.1.1 gives that the flux across  $\gamma_n$  also goes to zero. Furthermore, (VI.2.6) guarantees that the shrinking curves are separated; the points  $p_n$  may be close in  $\mathbf{R}^3$  but they are far apart in  $\Gamma$ .

<sup>41</sup>This follows exactly as does the analogous result for disks given in corollary 0.4 in [CM6]. Namely, if there were two such components, then we could put a stable surface between them. Interior estimates for stable surfaces then imply that each of the original components lies on one side of a plane that comes close to the center of the ball. However, this would contradict the one-sided lemma for non-simply connected surfaces, Lemma III.4.1, so we conclude that there could not have been two such components.

<sup>42</sup>Clearly, it is crucial here that  $C_d$  does not depend on the bound for the curvature.

Let  $\Gamma_n$  denote the connected component of  $\Gamma \setminus (\gamma_1 \cup \gamma_n)$  containing both  $\gamma_1$  and  $\gamma_n$  in its boundary. Note that we used that  $\gamma_1$  and  $\gamma_n$  are separating to guarantee that such a component exists.

Finally, let  $E_n$  denote the “sandwiched” region in  $\mathbf{R}^3$  that is between the stable graphs associated to  $p_1$  and  $p_n$  together with the balls  $B_{C_1 s_1}(y_1)$  and  $B_{C_1 s_n}(y_n)$ . We will need the following two properties of  $E_n$ :

$$\Gamma_n \subset E_n \text{ and } \overline{E_n} \cap \mathcal{S} = \emptyset. \quad (\text{VI.2.16})$$

The first property follows immediately from (2) in Lemma VI.1.1. To see the second, note that a point of  $\mathcal{S}$  in  $\overline{E_n}$  would come with a horizontal plane through it that is disjoint from  $\Gamma$ ; this is impossible since the connected leaf  $\Gamma$  intersects both above and below  $E_n$ .

- (e)  $\Gamma_n$  is properly embedded. We will prove this by contradiction, so suppose that some  $\Gamma_n$  is not proper. In this case, we would be able to choose a sequence  $y_j \in \Gamma_n$  with

$$\text{dist}_{\Gamma_n}(y_1, y_j) \rightarrow \infty \text{ and } |y_j - y| \rightarrow 0 \text{ for some } y \in \overline{\Gamma_n} \subset \overline{E_n}. \quad (\text{VI.2.17})$$

Since the union of the leaves of  $\mathcal{L}'$  is closed in  $\mathbf{R}^3 \setminus \mathcal{S}$  and  $\overline{E_n} \cap \mathcal{S} = \emptyset$ , the point  $y$  must be contained in some leaf  $\tilde{\Gamma}$  of  $\mathcal{L}'$ . As we have used several times, this implies that the universal cover of  $\tilde{\Gamma}$  must be stable; cf. the proof of Corollary B.20 for more details. Since  $\Gamma$  is not stable (see the proof of (a)), it follows that  $\tilde{\Gamma} \neq \Gamma$ .

We claim that

$$\tilde{\Gamma} \text{ is complete.} \quad (\text{VI.2.18})$$

Proof of (VI.2.18). We know from (c) that  $\Gamma$  is the only leaf of  $\mathcal{L}'$  that intersects  $\overline{B_{C s_1}(y_1)} \cup \overline{B_{C s_n}(y_n)}$ , so

$$y \notin \overline{B_{C s_1}(y_1)} \cup \overline{B_{C s_n}(y_n)}. \quad (\text{VI.2.19})$$

It is also easy to see that the stable graphs that form the top and bottom of the boundary of  $E_n$  cannot be contained in leaves of  $\mathcal{L}'$ <sup>43</sup>, so we must have that

$$y \in E_n \setminus (\overline{B_{C s_1}(y_1)} \cup \overline{B_{C s_n}(y_n)}). \quad (\text{VI.2.20})$$

However, (c') then implies that the entire leaf  $\tilde{\Gamma}$  must be trapped inside of  $E_n$ . Since  $\overline{E_n} \cap \mathcal{S} = \emptyset$ , it follows that  $\tilde{\Gamma}$  must be complete. QED of (VI.2.18).

Now that we have established (VI.2.18), the Bernstein theorem for stable surfaces implies that  $\tilde{\Gamma}$  is a plane. Since  $\tilde{\Gamma}$  does not cross  $\{x_3 = 0\}$ , it must be a horizontal plane. However, this is impossible since  $\tilde{\Gamma} \cap \Gamma = \emptyset$  and  $\Gamma$  intersects both above and below  $E_n$ . Therefore, we conclude that  $\Gamma_n$  must be proper.

- (f) The ends of  $\Gamma_n$  are graphs. We claim next that for each fixed  $n$ , there is a constant  $r_n$  so that

$$\Gamma_n \cap \{x_1^2 + x_2^2 \geq r_n^2\} \quad (\text{VI.2.21})$$

consists of a finite collection of graphs over  $\{x_3 = 0, x_1^2 + x_2^2 \geq r_n^2\}$ .

We will show first that  $\Gamma_n \cap \{x_1^2 + x_2^2 \geq r_n^2\}$  is locally graphical. The starting point is to observe that  $\Gamma_n$  is contained in the sandwich  $E_n$  and the height of this sandwich

---

<sup>43</sup>These stable graphs were obtained using limits of solutions to Plateau problems using the  $\Sigma_j$ 's as barriers.

grows at most logarithmically. Therefore, by the one-sided curvature estimate, it suffices to prove that  $\Gamma_n$  is scale-invariant ULSC with respect to the distance to 0; see, for instance, (D) in Subsection III.0.6. This follows from the “between the sheets” argument that we have used several times already, so we will just sketch the proof this time. Namely, since  $\Gamma_n$  is connected, we can fix a curve  $\sigma_n \subset \Gamma_n$  that connects  $\gamma_1$  to  $\gamma_n$ ; we will choose  $r_n$  so that

$$\sigma_n \subset \{x_1^2 + x_2^2 < r_n^2/4\}. \tag{VI.2.22}$$

If  $\Gamma_n \cap \{x_1^2 + x_2^2 \geq r_n^2\}$  were to contain a scale-invariant small neck, then a barrier argument would give a stable surface  $\Gamma_{\text{barrier}}$  in the complement of  $\Gamma_n$  that is also sandwiched in  $E_n$ . This sandwiching and the curvature estimates for stable surfaces imply that the stable surface  $\Gamma_{\text{barrier}}$  is graphical away from its boundary. Since the curve  $\sigma_n$  is away from the boundary of the stable surface and connects the top and bottom of the sandwich, the stable surface  $\tilde{\Gamma}$  is forced to intersect the curve  $\sigma_n$ , giving the desired contradiction.

After increasing  $r_n$ , we conclude that  $\Gamma_n \cap \{x_1^2 + x_2^2 \geq r_n^2\}$  is locally graphical and hence a union of graphs over  $\{x_3 = 0, x_1^2 + x_2^2 \geq r_n^2\}$ . (The other possibility is that it could contain a multi-valued graph; as we have argued before, this is impossible since such a multi-valued graph would have to spiral through the separating plane.) The properness of  $\Gamma_n$  proven in (e) implies that there can only be finitely many such graphs.

Note that, by the isoperimetric inequality, this gives area bounds for  $\Gamma_n$  in compact subsets of  $\mathbf{R}^3$ .

- (g) Slicing  $\Gamma_n$  with a plane to get the top curve. Each graphical end of each  $\Gamma_n$  is above  $\{x_3 = 0\}$  and, consequently, is asymptotic to either a plane or to an upward sloping half-catenoid. Since there are only finitely many such planes for each  $n$ , we can choose a height  $h$  between  $\sup_{\gamma_2} x_3$  and  $\inf_{\gamma_1} x_3$  that misses all of the heights of the planar ends for every  $\Gamma_n$  and so that the plane  $\{x_3 = h\}$  intersects  $\Gamma$  transversely. It follows that  $\{x_3 = h\}$  intersects each  $\Gamma_n$  transversely in a finite collection of simple closed curves. Note that this plane separates  $\gamma_1$  from  $\gamma_n$  (and, in particular, does not intersect  $\partial\Gamma_n$ ).

Let  $\Gamma'_n$  denote the component of  $\{x_3 < h\} \cap \Gamma_n$  with  $\gamma_n$  in its boundary.

- (h) The flux contradiction. The boundary of each  $\Gamma'_n$  consists of a “bottom curve”  $\gamma_n$  together with a collection of closed “top curves” in the plane  $\{x_3 = h\}$ . The collection of top curves is “increasing” in the following sense

$$\{x_3 = h\} \cap \partial\Gamma_n \subset \{x_3 = h\} \cap \partial\Gamma_{n+1}. \tag{VI.2.23}$$

Generally, one might expect equality in (VI.2.23); however, if  $\Gamma_{n+1}$  contained a catenoidal end that was not in  $\Gamma_n$ , then we would have a strict containment.

The integrand for the vertical flux is point-wise positive along the increasing boundary in  $\{x_3 = h\}$  and, hence, the vertical flux of  $\Gamma'_n$  across  $\{x_3 = h\}$  is positive and non-decreasing as a function of  $n$ . On the other hand, the flux across the bottom curve  $\gamma_n$  goes to zero as  $n \rightarrow \infty$  by (d). We can therefore fix some large  $n$  so that (the absolute value of) the flux across  $\gamma_n$  is less than the flux across  $\{x_3 = h\}$ . Since  $\Gamma'_n$  has only finitely many ends and each of these ends has non-negative flux at

infinity, the total flux of  $\Gamma'_n$  is positive. This gives the desired contradiction since, by Stokes' theorem, the total flux of  $\Gamma'_n$  must be zero.

□

**Remark VI.2.24.** The above argument did not really need that the leaf  $\Gamma$  was complete in order to conclude that it must be flat. Rather, we showed that  $\Gamma$  must be flat as long as there exists a sequence of points  $p_n \in \Gamma$  satisfying

$$x_3(p_n) \rightarrow 0, i(p_n) \rightarrow 0, \text{ and } \frac{i(p_n)}{\text{dist}_{\Gamma_{Clos}}(p_n, \mathcal{S})} \leq C_0, \quad (\text{VI.2.25})$$

where  $C_0$  is a fixed constant that does not depend on  $\Gamma$ . This will be useful when we consider in-complete leaves in the next section.

### VI.3. INCOMPLETE LEAVES OF $\mathcal{L}'$

It remains to show that each in-complete leaf  $\Gamma$  of  $\mathcal{L}'$  also must be flat. We do this in the next lemma.

**Lemma VI.3.1.** Suppose that  $\Gamma$  is an incomplete leaf of the lamination  $\mathcal{L}'$ , i.e, suppose that  $\Gamma_{Clos} \neq \Gamma$ . Then  $\Gamma$  is contained in a plane.

As proven earlier in Theorem 0.9, every leaf of  $\mathcal{L}'$  is flat when the sequence is ULSC. Therefore, by the no mixing theorem, i.e., Theorem 0.4, we can assume that  $\mathcal{S}_{ulsc} = \emptyset$  and  $\mathcal{S} = \mathcal{S}_{neck}$ .

Before getting into the proof, it is useful to consider an example of what a possible incomplete non-flat leaf  $\Gamma$  of  $\mathcal{L}'$  would have to look like. By assumption,  $\Gamma_{Clos} \setminus \Gamma \neq \emptyset$  and, hence,  $\Gamma_{Clos} \cap \mathcal{S}_{neck} \neq \emptyset$ . Since each point of  $\Gamma_{Clos} \cap \mathcal{S}_{neck}$  comes with a plane through it and none of the leaves of  $\mathcal{L}'$  can cross these planes, such a  $\Gamma$  would be contained in either

- an open slab between two singular planes, or
- an open half-space bounded by a singular plane.

Note that, by the strong maximum principle,  $\Gamma$  cannot intersect a singular plane and, hence, we can take the above slab and half-space to be open. We will see in the next subsection that  $\Gamma_{Clos} \cap \mathcal{S}$  consists of only one point in the boundary plane(s).

The basic idea behind the proof of Lemma VI.3.1 is again that a potential counterexample would lead to a flux contradiction. Much of the argument is very similar to the complete case:

- $\Gamma$  will be scale-invariant ULSC away from the singular points.
- $\Gamma$  will be proper in an open slab or open half-space.
- The ends of  $\Gamma$  will be asymptotic to planes or upward-sloping catenoids.
- We will slice between two planar ends to get a “top curve” with strictly positive flux.
- We will find a sequence of “bottom curves” where the flux goes to zero.

The main difficulty lies in finding the sequence of “bottom curves” where the flux goes to zero. One expects that the injectivity radius of  $\Gamma$  goes to zero as we approach the singular points. However, the rate at which it does so may be quite slow, so we cannot find large regions in  $\Gamma$  “on the smallest scale of non-trivial topology” as the injectivity radius goes to zero. The key for overcoming this will be to get some additional control over  $\Gamma$  near a singular point; in particular, we will prove scale-invariant curvature and area bounds for

$\Gamma$  near each singular point. Once we have this, we can use the co-area formula to find a sequence of “bottom curves” whose length goes to zero.

**VI.3.1. If  $\Gamma$  is not flat, then  $\Gamma_{Clos} \cap \mathcal{S}$  consists of at most two points.** As mentioned, we have already shown that the complete leaves of  $\mathcal{L}'$  must be flat, so the remaining case is when

$$\Gamma_{Clos} \cap \mathcal{S}_{neck} \neq \emptyset. \quad (\text{VI.3.2})$$

Each point of  $\Gamma_{Clos} \cap \mathcal{S}_{neck}$  comes with a plane through it and none of the leaves of  $\mathcal{L}'$  can cross this plane. Hence, by the strong maximum principle, this plane does not intersect any of the non-flat leaves of  $\mathcal{L}'$ . The starting point for Lemma VI.3.1 is to show that this plane contains exactly one point of  $\Gamma_{Clos} \cap \mathcal{S}_{neck}$ ; see Lemma VI.3.3 below. It follows immediately from this that  $\Gamma_{Clos} \cap \mathcal{S}$  consists of at most two points for any non-flat  $\Gamma$ .

**Lemma VI.3.3.** Suppose that  $\Gamma \subset \{x_3 > 0\}$  is a non-flat leaf of  $\mathcal{L}'$  with  $0 \in \Gamma_{Clos} \cap \mathcal{S}_{neck}$  and  $\{x_3 = 0\}$  is the associated stable limit plane through 0. Then we must have

$$\Gamma_{Clos} \cap \{x_3 = 0\} = \{0\}. \quad (\text{VI.3.4})$$

In fact, if  $\Gamma' \subset \{x_3 > 0\}$  is any non-flat leaf of  $\mathcal{L}'$  with  $\Gamma'_{Clos} \cap \{x_3 = 0\} \neq \emptyset$ , then

$$\Gamma'_{Clos} \cap \{x_3 = 0\} = \{0\}. \quad (\text{VI.3.5})$$

*Proof.* We will first argue by contradiction to prove (VI.3.4). Suppose therefore that there exists  $p \neq 0$  with

$$p \in \Gamma_{Clos} \cap \{x_3 = 0\}. \quad (\text{VI.3.6})$$

We begin by constructing a curve  $\gamma$  in  $\Gamma$  that connects  $\Gamma$  to 0 - or a singular point near 0 - and stays away from  $p$ . Precisely,  $\gamma$  will have the following properties:

$$\gamma : [0, 1) \rightarrow B_{|p|/3} \cap \Gamma, \quad (\text{VI.3.7})$$

$$\text{Length}(\gamma) \leq |p|/3, \quad (\text{VI.3.8})$$

$$\lim_{t \rightarrow 1} \gamma(t) \in \Gamma_{Clos} \cap \{x_3 = 0\}. \quad (\text{VI.3.9})$$

To construct  $\gamma$ , first use the definition of  $\Gamma_{Clos}$  to choose a point  $y \in \Gamma$  so that the closure of  $\mathcal{B}_{|p|/6}(y) \subset \Gamma$  contains 0. Then choose a sequence of length minimizing curves in  $\Gamma$  that start at  $y$  and whose second endpoints converge to 0. The Arzela-Ascoli theorem gives a subsequence of these curves that converges to a curve  $\tilde{\gamma}$  that starts at  $y$ , ends at 0, and is contained in  $\overline{\mathcal{B}_{|p|/6}(y)}$ . Finally, let  $\gamma$  be the component of  $\Gamma \cap \tilde{\gamma}$  that starts at  $y$ .

Note that the curve  $\tilde{\gamma}$  might hit another point of  $\mathcal{S}$  before it gets to 0. However, this point must be close to 0 and, hence, far from  $p$ ; this is all that the argument will use. For simplicity, we will assume that 0 was the first point of  $\mathcal{S}$  hit by  $\tilde{\gamma}$  so that  $\lim_{t \rightarrow 1} \gamma(t) = 0$ .

Since  $\gamma$  is contained in  $\Gamma$ , we get a sequence of curves  $\gamma_j : [0, t_j] \rightarrow \Sigma_j$  with  $t_j \rightarrow 1$  and so that the  $\gamma_j$ 's converge to  $\gamma$ . In particular,  $\gamma_j(t_j) \rightarrow 0$ .

**Claim:** The injectivity radius of  $\Sigma_j$  at  $\gamma_j(t_j)$  must go to zero.

**Proof of Claim:** Proposition IV.1.1 gives a stable graph disjoint from  $\Sigma_j$  for each  $j$  and this sequence is converging to  $\{x_3 = 0\} \setminus \{0\}$  as  $j$  goes to infinity. Moreover, exactly one component of  $\Sigma_j$  in a small ball near 0 intersects both sides of the stable graph. The

injectivity radius of this component (obviously) goes to zero as  $j$  goes to infinity. It follows that every other component sits on one side of this stable graph; see (B) in Proposition IV.1.1. In particular, if the component of  $B_\epsilon \cap \Sigma_j$  containing  $\gamma_j(t_j)$  was a disk for some fixed  $\epsilon > 0$  and all sufficiently large  $j$ , then the one-sided curvature estimate would imply that this component was graphical in a neighborhood of 0. Moreover, by the strong maximum principle, this sequence of graphs would have to converge to a subset of  $\{x_3 = 0\}$ . However, these graphs contain subsets of  $\gamma_j$  that are converging to (a component of)

$$B_\epsilon \cap \gamma \subset \Gamma. \quad (\text{VI.3.10})$$

It follows that  $\{x_3 = 0\}$  would have to contain a (smooth) point of the leaf  $\Gamma$ , violating the strong maximum principle. **QED for Claim.**

We can repeat the construction of  $\gamma$  near  $p$  to get curves  $\gamma'_j : [0, t'_j] \rightarrow \Sigma_j$  converging to a curve  $\gamma' : [0, 1) \rightarrow \Gamma$  so that the endpoints  $\gamma'_j(t'_j)$  converge to a singular point near  $p$ . For simplicity, we will assume that this second singular point is actually equal to  $p$ . Arguing as in the Claim, we see that the injectivity radius of  $\Sigma_j$  at  $\gamma'_j(t'_j)$  also goes to zero.

We can now apply Proposition IV.1.1 to shrinking balls centered at  $\gamma_j(t_j)$  and  $\gamma'_j(t'_j)$  to get disjoint stable graphs  $\Gamma_j$  and  $\Gamma'_j$  that are disjoint from  $\Sigma_j$  and so

$$\Gamma_j \rightarrow \{x_3 = 0\} \setminus \{0\} \text{ and } \Gamma'_j \rightarrow \{x_3 = 0\} \setminus \{p\}. \quad (\text{VI.3.11})$$

Since  $\Gamma_j$  and  $\Gamma'_j$  are disjoint, one must be above the other. After passing to a subsequence (and possibly switching  $\Gamma$  and  $\Gamma'$ ), we can assume that  $\Gamma_j$  is always above  $\Gamma'_j$ . It follows easily from the barrier construction used for the proof of Proposition IV.1.1 that the curve  $\gamma'_j$  must also be below the graph  $\Gamma_j$ .<sup>44</sup> However, this forces  $\gamma'_j$  to converge to a curve in  $\{x_3 = 0\}$ , contradicting the strong maximum principle as in the proof of Claim above. This completes the proof of (VI.3.4).

Finally, when  $p \in \Gamma'_{\text{Clos}} \cap \{x_3 = 0\}$ , the same argument applies with obvious changes. Hence, we also get (VI.3.5).  $\square$

**VI.3.2. The proof of Lemma VI.3.1.** As mentioned earlier, we can assume that we are in the case where  $\mathcal{S}_{\text{ulsc}} = \emptyset$  and we will use a flux argument to rule out the possibility of a non-flat leaf of  $\mathcal{L}'$ .

*Proof.* (of Lemma VI.3.1). We will prove the lemma by contradiction, so suppose that  $\Gamma \subset \{x_3 > 0\}$  is a non-flat leaf of  $\mathcal{L}'$  with  $0 \in \Gamma_{\text{Clos}} \cap \mathcal{S}_{\text{neck}}$  and  $\{x_3 = 0\}$  is the associated stable limit plane through 0. By Lemma VI.3.3, there are two possibilities:

- $\Gamma_{\text{Clos}} \cap \mathcal{S} = \{0\}$ .
- $\Gamma_{\text{Clos}} \cap \mathcal{S} = \{0, p\}$  for some point  $p$  with  $x_3(p) > 0$ .

$\Gamma$  is scale-invariant ULSC near 0. More precisely, there exist  $\delta > 0$  and  $r_0 > 0$  so that

$$\mathcal{B}_{\delta|x|}(x) \text{ is a disk for every } x \in B_{r_0} \cap \{x_3 > 0\} \cap \mathcal{L}'. \quad (\text{VI.3.12})$$

Recall that the argument used to prove that complete leaves of  $\mathcal{L}'$  must be flat actually gave a stronger statement; see Remark VI.2.24. This stronger statement implies that (VI.3.12) holds.

<sup>44</sup>Namely, the stable graph is actually a subset of a stable surface that is disjoint from  $\Sigma_j$  and has interior boundary lying in  $\Sigma_j$ ; this interior boundary connects within  $\Sigma_j$  to the curve  $\gamma'_j$ . This barrier construction is given in Lemma IV.1.2.

$\Gamma$  has quadratic curvature blowup near 0: We will next use a compactness argument to prove that there exist constants  $C_d$  and  $r_1 > 0$  so that

$$|A|^2(x) \leq C_d |x|^{-2} \text{ for every } x \in B_{r_1} \cap \{x_3 > 0\} \cap \mathcal{L}'. \quad (\text{VI.3.13})$$

The constant  $C_d$  above might depend on  $\mathcal{L}'$ , but it will be fixed throughout this proof.

Proof of (VI.3.13): We will argue by contradiction, so suppose that there is a sequence of points  $q_n \in \Gamma$  with  $q_n \rightarrow 0$  and

$$|q_n|^2 |A|^2(q_n) > n. \quad (\text{VI.3.14})$$

The idea of the proof is that dilating  $\mathcal{L}'$  by the factor  $|q_n|^{-1}$  about the point  $q_n$  gives a sequence of laminations

$$\mathcal{L}_n = |q_n|^{-1} (\mathcal{L}' - q_n) \quad (\text{VI.3.15})$$

with  $|A|^2(0) > n$  and so that  $\partial B_1$  intersects  $\mathcal{S}_{neck}(\mathcal{L}_n)$ ; here  $\mathcal{S}_{neck}(\mathcal{L}_n)$  is the singular set for the rescaled lamination  $\mathcal{L}_n$ . Moreover, (VI.3.12) gives a uniform lower bound for the injectivity radius of the leaves of  $\{x_3 > 0\} \cap \mathcal{L}_n$  in  $B_{1/2}$ ; see below for more details. Consequently, as  $n$  goes to infinity, a subsequence of the  $\mathcal{L}_n$ 's would converge to a lamination  $\mathcal{L}_\infty$  with

$$0 \in \mathcal{S}_{ulsc}(\mathcal{L}_\infty) \text{ and } \partial B_1 \cap \mathcal{S}_{neck}(\mathcal{L}_\infty) \neq \emptyset. \quad (\text{VI.3.16})$$

However, this would contradict the no mixing theorem, so we conclude that the sequence  $q_n$  could not have existed.

We need two things to make this outline rigorous. First, we do not have a compactness theorem for sequences of laminations, but rather only for sequences of embedded minimal surfaces. This is easily dealt with since the limit  $\mathcal{L}_\infty$  can be realized as a limit of a diagonal sequence of rescalings of the  $\Sigma_j$ 's; we will omit this standard argument. Second, we showed in (VI.3.12) above only that the leaves of  $\mathcal{L}'$  were scale-invariant ULSC near 0; what we need instead is that the sequence  $\Sigma_j$  is itself scale-invariant ULSC near 0. More precisely, we must show that there exists some  $\delta_0 > 0$  so that for each fixed  $n$  we have

$$\text{every component of } B_{\delta_0 |q_n|}(q_n) \cap \Sigma_j \text{ is a disk for } j \text{ large.} \quad (\text{VI.3.17})$$

Since the  $\Sigma_j$ 's are converging to  $\mathcal{L}'$  away from  $\mathcal{S}$  - and  $\Gamma$  does not intersect  $\mathcal{S}$  - then the component of  $B_{\delta |q_n|}(q_n) \cap \Sigma_j$  that is converging to  $\Gamma$  is a disk with large curvature. However, the intrinsic version of the one-sided curvature estimate implies that this is the only component of this ball intersecting a smaller concentric sub-ball about  $q_n$ . This gives the remaining ingredient needed to make the proof rigorous.

Extending flatness: We claim that there exist constants  $C_{flat} > 0$  and  $r_2 > 0$  so that if  $r < r_2$ ,  $x \in \partial B_r \cap \Gamma$ , and

$$\mathcal{B}_{r/4}(x) \text{ is a graph with gradient less than } C_{flat} \text{ over } \{x_3 = 0\}, \quad (\text{VI.3.18})$$

then  $x$  is contained in a graph  $\Gamma_x \subset \Gamma$  defined over (at least) the annulus

$$\{x_3 = 0, r^2/4 < x_1^2 + x_2^2 < r_2\}. \quad (\text{VI.3.19})$$

In other words, once  $\Gamma$  becomes very flat, then it extends to a very flat graph defined over some annulus of a definite size surrounding the singular point 0. Note that the outer radius  $r_2$  of this annulus is independent of  $r$ .

It is easy to prove from the gradient estimate and the quadratic curvature bound (VI.3.13) that  $x$  is contained in a very flat graph  $\Gamma_{x,r}$  defined over the annulus

$$\{x_3 = 0, r^2/4 < x_1^2 + x_2^2 < C r^2\}, \quad (\text{VI.3.20})$$

where the constant  $C = C(\alpha)$  can be as large as we want for  $\alpha$  sufficiently small. A priori, one might worry that this would give a multi-valued graph. However, by the usual argument,  $\Sigma_j$  cannot contain a multi-valued graph and, therefore, neither can  $\Gamma$ . It remains to extend  $\Gamma_{x,r}$  as a graph all the way out to  $\partial D_{r_2}$  for some fixed  $r_2$ . As long as  $C$  is sufficiently large, this can be done using the sublinear growth of the height of the graph. This sublinear growth is proven in proposition II.2.12 in [CM3]. The details of the proof will be left to the reader.

$\Gamma$  cannot be too “horizontal” near 0: We will show next that

$$\limsup_{s \rightarrow 0} \inf_{\Gamma \cap (B_{2s} \setminus B_s)} |\langle \mathbf{n}, (0, 0, 1) \rangle| < 1, \quad (\text{VI.3.21})$$

where  $\mathbf{n}$  is the unit normal to the surface  $\Gamma$ . Note that  $|\langle \mathbf{n}(x), (0, 0, 1) \rangle|$  is equal to one if and only if the tangent plane at  $x$  is horizontal.

Proof of (VI.3.21): Suppose first for some  $s$  that

$$\inf_{\Gamma \cap (B_{2s} \setminus B_s)} |\langle \mathbf{n}, (0, 0, 1) \rangle| > 0. \quad (\text{VI.3.22})$$

It follows  $\Gamma$  is locally graphical with bounded gradient in  $B_{2s} \setminus B_s$ . By the usual argument,  $\Sigma_j$  cannot contain a multi-valued graph and, therefore, neither can  $\Gamma$ . Hence, (VI.3.22) would imply that  $\Gamma \cap (B_{2s} \setminus B_s)$  is a collection of graphs.

Consequently, if we had a uniform lower bound for  $|\langle \mathbf{n}, (0, 0, 1) \rangle|$  in any neighborhood of 0, then standard removable singularity theorems for minimal graphs would imply that  $\Gamma$  has a removable singularity at 0. However,  $\Gamma$  would have to be flat by the strong maximum principle if the singularity at 0 was removable. We conclude therefore that

$$\liminf_{s \rightarrow 0} \inf_{\Gamma \cap (B_{2s} \setminus B_s)} |\langle \mathbf{n}, (0, 0, 1) \rangle| = 0. \quad (\text{VI.3.23})$$

Finally, (VI.3.21) follows easily from “Extending flatness” and (VI.3.23).

Using (VI.3.21) to blow up  $\mathcal{L}'$ . The point about (VI.3.21) is that any limit of rescalings of  $\mathcal{L}'$  about 0 will have a non-flat leaf. More precisely, if  $s_n$  is any sequence going to zero, then a subsequence of the rescaled laminations

$$\mathcal{L}_n = \frac{1}{s_n} (\mathcal{L}'), \quad (\text{VI.3.24})$$

will converge to a lamination  $\mathcal{L}_\infty$  of  $\mathbf{R}^3 \setminus \mathcal{S}(\mathcal{L}_\infty)$  with the following properties:

- (P1) The origin 0 is still in  $\mathcal{S}_{neck}(\mathcal{L}_\infty)$  and  $\{x_3 = 0\}$  is the corresponding limit plane.
- (P2) The leaves of  $\mathcal{L}_\infty$  satisfy the quadratic curvature bound (VI.3.13) in all of  $\{x_3 > 0\}$  (not just in  $B_{r_1}$ ), the singular set  $\mathcal{S}(\mathcal{L}_\infty)$  does not intersect the half-space  $\{x_3 > 0\}$ , and 0 is the only singular point in  $\{x_3 = 0\}$  “reachable” from  $\{x_3 > 0\}$ .
- (P3)  $\mathcal{L}_\infty$  contains a non-horizontal, and hence non-flat, leaf in  $\{x_3 > 0\}$ .

The lamination  $\mathcal{L}_\infty$  is given as a limit of a subsequence of rescalings of the  $\Sigma_j$ 's; see the proof of (VI.3.13) for such a diagonal argument. The first property (P1) follows immediately from this. The second property (P2) follows from immediately from (VI.3.13). Finally, (VI.3.21)

implies that  $\mathcal{L}_\infty$  contains a non-horizontal leaf. This non-horizontal leaf cannot be flat since it would otherwise intersect  $\{x_3 = 0\} \setminus \{0\}$ , thus giving (P3).

The key point about the rescaled limit lamination  $\mathcal{L}_\infty$  is that it has all of the same properties that  $\mathcal{L}'$  did. Therefore, we can repeat the construction to get that limits of rescalings of  $\mathcal{L}_\infty$  also satisfy (P1), (P2), and (P3). This will be important below, so we record it next:

Any limit of rescalings of  $\mathcal{L}_\infty$  will also satisfy (P1), (P2), and (P3). (VI.3.25)

*From now on, we will assume that  $\{x_3 > 0\} \cap \mathcal{L}'$  has quadratic curvature decay and*

$$\{x_3 > 0\} \cap \mathcal{S} = \emptyset; \tag{VI.3.26}$$

*this can be achieved by rescaling as above.*

No stable leaves in  $\{x_3 > 0\}$ : We will show that a lamination

$\mathcal{L}_\infty$  satisfying (P1), (P2), and (P3) cannot have a stable leaf in  $\{x_3 > 0\}$ . (VI.3.27)

The same argument also rules out a leaf in  $\{x_3 > 0\}$  whose oriented double cover is stable.

Proof of no stable leaves in  $\{x_3 > 0\}$ : Suppose instead that  $\mathcal{L}_\infty$  did contain a stable leaf  $\tilde{\Gamma}$  in  $\{x_3 > 0\}$ . We will show first that  $\tilde{\Gamma}$  must be a flat plane  $\{x_3 = t\}$  for some  $t > 0$ . Namely, if it wasn't flat, then it would be complete away from 0 by Lemma VI.3.3 (see equation VI.3.5) and then Lemma B.26 in Appendix B would give a contradiction.

Since the leaves of  $\mathcal{L}_\infty$  are - by definition - disjoint, it follows that the non-flat leaf  $\Gamma$  of  $\mathcal{L}_\infty$  must be contained in the open slab  $\{0 < x_3 < t\}$ . Set  $t_0 = \sup_\Gamma x_3$ , so that

$$\Gamma \subset \{x_3 < t_0\}, \tag{VI.3.28}$$

and

$\Gamma$  intersects every tubular neighborhood of the plane  $\{x_3 = t_0\}$ . (VI.3.29)

Moreover, the quadratic curvature bound (VI.3.13) for the leaves of  $\mathcal{L}'$  implies that

$$\sup_{\{t_0/2 < x_3 < t_0\} \cap \Gamma} |A|^2 \leq 4 C_d t_0^{-2} < \infty. \tag{VI.3.30}$$

However, the three properties (VI.3.28), (VI.3.29), and (VI.3.30) are impossible by the first paragraph of the proof of lemma 1.5 in [MeRo]. We conclude that (VI.3.27) must hold.

$\Gamma$  is proper: The first application of (VI.3.27) will be to show that  $\Gamma$  must be proper in compact subsets of  $\{x_3 > 0\}$ .

Proof of properness: The starting point is that  $\Gamma$  would otherwise accumulate into a stable leaf  $\tilde{\Gamma}$ ; we have used this argument several times and will omit the details (see, e.g., (e) in the proof of Lemma VI.2.1).<sup>45</sup> Clearly,  $\tilde{\Gamma}$  intersects the open half-space  $\{x_3 > 0\}$  and, hence,  $\tilde{\Gamma}$  must be contained in  $\{x_3 > 0\}$  by the strong maximum principle. However, this is impossible by (VI.3.27).

Scale-invariant area bounds: Given any  $\alpha > 0$ , there exists a constant  $C_\alpha$  so that

$$\text{Area}((B_{2r} \setminus B_r) \cap \{x_3 > \alpha |x|\} \cap \Gamma) \leq C_\alpha r^2. \tag{VI.3.31}$$

---

<sup>45</sup>To be precise, either  $\tilde{\Gamma}$  is stable or its oriented double cover is stable.

Proof of (VI.3.31): This will be pretty much the same argument as in the proof of “ $\Gamma$  is proper” combined with a compactness argument. We will argue by contradiction, so suppose that (VI.3.31) fails with  $r = r_n$  and  $C_\alpha = n$  for every integer. By a diagonal argument and rescaling, we get a sequence of embedded minimal planar domains  $\tilde{\Sigma}_j$  with

$$\text{Area} \left( (B_2 \setminus B_1) \cap \{x_3 > \alpha|x|\} \cap \tilde{\Sigma}_j \right) \rightarrow \infty. \quad (\text{VI.3.32})$$

Recall that we have proven in (VI.3.25) that a subsequence of the  $\tilde{\Sigma}_j$ 's converges to a limit lamination  $\mathcal{L}_\infty$  off of a singular set  $\mathcal{S}(\mathcal{L}_\infty)$  satisfying (P1), (P2), and (P3).

Next, we will use (VI.3.32) to show that  $\mathcal{L}_\infty$  contains a stable leaf in  $\{x_3 > 0\}$ , contradicting (VI.3.27). This would be obvious if  $\mathcal{L}_\infty$  itself had infinite area in  $(B_2 \setminus B_1) \cap \{x_3 > \alpha|x|\}$ . On the other hand, if  $\mathcal{L}_\infty$  had finite area in  $(B_2 \setminus B_1) \cap \{x_3 > \alpha|x|\}$ , then the  $\tilde{\Sigma}_j$ 's must converge with infinite multiplicity to some leaf  $\tilde{\Gamma}$  of  $\mathcal{L}_\infty$  that intersects

$$\overline{(B_2 \setminus B_1)} \cap \{x_3 \geq \alpha|x|\}. \quad (\text{VI.3.33})$$

Note that we used that  $\overline{(B_2 \setminus B_1)} \cap \{x_3 \geq \alpha|x|\}$  does not intersect the singular set  $\mathcal{S}_\infty$  (by (P2)) to guarantee the convergence of the  $\tilde{\Sigma}_j$ 's in this set. However, as we have used several times, this convergence with multiplicity implies that the leaf  $\tilde{\Gamma}$  is stable; see, e.g., the proof of Corollary B.20 for more details.<sup>46</sup> Finally, since  $\tilde{\Gamma}$  intersects the half-space  $\{x_3 \geq \alpha\}$ , it must be contained in the open half-space  $\{x_3 > 0\}$  by the strong maximum principle.

Low points in  $\Gamma$  are contained in graphs: We will need the following complete version of “Extending flatness”: There exists  $\alpha > 0$  so that if  $x \in \Gamma$  is in the “low cone”  $\{x_3 < \alpha|x|\}$ , then  $x$  is contained in a graph  $\Gamma_x \subset \Gamma$  defined over (at least)

$$\{x_3 = 0, r^2/4 < x_1^2 + x_2^2 < \infty\}, \quad (\text{VI.3.34})$$

where  $r = |x|$ . Moreover, the graph  $\Gamma_x$  must be asymptotic to a plane or to an upward-sloping half-catenoid. Finally, there is a positive lower bound for the height of the graph  $\Gamma_x$ , i.e.,

$$\inf_{\Gamma_x} x_3 > 0. \quad (\text{VI.3.35})$$

Proof that low points in  $\Gamma$  are contained in graphs: It follows from the gradient estimate and the quadratic curvature decay of  $\Gamma$  that  $\Gamma$  is “very flat” in a neighborhood of  $x$  in the sense of “Extending flatness.” It then follows from the sublinear growth of the height of the graph that  $\Gamma_x$  can then be extended over  $\{x_3 = 0, r^2/4 < x_1^2 + x_2^2 < \infty\}$  as long as  $\alpha$  is sufficiently small. The proof of this extension will be left to the reader.

Now that we know that  $\Gamma_x$  is defined over  $\{x_3 = 0, r^2/4 < x_1^2 + x_2^2 < \infty\}$ , it follows that  $\Gamma_x$  is asymptotic to either a plane, an upward-sloping half-catenoid, or a downward-sloping half-catenoid. The last is impossible since  $\Gamma_x$  is contained in  $\{x_3 > 0\}$ .

Finally, (VI.3.35) follows from the maximum principle at infinity of [LaRo].

The components of  $\Gamma \setminus B_r$  are proper: Given any  $r > 0$ , then

$$\text{each component of } \Gamma \setminus B_r \text{ is proper.} \quad (\text{VI.3.36})$$

<sup>46</sup>To be precise, this convergence with multiplicity implies that either  $\tilde{\Gamma}$  is stable or its oriented double cover is stable.

Proof of (VI.3.36): To prove (VI.3.36), we must show that any such component  $\Gamma_r$  cannot accumulate into  $\{x_3 = 0\}$ ; this is because we already know that  $\Gamma$  itself is proper in  $\{x_3 > 0\}$ . We divide this into two cases.

First, suppose that the boundary  $\partial\Gamma_r$  of the component  $\Gamma_r$  intersects the “low cone” - i.e., suppose that

$$\inf_{\partial\Gamma_r} x_3 < \alpha r. \quad (\text{VI.3.37})$$

In this case, it follows that the entire component  $\Gamma_r$  is a graph and, hence, proper.

Suppose now that (VI.3.37) does not hold. In this case, we will find a low component (for some smaller radius) that extends as a graph underneath  $\Gamma_r$ , thus keeping  $\Gamma_r$  strictly away from  $\{x_3 = 0\}$ . To get this barrier component, note that Lemma F.2 implies that  $\Gamma$  contains a sequence of points  $y_n \rightarrow 0$  contained in the low cone  $\{x_3 < \alpha|x|\}$ . If we choose  $y_n$  close enough to zero, then the resulting graph  $\Gamma_{y_n}$  must pass underneath  $\partial\Gamma_r$  in  $\partial B_r$ . It follows that  $\Gamma_r$  sits above  $\Gamma_{y_n} \cup B_r$  and, hence, cannot accumulate into  $\{x_3 = 0\}$ . This completes the proof of (VI.3.36).

The flux contradiction: We will show that the non-flat leaf  $\Gamma$  must contain a sequence of proper subdomains  $\Gamma_n$  with the following properties:

- (top)  $\partial\Gamma_n$  contains an increasing sequence of compact “top curves” in a fixed plane  $\{x_3 = h\}$  for some  $h$ . Here, increasing means that  $\{x_3 = h\} \cap \partial\Gamma_n \subset \partial\Gamma_{n+1}$  for every  $n$ .
- (ends)  $\Gamma_n$  has finitely many ends and each end is asymptotic to a plane or an upward-sloping half-catenoid.
- (bottom) The rest of  $\partial\Gamma_n$  consists of a finite collection of “bottom curves” whose total length goes to zero as  $n$  goes to infinity.

This will give a flux contradiction just as in the last step of the proof of Lemma VI.2.1. Namely, the flux of  $\Gamma_n$  across the top curves in  $\{x_3 = h\}$  is strictly positive and non-decreasing in  $n$ , the ends have non-negative flux, and the flux across the bottom curves goes to zero. However, this is impossible since the total flux for each  $\Gamma_n$  must be zero by Stokes’ theorem. It remains to construct the  $\Gamma_n$ ’s with these properties.

We will start with the “top curve” for  $\partial\Gamma_n$ . As in the proof of (VI.3.36), Lemma F.2 implies that  $\Gamma$  has infinitely many “low” ends that are asymptotic to either planes or upward-sloping half-catenoids. For simplicity, we will assume that these ends are planar; the catenoid case follows similarly and will be left to the reader. Since [LaRo] ensures that the planar ends are asymptotic to different planes, we can choose some  $h > 0$  between two consecutive planar ends so that  $\{x_3 = h\}$  intersects  $\Gamma$  transversely. Let  $\Gamma_h$  be a component of  $\{x_3 < h\} \cap \Gamma$  containing 0 in its closure and fix some component  $\gamma_h$  of  $\partial\Gamma_h \subset \{x_3 = h\}$ .

Combining the coarea formula with the area bounds from (VI.3.31), we can choose a sequence  $r_n \rightarrow 0$  so that

$$\text{Length}(\partial B_{r_n} \cap \{x_3 \geq \alpha r_n\} \cap \Gamma) \leq C r_n, \quad (\text{VI.3.38})$$

for a uniform constant  $C$  independent of  $n$ . The point here is that the length of these curves goes to zero as  $n$  goes to infinity.

For each  $n$ , let  $\Gamma_n$  be the component of  $\Gamma_h \setminus B_{r_n}$  with  $\gamma_h$  in its boundary. First, it follows immediately that (top) holds. Second, (VI.3.36) implies that  $\Gamma_n$  is proper. Next, when  $r_n$  is sufficiently small, then each point in  $\partial B_{r_n} \cap \{x_3 < \alpha r_n\} \cap \Gamma$  is contained in a graphical

(planar) end that never intersects  $\{x_3 = h\}$ . In particular, we must have that

$$\partial B_{r_n} \cap \partial \Gamma_n \subset \{x_3 \geq \alpha r_n\}, \quad (\text{VI.3.39})$$

so that the length bound (VI.3.38) gives (bottom). By construction, each  $\Gamma_n$  has compact boundary, is contained in the slab  $\{0 < x_3 < h\}$ , and has quadratic curvature decay. Therefore, the gradient estimate implies that each component of  $\Gamma_n$  outside of a cylinder  $\{x_1^2 + x_2^2 \leq R^2\}$  must be either an asymptotically planar graph or a multi-valued graph. However, as we have used several times,  $\Gamma$  cannot contain such a multi-valued graph, so we conclude that each component of

$$\Gamma_n \cap \{x_1^2 + x_2^2 > R^2\} \text{ is an asymptotically planar graph.} \quad (\text{VI.3.40})$$

There are only finitely many such ends for each  $n$  because  $\Gamma_n$  is proper. This gives (ends) and, hence, completes the proof.  $\square$

#### VI.4. THE PROOFS OF THEOREM 0.6 AND THEOREM 0.12

We now have all of the necessary ingredients to prove Theorems 0.6 and 0.12.

*Proof.* (of Theorem 0.6). We have already established properties (A) and (B) of Theorem 0.6 in Lemma II.1.2 and Definition/Lemma II.1.1, respectively. Therefore, it remains to show that every leaf of the lamination  $\mathcal{L}'$  is contained in a horizontal plane. Once we have shown this, then the lamination  $\mathcal{L}$  is obtained by taking the union of the horizontal planes in  $\mathcal{L}'$  together with a horizontal plane through each point in  $\mathcal{S}$ .

We have already proven that the leaves of  $\mathcal{L}'$  are planar when the sequence is ULSC in Theorem 0.9. Therefore, by the no mixing theorem, Theorem 0.4, the only remaining case is when  $\mathcal{S} = \mathcal{S}_{neck} \neq \emptyset$ . However, Lemma VI.2.1 and Lemma VI.3.1 together prove that every leaf of  $\mathcal{L}'$  is flat in this case. This completes the proof of the theorem.  $\square$

Theorem 0.12 now follows immediately:

*Proof.* (of Theorem 0.12). Now that we have established Theorem 0.6, it only remains to show that property  $(C_{neck})$  holds. However, property  $(C_{neck})$  was proven in (C1) in Theorem 0.14.  $\square$

## Part VII. Appendices

### APPENDIX A. COMPACT CONNECTED EXHAUSTIONS

We recall next that any connected surface  $\Gamma$  without boundary, but not necessarily complete, may be exhausted by connected open sets with compact closure. Just to be clear, the punctured plane  $\{(x, y) \mid x^2 + y^2 > 0\}$  is an example of such a surface. This lemma is elementary, but we include a proof below for completeness.

**Lemma A.1.** Given a connected surface  $\Gamma$  without boundary, there exists a sequence of connected open sets  $K_j$  with compact closure that exhaust  $\Gamma$ . That is, we have  $\Gamma = \cup_{j=1}^{\infty} K_j$  and  $K_j \subset K_{j+1}$  for every  $j$ .

*Proof.* To see this, first fix a point  $x \in \Gamma$ . For each  $r > 0$ , let  $\Gamma_r$  be the set of points  $y$  in  $\Gamma$  such that the geodesic ball of radius  $1/r$  about  $y$  is complete. Next define a compact subset  $K_r^{\text{comp}} \subset \Gamma_r$  to be the set of points  $z \in \Gamma$  such that there is a Lipschitz map

$$\gamma_z : [0, r] \rightarrow \Gamma_r \text{ with } \gamma_z(0) = x, \gamma_z(r) = z, \text{ and } |\gamma'_z| \leq 1. \quad (\text{A.2})$$

It follows immediately that each  $K_r^{\text{comp}}$  is connected. Moreover, since  $\Gamma$  is locally compact, the Arzela-Ascoli theorem implies that each  $K_r^{\text{comp}}$  is compact.

We will show that the  $K_r^{\text{comp}}$ 's exhaust  $\Gamma$ . Suppose that  $z \in \Gamma$  is a fixed but arbitrary point; we will show that  $z \in K_r^{\text{comp}}$  for some sufficiently large  $r$ . Observe first that  $\Gamma$  is path connected since it is connected and locally path connected; we therefore get a continuous map

$$f_z : [0, 1] \rightarrow \Gamma \text{ with } f_z(0) = x \text{ and } f_z(1) = z. \quad (\text{A.3})$$

Since  $[0, 1]$  is compact and  $f_z$  is continuous, the image  $f_z([0, 1]) \subset \Gamma$  is also compact. In particular, there exists  $r'$  so that

$$f_z([0, 1]) \subset \Gamma_{r'}. \quad (\text{A.4})$$

Finally, we will replace the curve  $f_z([0, 1])$  with a broken geodesic to get a Lipschitz curve in  $\Gamma_{2r'}$  from  $x$  to  $z$ . Namely, compactness allows us to cover  $f_z([0, 1])$  by a finite collection of balls of radius  $1/(4r')$  with centers on the curve. Replacing segments in  $f_z([0, 1])$  connecting the centers of overlapping balls by intrinsic geodesics gives a broken geodesic – with finitely many breaks – connecting  $x$  to  $z$ . The triangle inequality guarantees that this broken geodesic stays in  $\Gamma_{2r'}$ . This completes the proof that  $z$  is in some  $K_r^{\text{comp}}$  since the length of this curve is finite.

Finally, we define the open sets  $K_j$  by

$$K_j = \cup_{r < j} K_r^{\text{comp}}. \quad (\text{A.5})$$

The  $K_j$ 's are obviously nested and exhaust  $\Gamma$  since the  $K_j^{\text{comp}}$ 's do. The set  $K_j$  is path connected since it is the union of nested path connected sets; it is contained in the compact set  $K_j^{\text{comp}}$  and therefore has compact closure. Finally, it is easy to see that each  $K_j$  is open.  $\square$

## APPENDIX B. SURFACES WITH STABLE COVERS

**B.1. Going from stability of a covering space to stability of a surface itself.** If an oriented minimal surface is stable, then any covering space is also stable. However, the converse may not always be true. The next lemma states that the converse is true if in addition the holonomy group of the covering space has sub-exponential growth.

Before showing this, we will need to recall a few elementary properties of groups and covering spaces.

Growth of groups. Suppose that  $\Lambda$  is a finitely generated group and fix a set of generators. Such a choice of generators induces a natural metric on  $\Lambda$  called the word metric, cf. [Gr]. Let  $\Lambda_n$  denote the ball of radius  $n$  about the identity in this metric. The group is said to have sub-exponential growth if we have for every  $\epsilon > 0$  that

$$\lim_{n \rightarrow \infty} \frac{|\Lambda_n|}{e^{\epsilon n}} = 0 \quad (\text{B.1})$$

where  $|\Lambda_n|$  denotes the number of elements of  $\Lambda_n$ .<sup>47</sup> Given any fixed integer  $k$ , it follows, almost immediately, that sub-exponential growth guarantees that there is a sequence  $n_j \rightarrow \infty$  with

$$\frac{|\Lambda_{n_j+k} \setminus \Lambda_{n_j}|}{|\Lambda_{n_j}|} \rightarrow 0. \quad (\text{B.2})$$

Covering spaces. Recall that a connected covering space  $\hat{\Pi} : \hat{\Gamma} \rightarrow \Gamma$  with base point  $x \in \Gamma$  is uniquely determined by the *holonomy homomorphism*  $\text{Hol}$  from  $\pi_1(\Gamma)$  to the automorphisms of the fiber  $\hat{\Pi}^{-1}(x)$ . To define this homomorphism, suppose that  $\gamma : [0, 1] \rightarrow \Gamma$  is a curve with  $\gamma(0) = \gamma(1) = x$  and  $\hat{x}$  is a point in  $\hat{\Pi}^{-1}(x)$ . The lifting property for covering spaces gives a unique lift  $\gamma_{\hat{x}} : [0, 1] \rightarrow \hat{\Gamma}$  of  $\gamma$  with  $\gamma_{\hat{x}}(0) = \hat{x}$ . We define  $\text{Hol}(\gamma)(\hat{x})$  to be the endpoint  $\gamma_{\hat{x}}(1)$ .

We call the image  $\text{Hol}(\pi_1(\Gamma))$  the holonomy group of the covering space; to keep the notation simple, set  $\Lambda = \text{Hol}(\pi_1(\Gamma))$ .<sup>48</sup> If we fix a point  $\hat{x}$  with  $\Pi(\hat{x}) = x$ , then we can define a fundamental domain  $\Gamma_0$  in  $\hat{\Gamma}$  by

$$\Gamma_0 = \{y \in \hat{\Gamma} \mid \text{dist}_{\hat{\Gamma}}(y, \hat{x}) \leq \text{dist}_{\hat{\Gamma}}(y, z) \text{ for all } z \in \Pi^{-1}(x)\}. \quad (\text{B.3})$$

Using this, let  $\hat{\Gamma}_n = \cup_{\lambda \in \Lambda_n} \lambda(\Gamma_0)$  be the covering of  $\Gamma$  corresponding to  $\Lambda_n$ .

The next property that we will need is a positive lower bound for the distance between  $\hat{\Gamma}_n$  and  $\hat{\Gamma} \setminus \hat{\Gamma}_{n+k_0}$  when  $k_0$  is sufficiently large. Precisely, if  $\Gamma$  has compact closure (so, in particular,  $\pi_1(\Gamma)$  is finitely generated and  $\text{diam}(\Gamma_0)$  is finite), then an easy compactness argument gives a constant  $k_0$  so that

$$\text{dist}_{\hat{\Gamma}}(\hat{\Gamma}_n, \hat{\Gamma} \setminus \hat{\Gamma}_{n+k_0}) > 1. \quad (\text{B.4})$$

Here  $k_0$  depends on  $\hat{\Gamma}$ ,  $\Gamma$ , and  $\Lambda$  but does not depend on  $n$ .

The last fact that we will need is that the holonomy group extends to an action on  $\hat{\Gamma}$  when it is abelian; we include a proof for completeness.

**Lemma B.5.** If  $\hat{\Gamma} \rightarrow \Gamma$  is a connected covering space with abelian holonomy group  $\Lambda$ , then  $\Lambda$  extends to an action on  $\hat{\Gamma}$  as the group of deck transformations as follows:

Suppose that  $\gamma : [0, 1] \rightarrow \Gamma$  is a curve with  $\gamma(0) = \gamma(1) = x$  (where  $x$  is the base point in  $\Gamma$ ). We have to define the action of  $\text{Hol}(\gamma)$  on an arbitrary point  $\hat{y}$  in  $\hat{\Gamma}$ . To do this, choose a curve  $\sigma : [0, 1] \rightarrow \Gamma$  from  $y$  to  $x$  and define  $\text{Hol}(\gamma)(\hat{y})$  to be the second endpoint of the curve starting at  $\hat{y}$  that lifts the curve

$$(-\sigma) \circ \gamma \circ \sigma, \quad (\text{B.6})$$

where  $(-\sigma)$  denotes the curve  $\sigma$  traversed in the opposite direction.

*Proof.* The only thing to check is that this definition does not depend on the choice of the curve  $\sigma$ . Suppose therefore that  $\mu : [0, 1] \rightarrow \Gamma$  is a second curve from  $y$  to  $x$ . It is then easy to see that  $\sigma$  and  $\mu$  give the same endpoint in (B.6) if and only if

$$\mu \circ (-\sigma) \circ \gamma \circ \sigma \circ (-\mu) \circ (-\gamma) \quad (\text{B.7})$$

<sup>47</sup>It is not hard to see that having sub-exponential growth is independent of the choice of generators.

<sup>48</sup>If  $\hat{\Gamma}$  is the universal cover, then the holonomy group is exactly the group of deck transformations and, hence, isomorphic to  $\pi_1(\Gamma)$ . However, the deck group acts transitively on the fiber  $\Pi^{-1}(x)$  if and only if  $\pi_{\hat{\Gamma}}$  is a normal subgroup of  $\pi_1(\Gamma)$ ; when this is not the case, the holonomy group is bigger than the deck group.

lifts to a closed curve in  $\hat{\Gamma}$  starting at  $\hat{x}$ . However, the second endpoint of the curve in (B.7) is nothing more than

$$\begin{aligned} \text{Hol}(\mu \circ (-\sigma) \circ \gamma \circ \sigma \circ (-\mu) \circ (-\gamma))(\hat{x}) = \\ \text{Hol}(\mu \circ (-\sigma)) \circ \text{Hol}(\gamma) \circ \text{Hol}(\sigma \circ (-\mu)) \circ \text{Hol}(-\gamma)(\hat{x}) = \hat{x}, \end{aligned} \quad (\text{B.8})$$

since the holonomy group is abelian. This completes the proof.  $\square$

Stability of covering spaces. We will next show that if a cover of a minimal surface is stable and its holonomy group has sub-exponential growth, then the surface itself is stable. This would be obvious for finite covers; in that case, any compactly supported function on  $\Gamma$  lifts to a compactly supported function on  $\hat{\Gamma}$ . When the holonomy group is infinite, the lift of a compactly supported function on  $\Gamma$  no longer has compact support. To deal with this, we have to introduce a second cutoff function.

**Lemma B.9.** Suppose that  $\Gamma \subset \mathbf{R}^3$  is an oriented minimal surface with compact closure, possibly with boundary, and  $\hat{\Gamma}$  is a covering space of  $\Gamma$ . If  $\hat{\Gamma}$  is stable and its holonomy group has sub-exponential growth, then  $\Gamma$  itself is stable.

*Proof.* We will show that, for each function  $0 \leq \phi \leq 1$  compactly supported on  $\Gamma \setminus \partial\Gamma$ , we have the following stability inequality

$$\int_{\Gamma} |A|^2 \phi^2 \leq \int_{\Gamma} |\nabla \phi|^2. \quad (\text{B.10})$$

Since the holonomy group  $\Lambda$  of the covering space has sub-exponential growth, (B.2) gives a sequence  $n_j \rightarrow \infty$  with

$$\frac{|\Lambda_{n_j+k_0} \setminus \Lambda_{n_j}|}{|\Lambda_{n_j}|} \rightarrow 0, \quad (\text{B.11})$$

where  $k_0$  is given by (B.4).

Define a sequence of functions  $\psi_j$  on  $\hat{\Gamma}$  by

$$\psi_j = \begin{cases} 1 & \text{on } \hat{\Gamma}_{n_j}, \\ 1 - \text{dist}_{\hat{\Gamma}}(\hat{\Gamma}_{n_j}, \cdot) & \text{on } \{0 < \text{dist}_{\hat{\Gamma}}(\hat{\Gamma}_{n_j}, \cdot) < 1\}, \\ 0 & \text{otherwise.} \end{cases} \quad (\text{B.12})$$

In particular,  $\psi_j$  is one on  $\hat{\Gamma}_{n_j}$ , zero outside the 1-tubular neighborhood of  $\hat{\Gamma}_{n_j}$  and hence zero outside  $\hat{\Gamma}_{n_j+k_0}$  by (B.4). Moreover,  $\psi_j$  decays linearly in the distance to  $\hat{\Gamma}_{n_j}$  and hence satisfies

$$|\nabla \psi_j| \leq 1. \quad (\text{B.13})$$

Below, we will identify the functions  $\phi$  and  $|A|^2$  on  $\Gamma$  with their lifts to the cover  $\hat{\Gamma}$ .

Although the function  $\psi_j$  does not vanish on all of  $\partial\hat{\Gamma}$ , the function  $\psi_j\phi$  does. We can therefore use  $\psi_j\phi$  in the stability inequality for  $\hat{\Gamma}$  to get

$$\begin{aligned} |\Lambda_{n_j}| \int_{\Gamma} |A|^2 \phi^2 &= \int_{\hat{\Gamma}_{n_j}} |A|^2 \phi^2 \leq \int_{\hat{\Gamma}_{n_j+k_0}} |A|^2 (\psi_j \phi)^2 \\ &\leq \int_{\hat{\Gamma}_{n_j+k_0}} |\nabla(\psi_j \phi)|^2 = \int_{\hat{\Gamma}_{n_j}} |\nabla\phi|^2 + \int_{\hat{\Gamma}_{n_j+k_0} \setminus \hat{\Gamma}_{n_j}} |\nabla(\psi_j \phi)|^2 \\ &= |\Lambda_{n_j}| \int_{\Gamma} |\nabla\phi|^2 + \int_{\hat{\Gamma}_{n_j+k_0} \setminus \hat{\Gamma}_{n_j}} |\nabla(\psi_j \phi)|^2. \end{aligned} \quad (\text{B.14})$$

Since  $\phi$  is smooth and has compact support, there is a constant  $C_\phi$  so that  $2|\nabla\phi|^2 + 2 \leq C_\phi$ ; hence

$$|\nabla(\psi_j \phi)|^2 \leq 2(|\nabla\phi|^2 + |\nabla\psi_j|^2) \leq 2|\nabla\phi|^2 + 2 \leq C_\phi. \quad (\text{B.15})$$

We can use this to bound the last term in (B.14) as follows

$$\int_{\hat{\Gamma}_{n_j+k_0} \setminus \hat{\Gamma}_{n_j}} |\nabla(\psi_j \phi)|^2 \leq C_\phi \text{Area}(\hat{\Gamma}_{n_j+k_0} \setminus \hat{\Gamma}_{n_j}) = C_\phi \text{Area}(\Gamma) |\Lambda_{n_j+k_0} \setminus \Lambda_{n_j}|. \quad (\text{B.16})$$

Substituting (B.16) into (B.14) gives

$$\int_{\Gamma} |A|^2 \phi^2 \leq \int_{\Gamma} |\nabla\phi|^2 + C_\phi \text{Area}(\Gamma) \frac{|\Lambda_{n_j+k_0} \setminus \Lambda_{n_j}|}{|\Lambda_{n_j}|}. \quad (\text{B.17})$$

Finally, (B.11) implies that (B.17) goes to (B.10) as  $j \rightarrow \infty$ , completing the proof.  $\square$

**B.2. A surface and stable cover with cyclic holonomy group where the previous lemma applies.** We will show, in Corollary B.20 below, that a certain minimal surface  $\Gamma$  given as a limit of embedded minimal multi-valued graphs  $\Sigma_j$  must be stable. This will follow from Lemma B.9 once we show that there is a connected covering space  $\hat{\Gamma}$  satisfying the following two properties:

- The holonomy group  $\Lambda$  of the covering space is cyclic (and, hence, has sub-exponential growth).
- The cover  $\hat{\Gamma}$  is stable.

Throughout this subsection,  $\Gamma \subset \mathbf{R}^3$  will be an oriented minimal surface with compact closure, possibly with boundary, and  $\Pi : \hat{\Gamma} \rightarrow \Gamma$  a covering map with holonomy group  $\mathbf{Z}$  (in fact, abelian is sufficient) with the following properties:

- (G1)  $\Sigma_j$  is a sequence of embedded minimal multi-valued (normal exponential) graphs over  $\Gamma$ .
- (G2) There is a sequence  $K_1 \subset K_2 \subset \dots \subset \hat{\Gamma}$  of open domains exhausting  $\hat{\Gamma}$  and functions  $u_j : K_j \rightarrow \mathbf{R}$  with

$$|u_j| + |\nabla u_j| \leq 1/j, \quad (\text{B.18})$$

so that there is a bijection from  $K_j$  to  $\Sigma_j$  given by

$$x \rightarrow \Pi(x) + u_j(x) \mathbf{n}_\Gamma(\Pi(x)). \quad (\text{B.19})$$

The condition (G2) says that the  $\Sigma_j$ 's can be thought of as one to one graphs over the domains  $K_j$  in the cover  $\hat{\Gamma}$ .

**Corollary B.20.** If  $\hat{\Gamma} \rightarrow \Gamma$  satisfies (G1) and (G2), then the surface  $\Gamma$  is stable.

*Proof.* By assumption, the holonomy group  $\Lambda$  is cyclic and, thus, has sub-exponential growth. Therefore, to apply Lemma B.9, we must show that the cover  $\hat{\Gamma}$  is stable. We will prove the stability of  $\hat{\Gamma}$  by constructing a positive solution  $w$  of the Jacobi equation on  $\hat{\Gamma}$ .

First, since the holonomy group  $\Lambda$  is abelian, Lemma B.5 implies that it acts as the deck group of  $\hat{\Gamma}$ .

Next, define a sequence of subsets  $\tilde{K}_j^o \subset \hat{\Gamma}$  by

$$\tilde{K}_j^o = \{x \in K_j \mid h(1)(x) \in K_j\} = K_j \cap h(1)^{-1}(K_j), \quad (\text{B.21})$$

where  $h(1) \in \Lambda$  is the generator of the infinite cyclic subgroup  $\Lambda = \mathbf{Z}$ . Fix a point  $p \in \tilde{K}_1$  and let  $\tilde{K}_j$  be the connected component of  $\tilde{K}_j^o$  containing  $p$ .

We will need below that the  $\tilde{K}_j$ 's are nested, open, connected sets that exhaust  $\hat{\Gamma}$ . The only point to check is that they exhaust  $\hat{\Gamma}$ . To see this, suppose that  $y \in \hat{\Gamma}$  and choose a path  $\sigma : [0, 1] \rightarrow \hat{\Gamma}$  from  $p$  to  $y$ . Since the  $K_j$ 's are open and exhaust  $\hat{\Gamma}$ , the compact set  $\sigma([0, 1]) \cup h(1)(\sigma([0, 1]))$  is entirely contained in some  $K_j$  for  $j$  sufficiently large and, in particular,  $\sigma([0, 1]) \subset \tilde{K}_j$ .

Given  $x \in \tilde{K}_j$ , both  $x$  and  $h(1)(x)$  are in  $K_j$  and, therefore, we can define functions  $w_j$  on  $\tilde{K}_j$  by

$$w_j(x) = u_j(h(1)(x)) - u_j(x). \quad (\text{B.22})$$

Since the bijection (B.19) takes  $x$  and  $h(1)(x)$  to distinct points in the embedded surface  $\Sigma_j$  and these distinct points have the same projection to  $\Gamma$ , we conclude that

$$w_j(x) \neq 0. \quad (\text{B.23})$$

Therefore, we may as well assume that  $w_j$  is positive on the connected set  $\tilde{K}_j$ . Since  $u_j$  and  $|\nabla u_j|$  are going to zero by (B.18), a standard calculation (cf. lemma 2.4 in [CM4]) gives that  $u_j$  almost satisfies the Jacobi equation.<sup>49</sup> Likewise, the positive function  $w_j$  is almost a solution of the Jacobi equation. In particular, if we define normalized functions

$$\tilde{w}_j = \frac{w_j}{w_j(p)}, \quad (\text{B.24})$$

then a subsequence of the  $\tilde{w}_j$ 's converges to a positive solution  $w$  of the Jacobi equation on  $\hat{\Gamma}$  and, thus,  $\hat{\Gamma}$  is stable.  $\square$

**B.3. A Bernstein theorem for incomplete surfaces.** The results of the previous subsections will be used show that certain incomplete minimal surfaces must be stable. We will next prove a Bernstein theorem showing that such a stable surface  $\Gamma$  must then be flat, as long as it is “complete away from a single point.” This generalizes the well-known Bernstein theorem for complete stable surfaces of [FiSc], [DoPe].

More precisely, we will assume that the closure  $\Gamma_{\text{Clos}}$  of  $\Gamma$  is equal to the union of  $\Gamma$  and a single point. Recall that the closure  $\Gamma_{\text{Clos}}$ , defined in (II.2.10), is given by

$$\Gamma_{\text{Clos}} = \bigcup_r \overline{\mathcal{B}_r(x_\Gamma)}. \quad (\text{B.25})$$

<sup>49</sup>Precisely,  $\Delta u_j + |A|^2 u_j = Q(u_j)$ , where the nonlinear term  $Q(u_j)$  is at least quadratic in  $u_j$  and  $\nabla u_j$ .

The flatness of such a  $\Gamma$  follows from an argument of Gulliver and Lawson, [GuLa]; for completeness, we recall this in the next lemma.

**Lemma B.26.** Suppose that  $\Gamma \subset \mathbf{R}^3$  is a connected stable minimal surface without boundary and with trivial normal bundle. If

$$\Gamma_{\text{clos}} \setminus \Gamma = \{0\}, \quad (\text{B.27})$$

then  $\Gamma$  is a (punctured) plane.

*Proof.* We will use an argument of Gulliver and Lawson, [GuLa], to conformally change the metric  $ds^2$  on  $\Gamma$  so that:

- (1) The universal cover  $\Gamma_U$  of  $\Gamma$  is complete in the new metric  $d\tilde{s}^2$ .
- (2) The operator  $\tilde{L} = \tilde{\Delta} - 2\tilde{K}$  is non-negative on  $\Gamma_U$ ; i.e., if  $\phi$  is any compactly supported function on  $\Gamma_U$ , then

$$\int \phi \tilde{L} \phi \leq 0. \quad (\text{B.28})$$

Note that the sign convention here may be the opposite of what one would expect. Once we have done this, it follows from [FiSc] that  $(\Gamma_U, d\tilde{s}^2)$  is conformal to  $\mathbf{R}^2$  with the standard flat metric. Translating back to the original metric  $ds^2$  will then imply that the original  $\Gamma$  was flat.

Following [GuLa], we make the conformal change of metric

$$d\tilde{s}^2 = \frac{ds^2}{|x|^2}. \quad (\text{B.29})$$

Since the covering map from  $\Gamma_U$  to  $\Gamma$  is an immersion, the metric  $d\tilde{s}^2$  on  $\Gamma$  pulls back to give a metric on  $\Gamma_U$ ; we will also use  $d\tilde{s}^2$  to denote this pull back metric. It follows immediately that  $\Gamma_U$  is complete in the new metric  $d\tilde{s}^2$ . Set  $\tilde{L} = \tilde{\Delta} - 2\tilde{K}$  where the Laplacian  $\tilde{\Delta}$  and the curvature  $\tilde{K}$  are computed with respect to the metric  $d\tilde{s}^2$ . Corollary 2.13 in [GuLa]<sup>50</sup> gives that

$$\tilde{L} = |x|^2 L - 4(1 - |\nabla |x||^2). \quad (\text{B.30})$$

Combining (B.30) with the stability of  $\Gamma_U$  gives for any compactly supported  $\phi$  that

$$\int_{\Gamma_U} \phi \tilde{L} \phi d\tilde{\mu} = \int_{\Gamma_U} \phi (|x|^2 L \phi - 4(1 - |\nabla |x||^2) \phi) |x|^{-2} d\mu \leq \int_{\Gamma_U} \phi L \phi d\mu \leq 0; \quad (\text{B.31})$$

that is, the operator  $\tilde{L}$  is non-negative on  $\Gamma_U$  with the complete metric  $d\tilde{s}^2$ . However, theorem 2 in [FiSc] states that, for any complete surface conformal to the disk, the intrinsically defined operator  $\Delta - 2K$  must be negative.<sup>51</sup> Therefore, since the plane is the only other possible conformal type, we conclude that  $(\Gamma_U, d\tilde{s}^2)$  – and hence also  $(\Gamma_U, ds^2)$  – is conformally equivalent to  $\mathbf{R}^2$ . In particular, there is a sequence of compactly-supported logarithmic cutoff functions  $\phi_j$  defined on  $\Gamma_U$  with

$$\phi_j \leq \phi_{j+1} \text{ for every } j \text{ and } \phi_j(x) \rightarrow 1 \text{ for every } x \in \Gamma_U. \quad (\text{B.32})$$

$$\lim_{j \rightarrow \infty} \int_{\Gamma_U} |\tilde{\nabla} \phi_j|^2 d\tilde{\mu} = \lim_{j \rightarrow \infty} \int_{\Gamma_U} |\nabla \phi_j|^2 d\mu = 0. \quad (\text{B.33})$$

<sup>50</sup>Note that our operator  $L$  has the opposite sign convention from the operator  $L_2$  in [GuLa].

<sup>51</sup>Note that [FiSc] does not assume a sign on the curvature  $K$ .

Using the functions  $\phi_j$  in the stability inequality for  $L$  on  $\Gamma_U$  gives

$$-2 \int_{\Gamma_U} K \phi_j^2 d\mu \leq \int_{\Gamma_U} |\nabla \phi_j|^2 d\mu \rightarrow 0. \tag{B.34}$$

Since  $K \leq 0$  and the functions  $\phi_j$  go to 1, we conclude that  $\Gamma_U$  is flat. This completes the proof.  $\square$

### APPENDIX C. AN EXTENSION OF [CM9]

In the current paper, we need slight modifications of several results in [CM9]. We will give these results in this appendix and explain whatever modifications are needed for their proofs.

**C.1. Chord-arc bounds for ULSC surfaces.** The next lemma extends the chord-arc bounds of [CM9] from disks to ULSC surfaces.

**Lemma C.1.** Given a constant  $r$ , there exists  $R > r$  so that if  $\Sigma$  is an embedded minimal surface with  $\mathcal{B}_R(x_0) \subset \Sigma \setminus \partial\Sigma$  and

$$\mathcal{B}_1(x) \text{ is a disk for each } x \in \mathcal{B}_R(x_0) , \tag{C.2}$$

then the connected component of  $B_r(x_0) \cap \mathcal{B}_R(x_0)$  containing  $x_0$  has boundary in  $\partial B_r(x_0)$ .

*Proof.* The proof follows the proof of lemma 2.23 given in appendix B of [CM9] with one modification (the statement of lemma 2.23 from [CM9] is recalled below in Lemma C.3). The difference is that lemma 2.23 assumed a curvature bound and used this to show that two disjoint intrinsic balls whose centers were close (in  $\mathbf{R}^3$ ) could be written as graphs over each other. In the current case, the required curvature bound is not assumed but rather comes from the intrinsic version of the one-sided curvature estimate (corollary 0.8 in [CM9]).  $\square$

**C.2. Chord-arc and area bounds for surfaces with bounded curvature.** We also needed following lemma from [CM9] which gives chord-arc bounds for surfaces with bounded curvature<sup>52</sup>:

**Lemma C.3.** (lemma 2.23 in [CM9].) There exists  $C_0 > 1$  so that given a constant  $C_a$ , we get another constant  $C_b$  such that the following holds:

If  $\Sigma \subset \mathbf{R}^3$  is an embedded minimal surface with  $0 \in \Sigma \subset B_{C_0 R}$  and  $\partial\Sigma \subset \partial B_{C_0 R}$  and in addition

$$\sup_{B_{C_0 R} \cap \Sigma} |A|^2 \leq C_a R^{-2} , \tag{C.4}$$

then the component  $\Sigma_{0,R}$  of  $B_R \cap \Sigma$  containing 0 satisfies

$$\Sigma_{0,R} \subset \mathcal{B}_{C_b R}(0) . \tag{C.5}$$

In particular, we also get a constant  $C_c$  (depending only on  $C_a$ ) so that

$$\text{Area}(\Sigma_{0,R}) \leq C_c R^2 . \tag{C.6}$$

---

<sup>52</sup>Of course, any surface with bounded curvature is also ULSC and is therefore already covered by Lemma C.1. The usefulness of Lemma C.3 is that it makes the dependence very precise.

*Proof.* The first claim (C.5) follows precisely from the proof of lemma 2.23 in [CM9] that is given in appendix B in [CM9].<sup>53</sup>

Since  $|A|^2$  is bounded on  $\Sigma_{0,R}$  by assumption, (C.5) and standard comparison theorems give the area bound (C.6).  $\square$

A key point in Lemma C.3 is that the constant  $C_0$  does not depend on the constant  $C_a$  in the curvature bound (C.4).

#### APPENDIX D. ESTIMATES FOR STABLE SURFACES

Throughout this section,  $\Gamma$  will be a stable surface with connected “interior boundary”  $\gamma$ . We will use  $\text{An}_r(\gamma)$  to denote the intrinsic tubular neighborhood of radius  $r$  about a curve  $\gamma$ , i.e.,

$$\text{An}_r(\gamma) = \{x \in \Gamma \mid \text{dist}_\Gamma(x, \gamma) < r\}. \quad (\text{D.1})$$

Similarly, we will write  $\text{An}_{s,t}(\gamma)$  for the “annulus”  $\text{An}_t(\gamma) \setminus \text{An}_s(\gamma)$ .

The main result of this appendix is the following “stable graph” proposition. This proposition shows that a stable embedded minimal surface with a single interior boundary curve  $\gamma$  and an area bound near  $\gamma$  is graphical away from its boundary.

**Proposition D.2.** Given a constant  $C$ , there exists  $\omega > 1$  so that if  $\Gamma \subset B_R$  is a stable embedded minimal surface whose “interior boundary”  $\partial\Gamma \setminus \partial B_R$  is a simple closed curve  $\gamma \subset B_4$  satisfying

$$\text{Area}(\text{An}_2(\gamma)) \leq C, \quad (\text{D.3})$$

then each component of  $B_{R/\omega} \cap \Gamma \setminus B_\omega$  is a graph with gradient bounded by one.

**D.1. The regularity of the distance function to the interior boundary.** In proving the proposition, we will need some basic results on the level sets of the distance function to an interior boundary curve. Before stating these results, it will be helpful to recall the Gauss-Bonnet theorem with corners and set the notation.

The Gauss-Bonnet theorem with corners implies that a surface  $\Sigma$  with piecewise smooth boundary  $\partial\Sigma$  satisfies

$$\int_{\partial\Sigma} k_g + \int_\Sigma K_\Sigma + \sum \alpha_i = 2\pi \chi(\Sigma). \quad (\text{D.4})$$

Here  $K_\Sigma$  is the Gauss curvature of  $\Sigma$ ,  $\chi(\Sigma)$  is its Euler characteristic, and  $k_g$  is the geodesic curvature of  $\partial\Sigma$ . The sign convention of  $k_g$  is such that it is positive on the boundary of the unit disk in the plane. Finally, the  $\alpha_i$ ’s are the “jump angles” at the corners of  $\partial\Sigma$ ; see Figure 49. By convention,  $\alpha_i$  is positive at a corner where  $\Sigma$  is locally convex. For instance, on each corner of a square,  $\alpha_i$  is  $\pi/2$ .

The next lemma of Shiohama and Tanaka contains the main results that we will need (cf. the proof of theorem 1 in [Ro]):

---

<sup>53</sup>We should point out that we have slightly modified the statement of lemma 2.23 from [CM9]; in particular, the statement in [CM9] assumes that  $\Sigma$  is a disk. However, this was not used in the proof of the lemma given in appendix B in [CM9].

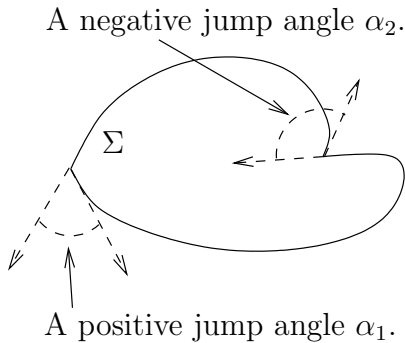
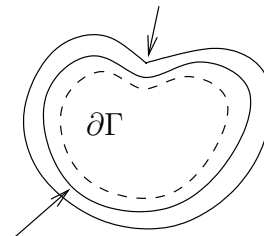


FIGURE 49. The jump angle  $\alpha_i$  at a corner.

Concave corners can develop (see  $(\star 1)$ ).



The distance level sets are initially smooth.

FIGURE 50. The level sets  $S(t)$  of the distance function to a curve.

**Lemma D.5.** [ShTa1], [ShTa2] Suppose that  $\Gamma$  is a complete noncompact oriented surface whose boundary  $\partial\Gamma$  is a smooth simple closed curve. The set

$$S(t) = \{x \in \Gamma \mid \text{dist}_\Gamma(x, \partial\Gamma) = t\} \tag{D.6}$$

satisfies the following properties:

- ( $\star 1$ ) For almost every  $t$ , the set  $S(t)$  is a finite union of piecewise smooth curves with length  $\ell(t)$ . Moreover, the “jump angle”  $\alpha_i(t)$  at each corner is negative and always between  $-\pi/2$  and  $0$ ; let  $-\theta_i(t)$  denote this negative angle at the  $i$ -th corner.<sup>54</sup>
- ( $\star 2$ ) For almost every  $t$ , the derivative  $\ell'(t)$  exists and satisfies

$$\ell'(t) = \int_{S(t)} k_g - \sum_i \tan(\theta_i(t)) \leq \int_{S(t)} k_g - \sum_i \theta_i(t). \tag{D.7}$$

The key for the inequality in (D.7) is that each  $\theta_i(t)$  is between  $0$  and  $\pi/2$  by ( $\star 1$ ).

Notice that the right-hand side of (D.7) is exactly the boundary term corresponding to  $S(t)$  in the Gauss-Bonnet formula with corners.<sup>55</sup>

- ( $\star 3$ ) Given any  $s > r \geq 0$ , we get

$$\ell(s) - \ell(r) \leq \int_r^s \ell'(t) dt. \tag{D.8}$$

- ( $\star 4$ ) The area of the “annulus”  $\text{An}_{r,s}(\partial\Gamma) = \{x \in \Gamma \mid r \leq \text{dist}_\Gamma(x, \partial\Gamma) < s\}$  is

$$\text{Area}(\text{An}_{r,s}(\partial\Gamma)) = \int_r^s \ell(t) dt. \tag{D.9}$$

**Remark D.10.** The papers [ShTa1] and [ShTa2] extend earlier results of Fiala, [Fa], for analytic surfaces and Hartman, [Ha], for simply connected surfaces. Since our surfaces are minimal in  $\mathbf{R}^3$  and, thus, analytic, the classical results of Fiala could be applied here. However, it is useful not to require analyticity so that the results easily generalize to local ones in a Riemannian 3-manifold.

The claim ( $\star 1$ ) was proven in [ShTa1], while the claims ( $\star 2$ ), ( $\star 3$ ), and ( $\star 4$ ) appear in [ShTa2]. Note also that ( $\star 4$ ) follows from the coarea formula. We should note that the

<sup>54</sup>This definition of  $\theta_i(t)$  is chosen for consistency with [Fa] and [Ha]. Note that each  $\theta_i(t)$  is positive.

<sup>55</sup>Unfortunately, the convention here is that  $\alpha_i = -\theta_i(t)$ .

formula (D.7) does not appear explicitly in [ShTa2], but is implicit there and can also be found in section 9.6 of [Fa].

We will need two additional properties of the level sets  $S(t)$  that hold if in addition  $\Gamma$  is stable:

- ( $\star 5$ ) There is a constant  $C_g$  so that if  $\Gamma$  is embedded and stable, then we get the upper bound

$$\sup_{S(t)} k_g \leq C_g t^{-1}. \quad (\text{D.11})$$

Recall that given our sign convention for  $k_g$ , (D.11) means that  $S(t)$  cannot be “too convex” when it is thought of as part of the boundary of  $\text{An}_t(\gamma)$ .

- ( $\star 6$ ) There is a constant  $\epsilon_g$  so that if  $\Gamma$  is embedded and stable and  $\sigma \subset S(t)$  is a closed curve with

$$\text{Length}(\sigma) \leq \epsilon_g t, \quad (\text{D.12})$$

then  $\sigma$  bounds a disk  $\Gamma_\sigma \subset \Gamma$  and  $\Gamma_\sigma \subset \text{An}_{3t/4, 4t/3}$ .

*Proof.* (of ( $\star 5$ ) and ( $\star 6$ )). The upper bound ( $\star 5$ ) follows immediately from a barrier argument using standard comparison theorems and the interior curvature estimate for stable surfaces. Namely, suppose that  $p \in S(t)$  is a smooth point. Let

$$\gamma_p : [0, t] \rightarrow \Gamma \quad (\text{D.13})$$

be a minimizing geodesic connecting  $\partial\Gamma$  to  $p$ . The triangle inequality then implies that  $S(t)$  does not intersect the interior of the geodesic ball  $\mathcal{B}_s(\gamma_p(t-s))$  for any  $s$  between 0 and  $t$ . Standard comparison theorems and the curvature estimate for stable surfaces then give some  $a > 0$  and  $C_g$  so that  $\partial\mathcal{B}_{at}(\gamma_p(t-at))$  is a smooth curve with geodesic curvature at most  $C_g t^{-1}$ . Since the  $p$  is in the boundaries of these balls and is a smooth point of  $S(t)$ , we conclude that the geodesic curvature of  $S(t)$  at  $p$  is also at most  $C_g t^{-1}$ .<sup>56</sup> Note that we do not claim a lower bound for  $k_g$  (in fact, easy examples show that  $k_g$  can go to  $-\infty$ ; see [Ha]).

To see ( $\star 6$ ), fix a point  $p \in \sigma$  and note that the entire curve  $\sigma$  is contained in the intrinsic geodesic ball  $\mathcal{B}_{\epsilon_g t}(p)$  and this ball stays away from  $\partial\Gamma$ . Taking  $\epsilon_g$  small, the interior curvature estimates for stable surfaces imply that  $\mathcal{B}_{\epsilon_g t}(p)$  is a graph over some plane. In particular, the curve  $\sigma$  is contractible in  $\mathcal{B}_{\epsilon_g t}(p)$ , giving the desired  $\Gamma_\sigma$ .  $\square$

**Remark D.14.** We will actually use a very slight generalization of these results. Namely, in applications,  $\Gamma$  will not be complete, but will rather be allowed to have other boundary components. This does not matter since we will always work with level sets  $S(t)$  where  $t$  is less than the distance to any of the other boundary components. It’s easy to see that the above results extend to this case.

**D.2. The proof of the “stable graph” proposition.** The key point for proving Proposition D.2 will be to show that  $\Gamma$  has quadratic area growth. This quadratic area estimate formally follows from the argument in [CM2], but we need the results of the previous subsection to deal with technical difficulties that arise from the lack of regularity of the level sets of the distance function.

<sup>56</sup>This argument also shows that the jump angles at the corners of  $S(t)$  are negative as claimed in ( $\star 1$ ).

*Proof.* (of Proposition D.2.) The key point is to prove that the intrinsic annuli  $\text{An}_r(\gamma)$  have quadratic area growth:

$$\text{Area}(\text{An}_r(\gamma)) \leq C_1 r^2 + C, \quad (\text{D.15})$$

where the constant  $C_1$  depends on the constant  $C$  in (D.3). Once we have (D.15), the lemma follows easily from the proof of lemma II.1.34 in [CM5]. For the reader's convenience, we will sketch the proof of the lemma assuming (D.15) next:

First, (D.15) allows us to use a logarithmic cutoff function to get sub-annuli with small total curvature. Since these sub-annuli have small total curvature and are stable, the mean value inequality gives a small scale-invariant pointwise curvature estimate. Here the scale refers roughly to the distance to  $\gamma$ . In particular, integrating this curvature bound implies that each component of a level set of the distance to  $\gamma$  is itself a graph over (a curve in) some plane. Moreover, proposition 1.12 in [CM13] uses the fact that the Gauss map is conformal to piece these together and get a graph over one fixed plane, as desired.

It remains therefore to establish (D.15). Note that proposition II.1.3 in [CM5] gives (D.15) directly under the additional assumption that  $\Gamma$  is a topological annulus. We will see that the general case follows similarly if we also use the regularity of the length of level sets of the distance function from  $\gamma$  given by Lemma D.5.

The proof of (D.15). There are two steps in the proof of (D.15):

- (1) The stability inequality allows us to bound the total curvature in terms of the energy of a cutoff and this in turn is bounded by the area.
- (2) The area growth is always controlled by the total curvature. This follows easily from Gauss-Bonnet when the exponential map is smooth but holds more generally by Lemma D.5.

Step (1): Set  $d(\cdot) = \text{dist}_\Gamma(\gamma, \cdot)$  and define a (radial) cut-off function  $\phi$  by

$$\phi = \begin{cases} d & \text{on } \text{An}_1(\gamma), \\ (r - d)/(r - 1) & \text{on } \text{An}_{1,r}(\gamma), \\ 0 & \text{otherwise .} \end{cases} \quad (\text{D.16})$$

By the stability inequality applied to  $\phi$ , we get

$$\begin{aligned} \int_{\text{An}_{1,r}(\gamma)} |A|^2 [(r - d)/(r - 1)]^2 &\leq \int |A|^2 \phi^2 \leq \int |\nabla \phi|^2 \\ &\leq \text{Area}(\text{An}_1(\gamma)) + (r - 1)^{-2} \text{Area}(\text{An}_{1,r}(\gamma)). \end{aligned} \quad (\text{D.17})$$

If we set  $K(s) = \int_{\text{An}_{1,s}(\gamma)} |A|^2$ , then the coarea formula gives

$$K(s) = \int_{\text{An}_{1,s}(\gamma)} |A|^2 = \int_1^s \left[ \int_{\{d=t\}} |A|^2 \right] dt. \quad (\text{D.18})$$

In particular, we can integrate by parts twice to get

$$\begin{aligned} 2(r-1)^{-2} \int_1^r \int_1^t K(s) ds dt &\leq 2/(r-1) \int_1^r K(s)(r-s)/(r-1) ds \\ &\leq \int_1^r K'(s) ((r-s)/(r-1))^2 ds \leq \text{Area}(\text{An}_1(\gamma)) + (r-1)^{-2} \text{Area}(\text{An}_{1,r}(\gamma)), \end{aligned} \quad (\text{D.19})$$

where the last inequality is (D.17).

Step (2): We will now use Lemma D.5 to estimate the area by the total curvature. Set  $\ell(t)$  equal to the length of the level set  $\{d = t\}$ . The key will be to prove the following estimate for  $\ell(t)$  for  $t \geq 1$ :

$$\ell(t) \leq C_2(1+t) + \frac{1}{2} \int_1^t \int_{\text{An}_{1,s}(\gamma)} |A|^2 ds = C_2(1+t) + \frac{1}{2} \int_1^t K(s) ds, \quad (\text{D.20})$$

where  $C_2$  depends only on the constant  $C$  in (D.3).

The proof of the proposition assuming (D.20): Integrating the length bound (D.20) gives the area bound

$$\begin{aligned} \text{Area}(\text{An}_r(\gamma)) &\leq \text{Area}(\text{An}_1(\gamma)) + \int_1^r \ell(t) dt \\ &\leq C + C_2 r + C_2 r^2/2 + \int_1^r \int_1^t \frac{K(s)}{2} ds dt. \end{aligned} \quad (\text{D.21})$$

Combining (D.19) and (D.21) gives the needed bound (D.15).

The proof of (D.20): We will prove (D.20) by integrating a bound on  $\ell'(t)$ . There will be two steps; namely, bounding  $\ell'(t)$  and then finding some value of  $t$  where  $\ell(t)$  is bounded (this is where we will integrate the bound on  $\ell'(t)$  from).

The bound on  $\ell'(t)$ : Roughly speaking, we will bound  $\ell'(t)$  in terms of the total curvature by using the Gauss-Bonnet theorem in the ‘‘annulus’’  $\text{An}_{t_0,t}$  for a specific choice of  $t_0$ . Recall that  $(\star 2)$  implies that  $\ell'(t)$  is bounded by the Gauss-Bonnet terms corresponding to  $S(t)$ . To get the desired upper bound, we will need to control the contributions from the geodesic curvature of the ‘‘inner boundary’’  $S(t_0)$  as well as the Euler characteristic of the ‘‘annulus’’. We will do this next.

First, the area bound (D.3) and  $(\star 4)$  imply that there must exist some  $t_0 \in (1/3, 2/3)$  with

$$\ell(t_0) \leq 3 \text{Area}(\text{An}_{1/3,2/3}(\gamma)) \leq 3C. \quad (\text{D.22})$$

Moreover, by the regularity property  $(\star 1)$ , we may assume that the level set  $S(t_0)$  is a finite union of simple closed piecewise smooth curves. We will sort these curves into two groups, depending on their length. Namely, let  $\sigma_1^{long}, \dots, \sigma_n^{long}$  be the components of  $S(t_0)$  with

$$\text{Length}(\sigma_i^{long}) \geq \epsilon_g/3, \quad (\text{D.23})$$

where  $\epsilon_g$  is given by  $(\star 6)$ . Let  $\sigma_1^{short}, \dots, \sigma_m^{short}$  be the remaining components. Combining (D.23) with the upper bound on the total length of  $S(t_0)$  from (D.22) immediately gives the bound

$$n \leq n(C), \quad (\text{D.24})$$

where  $n(C)$  depends only on the area bound (D.3).<sup>57</sup>

We will not actually apply the Gauss-Bonnet theorem to all of  $\text{An}_{t_0,t}(\gamma)$ , but rather to the subset  $\Gamma_t$  that “sees the outer boundary”  $S(t)$ . To be precise, define  $\Gamma_t$  to be the union of all connected components of  $\text{An}_{t_0,t}(\gamma)$  whose boundaries intersect  $S(t)$ ; see Figure 51.

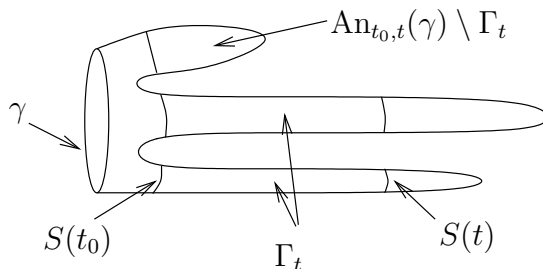


FIGURE 51. An example illustrating  $\Gamma_t$  in a case where  $\Gamma_t \neq \text{An}_{t_0,t}(\gamma)$ .

By construction, we have

$$S(t) \subset \partial\Gamma_t \text{ and } \partial\Gamma_t \setminus S(t) \subset S(t_0). \quad (\text{D.25})$$

Consequently, combining the length bound (D.22) with the pointwise geodesic curvature bound  $(\star 5)$ , we get a total (geodesic) curvature bound for  $\partial\Gamma_t \setminus S(t)$

$$\int_{\partial\Gamma_t \setminus S(t)} k_g \leq \ell(t_0) \sup_{S(t_0)} k_g \leq k(C), \quad (\text{D.26})$$

where  $k(C)$  depends only on the area bound (D.3). We should make two remarks about (D.26):

- The integration in (D.26) is over only the smooth part of  $\partial\Gamma_t \setminus S(t)$ .
- The sign convention on  $k_g$  in (D.26) is as part of the boundary of  $\text{An}_{t_0}(\gamma)$ ; this is the opposite as it would be as part of the boundary of  $\Gamma_t$ . This is important later when we apply the Gauss-Bonnet theorem.

The last ingredient that we will need to bound  $\ell'(t)$  is a bound on the Euler characteristic  $\chi(\Gamma_t)$  that depends only on the area bound (D.3). This bound follows immediately from the bound (D.24) on the number of long components of  $S(t_0)$  together with the following claim:

(Claim) For  $t \geq 3/4$ , each connected component of  $\Gamma_t$ , i.e., each component of  $\text{An}_{t_0,t}(\gamma)$  whose boundary touches  $S(t)$ , contains at least one long component  $\sigma_i^{long}$  in its boundary.

The point here is that the short components of  $S(t_0)$  are contractible near  $S(t_0)$ , so  $S(t)$  never sees them. More precisely,  $(\star 6)$  implies that each  $\sigma_i^{short}$  bounds a disk

$$\Gamma_i^{disk} \subset \text{An}_{1/4,3/4}(\gamma). \quad (\text{D.27})$$

Therefore, if  $p$  is an arbitrary point in  $S(t)$ , then we know that  $p$  and  $\gamma$  are in the same connected component of

$$\overline{\text{An}_t(\gamma)} \setminus \cup_{i=1}^m \sigma_i^{short}. \quad (\text{D.28})$$

Note that we have used here that  $\text{An}_t(\gamma)$  is itself connected. Since  $S(t_0)$  separates  $\gamma = S(0)$  from  $S(t)$ , we conclude that it must be  $\cup_i \sigma_i^{long}$  that separates  $p$  and  $\gamma$ . In particular, the

<sup>57</sup>We are not claiming a bound on the total number  $m + n$  of components of  $S(t_0)$ .

component of  $\text{An}_{t_0,t}$  with  $p$  in its boundary also contains at least one  $\sigma_i^{long}$  in its boundary. This completes the proof of (Claim).

We can now bound  $\ell'(t)$  for  $t \geq 3/4$ . Namely,  $(\star 2)$  implies that  $\ell'(t)$  is bounded by the Gauss-Bonnet integrand along  $S(t)$  so the Gauss-Bonnet theorem gives for almost every  $t$  that

$$\ell'(t) \leq \int_{S(t)} k_g - \sum_i \theta_i(t) \leq \frac{1}{2} \int_{\Gamma_t} |A|^2 + 2\pi\chi(\Gamma_t) + \int_{\partial\Gamma_t \setminus S(t)} k_g. \quad (\text{D.29})$$

We have thrown away the angle contributions at the corners of  $\partial\Gamma_t \setminus S(t)$  in (D.29) since these are all negative by  $(\star 1)$ . Since  $\Gamma_t \subset \text{An}_{1/3,t}(\gamma)$ , we can use interior curvature estimates for stable surfaces and the area bound on  $\text{An}_1(\gamma)$  to get

$$\int_{\Gamma_t} |A|^2 \leq \int_{\text{An}_{1,t}(\gamma)} |A|^2 + \text{Area}(\text{An}_1(\gamma)) \sup_{\text{An}_{1/3,1}(\gamma)} |A|^2 \leq \int_{\text{An}_{1,t}(\gamma)} |A|^2 + C_3, \quad (\text{D.30})$$

where  $C_3$  depends only on the initial area bound (D.3). Substituting the above bounds into (D.29), we get for almost every  $t \geq 3/4$  that

$$\ell'(t) \leq \frac{1}{2} \int_{\text{An}_{1,t}(\gamma)} |A|^2 + C_4, \quad (\text{D.31})$$

where  $C_4$  depends only on the initial area bound (D.3).

To complete the proof, use the area bound and  $(\star 4)$  again to find  $t_1$  between  $3/4$  and  $1$  with  $\ell(t_1) \leq 4C$ . Given  $t \geq 1$ , we can then use  $(\star 3)$  to integrate (D.31):

$$\begin{aligned} \ell(t) &\leq \ell(t_1) + \int_{t_1}^t \ell'(s) ds \\ &\leq 4C + C_4(t - t_1) + \frac{1}{2} \int_{t_1}^t \int_{\text{An}_{1,s}(\gamma)} |A|^2 ds. \end{aligned} \quad (\text{D.32})$$

This gives (D.20), thus completing the proof.

We should point out that we have actually shown only that the components coming from the tubular neighborhood  $\text{An}_r(\gamma)$  are graphs. However, the other components are easily also seen to be graphs by combining the curvature estimate and embeddedness. Namely, any other component is intrinsically far from the boundary and hence graphical over some plane. By embeddedness, these graphs do not cross, and we can take these planes to be parallel.  $\square$

## APPENDIX E. BLOWING UP INTRINSICALLY ON THE SCALE OF NON-TRIVIAL TOPOLOGY

The next lemma uses a standard blowup argument to locate the smallest scale of non-trivial topology:

**Lemma E.1.** Suppose that  $\Sigma \subset \mathbf{R}^3$  is a smooth minimal surface, possibly with boundary  $\partial\Sigma$ . If the ball  $\mathcal{B}_{5C_1 r_1}(y_0) \subset \Sigma$  is disjoint from  $\partial\Sigma$  for some  $C_1 > 1$  and

$$\mathcal{B}_{r_1}(0) \text{ is not a disk,} \quad (\text{E.2})$$

then there exists a sub-ball  $\mathcal{B}_{C_1 s}(y_1) \subset \mathcal{B}_{4C_1 r_1}(y_0)$  so that

$$\mathcal{B}_{4s}(y_1) \text{ is not a disk,} \quad (\text{E.3})$$

$$\mathcal{B}_s(y) \text{ is a disk for any } y \in \mathcal{B}_{C_1 s}(y_1). \quad (\text{E.4})$$

*Proof.* After rescaling, we can assume that  $r_1 = 1$ . The lemma will follow from a simple rescaling argument as in Lemma 5.1 of [CM4], except we define  $F$  intrinsically on  $\mathcal{B}_{4C_1}(y_0)$  by

$$F(x) = d^2(x) i^{-2}(x), \tag{E.5}$$

where  $i(x)$  is the injectivity radius of  $\Sigma$  at  $x$  and

$$d(x) = 4C_1 - \text{dist}_\Sigma(x, y_0) \tag{E.6}$$

is the distance to  $\partial\mathcal{B}_{4C_1}(y_0)$ . It follows that  $F = 0$  on  $\partial\mathcal{B}_{4C_1}(y_0)$  and  $F(y_0) \geq 16C_1^2$ . Also, since  $\mathcal{B}_{5C_1}(y_0)$  is smooth, it follows that  $F$  is bounded from above on  $\mathcal{B}_{4C_1}(y_0)$ . We can therefore choose a point  $y_1$  where  $F(y_1)$  is at least half of its supremum<sup>58</sup>, i.e.,

$$F(y_1) > 1/2 \sup_{\mathcal{B}_{4C_1}(y_0)} F. \tag{E.7}$$

Set  $s^2 = i^2(y_1)/8$ .

To see that (E.3) holds, first note that  $4s > i(y_1)$ . In particular, there must be two distinct geodesics,  $\gamma_1$  and  $\gamma_2$ , contained in  $\mathcal{B}_{4s}(y_1)$  with

$$\gamma_1(0) = \gamma_2(0) = y_1 \text{ and } \gamma_1(i(y_1)) = \gamma_2(i(y_1)). \tag{E.8}$$

Since  $\Gamma$  has non-positive curvature, it follows immediately from the Gauss-Bonnet theorem with corners that the closed curve  $\gamma_1 \cup \gamma_2$  cannot bound a disk in  $\Gamma$ , thus giving (E.3).<sup>59</sup>

We will use (E.7) twice to prove (E.4). First, since  $d \geq d(y_1)/2$  on  $\mathcal{B}_{\frac{d(y_1)}{2}}(y_1)$ , (E.7) implies that

$$\sup_{\mathcal{B}_{\frac{d(y_1)}{2}}(y_1)} i^{-2} \leq \frac{4}{d^2(y_1)} \sup_{\mathcal{B}_{\frac{d(y_1)}{2}}(y_1)} F < \frac{8F(y_1)}{d^2(y_1)} = s^{-2}, \tag{E.9}$$

so that  $i > s$  on  $\mathcal{B}_{\frac{d(y_1)}{2}}(y_1)$ . Second, using  $F(y_0)$  as a lower bound for the sup of  $F$  in (E.7) implies that

$$8C_1^2 \leq F(y_1) = \frac{d^2(y_1)}{8s^2}, \tag{E.10}$$

so that  $d(y_1)/2 > C_1 s$ . □

## APPENDIX F. MINIMAL SURFACES WITH A QUADRATIC CURVATURE BOUND IN A HALF-SPACE

The next lemma deals with a minimal surface whose curvature blows up at most quadratically at a point  $z$  in its closure. The lemma shows that the surface must come arbitrarily scale-invariant close to any plane through  $z$ . Roughly speaking, this means that the surface does not lie in any strictly mean convex cone through  $z$ ; see Figure 52.

To state the lemma precisely, given a plane through  $z$ , we will define a scale-invariant function  $\beta(s)$  that measures how close in the sphere  $\partial\mathcal{B}_s(z)$  a surface  $\tilde{\Gamma} \subset \mathbf{R}^3 \setminus \{z\}$  comes

---

<sup>58</sup>Note that we are not claiming that  $i$ , or  $F$ , is continuous, so we do not know that it achieves its maximum. However, since it is bounded, there must be points where it is at least half of its supremum.

<sup>59</sup>The Gauss-Bonnet theorem with corners implies that a disk  $D$  has  $\int_{\partial D} k_g + \int_D K + \sum \alpha_i = 2\pi$ , where  $\partial D$  has jump angles  $\alpha_i$  at the corners. In this case, both integrals are non-positive and there are only two corners with each contributing less than  $\pi$ , so no such disk can exist.

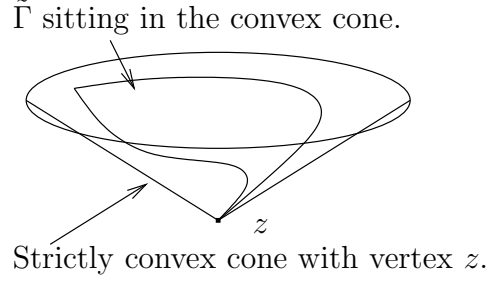


FIGURE 52. We prove Lemma F.2 by contradiction, so suppose that  $\tilde{\Gamma}$  lies in a strictly mean convex cone.

to the plane. After a rotation, we can assume that the plane is the horizontal plane  $\{x_3 = x_3(z)\}$ . Define the function  $\beta(s)$  by setting

$$\beta(s) = \frac{\inf_{\partial B_s(z) \cap \tilde{\Gamma}} |x_3 - x_3(z)|}{s}. \quad (\text{F.1})$$

The next lemma shows that the  $\liminf$  of  $\beta(s)$  is zero, so that  $\tilde{\Gamma}$  comes arbitrarily scale-invariant close to the plane as we approach  $z$ .

**Lemma F.2.** Let  $\tilde{\Gamma} \subset \mathbf{R}^3 \setminus \{z\}$  be a minimal surface (embedded or not) with  $z$  in its closure. Suppose that, for each  $\epsilon > 0$ , each component of  $\tilde{\Gamma} \setminus B_\epsilon(z)$  is complete and has boundary in  $\partial B_\epsilon(z)$ .

If there exist constants  $r_0 > 0$  and  $C$  so that for  $x \in B_{r_0}(z) \cap \tilde{\Gamma}$  we have

$$|A|^2(x) \leq C |x - z|^{-2}, \quad (\text{F.3})$$

then the function  $\beta(s)$  defined in (F.1) satisfies

$$\liminf_{s \rightarrow 0} \beta(s) = 0. \quad (\text{F.4})$$

*Proof.* We will prove (F.4) by contradiction (see Figure 52), so suppose that

$$\liminf_{s \rightarrow 0} \beta(s) = \beta_0 > 0. \quad (\text{F.5})$$

In particular, given any  $\delta > 0$ , equation (F.5) implies that there exists  $s_0 > 0$  so that  $\beta(s) > \beta_0 - \delta$  for every  $s < s_0$  and, hence,  $B_{s_0}(z) \cap \tilde{\Gamma}$  lies inside a strictly mean convex (double) cone:

$$B_{s_0}(z) \cap \tilde{\Gamma} \subset \{|x_3 - x_3(z)| > (\beta_0 - \delta) |x - z|\}. \quad (\text{F.6})$$

On the other hand, (F.5) also implies that there is an  $s < s_0/2$  with  $\beta(s) < \beta_0 + \delta$  and, consequently, there is a point  $y_s \in \partial B_s(z) \cap \tilde{\Gamma}$  close to the strictly mean convex cone:

$$y_s \in \partial B_s(z) \cap \{|x_3 - x_3(z)| < (\beta_0 + \delta) s\} \cap \tilde{\Gamma}. \quad (\text{F.7})$$

Note that (F.6) and (F.7) imply that the intrinsic ball  $\mathcal{B}_{s/2}(y_s)$  stays inside, but comes close to, the strictly mean convex cone

$$\{|x_3 - x_3(z)| = (\beta_0 - \delta) |x - z|\}. \quad (\text{F.8})$$

We will assume below that  $\delta < \beta_0$ .

We will see that (F.6) and (F.7) lead to a contradiction for  $\delta$  sufficiently small, thus proving (F.4).

First, recall that the quadratic curvature bound (F.3) gives an  $\alpha > 0$  so that the component  $\tilde{\Gamma}_{\alpha s}$  of  $B_{\alpha s}(y_s) \cap \tilde{\Gamma}$  containing  $y_s$  is a graph with gradient bounded by one (see, e.g., lemma 2.2 in [CM1]). After possibly reducing  $\alpha$ , we can therefore assume that

$$\tilde{\Gamma}_{\alpha s} \subset \mathcal{B}_{s/2}(y_s). \quad (\text{F.9})$$

Since  $\tilde{\Gamma}_{\alpha s}$  is connected and does not intersect the (double) cone (F.8), it must be in one of the two components of  $\{|x_3 - x_3(z)| > (\beta_0 - \delta)|x - z|\}$ . After possibly reflecting, we can assume that

$$\tilde{\Gamma}_{\alpha s} \subset \{x_3 - x_3(z) > (\beta_0 - \delta)|x - z|\}. \quad (\text{F.10})$$

Define a function  $f$  that vanishes on the cone  $\{x_3 - x_3(z) = (\beta_0 - \delta)|x - z|\}$  by setting

$$f(x) = x_3 - x_3(z) - (\beta_0 - \delta)|x - z|. \quad (\text{F.11})$$

Note that (F.6) and (F.7) imply that

$$0 \leq \inf_{\tilde{\Gamma}_{\alpha s}} f \leq f(y_s) < 2\delta s. \quad (\text{F.12})$$

Using that  $\tilde{\Gamma}_{\alpha s}$  is minimal, we have that

$$\Delta f = -(\beta_0 - \delta)\Delta|x - z| < -\frac{\beta_0 - \delta}{|x - z|}. \quad (\text{F.13})$$

Define a function  $g$  on  $\tilde{\Gamma}_{\alpha s}$  by setting

$$g = f + |x - y_s|^2 \frac{\beta_0 - \delta}{6s}. \quad (\text{F.14})$$

Using that  $|x - z| < 3s/2$  on  $\tilde{\Gamma}_{\alpha s}$ , we get that  $g$  is superharmonic since

$$\Delta g < -\frac{\beta_0 - \delta}{|x - z|} + 4\frac{\beta_0 - \delta}{6s} < 0. \quad (\text{F.15})$$

Therefore, the minimum of  $g$  is achieved on  $\partial\tilde{\Gamma}_{\alpha s}$  and thus

$$\min_{\partial\tilde{\Gamma}_{\alpha s}} \left[ f + (\alpha s)^2 \frac{\beta_0 - \delta}{6s} \right] = \min_{\tilde{\Gamma}_{\alpha s}} g < g(y_s) = f(y_s) < 2\delta s, \quad (\text{F.16})$$

where the last inequality is from (F.12). Combining the first inequality from (F.12) and (F.16) gives

$$0 \leq \min_{\partial\tilde{\Gamma}_{\alpha s}} f < 2\delta s - \alpha^2 s (\beta_0 - \delta)/6. \quad (\text{F.17})$$

This gives the desired contradiction for  $\delta$  sufficiently small.  $\square$

## REFERENCES

- [CM1] T.H. Colding and W.P. Minicozzi II, Minimal surfaces, Courant Lecture Notes in Math., v. 4, 1999.
- [CM2] T.H. Colding and W.P. Minicozzi II, Estimates for parametric elliptic integrands, *International Mathematics Research Notices*, no. 6 (2002) 291–297.
- [CM3] T.H. Colding and W.P. Minicozzi II, The space of embedded minimal surfaces of fixed genus in a 3-manifold I; Estimates off the axis for disks, *Annals of Math.*, 160 (2004) 27–68, math.AP/0210106.
- [CM4] T.H. Colding and W.P. Minicozzi II, The space of embedded minimal surfaces of fixed genus in a 3-manifold II; Multi-valued graphs in disks, *Annals of Math.*, 160 (2004) 69–92, math.AP/0210086.
- [CM5] T.H. Colding and W.P. Minicozzi II, The space of embedded minimal surfaces of fixed genus in a 3-manifold III; Planar domains, *Annals of Math.*, 160 (2004) 523–572, math.AP/0210141.
- [CM6] T.H. Colding and W.P. Minicozzi II, The space of embedded minimal surfaces of fixed genus in a 3-manifold IV; Locally simply connected, *Annals of Math.*, 160 (2004) 573–615, math.AP/0210119.
- [CM7] T.H. Colding and W.P. Minicozzi II, Multi-valued minimal graphs and properness of disks, *International Mathematics Research Notices*, no. 21 (2002) 1111–1127.
- [CM8] T.H. Colding and W.P. Minicozzi II, On the structure of embedded minimal annuli, *International Mathematics Research Notices*, no. 29 (2002) 1539–1552.
- [CM9] T.H. Colding and W.P. Minicozzi II, The Calabi–Yau conjectures for embedded surfaces, preprint, math.DG/0404197.
- [CM10] T.H. Colding and W.P. Minicozzi II, Embedded minimal disks, Minimal surfaces (MSRI, 2001), ed. D. Hoffman, Clay Mathematics Proceedings, AMS, Providence (2004), 405–438, math.DG/0206146.
- [CM11] T.H. Colding and W.P. Minicozzi II, Disks that are double spiral staircases, *Notices of the AMS*, Vol. 50, no. 3, March (2003) 327–339.
- [CM12] T.H. Colding and W.P. Minicozzi II, Embedded minimal disks: Proper versus nonproper - global versus local, *Transactions of the AMS*, 356 (2004) 283–289.
- [CM13] T.H. Colding and W.P. Minicozzi II, Minimal annuli with and without slits, *Jour. of Symplectic Geometry*, vol. 1, issue 1 (2001) 47–62.
- [CM14] T.H. Colding and W.P. Minicozzi II, Complete properly embedded minimal surfaces in  $\mathbf{R}^3$ , *Duke Math. J.* 107 (2001) 421–426.
- [DoPe] M. do Carmo and C.K. Peng, Stable complete minimal surfaces in  $\mathbf{R}^3$  are planes, *Bull. Amer. Math. Soc. (N.S.)* 1 (1979), no. 6, 903–906.
- [Fa] F. Fiala, Le problme des isoprimitives sur les surfaces ouvertes courbure positive, *Comment. Math. Helv.* 13, (1941) 293–346.
- [FiSc] D. Fischer-Colbrie and R. Schoen, The structure of complete stable minimal surfaces in 3-manifolds of nonnegative scalar curvature, *Comm. Pure Appl. Math.* 33 (1980), no. 2, 199–211.
- [Gr] M. Gromov, *Groups of polynomial growth and expanding maps*, Inst. Hautes Études Sci. Publ. Math. No. 53, (1981), 53–73.
- [GuLa] R. Gulliver and H. B. Lawson, Jr., The structure of stable minimal hypersurfaces near a singularity, *Geometric measure theory and the calculus of variations* (Arcata, Calif., 1984), 213–237, Proc. Sympos. Pure Math., 44, Amer. Math. Soc., Providence, RI, 1986.
- [HSi] R. Hardt and L. Simon, Boundary regularity and embedded solutions for the oriented Plateau problem, *Ann. of Math. (2)* 110 (1979), no. 3, 439–486.
- [Ha] P. Hartman, Geodesic parallel coordinates in the large, *Amer. J. Math.* 86 (1964) 705–727.
- [Hi] S. Hildebrandt, Boundary behavior of minimal surfaces, *Arch. Rational Mech. Anal.* 35 (1969) 47–82.
- [HoKrWe] D. Hoffman, H. Karcher, and F. Wei, Adding handles to the helicoid, *Bull. Amer. Math. Soc. (N.S.)* 29 (1993), no. 1, 77–84.
- [HoWeWo] D. Hoffman, M. Weber, and M. Wolf, An embedded genus-one helicoid, math.DG/0401080.
- [HoMe] D. Hoffman and W. Meeks III, The strong halfspace theorem for minimal surfaces, *Invent. Math.* 101 (1990) 373–377.
- [LaRo] R. Langevin and H. Rosenberg, A maximum principle at infinity for minimal surfaces and applications, *Duke Math. J.* 57 (1988), no. 3, 819–828.
- [Me1] W. Meeks III, The regularity of the singular set in the Colding and Minicozzi lamination theorem, *Duke Math. Jour.* 123 (2004), no. 2, 329–334.

- [Me2] W. Meeks III, The lamination metric for the Colding-Minicozzi minimal lamination, preprint.
- [MeP] W. Meeks III and J. Perez, Conformal properties in classical minimal surface theory, *Surveys in Differential Geometry - Eigenvalues of Laplacian and other geometric operators*, Vol. 9, edited by A. Grigor'yan and S.T. Yau (2004), 275–336.
- [MePRs1] W. Meeks III, J. Perez, and A. Ros, The geometry of minimal surfaces of finite genus I; Curvature estimates and quasiperiodicity, *J. Diff. Geom.* 66 (2004), no. 1, 1–45.
- [MePRs2] W. Meeks III, J. Perez, and A. Ros, The geometry of minimal surfaces of finite genus II; Nonexistence of one limit end examples, *Invent. Math.*, 158 (2004), no. 2, 323–341.
- [MePRs3] W. Meeks III, J. Perez, and A. Ros, The geometry of minimal surfaces of finite genus III; bounds on the topology and index of classical minimal surfaces, preprint.
- [MeRo] W. Meeks III and H. Rosenberg, The uniqueness of the helicoid and the asymptotic geometry of properly embedded minimal surfaces with finite topology, *Annals of Math.*, 161 (2005) 727–758.
- [MeWe] W. H. Meeks III and M. Weber, Existence of bent helicoids and the regularity of the singular set in the Colding-Minicozzi lamination theorem, in preparation.
- [MeYa1] W. Meeks III and S. T. Yau, The classical Plateau problem and the topology of three-dimensional manifolds. The embedding of the solution given by Douglas–Morrey and an analytic proof of Dehn's lemma, *Topology* 21 (1982) 409–442.
- [MeYa2] W. Meeks III and S. T. Yau, The existence of embedded minimal surfaces and the problem of uniqueness, *Math. Zeit.* 179 (1982) 151–168.
- [P] J. Perez, Limits by rescalings of minimal surfaces: Minimal laminations, curvature decay and local pictures, notes for the workshop “Moduli Spaces of Properly Embedded Minimal Surfaces”, American Institute of Mathematics, Palo Alto, California (2005).
- [Ro] H. Rosenberg, Some recent developments in the theory of minimal surfaces in 3-manifolds. IMPA Mathematical Publications. *24th Brazilian Mathematics Colloquium*, Instituto de Matemática Pura e Aplicada (IMPA), Rio de Janeiro, 2003.
- [Sc1] R. Schoen, Estimates for stable minimal surfaces in three-dimensional manifolds, Seminar on Minimal submanifolds, *Ann. of Math. Studies*, v. 103, Princeton University Press (1983).
- [Sc2] R. Schoen, Uniqueness, symmetry, and embeddedness of minimal surfaces, *J. Differential Geom.* 18 (1983), no. 4, 791–809.
- [ShTa1] K. Shiohama and M. Tanaka, An isoperimetric problem for infinitely connected complete open surfaces. *Geometry of manifolds (Matsumoto, 1988)*, 317–343, *Perspect. Math.*, 8, Academic Press, Boston, MA, 1989.
- [ShTa2] K. Shiohama and M. Tanaka, The length function of geodesic parallel circles, *Progress in differential geometry*, (1993) 299–308.
- [So] B. Solomon, On foliations of  $\mathbf{R}^{n+1}$  by minimal hypersurfaces, *Comm. Math. Helv.* 61 (1986) 67–83.

COURANT INSTITUTE OF MATHEMATICAL SCIENCES, 251 MERCER STREET, NEW YORK, NY 10012

DEPARTMENT OF MATHEMATICS, JOHNS HOPKINS UNIVERSITY, 3400 N. CHARLES ST., BALTIMORE, MD 21218

*E-mail address:* colding@cims.nyu.edu and minicozz@math.jhu.edu